Structural and functional analyses of H-Ras and R-Ras

Julie Ann Love

A thesis submitted for the degree of Doctor of Philosophy

University of Edinburgh, 2004

Declaration

I hereby declare that this thesis has been composed solely by myself and has not been accepted in any previous candidature for a higher degree. All work in presented in this thesis was, unless acknowledged, initiated and executed by myself. All sources of information in the text have been acknowledged by reference.

Julie Ann Love

March 2004

Abstract

Integrins are heterodimeric transmembrane glycoproteins present on the surface of virtually every cell. They play a key role in growth, survival, migration and tumour metastasis, by maintaining and controlling cell-cell and cell-substratum adhesion. The precisely controlled changes in cell adhesion, governed by integrins, are a hallmark of many basic physiological processes. These include leukocyte migration during infiltration into inflammatory sites, and platelet aggregation. Many cancers have abnormal integrin function as a result of oncogenic transformation. However, the precise effect of integrin function on transformation is not well defined.

Central to the role of integrins in regulating adhesion is the ability to modulate affinity for ligand binding in response to intracellular signal transduction pathways. The mechanism by which this 'inside-out' signalling governs integrin affinity requires further definition.

Previous studies have identified H-Ras and its downstream effector Raf-1 as key suppressors of integrin activation. H-Ras is the most prevalent oncogenic mutation in human solid tumours and has been implicated in cellular transformation. The related small GTP-binding protein, R-Ras, was originally identified as a result of its high homology to H-Ras. The activated variant of R-Ras, R-Ras (G38V), strongly antagonises the H-Ras/Raf- initiated integrin suppression pathway, leading to integrin activation and an increase in adhesion in CHO cells. The different effects H- and R-Ras have on cellular function have provided the first system whereby these proteins can be distinguished.

In this thesis I have sought to gain further insight into the regulation of integrin affinity and cellular function by Ras GTPases. A series of H-and R-Ras chimeras have been used to examine the hypothesis that specific sequences within these molecules govern their differential effects on integrin function and cellular transformation. Understanding the structure/function relationship between H-Ras and R-Ras may help to elucidate their downstream effectors which regulate integrin function, and define the relevance of MAP kinase activation with regards to integrin

activation and cellular transformation. This may lead to a better understanding of the development of cancer.

Expression of the H-and R-Ras chimeras within an integrin reporter system ($\alpha\beta$-py cells) revealed that a C-terminal 25-amino acid stretch of H-Ras was required for full suppressive activity, and that the equivalent C-terminal 28-amino acid stretch of R-Ras was required to fully reverse H-Ras/Raf- initiated integrin suppression. The effect of these amino acid stretches on integrin function was further confirmed by investigations into the changes in cytoskeletal organisation and overall cellular morphology. Furthermore, the data suggest that the effects on integrin function are independent of the activation of the ERK1/2 MAP kinase pathway. This implicates a novel mechanism whereby Ras modulates integrin affinity.

In summary, it is shown that H-Ras- and R-Ras-mediated integrin affinity is regulated by distinct C-terminal domains. Moreover, integrin affinity modulation is independent of ERK1/2 MAP kinase activation. In addition there is an apparent correlation between suppression of integrin function and cellular transformation.

Acknowledgements

Although there have been numerous people who have helped me during the course of my PhD, a few are deserving of special mention.

Very special thanks to my parents and sister, who have provided me with a considerable amount of support and encouragement over the last few years. I'm quite sure they will be glad to see the back of this project.

I am most grateful to Dr Tariq Sethi for providing me with the opportunity to work with such a lively and sociable group, making the time I have spent in the laboratory enjoyable and fulfilling. Tariq has been a source of constant optimism throughout this project.

I would like to thank Dr Alison MacKinnon and Dr Yatish Lad who have provided me with a great deal of guidance, patience and advice throughout my lab work and subsequent write-up. I also have to thank Linda Wilson for her help with the confocal microscopy, Steve Mitchell for his help with the scanning electron microscope and Dr M. H. Ginsberg and Dr Paul Hughes for providing me with the chimeras used throughout this project.

To the remaining members of my group (past and present), I would like to thank you all for your friendship and support, both in the lab and in various public houses, which has helped me through the ups and downs of this thesis. A special thanks to Liz Collis, a most unselfish friend who has shared in this experience since day one. Also thanks to Dr Niall McLaren, a friend from the beginning of university, who has always been one step ahead!

And last but by no means least, many thank-yous and love to my partner Jonny, who has been a source of patience and support throughout the process of this PhD. His company during the write-up of this thesis has helped me to keep a balanced outlook on life, as well as providing me with some much needed laughs.

This work was supported by the MRC.

Abbreviations

AI	Activation Index
Ala	Alanine
APS	Ammonium persulphate
Arg	Arginine
Asn	Asparagine
Asp	Aspartic acid
ATP	Adenosine 5' triphosphate
AU	Arbitrary Units
Bcl-2	B cell leukaemia oncogene 2
bp	base pair
BSA	Bovine serum albumin
Ca^{2+}	Calcium
CAAX	Cysteine-Aliphatic amino acid-Aliphatic amino acid Serine/ Methionine
$CaCl_2$	Calcium chloride
CD	Cluster of Differentiation
cDNA	Complementary DNA
CHO	Chinese hamster ovary
CKI	Cyclin-dependent kinase inhibitor
COOH-	Carboxyl-
Ctx	Cholera toxin
dH_2O	Distilled H_2O
DMEM	Dulbeccos Modified Eagles Medium
DNA	Deoxyribonucleic acid
dNTP	Deoxynucleotide triphosphate
E.coli	*Escherichia coli*
ECL	Enhanced chemiluminescence
ECM	Extracellular matrix
EDTA	Ethylenediaminetetraacetic acid
EGF	Epidermal growth factor
EGTA	Ethylene glycol-bis (β-aminoethyl ether) N,N,N',N'-tetraacetic acid

ELISA	Enzyme-linked immunosorbant assay
ER	Endoplasmic reticulum
ERK	Extracellular signal-regulated kinase
FA	Focal adhesion
FACS	Fluorescence activated cell sorter
FAK	Focal adhesion kinase
Fg	Fibrinogen
FITC	Fluorescein isothiocyanate
FN	Fibronectin
FSG	Fish skin gelatine
G12V	Glycine^{12} to Valine^{12}
G418	Geneticin
GAP	GTPase Activating Protein
GDP	Guanine diphosphate
GEF	Guanine Exchange Factor
GFP	Green fluorescent protein
Gln	Glutamine
Glu	Glutamic acid
Gly	Glycine
GPI	glycophosphatidylinositol
Grb2	Growth-factor-receptor-bound protein 2
GTP	Guanine triphosphate
HCl	Hydrochloric acid
HEPES	EGTA Ethylene glycol-bis (β-aminoethyl ether) N,N,N',N'-tetraacetic acid
His	Histidine
HRP	Horse radish peroxidase
HVR	Hypervariable region
ICAM	Immunoglobulin-like Cell Adhesion Molecule
ILK	Integrin linked kinase
IPTG	Isopropylthio-β-D-galactoside
JNK	c-Jun N-terminal kinase
Kb	Kilobase
kDa	Kilodalton

LB media	Luria-Bertani Media
Leu	Leucine
LFA	Lymphocyte function associated antigen
LN	Laminin
mAb	Monoclonal antibody
MAPK	Mitogen Activated Protein kinase
MBP	Myelin basic protein
MDCK	Madin-Darby canine kidney
MEK	MAPK/ERK kinase
MFI	Mean fluorescence intensity
$MgCl_2$	Magnesium chloride
MIDAS	Metal ion-dependent adhesion site
MKP	MAP kinase phosphatase
Mn^{2+}	Manganese
mRNA	messenger RNA
MSV	Murine sarcoma virus
MβCD	Methyl-β-cyclo dextrin
NaCl	Sodium chloride
NaF	Sodium fluoride
NF-1	Nuclear factor 1
NH_2-	Amino-
NMR	Nuclear magnetic resonance
PBS	Phosphate buffered saline
PCR	Polymerase chain reaction
PDGF	Platelet derived growth factor
pERK	Phosphorylated ERK
PFA	Para formaldehyde
PI3-kinase	Phosphoinositide-3-OH kinase
PKB	Protein kinase B
PLC	Phospholipase C
Pro	Proline
PS	Phosphatidylserine
Ral-GDS	Ral guanine nucleotide dissociation stimulator
RBD	Ras binding domain

RGD	Arg-Gly-Asp sequence
RNA	Ribonucleic acid
RPE	R-phycoerythrin
RTK	Receptor tyrosine kinase
SAP	Shrimp alkaline phosphatase
SDM	Site-directed mutagenesis
SDS	Sodium dodecyl-sulphate
SDS-PAGE	Sodium dodecyl-sulphate polyacrylamide gel electrophoresis
SEM	Standard error mean
Ser	Serine
SH	Src homology
Shc	SH2-domain-containing $\alpha 2$-collagen related protein
SOE by PCR	Splice-overlap extension by PCR
SOS	Son of sevenless
TBS	Tris buffered saline
TEMED	N,N,N',N'-tetramethylethylenediamine
Thr	Threonine
Trp	Tryptophan
Tyr	Tyrosine
VCAM	Vascular Cell Adhesion Molecule
VLA	very late antigens
X-Gal	5-Bromo-4-Chloro-β-D-galactopyranoside

Table of Contents

List of Figures

CHAPTER 7

List of Tables

Chapter 1: Introduction

Integrins and integrin signalling

Integrins are a widely expressed family of cell adhesion receptors that enable cells to bind to extracellular matrix (ECM) proteins and to each other via cell surface Ig counter-receptors. Integrins provide a physical link between the extracellular environment and the cytoskeletal elements of the cell interior. The term 'integrin' relates to the role of the cell adhesion glycoprotein as an integral membrane complex involved in the transmembrane association between the extracellular matrix and cytoskeleton (Tamkun *et al.*, 1986). Early studies carried out on the platelet glycoprotein GPIIb-IIIa, the fibronectin receptor on chick fibroblasts and the leukocyte antigens (LFA-1, Mac-1 and the VLA antigens), revealed that these proteins were composed of two non-covalently linked subunits, termed α and β, which form heterodimeric receptor complexes. Sequence analysis of the subunits revealed sequence homology between the α and β subunits from these proteins groups (Hynes, 1987; Ruoslahti and Pierschbacher, 1987). The $\alpha\beta$ nomenclature, adopted to classify the subunits according to their sequence identity, is the most widely used and most widely applicable (Hynes, 1992).

1.1 Integrin subunits and ligands

Currently, there have been 18α and 8β integrin subunits described. Although these subunits could in theory associate to create more than 100 integrin heterodimers, the diversity appears to be much more restricted with only 24 different receptors identified (Plow *et al.*, 2000). Table 1.1 lists the receptors identified to date, along with their respective ligands and ligand-recognition sequences. Several α subunits have been shown to associate with only a single β subunit, α_{IIb} associates exclusively with β_3; while others, in particular α_v, have been shown to be capable of associating with more than one β subunit. Thus, integrins have been classified into subgroups according to their β subunit interactions (Table 1.1). Integrins are expressed on virtually every mammalian cell, with β_1 integrins having the most widely expressed profile whereas expression of the β_2 integrins is restricted to leukocytes.

Subunit		Previous Names	Ligands	Binding Site
β1	α1	VLA-1, CD41a/CD29	Collagens, laminin	
	α2	VLA-2, CD41b/CD29	Collagens, laminin	DGEA (in collagen only)
	α3	VLA-3, CD41c/CD29	Fibronectin, laminin, collagens	RGD (all ligands)
	α4	VLA-4, CD41d/CD29	Fibronectin, VCAM-1	EILDV (FN only)
	α5	VLA-5, CD41e/CD29	Fibronectin	RGD
	α6	VLA-6, CD41f/CD29	Laminin	
	α7		Laminin	
	α8		Fibronectin, tenascin	
	α9		Tenascin	
	α10		Collagens	
	α11		Collagens	
	αV	CD51/CD29	Vitronectin, fibronectin	RGD
β2	αL	LFA-1, CD11a/CD18	ICAM1-5	
	αM	Mac-1, CD11b/CD18	Fibrinogen, ICAM-1, FactorX, C3bi	
	αX	P150/95, CD11c/CD18	Fibrinogen, C3b1	GPRP
	αD		VCAM-1	
β3	αIIb	GPIIIb/IIa, CD41/CD61	Fibronectin, collagens, fibrinogen, vitronectin, von Willebrand factor, thrombospondin	RGD (all ligands) KQAGDV (Fb only)
	αV	CD51/CD61	Fibronectin, collagens, von Willebrand factor, fibrinogen, vitronectin, thrombospondin, tenascin, osteopontin	RGD
β4	α6		Laminin, basement membrane	
β5	αV		Vitronectin, fibronectin	RGD
β6	αV		Fibronectin, tenascin	RGD
β7	α4		Fibronectin, VCAM-1	EILDV (FN only)
	αE		E-cadherin	
β8	αV		Fibronectin	

Table 1.1 Integrin heterodimers and their ligands

Adapted from Hynes *et al.*, (1992) and Plow *et al.*, (2000). Abbreviations used: FN-fibronectin and Fb-fibrinogen.

Although the $\alpha\beta$ nomenclature is the most widely used, many of the integrins were described prior to the $\alpha\beta$ nomenclature being adopted and earlier names still exist in the literature. The platelet integrin $\alpha_{IIb}\beta_3$, is often referred to as GPIIb-IIIa (Philips *et al.*, 1991) and several β_1 integrins are sometimes referred to as VLA (very late after activation) antigens (Hemler, 1990). The leukocyte-specific β_2 integrins are routinely referred to by their earlier names; $\alpha_L\beta_2$ - lymphocyte function associated antigen-1 (LFA-1) and $\alpha_M\beta_2$ - macrophage-1 receptor (Mac-1) (Hemler, 1990) (see Table 1.1).

Integrins were initially described by their ability to bind to extracellular matrix proteins (collagens, laminin, vitronectin and fibronectin) and mediate cell-substratum adhesion. Other integrin-ligands such as fibrinogen and the integral membrane proteins of the immunoglobulin superfamily (ICAM-1/2 and VCAM-1) mediate cell-cell adhesion. Table 1.1 shows that individual integrins can often bind to more than one ligand and that individual ligands are often recognised by more than one integrin.

Within the ligand macromolecules, specific integrin recognition sites have been identified that are essential for ligand binding. Many members of the integrin family (including $\alpha_5\beta_1$, $\alpha_{IIb}\beta_3$ and most $\alpha_V\beta$ integrins) recognise the Arg-Gly-Asp (RGD) sequence within their ligands. These ligands include fibronectin, vitronectin, von Willebrand factor and many other large glycoproteins. The RGD motif is essential, as peptides containing this motif can effectively block integrin-ligand interaction (Fernandez *et al.*, 1998). However, it is the residues outside the RGD motif that provide specificity as well as high affinity for each ligand-integrin pair (Hynes and Yamada, 1982; Pierschbacher and Ruoslahti, 1984). Different ligand sequences are also used as integrin recognition sites, one such example is the Lys-Gln-Ala-Gly-Asp-Val (KQAGDV) sequence in fibrinogen recognised by the $\alpha_{IIb}\beta_3$ integrin (Hynes, 1992).

1.2 Integrin structure

All integrins are $\alpha\beta$-subunit heterodimers. The α subunits vary in size between 120 and 180kDa, while the β subunits are between 90 and 110kDa (Hynes, 1992). Both types of integrin subunit contain a relatively large N-terminal extracellular domain, a single hydrophobic membrane-spanning region and with most integrins, a short

cytoplasmic domain (less than 50 amino acids). The notable exception is β_4, as its cytoplasmic domain comprises over 1000 amino acids (Hynes, 1992).

The overall shape and dimensions of integrins have been determined by electron microscopy. Early studies by Carrell *et al.*, (1985) revealed that the $\alpha_{IIb}\beta_3$ integrin comprised of a globular oblong head and two rod-like tails extending into the lipid bilayer. Electron microscopic analysis of the $\alpha_5\beta_1$ integrin revealed similar results (Nermut *et* al., 1988). Most of the proposed integrin structures have relied on primary sequence analysis and structure predictions based on homology to proteins to which tertiary structure have already been determined. Figure 1.1 shows a schematic representation of the domain structure of an integrin dimer.

On the basis of primary sequence analysis, the N-terminal region of all α subunits contain a seven-fold repeat of a homologous region, encoding 4 β-sheets that come together in a structure known as a β-propeller (Springer, 1997). The final three or four of these repeats contain sequences that are similar to the EF-hand-like motif, that display divalent cation-binding properties. The α subunits can be divided into two groups, those that contain an inserted A-domain (found in the α_1, α_2, α_L, α_M and α_X subunits), and those with a post-translational proteolytic cleavage site. The A-domain comprises five parallel and one anti-parallel hydrophobic β-strands surrounded by seven hydrophilic α-helices forming a Rossmann fold (Fernandez *et al.*, 1998). The A-domains contain a metal ion-dependent adhesion site or MIDAS motif. Cleavage at the proteolytic site of the α_3, α_5, α_6, α_7, α_8, α_{IIb} and α_V subunits, found close to the transmembrane domain, yields an N-terminal heavy and C-terminal light chain (Fernandez *et al.*, 1998).

An A-domain-like region has also been predicted in the N-terminal half of the β subunit. The A-domain of the β subunits is preceded by a PSI (plexins, semaphorins and integrins) domain and is followed by a cysteine-rich region composed of four epidermal-growth-factor (EGF)-like repeats (Humphries, 2000). As with α subunits, the A-domain of the β subunits contains a MIDAS motif.

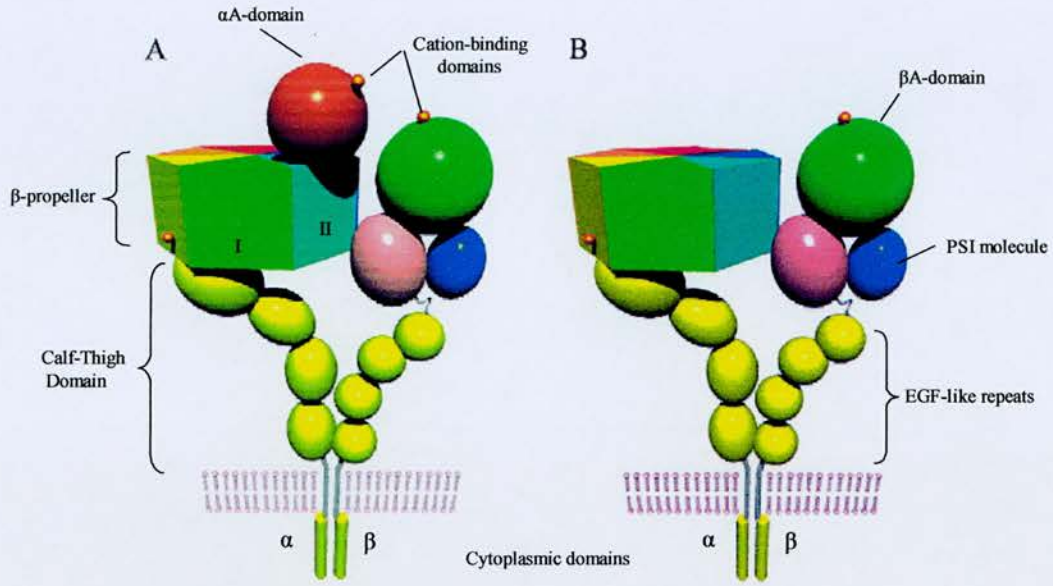

Figure 1.1 Schematic representation of integrin structure

Schematic shows the proposed domain structure of an integrin heterodimer with (A) or without (B) an αA-domain.
The schematic diagram has been modified from Humphries, (2000).

For α subunits containing A-domains, the ligand-binding pocket has been mapped to the A-domain (Fernandez *et al.*, 1998). For those integrins which lack an α subunit A-domain such as α_{IIb}, the ligand-binding pocket has been mapped to the upper face in the β-propeller motif (Bajt and Loftus, 1994; D'Souza *et* al., 1994). Ligand binding sites which have been identified in β subunits have been mapped to the presumed A-domain (Humphries, 2000). The presence of divalent cation binding sites (MIDAS) in the ligand binding sites of both integrin subunits reflects their importance in integrin structure. The regulatory role of metal ions on ligand binding is highlighted by the lack of ligand binding upon removal of cations by chelating agents (Fernandez *et al.*, 1998).

The short cytoplasmic domains link the integrin with the cytoskeleton either directly or via adaptor proteins. There are few direct interactions known between the α subunit tail and the components of the cytoplasm although α4 has been shown to have a high affinity for paxillin (Liu *et al.*, 1999). The large cytoplasmic domain of β_4 connects with the intermediate filament network and has a role in hemidesmosome formation. The other β subunit cytoplasmic domains have three conserved regions designated Cyto 1, 2 and 3 (Reszka *et al.*, 1992). Cyto 1 is necessary for binding focal adhesion components such as FAK, filamen and α-actinin (Lewis and Schwartz, 1995; Otey *et al.*, 1993 and Sharma *et al.*, 1995). Cyto 2 and 3 are NPXY motifs which are phosphorylation sites for protein kinases (Bodeau *et al.*, 2001; Mulrooney *et al.*, 2001). All three Cyto domains are required for adhesive function (Levy *et al.*, 2000). A number of proteins have been shown to bind to the NPXY motif, including the integrin cytoplasmic domain-associated protein 1 (ICAP-1) (Chang *et al.*, 1997), and more recently talin has been shown to bind directly with the β_3 tail via the NPXY motif (Garcia-Alvarez, 2003).

1.3 Integrin signalling

The interaction of cells with the ECM regulates many cellular processes including cell survival, proliferation, differentiation and migration. The binding of ligands to integrins results in the clustering of ligand-occupied integrins, which increases the avidity of the cell for its ligand. Integrin clustering also leads to the formation of specialised sites within the plasma membrane termed focal adhesions, where

integrins link the outside matrix with intracellular cytoskeletal complexes (Burridge *et al.*, 1988).

The assembly of many of the signalling components in focal adhesions depends on focal adhesion kinase (FAK) activity. FAK is recruited to focal adhesions through interactions with the adaptor proteins talin (Chen *et al.*, 1996), vinculin and paxillin (Brown *et al.*, 1996). It has been proposed that following recruitment to focal adhesions, FAK undergoes a conformational change which allows its N-terminal domain to interact with the β subunit tail and subsequent activation of FAK by autophosphorylation (Richardson and Parsons, 1996).

Despite lacking intrinsic tyrosine kinase activity, integrins have been shown to influence a number of classical signalling pathways by recruiting adaptor proteins and kinases through interactions with both the extracellular and cytoplasmic domains (Kumar, 1998; Giancotti and Ruoslahti, 1999).

1.3.1 Integrin and cytoskeletal organisation

Following the interaction of integrins with ECM proteins, a diverse number of structural and signalling proteins are targeted to focal adhesions. Structural actin binding proteins that localise with integrins at focal adhesions include α-actinin, talin, tensin, paxillin, vinculin and tensin (Dedhar and Hannigan, 1996). Signalling proteins that colocalise with focal adhesions include the following protein kinases: focal adhesion kinase (FAK), Src and integrin linked kinase (ILK) (Yamada and Miyamoto, 1995; Dedhar and Hannigan, 1996). Rho family members have also been shown to be activated by integrin ligation. Hotchin and Hall (1995) demonstrated that the interaction of integrins with the ECM is not sufficient to induce integrin clustering, but requires the activity of the GTP-binding protein Rho.

Cell migration is a key aspect in many normal and abnormal cellular processes, including wound healing and tumor metastasis. The driving force for cell motility is provided by dynamic actin reorganisation. Integrins and receptors for soluble mitogens such as growth factors can regulate cell spreading and migration through activation of the Rho-family proteins (Nobes and Hall, 1999). Each of the Rho-family proteins has control over the actin cytoskeleton. Rho regulates the formation

of contractile actin-myosin filaments to form stress fibres, generating tension within the cell (Ridley and Hall, 1992), while Rac and Cdc42 regulate lamellipodia and filopodia formation respectively, which are protrusive structures found at the leading edge of the cell (Ridley and Hall, 1992; Nobes and Hall, 1995). The activation of the Ras-ERK1/2 signalling pathway by integrin ligation (see below) has also been shown to influence cell motility. Signalling by ERK1/2 results in the phosphorylation of myosin light chain kinase (MLCK), which in turn phosphorylates myosin light chains (MLC) resulting in a fully functional actin-myosin motor unit which serves to produce the contractile forces within the cell required for cell motility (Klemke *et al.*, 1997).

1.3.2 Integrins and cell proliferation

The biological effects attributed to integrin-ligand interaction are a consequence of recruited signalling molecules. One such molecule, FAK, has been linked to a number of intracellular signalling pathways described in Figure 1.2. FAK localises to the plasma membrane at sites of integrin-mediated adhesion. Following integrin clustering, autophosphorylation of FAK at Tyr^{397} results in the formation of a Src homology 2 (SH2) binding domain (Schaller *et al.*, 1994). The recruitment of Src family kinases to the focal adhesion and subsequent tyrosine phosphorylation of FAK leads to the phosphorylation of a number of focal adhesion components including paxillin, tensin and $p130^{CAS}$, a docking protein that recruits Crk and Nck (Vuori *et al.*, 1996). These events lead to the recruitment of adaptor proteins CAS and Crk and to the subsequent activation of the JNK pathway (Schlaepfer *et al.*, 1994). Autophosphorylated FAK can also combine with and activate PI 3-kinase (Chen *et al.*, 1996).

Src can also phosphorylate FAK on Tyr^{925}, creating a binding site for the Grb2-mSOS complex (Schlaepfer *et al.*, 1994) resulting in the activation of the Ras signalling pathway (Giancotti and Ruoslathi, 1999). The activation of the Ras-ERK1/2 signalling pathway by integrin ligation has been shown to require an intact cytoskeleton suggesting that integrin-dependent cytoskeletal complexes, such as focal adhesions, are involved in the activation of the MAP kinase pathway (Kumar, 1998). ERK1/2 MAPK activation by integrins can also occur independently of FAK.

The integrin subunits α_V, α_5, and α_1 can associate laterally with caveolin which in turn binds Fyn (Wary *et al.*, 1996). Shc can bind to the SH3 domain of Fyn resulting in its phosphorylation. Once phosphorylated, Shc can recruit the Grb/SOS complex leading to Ras activation (Wary *et al.*, 1996).

Normal adherent cells require anchorage to ECM to proliferate. There are several mechanisms by which integrin engagement may influence the cell cycle. Integrin–mediated cell attachment is necessary for optimal activation of growth factor receptors (Giancotti and Ruoslahti, 1999). Several β_1 integrins, including $\alpha_5\beta_1$, have been shown to associate with the EGF receptor (Miyamoto *et al.*, 1996).

Integrin-growth factor complexes appear to be required for optimal mitogenic signal pathway activation (Kumar *et al.*, 1998).

Signals from Shc-linked integrins can co-operate in a synergistic manner with growth factor receptors to promote cell cycle progression. Cell adhesion is specifically required for the induction of cyclin D1 transcription and for the activation of the cyclin E-cdk2 complex (Fang *et al.*, 1996; Giancotti and Ruoslahti, 1999). Integrin signalling may be directly needed for cyclin D1 transcription, as the cyclin D1 promoter is co-ordinately regulated by ERK1/2 and JNK (Albanese *et al.*, 1995). The effects of cell adhesion on cyclin E-cdk2 complex appears to be indirect and mediated by downregulation of the cdk inhibitors p21 and p27 (Zhu *et al.*, 1996). The anchorage-dependent regulation of cyclin-D1 and the cdk inhibitors enables cells to progress through the G1 phase of the cell cycle in response to growth factors.

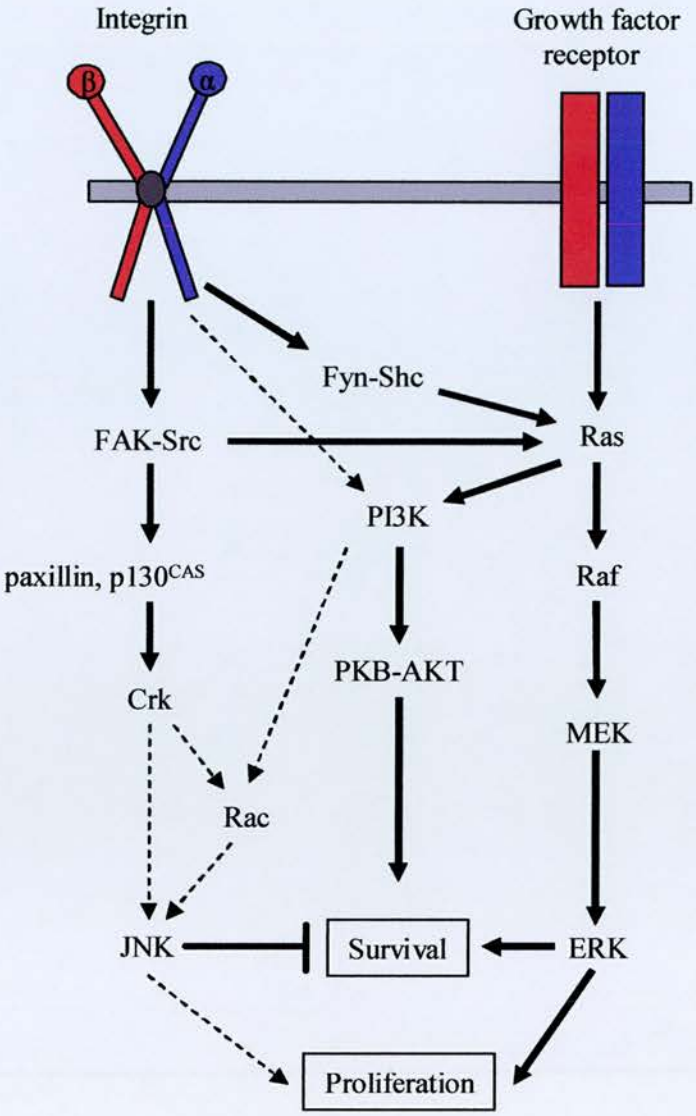

Figure 1.2 Convergence of integrin and growth factor pathways

The major integrin and growth factor pathways involved in cell proliferation and survival. Diagram shows signalling pathways which have been well established (bold arrows) or presumed (dashed arrows) to be co-ordinately regulated by integrins and growth factor receptors (Giancotti and Ruoslahti, 1999; Kumar, 1998).

1.3.3 Integrins and cell survival

One of the most important functions of the integrin signalling pathways is to regulate anchorage dependence. Epithelial and endothelial cells that detach from the extracellular matrix undergo apoptosis, this has been termed anoikis (Frisch and Francis, 1994; Meredith *et al.*, 1993). Anoikis is a mechanism to ensure that when cells are detached from their natural environment, they are eliminated prior to their colonisation of another inappropriate environment.

FAK is involved in conveying survival signals from the ECM (see Figure 1.2). Activated FAK can activate the phosphatidyl-inositide-3 kinase (PI-3 kinase) pathway (Chen *et al.*, 1996). Activation of the PI 3-kinase/Akt pathway results in Akt promoting survival, by phosphorylation and subsequent inactivation of two pro-apoptotic proteins Bad and caspase-9 (Khwaja *et al.*, 1997). Since the inhibition of ERK1/2 or activation of JNK cause apoptosis (Xia *et al.*, 1995), integrins that combine with Shc promote cell survival by increasing the activity of ERK1/2 thus increasing the ratio of ERK1/2 to JNK signalling. The β_1 integrins and fibronectin have been implicated as playing a role in suppression of apoptosis and cell survival. Fibronectin adhesion through $\alpha_5\beta_1$ prevented CHO cells from undergoing serum-starved induced apoptosis by increasing Bcl-2 expression (Zhang *et al.*, 1995). However, CHO cells engineered to express $\alpha_V\beta_1$ as their fibronectin receptor did not survive in serum-free conditions (Zhang *et al.*, 1995) suggesting that cells may differ in their integrin specificity to activate survival signals. Therefore, attachment to an inappropriate surface through the wrong integrin would result in cell apoptosis.

1.3.4 Integrins and cellular transformation

Normal cells require both adherence to matrix proteins and stimulation by serum or growth factors in order to proliferate. The convergence of the signalling pathways by integrins and growth factor receptors determines cell cycle progression. Oncogenes are components of the normal growth regulatory pathways that are constitutively activated by mutation or overexpression, leading to irreversible activation of these pathways.

Constitutive activation of a step succeeding convergence of integrin and growth factor signalling pathways would elicit both anchorage-and serum-independent proliferation to the transformed cells (see Figure 1.3) (Kumar *et al.*, 1998; Schwartz, 1997). The Ras oncogene results in both anchorage-and serum-independent proliferation (Schwartz, 1997). Activation of the integrin signalling pathway, prior to convergence would give rise to anchorage-independent but serum-dependent growth. Rho family oncogenes are capable of inducing this phenotype (Schwartz *et al.*, 1996). Conversely, activation of the growth factor signalling pathway, before convergence, should induce accelerated proliferation without causing anchorage independence.

Tumour cell invasion and metastasis relies on constitutive activation of the integrin-dependent signalling pathways, resulting in inhibition of anoikis (Schwartz *et al.*, 1997).

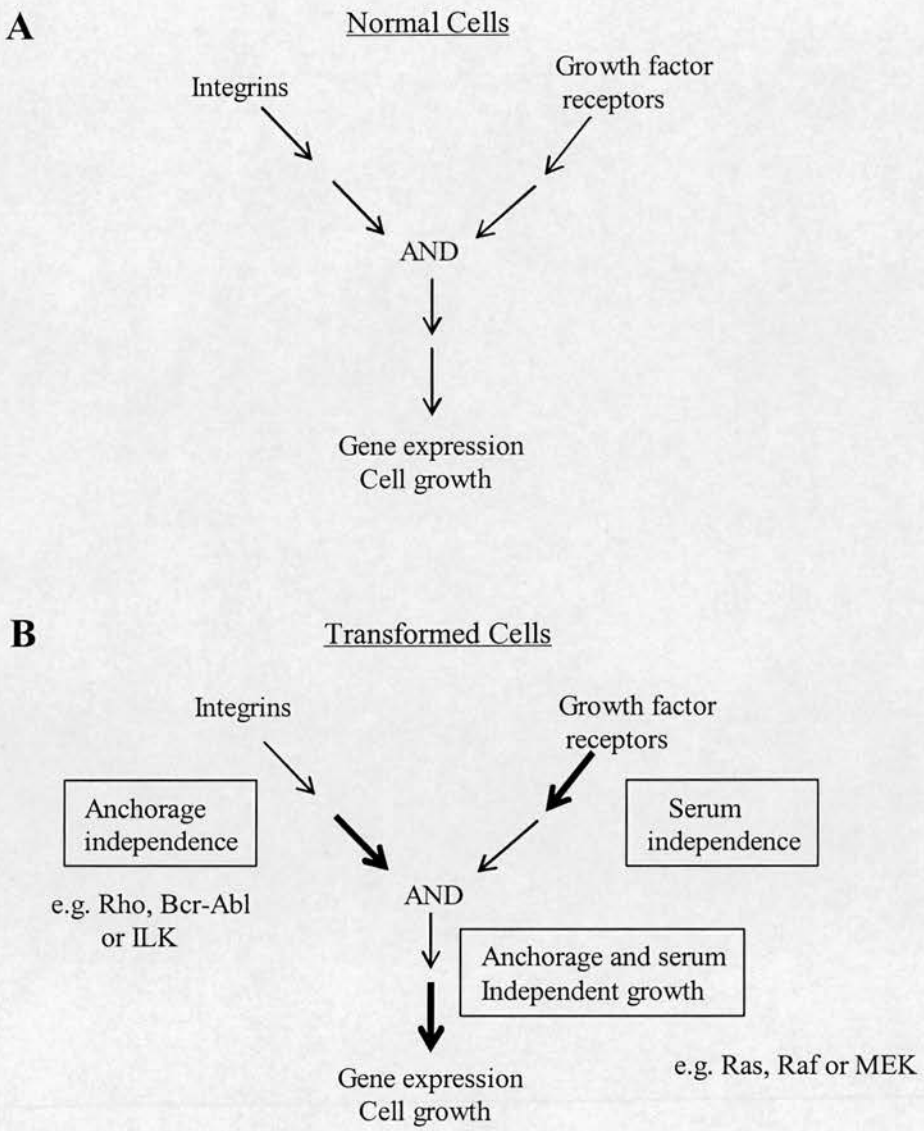

Figure 1.3 Oncogenes and cellular transformation

(A) General proposal for the convergence of integrin-and growth factor-mediated pathways in normal cells. Both pathways are required for normal activation of gene expression and cell proliferation.
(B) Constitutive activation indicated by boldface arrows. Constitutive activation of the integrin pathway, prior to convergence, should lead to anchorage-independent growth. Anchorage-independent growth can be mediated by Rho, Bcr-Abl and ILK. Constitutive activation of the growth factor pathway, prior to convergence, should lead to serum-independent growth. Activation of a step subsequent to convergence, by oncogenes such as Ras, Raf and MEK, induces anchorage-and serum-independent growth (Schwartz, 1997).

1.4 Integrin dysfunction and disease.

The *in vivo* function of integrins has been studied by the generation of monoclonal blocking-antibodies and by studies of knock-out mice lacking a specific integrin molecule. The largest subfamily of integrins is the β_1 subfamily, which comprises of twelve heterodimers that share the β_1 subunit. Knocking-out the β_1 subunit gene results in very early embryonic lethality (Fässler and Meyer, 1995; Stephens *et al.*, 1995), due to the critical roles played by specific β_1 integrins at early stages in development. Figure 1.4 shows the critical roles of the β_1 subfamily. The interaction between $\alpha_5\beta_1$ and fibronectin is fundamental for invertebrate development, since lack of $\alpha_5\beta_1$ binding to fibronectin results in embryonic lethality (Yang *et al.*, 1993). Knock-out of the β_2 subunit gene results in mice exhibiting most of the features of the leukocyte adhesion deficiency seen in humans (see below) (Schmits *et al.*, 1996). β_3 null mice exhibit some embryonic loss due to placental defects and show reduced survival after birth as a result of haemorrhaging (Hodivala-Dilke *et al.*, 1999).

Studies of patients who have inherited rare and specific genetic defects of integrin expression have provided an opportunity to observe the *in vivo* effect of the loss of proper control of integrin expression or signalling.

Leukocyte adhesion deficiency-1 (LAD-1) disorder results from a lack of normal β_2 expression. Mutations within the β_2 subunit gene give rise to an altered precursor protein which fails to bind to the α subunit precursor and prevents $\alpha\beta$ heterodimer formation (Hogg and Bates, 2000). As a result, there is a lack of LFA-1, Mac-1 p95 and $\alpha_D\beta_2$ integrin expression (Anderson and Springer, 1987). The disease characteristics include re-occurring soft tissue infections, impaired wound healing and severe gingivitis, primarily as a result of the absence of neutrophil infiltration (Hogg and Bates, 2000).

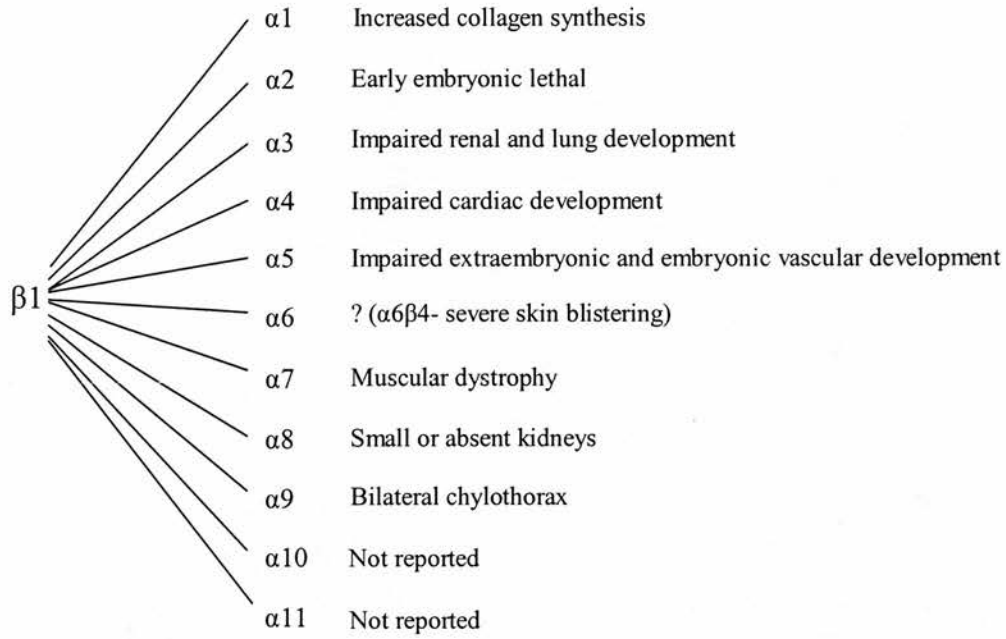

Figure 1.4 Critical roles of the β_1 integrin subfamily

Diagram shows the large group of heterodimers that share the β_1 subunit. Also described are the phenotypes produced by a homozygous null mutation of the β_1 subunit gene, highlighting the critical roles played by these subunits in development (Sheppard, 2000).

Glanzmann thrombasthenia (GT) is a bleeding disorder resulting from mutations in the $\alpha_{IIb}\beta_3$ platelet integrin. Mutations have been observed in genes encoding both the α-subunit α_{IIb}, and the β-subunit β_3 (Newman *et al.*, 1991), resulting in deficient expression or faulty function of the $\alpha_{IIb}\beta_3$ integrin. The absence of $\alpha_{IIb}\beta_3$-mediated fibrinogen crosslinking, essential for platelet aggregation and clot formation, results in excessive bleeding of the gums, cuts, wounds and other abnormal bleeding (Hogg and Bates, 2000). The reverse effect is seen when excessive aggregation of platelets occurs, resulting in embolism and blockage of small blood vessels (Clemetson and Clemetson, 1998).

A patient has been described with defective function of both the β_1 and β_2 integrins on leukocytes (LAD-1) and $\alpha_{IIb}\beta_3$ (GT) integrin (Kuijpers *et al.*, 1997). While expression of the integrins was not affected, they were not able to become activated and as a result leukocyte adhesion and platelet aggregation were impaired (Etzioni, 1999). This resulted from defective inside-out signalling (see below), leading to abnormal integrin clustering and deficiency of high avidity ligand binding (McDowall *et al.*, 2003). This is the first description of a dysfunction affecting three classes of integrin (β_1, β_2 and β_3) (McDowall *et al.*, 2003).

As discussed in section 1.3.4, malignant transformation relies on constitutive activation of the integrin-dependent signalling pathways. Oncogene expression associated with integrin signalling has been observed in tumour cells, resulting in anchorage-independent growth. Studies of integrin expression profiles have suggested that various integrin subunits may also contribute positively or negatively to the transformed phenotype (Ruoslahti, 1992). High levels of $\alpha_5\beta_1$ expression seem to correlate with low levels of transformation (Plantefaber and Hynes, 1989). Over expression of $\alpha_5\beta_1$ in CHO cells increased fibronectin matrix assembly, inhibiting tumour growth when injected into nude mice (Giancotti and Ruoslahti, 1990). In contrast, increased expression of $\alpha_V\beta_3$ is positively correlated with increased malignancy in melanomas (Chan *et al.*, 1991). In human melanoma patients, the increased expression of $\alpha_4\beta_1$ together with decreased expression of $\alpha_6\beta_1$ correlates significantly with the occurrence of metastases (Juliano and Varner, 1993).

Analysis of knock-out mice and human disease pathology has provided insight into the mechanisms by which integrins can affect cell behaviour. The precise control of cell migration and adhesion is key to many biological processes and central to this control is the interaction between integrins and their ligands. Levels of integrin activation and expression must be tightly controlled in order to prevent diseases arising from integrin dysfunction. The use of mAbs against integrins in vivo has demonstrated that several integrins are valid therapeutic targets for the treatment of inflammatory and cardiovascular responses. One such example is ReoPro (Centocor, Leiden, The Netherlands), a chimeric antibody against the platelet integrin αIIbβ3, which is a potent anti-thrombotic agent used in patients with cardiovascular complications following coronary angioplasty (Newham and Humphries, 1996).

1.5 Control of integrin affinity state

The ligand–binding activity of integrins is a dynamic and highly regulated process. Inactivated integrins usually have a low-affinity for their ligand however, upon activation integrins can participate in high-affinity ligand binding. There are two non-exclusive mechanisms which can transiently alter the integrin activation state without changing expression levels; integrin affinity modulation is a conformational change within the integrin subunits determining integrin binding-state and integrin avidity modulation is mediated by receptor clustering. Figure 1.5 shows a schematic representation of integrin affinity and avidity modulation. Both of these mechanisms are regulated by intracellular signalling proteins acting upon the cytoplasmic domains of the integrin in a process termed 'inside-out signalling' (Bazzoni and Hemler, 1998).

1.5.1 Integrin avidity modulation

The activation of β_1 and β_2 integrins on leukocytes is characteristic of integrin avidity modulation, as no physiological activators have ever been shown to induce integrin affinity modulation (Brown and Hogg, 1996). Studies have shown that leukocyte β_2 integrins, in particular $\alpha_L\beta_2$, (LFA-1) are maintained in a dispersed state due to constraints imposed by the cytoskeleton (Kucik *et al.*, 1996). Treatment of these cells with phorbol ester released the cytoplasmic restraints and stimulated LFA-1

mediated adhesion by rapid integrin clustering (Stewart and Hogg, 1996). In the physiological environment, leukocyte activation is induced by various inflammatory mediators including tumour necrosis factor (TNF) and platelet activating factor which are produced at the endothelium or at sites of inflammation (Hynes *et al.*, 1992). The actin cytoskeleton is critical for integrin clustering, as treatment of cells with cytochalasin D (which inhibits actin polymerisation) can inhibit integrin clustering and cell adhesion (van Kooyk and Figdor, 2000).

Thus, the proposed model for leukocyte adhesion follows a cascade of events. First, selectin interaction slows the flow-rate of migrating leukocytes over the endothelium at sites of inflammation allowing the cell time to sense inflammatory mediators. Following cell activation by the inflammatory mediators, rapid integrin clustering occurs, increasing leukocyte adhesion to ligands such as ICAM-1, ICAM-2, VCAM-1 and fibrinogen. This integrin-mediated adhesion is essential for transendothelial migration to sites of infection (Brown and Hogg, 1996), and the requirement of this step is highlighted by diseases such as LAD-1 arising from genetic defects in β_2 expression.

1.5.2 Integrin affinity modulation

Integrins in the β_1, β_2, β_3 and β_7 subfamilies have been shown to modulate their integrin-binding affinity, in response to inside-out signalling (Hughes and Pfaff, 1998). Platelet aggregation is a physiological process dependent on integrin-affinity modulation. The function of the $\alpha_{IIb}\beta_3$ integrin in platelet aggregation is the best-described example of integrin-affinity modulation.

The $\alpha_{IIb}\beta_3$ integrin on resting platelets does not bind to any of its soluble ligands, therefore preventing thrombosis. Following platelet activation by specific agonists such as thrombin and ADP, which signal through heterotrimeric G-proteins or by activation of non-receptor tyrosine kinases such as Src (Payrastre *et al.*, 2000), a conformational change in $\alpha_{IIb}\beta_3$ is induced, leading to an increase in affinity for soluble fibrinogen (Shattil *et al.*, 1985). The subsequent clustering of the $\alpha_{IIb}\beta_3$ integrin then increases the cell avidity for fibrinogen and this results in irreversible binding of ligand to $\alpha_{IIb}\beta_3$ (Hato *et al.*, 1998).

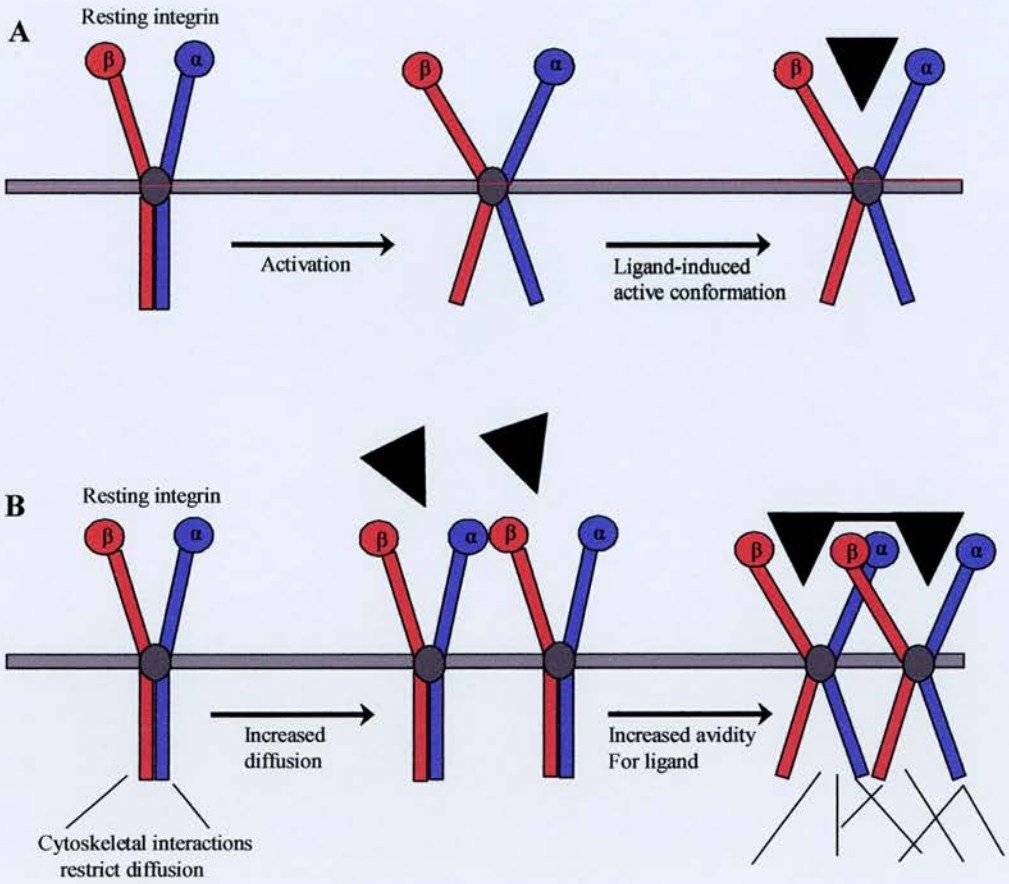

Figure 1.5 Models of integrin activation and ligand binding

(A) In integrin affinity modulation, a conformational change occurs and the integrin acquires elevated affinity for ligand. Following ligand binding, the active conformation is stabilised and further activation epitopes are exposed.
(B) Integrin avidity modulation occurs when integrin diffusion is elevated. Integrins cluster at adhesive sites to increase avidity for ligand. Conformational changes only occur following ligand binding.

1.5.3 Regulation of ligand binding by inside-out signalling

Experimental approaches using recombinant integrins and the generation of ligand-mimetic antibodies, which mimic ligand binding to the activated integrin and anti-CLIBS (cation-and-ligand-influenced binding site) antibodies, have enabled further analyses of the conformational changes which occur within integrins in response to inside-out signalling. The PAC-1 ligand-mimetic antibody mimics fibrinogen's ability to bind to the activated $\alpha_{IIb}\beta_3$ integrin (Shattil, *et al.*, 1985). PAC-1 contains an RGD sequence within its heavy chain which enables affinity-specific recognition of $\alpha_{IIb}\beta_3$ (Kunicki *et al.*, 1996). The binding of PAC-1 can therefore be used as a measure for activated $\alpha_{IIb}\beta_3$.

The cytoplasmic domains of integrins play a central role in affinity modulation. Chinese hamster ovary (CHO) cells do not naturally express the $\alpha_{IIb}\beta_3$ integrin. CHO cells expressing $\alpha_{IIb}\beta_3$ were unable to bind to soluble fibrinogen or PAC-1, even in the presence of platelet agonists (O'Toole *et al.*, 1990). However, anti-CLIBS antibodies were capable of inducing PAC-1 binding which indicated that this integrin was capable of undergoing a conformational change (O'Toole *et al.*, 1990). CHO cells naturally express the $\alpha 5\beta 1$ (fibronectin receptor), which is maintained in a high-affinity state (Faull and Ginsberg, 1996). CHO cells expressing $\alpha_{IIb}\beta_3$ chimeras containing the cytoplasmic domains of $\alpha_5\beta_1$ were capable of binding soluble fibrinogen and PAC-1 (O'Toole *et al.*, 1991; O'Toole *et al.*, 1994). This indicates that the cytoplasmic domains of $\alpha_5\beta_1$ are sufficient to induce a conformational change of the chimeric integrin.

Specific sequences within the integrin cytoplasmic domains control the integrin affinity state and both integrin subunits are required to regulate integrin affinity state. Integrin α and β subunit cytoplasmic domains share a similar membrane-proximal organisation (Hughes *et al.*, 1996). The conserved sequences for the α and β subunits are -GFFKR and LLv-iHDR (highly conserved residues are in uppercase, less conserved residues are in lower case and dashes represent nonconserved residues) respectively (Fernandez *et al.*, 1998; Hughes *et al.*, 1996). The associations between the conserved sequences of the α and β subunits has been investigated using mutagenesis of the $\alpha_{IIb}\beta_3$ integrin. Deletion of the either of the conserved sequences

of the α and β subunits activates the integrin, locking it in a high affinity state (Hughes *et al.*, 1996). This region, termed the 'hinge-domain', results from the formation of a salt-bridge between the two conserved regions of the α and β subunits and may serve as a physical 'on-off' switch in determining integrin affinity state (Ginsberg *et al.*, 2001; Hughes *et al.*, 1996). Recent nuclear magnetic resonance (NMR) studies by Vinogradova *et al.*, (2002), who looked at the interaction of the cytoplasmic domains following mutations that disrupt the salt bridge, support the suggestion of a spatial separation of the integrin cytoplasmic domains upon integrin activation.

Another conserved sequence has been identified in many β subunits, the NPXY motif. Point mutations within this motif abolished PAC-1 binding from the $\alpha_{IIb}\beta_3$/ $\alpha_5\beta_1$ chimeric integrin (O'Toole *et al.*, 1995). Mutation of this sequence in the β_1 integrin was also shown to be important for integrin activation (Mastrangelo *et al.*, 1999). Additionally, a similar motif (NXXY) has also been identified on the cytoplasmic domains of the β_1, β_2, and β_3 subunits (Fernandez *et al.*, 1998). These sequences regulate integrin affinity states by interacting with inside-out signalling pathways and with cytoskeletal components.

A number of intracellular proteins have been reported to interact with integrin cytoplasmic domains. These molecules have been implicated in both outside-in and inside-out signalling. Several molecules including the calcium-and integrin-binding protein (CIB), β_3-endonexin, cytohesin-1 and talin, have been shown to bind to the β subunit cytoplasmic tails resulting in integrin activation (Travis *et al.*, 2003).

Talin has been shown to bind to the β subunit cytoplasmic tails through its N-terminal head domain, leading to integrin activation (Calderwood *et al.*, 1999). Crystal structure analysis of talin-integrin interactions has indicated that the phosphotyrosine binding (PTB)-like domain of talin interacts directly with the β_3 tail through the region containing the NPXY motif (Garicia-Alvarez, 2003). It was hypothesised that talin binding to the β_3 tail could perturb the $\alpha\beta$-interface, resulting in integrin activation (Calderwood *et al.*, 1999; Garcia-Alvarez, 2003). This was confirmed by Vinogradova *et al.*, (2002) who, using NMR studies, demonstrated that talin binding could activate $\alpha_{IIb}\beta_3$ by separating the $\alpha\beta$ complex. Other proteins that

are associated with integrin cytoplasmic tails may also act like talin by directly binding to and perturbing the $\alpha\beta$ subunit interface.

A number of intracellular signalling pathways have been implicated in modulating integrin affinity, however they have yet to be fully defined. Studies on platelets revealed that agonists, such as thrombin, activate the $\alpha_{IIb}\beta_3$ integrin via heterotrimeric G-protein coupled receptor signalling and tyrosine phosphorylation (Shattil and Brass, 1987). Other studies have indicated that the Ras family of small GTP-binding proteins, and their effectors, play a crucial role in integrin affinity modulation (Keely *et al.*, 1998; Hughes *et al.*, 1997).

1.5.4 Current model of inside-out integrin signalling

Structural analysis of the $\alpha_V\beta_3$ full-length integrin has indicated that in a low-affinity state, the extracellular domain of the integrin is in a bent conformation, with the N-terminal ligand-binding pocket close to the membrane (Xiong *et al.*, 2001). Electron microscope analyses of the $\alpha_5\beta_1$ integrin suggest that upon activation, there is a 'flick-knife' opening of the integrin, with the extracellular domain straightening out, exposing the ligand binding pocket (see Figure 1.6) (Takagi *et al.*, 2003). This is accompanied by subtle changes in the ligand-binding pocket of the integrin to create a high-affinity ligand-binding site (Takagi *et al.*, 2002). Currently integrin cytoplasmic tail separation, following intracellular signalling or intracellular protein interaction, is at the centre of models of inside-out signalling.

Inside-out signalling is crucial to normal integrin function, allowing integrins to bind to ligand only when appropriate signals and stimuli are present.

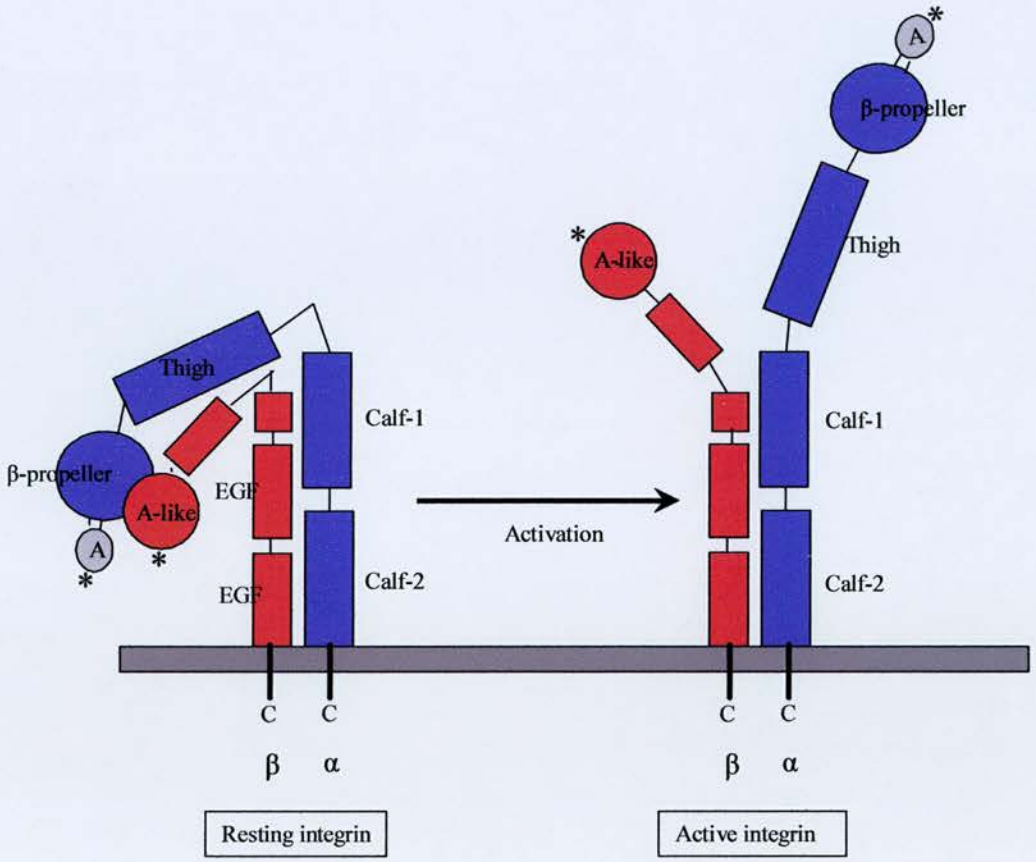

Figure 1.6 'Flick-knife' model of integrin activation

Diagrammatic representation of the 'flick-knife' model of integrin activation.
The α-subunit is shown in red and the β-subunit is shown in blue. Asterisks mark the position of ligand binding sites either at a β-propeller-A-like domain interface in integrins lacking αA-domains, or at the top of the A-domain in integrins containing αA-domains (αA-domains represented by light grey circle). Ligand-binding domains are kept hidden, close to membrane surface. Following activation, the integrin subunits bend at the 'knee' (between α-subunit thigh and calf regions). The straighter conformation exposes the ligand-binding domains. Adapted from Takagi *et al.*, (2002).

Ras and Ras signalling

Research into the Ras proteins began almost forty years ago with the discovery of the Harvey and Kirsten strains of mouse sarcoma retrovirus (Malumbres and Barbacid, 2002). These were isolated from mouse tumours induced by the murine leukaemia virus that were passaged through rats (Harvey *et al.*, 1964; Kirsten and Mayer, 1969). The acronym Ras was derived from the words rat sarcoma, from which these genes were initially identified. A protein of 21kDa was found to be encoded by the Harvey and Kirsten strains of mouse sarcoma retrovirus, in cells transformed by these two viruses (Shih *et al.*, 1979). The p21 viral oncogenes from Ha-MSV and Ki-MSV were shown to originate from a divergent family of normal rat cellular proteins called Harvey-Ras (Ha-/H-Ras) and Kirsten-Ras (Ki-/K-Ras) (Ellis *et al.*, 1981; Langbeheim *et al.*, 1980; Shih *et al.*, 1979).

1.6 Ras genes

The importance of the *Ras* genes has been highlighted following the identification of human genetic mutations, found in 30% of all human tumours, which were homologous to the viral *H-ras* and *K-ras* (Der *et al.*, 1982; Santos *et al.*, 1982; Parada *et al.*, 1982). In 1983, Shimizu *et al.*, (1983) and Hall *et al.*, (1983), both identified a third member of the Ras family, N-Ras (neuroblastoma). Molecular cloning of the normal human *ras* proto-oncogenes and their oncogenic alleles revealed that functional differences could be mapped to a single point mutation (Reddy *et al.*, 1982; Tabin *et al.*, 1982). The normal cellular *H-ras* gene encodes a glycine residue at position 12 (gly12), while the activated form of the *H-ras* gene isolated from a bladder sarcoma cell line contains a gly12 to val12 mutation (Capon *et al.*, 1983; Reddy *et al.*, 1982).

The *ras* genes have been isolated from organisms as diverse as *Saccharomyces cerevisae* (DeFeo-Jones *et al.*, 1983), Drosophila melangogaster (Neuman-Silberberg *et* al., 1984) and humans. There is up to 65% amino acid sequence homology between the *ras* genes from different species compared with the human *ras* proto-oncogene (Lowe *et al.*, 1987). The high degree of sequence conservation between

species suggests that the *ras* genes serve important roles in fundamental cellular processes.

The H-, K- and N-ras genes contain five exons, the first of which is noncoding (Lowy and Willumsen, 1993). The introns differ in their sequence and size, with the human genomic DNA sequences spanning 3kb (*H-ras*), 7kb (*N-ras*) and 35kb for *K-ras*. *K-ras* is alternatively spliced into two isoforms: *K-ras*4A and *K-ras*4B (Barbacid, 1987). The main products of the *ras* genes are proteins of about 21kDa, hence the name p21Ras. While the *ras* genes are ubiquitously expressed, the expression levels vary in different tissue types: *H-ras* is highly expressed in the skin and in the skeletal muscles; *K-ras* is mostly expressed in the colon and thymus, and *N-ras* in male germinal tissue and thymus (Lowy and Willumsen, 1993).

Of the three *ras* genes only *K-ras* appears to be essential and sufficient for development, as mice with a double knock-out of *H-ras* and *N-ras* are viable (Esteban *et al.*, 2001; Koera *et al.*, 1997).

1.6.1 The R (Related)-*ras* gene

The *R-ras* gene was first identified in a screen to identify genomic sequences related to the *ras* gene family. Using low-stringency hybridisation to a v-H-ras gene probe (Lowe *et al.*, 1987), R-Ras was isolated due to its 55% sequence homology in the region of overlap with *H-ras*. In contrast to the family of *ras* genes, *R-ras* had a completely different exon-intron structure which suggests evolutionary distance between the genes (Lowe *et al.*, 1987). The *R-ras* gene contains six coding exons, and the main product is a protein of about 23kDa (Lowe *et al.*, 1987).

1.6.2 The Ras superfamily

The Ras superfamily now includes over 150 small GTPases. It comprises six subfamilies, the Ras, Rho, Ran, Rab, Arf and Kir/Rem/Rad/Gem subfamilies (Ehrhardt *et al.*, 2002). The Rho family members are associated with the cell cytoskeleton and gene expression (Ridley and Hall, 1992). The Rab family are associated with secretory and endocytic pathways (Schimmoller *et al.*, 1998) The Arf family are associated with vesicular trafficking pathways and phospholipase D activation (Brown *et al.*, 1993). The cellular functions of the Kir/Rem/Rad/Gem

subfamily remains to be fully established (Finlin *et al.*, 2000) however, Rem and Rad have been implicated in the regulation of Ca^{2+} channels (Finlin *et al.*, 2003).

The Ras subfamily contains 13 members: H-Ras, N-Ras, K-Ras4A, K-Ras4B, R-Ras proteins (R-Ras, R-Ras2/Tc21 and R-Ras3/M-Ras), Ral proteins (A and B), the Raps (1A, 1B, 2A and 2B), Rheb, Rin and Rit.

1.7 Structural comparison between Ras proteins and R-Ras

The amino terminal 84 residues of the three main Ras proteins are identical. The importance of this sequence homology is highlighted by the fact that this region includes the effector domain (residues 25 to 45), as well as the switch I (residues 30 to 38) and switch II (residues 59 to 76) domains. The next 80 residues of the Ras proteins share 90% homology however, the remaining 25 residues of the carboxyl-terminal region are highly variable. The carboxyl-terminal region has been termed the 'hypervariable' region (HVR) and it comprises two distinct areas, the HVR linker domain (H-Ras 166-179) and the carboxyl terminal (CAAX) targeting domain (H-Ras 180-189) (see Figure 1.7) (Prior *et al.*, 2001)

The main difference between the R-Ras protein and the N-, K- and H-Ras proteins is the presence of an additional N-terminal 26 amino acids. The R-Ras protein contains several sequences, which are conserved between the Ras proteins; these include four blocks of amino acids, from R-Ras residues 32 to 46, 82 to 90, 102 to 110 and 138 to 146 (Lowe *et al.*, 1987). These residues are conserved throughout the GTP-binding protein superfamily (Halliday *et al.*, 1984; Lebermann and Egner, 1984). In common with the Ras proteins, R-Ras also contains a hypervariable linker domain (residues 193 to 206) and a C-terminal CAAX box (residues 215 to 219). See Figure 1.8 for H-Ras and R-Ras amino acid sequence alignment.

1.7.1 Ras proteins function as GTP-binding proteins

The *ras* and *R-ras* genes code for proteins that bind guanine nucleotides and have an intrinsic GTPase activity (McGrath *et al.*, 1984; Gibbs *et al.*, 1984; Lowe *et al.*, 1987). The Ras and R-Ras proteins function as molecular switches, when bound to guanosine triphosphate (GTP) they are active and following hydrolysis of GTP to

GDP they are inactive (Field *et al.*, 1987; Sweet *et al.*, 1984). The mechanisms of GDP to GTP exchange will be described later.

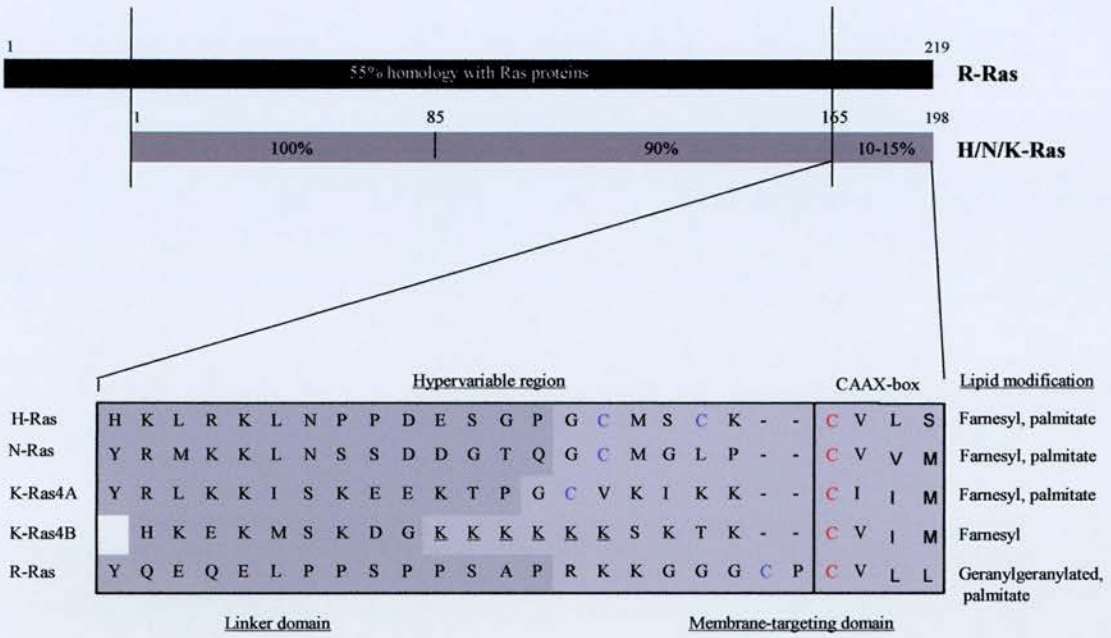

Figure 1.7 The Ras proteins and R-Ras hypervariable regions

Sequence alignment of the four Ras isoforms and R-Ras, focusing on the hypervariable regions. The hypervariable domain comprises the linker domain (dark grey) and membrane-targeting domain (light grey). Within the membrane-targeting domain the C-terminal CAAX box, common to all the proteins, contains a conserved cysteine residue (red). Second signalling sequences include: cysteine palmitoylation sites (shown in blue) in H-Ras, N-Ras, K-Ras4A and R-Ras and a polybasic domain in K-Ras4B (underlined residues). Modified from Prior and Hancock (2001).

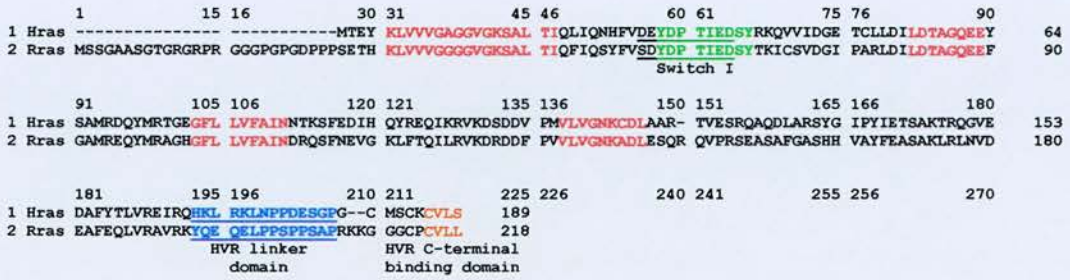

Figure 1.8 H-Ras and R-Ras amino acid sequence alignment

Sequence alignment of H-Ras and R-Ras with homologous amino acids, shown to be conserved throughout GTP-binding proteins, shown in red. Regions in green denote areas of high sequence homology within the effector region. Green residues overlap with Switch I region (underlined). The blue residues highlight the hypervariable–linker domain, which is the area of most sequence divergence between the Ras proteins. The orange residues show the conserved CAAX box, found in all Ras proteins in the C-terminal binding region of the hypervariable domain. HVR domains labelled.

1.8 Post-translational modification and membrane-targeting of Ras and R-Ras proteins

The Ras proteins (H, N and K-Ras) exhibit significant biological differences despite their high degree of sequence homology. The main sequence divergence is confined to 23-amino acids of the carboxy-terminal hypervariable region (HVR) (Prior *et al.*, 2001). The main difference between the R-Ras protein and the N-, K- and H-Ras proteins is the presence of an additional N-terminal 26 amino acids, as well as the HVR. The localisation of Ras to the plasma membrane is essential for its correct biological activity (Williumsen *et al.*, 1984). Figure 1.9 shows the C-terminal modifications and membrane-trafficking pathways of the Ras proteins.

1.8.1 C-terminal modifications

The two signals responsible for the correct localisation of Ras are contained in the Ras HVR (Jaumot *et al.*, 2002). The first signal sequence, common to all Ras proteins, is the C-terminal CAAX box (C, cysteine; A, aliphatic; and X, any amino acid) (Hancock *et al.*, 1989). Ras proteins undergo a series of post-translational modifications on their CAAX motif (Okada *et al.*, 1996). The first stage of the processing involves three successive modifications of the CAAX motif (i) farnesylation (polyisoprenylation) of the cysteine residue, (ii) proteolytic cleavage of the amino acids –AAX, and (iii) methyl esterification of the new C-terminal cysteine. This first stage of modification coverts the primary translation product into an intermediate form. H-, N-Ras and K-Ras4A are further modified by acylation with palmitic acid on cysteine residues (Cys^{181} and Cys^{184}) immediately upstream of the CAAX motif, yielding the final, fully modified form (Hancock *et al.*, 1990). Palmitoylation of H-, N-Ras and K-Ras4A and the poly-lysine stretch in K-Ras4B, contribute to the correct membrane localisation of the proteins.

H-Ras mutants, H-Ras $Ser^{181, 184}$ (which were farnesylated but lacked the cysteine residues to be palmitoylated) activated Raf as efficiently as fully modified H-Ras (Okada *et al.*, 1996). In contrast, H-Ras Ser^{186} (which lacked the cysteine residue to be farnesylated) had almost negligible activity, indicating that the post-translational modifications of H-Ras, especially the farnesylation step, are critical for normal

activation of Raf (Okada *et al.*, 1996). Moreover, it has recently been observed that intracellular galectin-1 is essential for, and stabilises the interactions of H-Ras GTP within the cell membrane and that the H-Ras farnesyl moiety is essential for this interaction (Paz *et al.*, 2001).

R-Ras is also palmitoylated (Lowe and Goeddel, 1987) but possesses a different C-terminal prenylation motif to H-Ras for post-translational modification and is geranyl-geranylated rather than farnesylated (Lowe *et al.*, 1988; Osada *et al.*, 1999).

An important consequence of HVR divergence between the proteins is that the plasma membrane anchors for each of the proteins is different. Since the H-Ras, N-Ras and K-Ras proteins all contain identical sequences including the effector, exchange factor and guanine-nuclcotide-binding domains, perhaps the biological differences between the isoforms could be attributed to the differences in membrane microlocalisation.

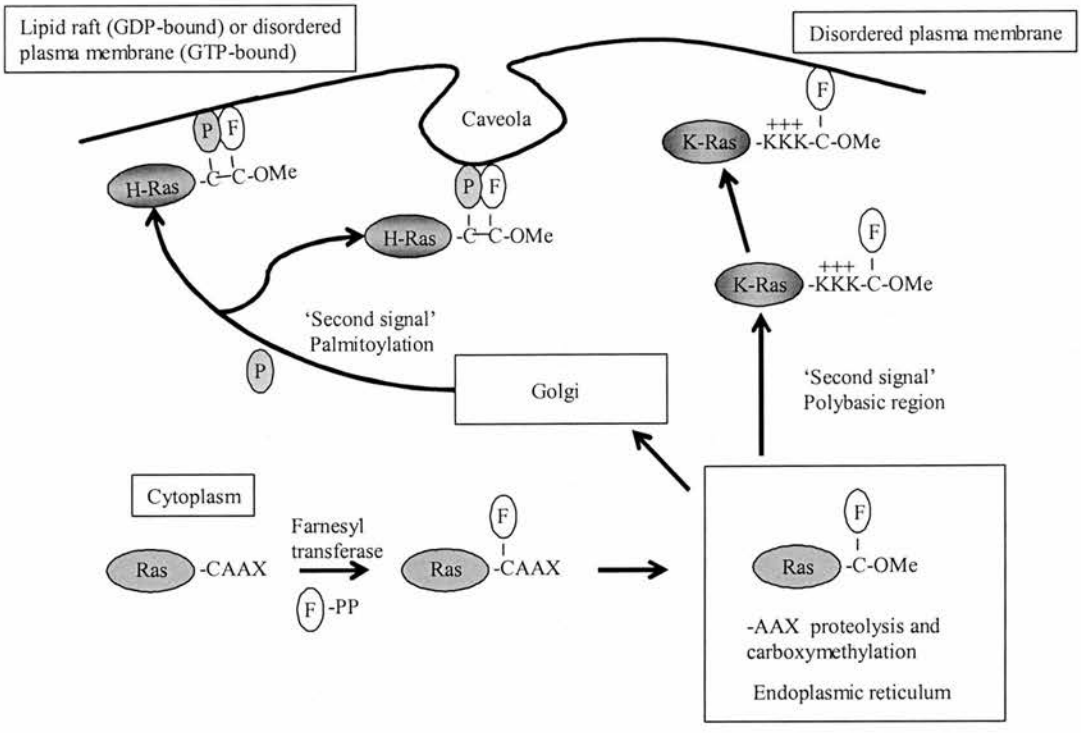

Figure 1.9 C-terminal modification and membrane-trafficking of Ras proteins

Ras proteins are synthesised as cytosolic proteins (light grey circles). The common CAAX box is recognised by the cytosolic farnesyltransferase enzyme, which catalyses the addition of the farnesyl isoprenoid lipid (F) to the cysteine residue. Endoplasmic reticulum associated enzymes catalyses the proteolytic removal of the AAX residues and carboxyl methylation of the farnesylated cysteine residue. H-Ras, N-Ras and K-Ras4A then migrate through the Golgi. A second set of signalling sequences are required to traffic Ras proteins to the plasma membrane. The lysine-rich sequence of K-Ras4B (referred to in diagram as K-Ras) provides the second signal required for transit to the membrane. H-Ras, N-Ras and K-Ras4A undergo covalent addition of palmitate fatty acid moieties to cysteine residues located upstream of CAAX motif. The palmitate modification of H-Ras targets it to the lipid rafts and caveolae of the plasma membrane. This is dependent on activation state of H-Ras. The lysine-rich sequences of K-Ras4B target it to the disordered plasma membrane. Modified from Prior and Hancock, (2001); Reuther and Der, (2000).

1.8.2 Trafficking of proteins to the plasma membrane

The post-translational modifications of the Ras and R-Ras proteins increase the hydrophobic nature of the C-terminal domains of the proteins, increasing their affinity for membranes. The enzymes required for post-translational farnesylation and palmitoylation have been identified on the endoplasmic reticulum (ER) (reviewed by Prior and Hancock, 2001). A mammalian homologue to the recently cloned *Saccromyces cerevisae,* ER localised, Ras palmitoyltranferase (RPT) is thought to exist (Lobo *et al.*, 2002; Hancock, 2003). Following palmitoylation on the ER, H-Ras and N-Ras proteins access the plasma membrane by vesicular trafficking through the classical exocytic pathway, on the cytoplasmic surface of the vesicles (Apolloni *et al.*, 2000; Choy *et al.*, 1999). In contrast, the polybasic K-Ras4B is largely excluded from the Golgi (see Figure 1.9). The K-Ras trafficking pathway remains elusive, although it has been suggested that it may involve microtubule binding (Apolloni *et al.*, 2000; Choy *et al.*, 1999) or simple passive diffusion from the ER to the plasma membrane (Roy *et al.*, 2000). The trafficking pathway for R-Ras has yet to be defined.

A consequence of the alternative trafficking pathways adopted by the Ras proteins is that their eventual membrane microlocalisations are different.

1.8.3 Targeted membrane microdomains

The simple fluid mosaic model of the plasma membrane has been made more complex by the discovery of microdomains which have distinct protein and lipid compositions. The lipid raft, comprising sphingolipids and glycosphingolipids packed together with cholesterol, is the best characterised microdomain (Simons and Ikonen, 1997). The liquid-ordered structure of lipid rafts promotes phase separation from the loosely packed, disordered glycosphingolipids of the bulk plasma membrane (Prior and Hancock, 2001). Lipid rafts have been proposed as important structures of the plasma membrane which serve as signalling platforms (Simons and Ikonen, 1997).

Membrane proteins which associate with the lipid rafts, such as glycophosphatidylinositol (GPI)-anchored proteins, are anchored with long, saturated

acyl chains (Simons and Ikonen, 1997). While proteins anchored by farnesyl or geranylgeranyl groups alone are excluded from lipid rafts (Melkonian *et al.*, 1999). H-Ras has been shown to be efficiently targeted to the lipid rafts following post-translational modification (Prior *et al.*, 2001). It is thought that H-Ras is initially trafficked to lipid rafts and caveolae, where lipid rafts have been aggregated into invaginations of the plasma membrane by caveolin (Simons and Toomre, 2000), but then exists in a dynamic equilibrium between lipid rafts (in the GDP-bound state) and the disordered bulk plasma membrane (in the GTP-bound state) (Prior *et al.*, 2001). In contrast K-Ras, which is anchored by prenylation and electrostatic charge, resides in the disordered, non-raft plasma membrane regardless of activation state (Prior *et al.*, 2001). As yet, the targeted membrane microdomain of R-Ras has not been elucidated.

The importance of correct membrane localisation of the Ras proteins has been illustrated by Prior *et al.*, (2001), who compared Raf-1 activation by activated H-Ras with an H-Ras HVR mutant confined to the lipid rafts. Although Raf-1 can be recruited to the lipid rafts and bulk plasma membrane equally well, activation is much less efficient in the lipid rafts (Prior *et al.*, 2001).

1.9 Regulating Ras/R-Ras activity

1.9.1 The Ras/R-Ras-GTP/GDP cycle

In addition to post-translational modification, the Ras and R-Ras proteins require GTP-binding for activation. The proteins cycle between an inactive GDP-bound state and an active GTP-bound state (see Figure 1.10). Inactive GDP-bound proteins are activated by interaction with proteins known as Guanine Exchange Factors (GEF), which catalyse the release of GDP. The lost GDP is then rapidly replaced by the more abundant GTP (Lenzen *et al.*, 1998). The exchange of GDP for GTP drives an allosteric change in the Switch I and Switch II regions (Boriack-Sjodin *et al.*, 1998). The Switch I region, which forms part of the effector binding domain, permits the binding of effectors when Ras is in the GTP-bound configuration (Ehrhardt *et al.*, 2002). Several Ras-GEFs have been characterised. Mammalian SOS, a homologue of the *Drosophila son of sevenless* gene product, has been identified as a Ras activator,

which responds to signals which generate tyrosine phosphorylation at the interior of the cell (Bowtell *et al.*, 1992; Gotoh *et al.*, 2001; Lai *et al.*, 1993). Other Ras-GEFs include RasGRF1and 2 (Farnsworth *et al.*, 1995; Fam *et al.*, 1997) and Ras-GRP (Ebinu *et al.*, 1998), which all respond to different signals.

GTPase-activating proteins (GAPs) also bind to the GTP-bound Ras proteins, these proteins serve to enhance the intrinsic GTPase activity of the proteins, resulting in the hydrolysis of GTP to GDP and returning the protein configuration to the inactive state (Wittinghoffer *et al.*, 1997). There have been several distinct Ras-GAPs identified: p120GAP, a predominantly cytosolic protein (McCormick, 1998), neurofibromatosis type1 protein (NF-1) (Ballester *et al.*, 1990) and $Gap1^{m}$ (Li *et al.*, 1996).

The R-Ras GTP-binding protein also cycles between an inactive GDP-bound state and an active GTP-bound state. The Ras proteins GEFs, Ras-GRP and RasGRF1and 2, as well as a Ral1 GEF called C3G, have been shown to activate R-Ras (Ohba *et al.*, 2000). As yet, no GEFS specific for R-Ras have been identified. The GAPs for the Ras family p120GAP, NF-1 and $Gap1^{m}$, have all been shown to increase R-Ras GTPase activity (Ohba *et al.*, 2000). A GAP specific for the activation of R-Ras has been identified and termed R-RasGAP (Emkey *et al.*, 1991; Yanamoto *et al.*, 1995). As this regulatory protein seems more specific, it may play a critical role in the specific regulation of the R-Ras subfamily (Ohba *et al.*, 2000). Figure 1.10(B) provides a table of all the known H-Ras and R-Ras GAPs and GEFs.

Point mutations within the Switch I and Switch II regions of the Ras and R-Ras proteins block the GTPase activity, leading to constitutively active proteins. The amino acids in Ras, Gly^{12} and Glu^{61}, are essential for Ras GTPase activity by GAP stimulation (Macaluso *et al.*, 2002) and mutating them inhibits GTP hydrolysis. Mutation of the R-Ras Gly^{38} amino acid, equivalent to Ras Gly^{12}, also results in a constitutively active protein.

A

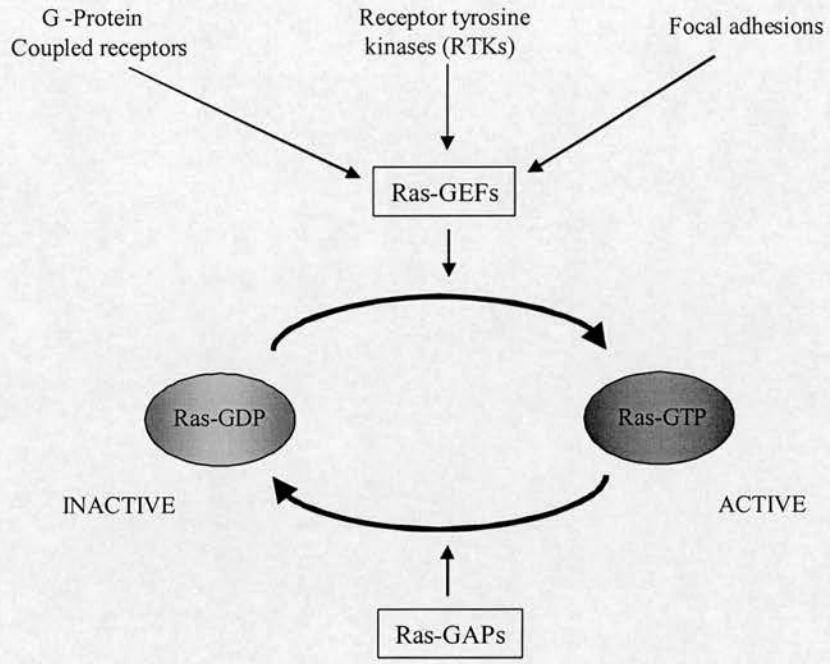

B

H-Ras		R-Ras	
GEFs	**GAPs**	**GEFs**	**GAPs**
RasGRF1	NF1	RasGRF1	NF1
RasGRF2	GAP1m	RasGRP1	GAP1m
RasGRF3	GAPIII	RasGRP3	GAPIII
RasGRP1	p120RasGAP	CalDAG-GEF1	p120RasGAP
SOS1/2	GAP^{IP4BP}		GAP^{IP4BP}

Figure 1.10 The Ras GDP/GTP activation cycle

(A) Schematic representation of the regulation of Ras proteins. Extracellular stimuli mediated by G-protein coupled receptors, RTKs and adhesion molecules activated various GEFs which exchange bound GDP for GTP producing the active Ras protein. Ras GAPs enhance the intrinsic Ras GTPase activity, resulting in the hydrolysis of GTP to GDP and returning protein to inactive state.
(B) Table to show and compare the known H-Ras and R-Ras GAPs and GEFs. Abbreviations used: GAP, GTPase-activating protein; GEF, guanine-nucleotide exchange factor; GRF, guanine-nucleotide-releasing factor; GRP, guanine-nucleotide-releasing protein; SOS, Son of Sevenless; NF1, neurofibromin 1; CalDAG, calcium and diacylglycerol. Modified from Kinabara *et al.*, (2003).

1.9.2 Ras activation

Ras activation can be mediated by a number of different receptors including receptor tyrosine kinases (e.g. the epidermal-growth-factor (EGF) receptors, G- protein coupled receptors and ligand-stimulated integrins (see section 1.3.2). The best described of these signalling pathways is that of growth factor stimulation of Ras activity.

Following ligand (EGF) binding, activated receptor tyrosine kinases (RTK) auto-phosphorylate key tyrosine kinases at their carboxyl terminus (Pazin and Williams, 1992). These phosphotyrosines serve as binding sites for adaptor proteins such as Shc and Grb2, which contain SH2-binding domains (Gale *et al.*, 1993; Lowenstein *et al.*, 1992). Grb2 consists of one SH2 and two SH3 domains. Grb2 is constitutively associated with the Ras-GEF SOS via its SH3 domain, whilst the SH2 domains of Grb2 mediate binding to the EGFR phosphotyrosines either directly or through the adaptor protein Shc (Li *et al.*, 1993; Rozakis-Adcock *et al.*, 1993; Okutani *et al.*, 1994). Recruitment of the Grb2-SOS complex to the EGFR positions SOS adjacent to the membrane-bound Ras, thus facilitating the release of GDP from Ras and replacement with GTP.

The heterotrimeric G-protein coupled receptors, in particular the pertussis toxin-inhibitable (G_i) receptors, can influence Ras activity via their G-protein subunits (α and $\beta\gamma$). Activation of the G-protein receptors increases the phosphorylation of the adaptor protein Shc, leading to increased Shc-Grb2-SOS complex formation and subsequent Ras activation (Denhart, 1996; Lowes *et al.*, 2002). G-proteins are also capable of activating Ras-GEFs such as RasGRF1 and RasGRP, resulting in GDP-GTP exchange (Reuther and Der, 2000).

While the activation pathways for Ras have been described, the upstream-signalling pathways involved in the activation of R-Ras have yet to be elucidated. Activation of the Ras family proteins family leads to their interactions with a variety of downstream effector proteins. While methods of activation for the Ras proteins and R-Ras cannot yet be compared, R-Ras has been shown to bind to similar effector proteins as the Ras proteins. The interactions and subsequent signalling pathways will be discussed below.

1.10 Effector proteins

Activated Ras stimulates a multitude of downstream signalling cascades and it is through these pathways that Ras controls cell proliferation, survival and cell behaviour contributing to a transformed phenotype. Ras effectors preferentially bind to GTP-bound Ras. The three main Ras effectors Raf kinase, PI3-kinase and Ral-GEFs, bind to the minimal effector region of Ras (residues 32-40) and increase their '*in-vivo*' activity after Ras binding. R-Ras and the other Ras proteins have highly homologous effector binding domains; consequently GTP-bound R-Ras is capable of binding to several common effectors. Figure 1.11 shows the main effectors of Ras and their associated pathways.

1.10.1 Raf kinase

The serine/threonine kinase Raf was one of the first Ras effectors to be identified and has been the most intensely studied. The *raf* gene was first discovered as the transforming oncogene in the mouse sarcoma virus 3611 (Rapp *et al.*, 1983). The proto-oncogene, *c-raf-1*, was identified in non-transformed cells (Kozak *et al.*, 1984). Upon activation, Raf-1 was demonstrated to activate the p42/44 mitogen activated protein kinases (MAPKs) or extracellular-signal-regulated kinases (ERK1/2) (Howe *et al.*, 1992). Three Raf isoforms have been identifed: Raf-1, A-Raf and B-Raf. The Raf isoforms display differential catalytic activity towards MEK (B-Ras>Raf-1>A-Raf), and this activity is represented by different levels of ERK1/2 activation (Pritchard *et al.*, 1995). A key observation that implicated the Raf-1 serine/threonine kinase as a critical effector of Ras function was that Ras-GTP forms a high affinity complex with Raf-1 (Zhang *et al.*, 1993; Moodie *et a*l., 1993; Vojtek *et al.*, 1993).

The Raf protein consists of an N-terminal noncatalytic domain and a C-terminal kinase domain. The N-terminal regulatory domain contains two Ras binding domains (RBD) and a cysteine rich domain (CRD). Removal of the N-terminal domain results in a constitutively active Raf (Raf-BxB) (Morrison and Cutler, 1997). The mechanisms by which Ras mediate Raf activation, and subsequent ERK1/2 activation have been intensely studied. Inactive Raf exists in the cytosol where it is constitutively associated with several proteins, including the phosphoserine binding protein, 14-3-3, which may serve as a negative regulator (Wartmann and Davis,

1994; Campbell *et al.*, 1998). Activated Ras binds to the first RBD and recruits the Raf complex to the plasma membrane. At the membrane, phosphatidylserine (PS) facilitates the binding of Ras binds to Raf CRD, by displacing 14-3-3 (Hu *et al.*, 1995). Other factors including kinase suppressor of Ras (KSR), phospholipids, HSP90 and both serine/threonine kinases lead to full Raf activation (reviewed by Morrison and Cutler, 1997; Kolch, 2000).

R-Ras also interacts with the Raf serine/threonine kinases in a GTP-dependent manner (Spaargaren *et al.*, 1994) however, in contrast to Ras, R-Ras does not activate Raf (Marte *et al.*, 1997).

1.10.2 PI 3-kinase

Phosphatidylinositol-3-OH kinase (PI 3-kinase) is another effector of the Ras family that has kinase activity against lipids and proteins. PI 3-kinase can phosphorylate the 3' position of the inositol ring on phosphoinositides (Carpenter and Cantley, 1996). PI 3-kinase is composed of a p110 catalytic and a p85 regulatory subunit. The p110 catalytic domain of PI 3-kinase has a high affinity for the GTP-bound form of Ras G12V through the Ras effector domain (Rodriguez-Viciana *et al.*, 1994; Rodriguez-Viciana *et al.*, 1996). Ras stimulation of PI 3-kinase activity is required for its optimal activation in response to growth factors (Rodriguez-Viciana *et al.*, 1994). The phosphorylated lipid products of PI 3-kinase can regulate a number of proteins including Rac, p70S6 kinase, PKB/AKT and isoforms of protein kinase C (Carpenter and Cantley, 1996). PKB/AKT enzyme activity has been implicated in cell survival by inactivating BAD (pro-apoptotic factor) by phosphorylation (Datta *et al.*, 1999; Downward *et al.*, 1998). The Ras family are also able to mediate activation of the Rho subfamily proteins via PI 3-kinase activation of Rac (Ehrhardt *et al.*, 2002).

R-Ras also binds to the p110 catalytic subunit of PI 3-kinase *in vitro* and induces an elevation in the levels of PI 3-kinase lipid products *in vivo*, demonstrating that PI 3-kinase is downstream of R-Ras (Marte *et al.*, 1997). Activated R-Ras may increase the activity of PI 3-kinase more efficiently than H-Ras, which in turn is more efficient than K-Ras4B (Yan *et al.*, 1998).

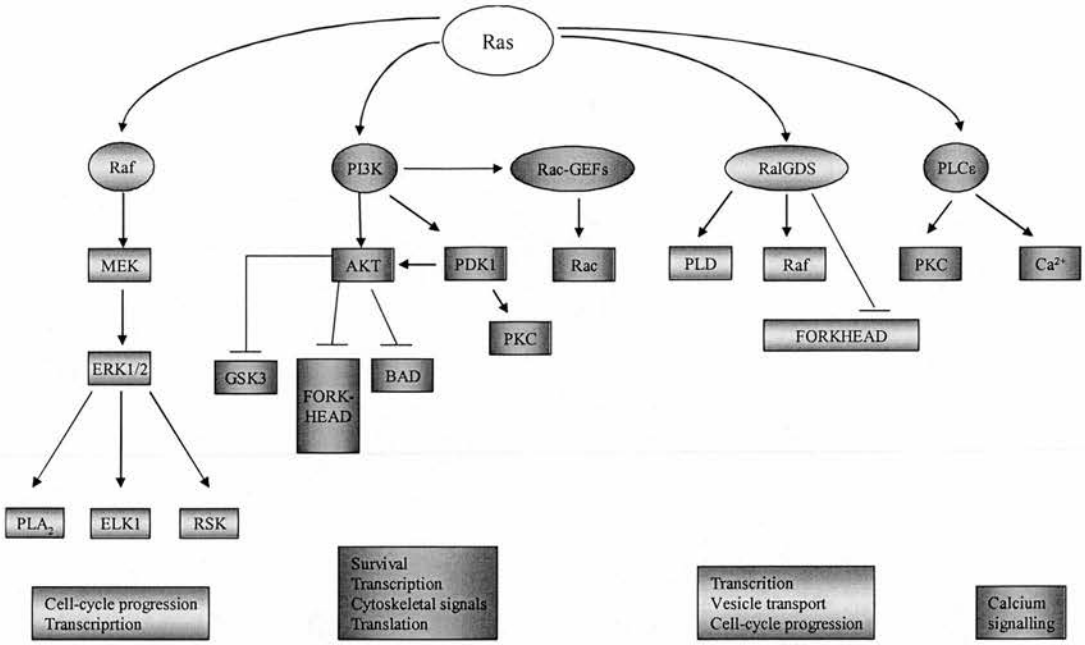

Figure 1.11 Common Ras effector pathways

Active Ras will interact with several families of effector proteins. The main effectors are shown here along with their downstream effectors and cellular effects. Abbreviations: ERK, extracellular regulated kinase; GSK3, glycogen synthase kinase 3; MEK, mitogen-ctivated kinase/ERK kinase; PDK1, phosphatidylinositol trisphosphate-dependent kinase 1; PLA_2, phospholipase A_2; PLD, phospholipase D; RSK, ribosomal protein S6 kinase (Downward, 2003).

1.10.3 Ral guanine exchange factors

The Ral-GEFs are Ras effectors, which activate the Ras related proteins RalA and RalB. These RalGEFs include Ral guanine nucleotide dissociation factor (RalGDS), RalGDS-like1/2 (Rgl1/2) and RalGDS-like factor (Rlf) (Hofer *et al.*, 1994; Peterson *et al.*, 1996; Wolthuis and Bos, 1999). The C-terminal noncatalytic domains of RalGDS, Rgl1/2 and Rlf interact with the effector domain of Ras in a GTP-dependent manner *in vitro* and can compete with Raf-1 for binding to the Ras effector binding region *in vitro* (Campbell *et al.*, 1998). A role for Ral in the regulation of the cell cycle has been demonstrated by its ability to upregulate the expression of cyclin D1 (Henry *et al.*, 2000).

R-Ras also binds RalGDS however, in contrast to Ras it does not enhance the Ral-GEF activity of RALGDS (Urano *et al.*, 1996).

1.11 The ERK1/2 signalling pathway

The mitogen-activated protein (MAP) kinases, also termed ERK 1 and 2 (extracellular-regulated kinases), control many cellular responses. In fact, ERK activity has been implicated as a regulatory component in nearly every fundamental cellular activity. The Raf/MEK/ERK pathway is perhaps the best described Ras effector pathway.

The activation of ERK1/2 pathway first requires the activation of the dual specificity kinases MAPK/ERK Kinase1/2 (MEK1/2), also called MKK1 and MKK2 (Dhanasekaran and Reddy, 1998). The predominant MEK activators are Raf kinases (Schaeffer and Weber, 1999). MEK1/2 can directly associate with the C-terminal catalytic domain of Raf-1, resulting in its phosphorylation (Crewes and Erikson, 1993). MEK1 is activated by phosphorylation on two serine residues, Ser218 and Ser222 and MEK2 is activated by phosphorylation on serine residues Ser219 and Ser223 (Alessi *et al.*, 1994) leading to full activation of MEK activity. The interaction between Raf and MEK can be disrupted by Raf kinase inhibitor protein (RKIP) (Kolch, 2000). RKIP seems to act as a physiological regulator of ERK signalling by controlling Raf/MEK interactions (Kolch, 2000). Activated MEKs function as dual specificity kinases and phosphorylate ERK1/2 threonine and

tyrosine residues (Crews *et al.*, 1992). These residues Thr183 and Tyr185 (on ERK2), reside within a TEY-motif (Thr-X-Tyr, where X is glutamic acid) (Payne *et al.*, 1991). Phosphorylation of both of these residues is required for full activation and subsequent increase in ERK activity (Anderson *et al.*, 1990; Robbins *et al.*, 1993). Map kinase phosphatases (MKP) can specifically dephosphorylate threonine and tyrosine residues, regulating in vivo ERK activity (Alessi *et al.*, 1993).

Once activated, ERK1/2 translocate to the nucleus where they phosphorylate and activate a variety of transcription factors that include Elk-1 nuclear transcription factor (Marais *et al.*, 1993). Elk-1 forms a complex with serum response factor (SRF) at the serum response DNA element (SRE) present in many promoters (Price *et al.*, 1996), promoting transcription of genes such as the transcription factor *c-fos* (Janknecht *et al.*, 1993).

Ras-ERK1/2 signalling can lead to cell proliferation through the induction of cyclin D1 expression and degradation of the cell cycle inhibitor p27kip which is induced by Ras-ERK1/2 signalling. This facilitates passage through G1 and entry into the S-phase of the cell-cycle (Woods *et al.*, 1997).

Not all activated ERK1/2 translocates to the nucleus, ERK1/2 is also capable of activating a number of cytoplasmic proteins. Myosin light chain kinase (MLCK) is activated by ERK1/2 phosphorylation (Morrison *et al.*, 1996). Phosphorylated myosin light chains (MLC) result in a fully functional actin-myosin motor unit, which serves to produce the contractile forces within the cell required for cell motility (Klemke *et al.*, 1997).

1.12 Biological effects of Ras and Ras-related proteins

Despite sharing common activators and effectors the Ras proteins and R-Ras have distinct biological functions. Ras is the most commonly mutated gene in human tumours (Bos, 1989). Constitutively active mutants of Ras (G12V) promote transformation of a variety of fibroblast and epithelial cell lines, whereas R-Ras (G38V) only causes the transformation of NIH-3T3 cells (Huff *et al.*, 1997; Shields *et al.*, 2000). Ras activation of the Raf-MEK-ERK1/2 kinase cascade has been shown to be necessary for cellular transformation (Cowley *et al.*, 1994; Mansour *et al.*, 1994). H-Ras G12V transformed cells show constitutively elevated Raf-1 kinase

activity in contrast, no elevated Raf kinase activities were observed in R-Ras G38V transformed NIH-3T3 cells (Huff *et al.*, 1997). R-Ras, but not H-Ras, has been observed in complex with the anti-apoptotic protein Bcl-2 suggesting a role for R-Ras in apoptosis (Fernandez-Sarabia, 1993).

The functions of the Ras and R-Ras GTPases are not restricted to their roles in cell growth and proliferation, 'inside-out' signalling pathways involving these GTPases have also been implicated in mediating integrin-affinity modulation. Zhang *et al.*, (1996), demonstrated that R-Ras, but not H-Ras, can increase cell adhesion by modulating integrin function.

Regulation of integrins by Ras proteins

1.13 Modulating integrin expression levels

In order to achieve correct cellular function, the interactions between integrins and their ligands must be strictly regulated. Cellular adhesive strength to the ECM or other cells can be regulated in a number of ways including modulation of surface expression levels of integrins. Leukocytes increase β_2 expression levels to facilitate recruitment to sites of tissue injury (Hillis and MacLeod, 1996).

Ras signalling activates several pathways which can result in transcriptional changes, including levels of integrin expression. The modulation of integrin surface expression by *ras* genes is cell-and integrin-specific. Constitutively active Ras (probably H-Ras) increased β_3 expression levels in human melanoma and pancreatic carcinoma cell lines (Woods *et al.*, 2001). Conversely, expression of a constitutively active Ras mutant in an endothelial cell line resulted in a reduction in $\alpha_3\beta_1$ integrin expression (Shin *et al.*, 1999). While expression of H-Ras G12V in human osteoblasts reduced the expression levels of β_1, α_4, α_5, α_6 (Tanaka, 2002), expression of H-Ras G12V in a pro-B cell line had no significant effect on the expression levels of the $\alpha_4\beta_1$, $\alpha_5\beta_1$, $\alpha_6\beta_1$ integrins (Fujimoto *et al.*, 2001; Shibayama *et al.*, 1999; Tanaka *et al.*, 1999).

1.14 Regulation of integrin affinity

The rapid activation of integrins is essential for the ability of a cell to respond to environmental changes. Activation of integrins is often gauged by an increase in cell adhesion to immobilised substrate. Cell adhesion requires a combination of integrin affinity and avidity and therefore, pathways which modulate cell adhesion can not be solely credited to affinity changes (Hughes and Pfaff, 1998). Cell binding to soluble ligand and ligand-mimetic antibodies provide a better model for measuring integrin affinity changes.

Soluble fibrinogen and PAC-1 (ligand-mimetic antibody to $\alpha_{IIb}\beta_3$) binding to platelets increases upon platelet activation (Bennett and Vilaire, 1979). $\alpha_{IIb}\beta_3$ expressed in CHO cells, however, failed to respond to any $\alpha_{IIb}\beta_3$-stimulating agonists such as ADP, thrombin and phorbol esters (O'Toole *et al.*, 1990). Substitution of the $\alpha_{IIb}\beta_3$ cytoplasmic domain with that of the laminin ($\alpha_{6A}\beta_1$) integrin produces a constitutively active chimeric integrin in CHO cells ($\alpha\beta$-py cells) (O'Toole *et al.*, 1991; O'Toole *et al.*, 1994). Binding of the PAC-1 ligand-mimetic antibody (acts like soluble fibrinogen) to the chimeric integrin can be used to determine integrin activation state. This $\alpha\beta$-py cell model system and adhesion assays have been used to help investigate the cytoplasmic signalling pathways involved in integrin-affinity modulation.

1.14.1 H-Ras modulates integrin affinity

Expression of activated H-Ras (G12V) in $\alpha\beta$-py cells suppressed the active chimeric integrin by means of a pathway that was sensitive to MAP kinase phosphatase-1 (Hughes *et al.*, 1997). Suppression of the integrin was not related to protein synthesis, integrin phosphorylation or mRNA transcription (Hughes *et al.*, 1997). Suppression of integrin affinity by H-Ras is cell- and integrin-type specific. Expression of constitutively active H-Ras suppresses integrin activation in fibroblasts (Hughes *et al.*, 2002). In contrast, constitutively active H-Ras induces the activation of $\alpha_4\beta_1$, $\alpha_5\beta_1$, and $\alpha_6\beta_1$, (in a pro-B cell line) without altering integrin expression levels (Fujimoto *et al.*, 2001; Shibayama *et al.*, 1999; Tanaka *et al.*, 1999).

Investigations into H-Ras downstream effectors and their roles in suppressing integrin activation highlighted the ability of an activated variant of Raf-1 to effectively suppress integrins in CHO cells (Hughes *et al.*, 1997). As the suppression of integrins by activated H-Ras and Raf-1 was alleviated by the MAP kinase phosphatase-1 (Hughes *et al.*, 1997), it was hypothesised that H-Ras/Raf-mediated integrin suppression was dependent on ERK1/2 activation. However, more recent studies have indicated that suppression of integrins by H-Ras/Raf does not require with ERK1/2 activation (Hughes *et al.*, 2002). Suppression of $\alpha_5\beta_1$ integrin by active Raf-1 was shown to be independent of ERK1/2 activity, as inhibition of ERK1/2 by a MEK inhibitor failed to alleviate Raf-1-mediated integrin suppression (Hughes *et al.*, 2002). Consistent with this, an active variant of MEK1 (which potently activates ERK1/2) fails to suppress integrins (Hughes *et al.*, 2002; Kinbara *et al.*, 2003).

In cells where H-Ras was shown to enhance integrin activation, the downstream effector PI 3-kinase has been implicated in mediating the H-Ras effect. In bone-marrow-derived mast cells H-Ras induced adhesion, through activation of $\alpha_5\beta_1$ integrin, was susceptible the PI 3-kinase inhibitor wortmannin (Kinashi *et al.*, 2000). In the study by Kinashi *et al.*, (2000), targeting PI 3-kinase to the cell membrane using a CAAX tail, resulted in enhanced adhesion and spreading of the mast cells whereas membrane-targeted Raf-CAAX failed to enhance adhesion and spreading of the cells. The choice of effector pathway utilised by H-Ras in mediating integrin affinity may be cell-type dependent (Kinbara *et al.*, 2003).

1.14.2 R-Ras promotes integrin activation

R-Ras was first implicated in integrin regulation when expression of constitutively active R-Ras (G38V) converted the suspension-cell lines, mouse 32D and human myeloid cells, into highly adherent cells (Zhang *et al.*, 1996). Stable expression of activated R-Ras significantly enhanced $\alpha_2\beta_1$-dependent cell migration in human breast carcinoma cells, promoting cell invasion across collagen (Keely *et al.*, 1999). R-Ras causes extensive cell spreading when injected into PC12 cells, although the identity of the integrins involved in PC12 cells is not clear (Self *et al.*, 2001). Expression of R-Ras G38V also induces the adhesion of bone-marrow-derived mast cells through activation of $\alpha_5\beta_1$ (Kinashi *et al.*, 2000). Expression of R-Ras G38V in

retinal neurons promoted late embryonic stage retinal neurite outgrowth on laminin-1 (LN-1) through activation of $\alpha_6\beta_1$ integrin (Ivins *et al.*, 2000).

The downstream effectors involved in R-Ras-mediated integrin activation remain to be elucidated; however a proline-rich, SH3-binding C-terminal motif (Wang *et al.*, 2000) and C-terminal prenylation (Oertli *et al.*, 2000) within R-Ras have been shown to be important for integrin activation. The ability of R-Ras to control integrin activity can be regulated by phosphorylation. Activation of the Eph (ephrin) receptor EphB2 phosphorylates a tyrosine residue (Tyr^{66}) in the effector domain of R-Ras, this phosphorylated R-Ras can no longer support integrin activity and cell-ECM adhesion is lost (Zou *et al.*, 1999; Zou *et al.*, 2002). Zou *et al.*, (2002) found that oncogenic Src also phosphorylates R-Ras on Tyr^{66}, which may explain the reduced cell adhesion that is characteristic of Src-transformed cells.

A recent study has implicated PI 3-kinase in R-Ras-induced cell spreading. Keely *et al.*, (1999) demonstrated that PI 3-kinase inhibitors prevented the restoration of fibroblastic cell spreading by R-Ras.

1.14.3 R-Ras antagonises H-Ras/Raf-mediated integrin suppression

Despite their sequence homology and overlapping use of effectors and GEFs, H-Ras and R-Ras have different functional effects on integrins. In CHO cells, expression of R-Ras promotes the active integrin state while expression of H-Ras suppresses the integrin activation. Furthermore, co-expression of active R-Ras G38V with active H-Ras G12V, in CHO cells, reversed H-Ras-mediated integrin suppression (Sethi *et al.*, 1999). The reversal of H-Ras-mediated integrin suppression by R-Ras is not due to competition for the common effector Raf-1, as R-Ras can reverse the integrin suppression caused by an active Raf-1 which lacks the Ras-binding domain (Raf-BxB CAAX) (Sethi *et al.*, 1999). The mechanism by which R-Ras antagonises H-Ras/Raf-mediated integrin suppression is currently under investigation however, several candidate proteins have been proposed which may influence the R-Ras effect. Figure 1.12 shows the known and proposed pathways involved in R-Ras reversal of H-Ras-mediated integrin suppression.

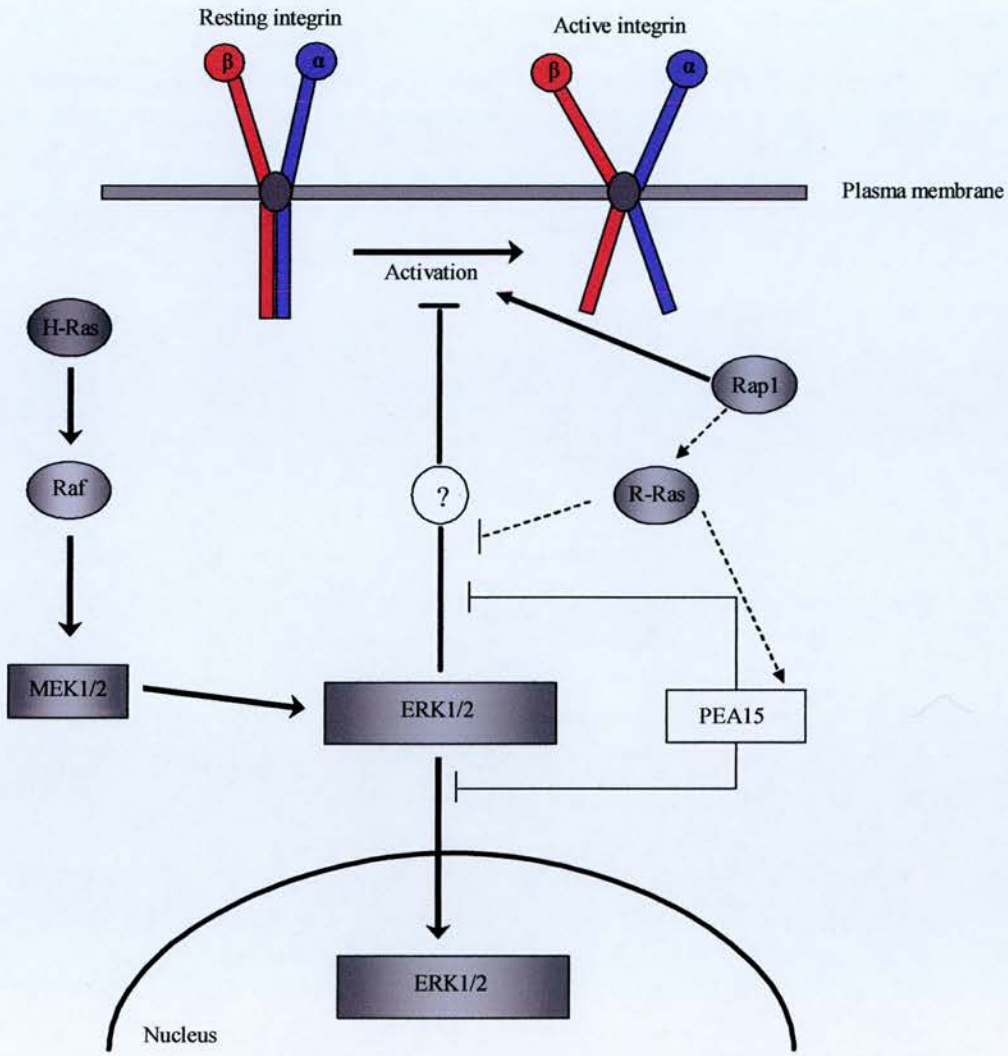

Figure 1.12 R-Ras antagonism of H-Ras/Raf integrin suppression pathway

Boldface arrows highlight the well established pathways. Where a mechanism/pathway remains to be elucidated, the proposed pathway is shown by dashed arrows.

H-Ras activates the Raf/MEK/ERK pathway, which can lead to the suppression of integrin activation. PEA-15 binds directly to ERKs and prevents their translocation to nucleus, although it has no affect on ERK activity. PEA-15 is capable of reversing Ras-mediated integrin suppression. Expression of R-Ras reverses H-Ras-mediated integrin suppression. PEA-15 has been identified as a possible R-Ras effector. Activated Rap-1 can activate integrins. Rap-1 activation of R-Ras has been proposed as a mechanism for reversing H-Ras-mediated integrin suppression (Kinbara *et al.*, 2003).

In a screen to identify proteins that antagonise Ras-mediated integrin suppression in fibroblasts, Ramos *et al.*, 1998, identified PEA-15. PEA-15, a small death effector domain (DED)-containing protein, does not block the capacity of Ras to activate the ERK1/2 mitogen-activated protein kinase pathway (Ramos *et al.*, 1998). It has been hypothesised that PEA-15 reverses H-Ras-mediated integrin suppression by means of R-Ras, as PEA-15's action is blocked by a dominant negative R-Ras (Ramos *et al.*, 1998).

It is interesting to note that PEA-15 interacts directly with ERK/ MAPKs, to sequester them to the cytoplasm thus preventing ERK/MAPK-dependent transcription and cellular proliferation, but does not inhibit ERK/ MAPK activity (Formstecher *et al.*, 2001). R-Ras G38V reversal of H-Ras-mediated integrin suppression does not result in diminished levels of ERK1/2 phosphorylation. As PEA-15 reverses Ras-mediated integrin suppression but does not inhibit ERK/ MAPK activity, this could implicate PEA-15 as a possible R-Ras effector.

Rap1, a member of the Ras subfamily, has been shown to be activated following stimulation by cytokines and growth factors. Similar to R-Ras, activated Rap-1 has been shown to activate integrins. Erythropoietin and IL-3 activate Rap-1 to promote the adhesion of haematopoietic cells through $\alpha_4\beta_1$ or $\alpha_5\beta_1$ integrins (Arai *et al.*, 2001). Activated Rap-1 (V12) increased $\alpha_{IIb}\beta_3$ affinity in megakaryocytes, as measured by binding of an $\alpha_{IIb}\beta_3$ activation-specific monovalent Fab fragment (antigen-binding fragment) (Bertoni *et al.*, 2002). Both R-Ras and Rap-1 activate the $\alpha_M\beta_2$ macrophage integrin to initiate complement-mediated phacocytosis (Caron *et al.*, 2000). Microinjection of Rap-1GAP in to a macrophage cell line eradicated R-Ras induced $\alpha_M\beta_2$ activation (Self *et al.*, 2001), indicating that R-Ras requires Rap-1 activity to activate the integrin, in this cell line.

General aims of this thesis

As discussed in the first part of the introduction, the strict regulation of integrin function is essential for normal cellular processes. Despite having 55% homology, H-Ras and R-Ras have very different effects on integrin affinity. Studies have shown that expression of the H-Ras oncogene (H-Ras G12V) in CHO $\alpha\beta$-py cells can result in the suppression of activation of the stably expressed chimeric integrin. However, expression of activated R-Ras (G38V) reverses H-Ras-mediated integrin suppression.

One of the main aims of this thesis is to further examine the role of H-Ras and R-Ras in integrin affinity. For this, a series of H-Ras and R-Ras chimeric molecules will be utilised. These chimeras have been designed on the basis of transposing the most variable regions of H-Ras and R-Ras, in the hope of identifying the specific regions of the proteins involved in conferring their contrasting effects on integrin affinity state.

A further aim will be to investigate the different functional effects of H-Ras and R-Ras on CHO cells. Using CHO cells stably expressing the H-and R-Ras chimeric proteins, it is hoped that the specific areas of the H-Ras and R-Ras proteins relating to their differing functional effects may be investigated. Results from functional assays will then be linked back to integrin-affinity status to see if the H-Ras and R-Ras proteins affect their functional effects through integrin affinity modulation.

Chapter 2

Materials and Methods

2.1 Materials

Unless otherwise stated, all chemicals were purchased from Sigma (Dorset, UK). The following reagents were obtained from Life Technologies (Paisley, UK): Dulbecco's Modified Eagles Medium (DMEM); penicillin; streptomycin; dialysed foetal calf serum (FCS); L-glutamine 30% (w/v) and non-essential amino acids.

Antibodies were obtained from the following sources: anti-HA (Y-11), anti-myc (9E10 and A14), anti-ERK2 (C-14), anti-Raf-1 (E-10) were from Santa Cruz Biotechnology (Santa Cruz, CA, USA). Phospho-ERK1/2 (ERK-PT115); anti-FLAG M2 monoclonal antibody; anti-FLAG M2 monoclonal antibody-FITC conjugate; anti-Cholera toxin and anti-mouse IgG (whole molecule) were from Sigma (Dorset U.K). All anti-species specific horseradish peroxidase-conjugated antibodies and RPE-Conjugated monoclonal mouse anti-Human CD25 Interleukin-2 receptor were from DAKO (Bucks, UK). All anti-species specific Alexa-Fluor–conjugated antibodies were purchased from Molecular Probes (The Netherlands). Function-blocking β_1 antibody, 4B4, was purchased from Coulter (Hialeah, Florida). Function-activating β_1 antibody, TS2-16, was obtained from an in-house hybridoma.

Transformation competent *Escherichia coli* strain DH5α cells were purchased from Life Technologies (Paisley, UK); strain TOP10 cells were purchased from Invitrogen (Groningen, Netherlands); XL-1 Blue Subcloning-Grade competent cells and XL-1 Blue Competent cells were purchased from Stratagene (La Jolla, CA, USA).

DNA constructs were obtained from the following sources: all pCDNA3.1(+) - H/R-Ras chimeras (CH1, CH3, CH5, CH6, H197, R197, H201 and R201), Tac-α5 (permission from Dr. S. E. LaFlamme, Centre for Cell Biology and Cancer research, NY, USA), pDCR-H-Ras (G12V) (permission from Dr. D. H. Wiger, Cold Stream Harbour Laboratory, NY, USA), pSG5-R-Ras G38V (permission from Prof. J. Downward, ICRF, London, UK) were provided by Dr. M. H. Ginsberg (Scripps

Research Institute, La Jolla, USA). pCDNA3-Raf-BxB CAAX was provided by Dr. C. K. Weber (University of Ulm, Germany), pEGFP-C3 (empty vector, H-Ras WT and H-Ras G12V) were provided by Dr Yoel Kloog (Department of Neurobiochemistry, Tel-Aviv University).

2.2 Cell Culture

The $\alpha\beta$-py CHO cell line was a generous gift from Dr. Mark Ginsberg (Scripps Institute, La Jolla, USA). This cell line stably expresses a chimeric integrin comprised of $\alpha_{IIb}\alpha_{6A}\beta_3\beta_1$ (Hughes *et al*, 1997). Stable expression of the chimeric integrin is maintained through culture in the presence of G418.

The $\alpha\beta$-py cell line was cultured in Dulbeccos Modified Eagles Media (DMEM), supplemented with 10% (or 0.1% for quiescent media) (v/v) FCS (heat inactivated at 57°C for 1 hour, unless pre-inactivated), 1% (v/v) non-essential amino acids and G418 antibiotic (400µg/ml) (Invitrogen), this will be referred to as complete media. The CHO-K1 cell line was cultured in the same media as the $\alpha\beta$-py cell line, without the G418 antibiotic. Stable lines were cultured in the same media as the $\alpha\beta$-py cell line, with G418 antibiotic (800µg/ml) to maintain selection.

All media contained 50 IU/ml streptomycin and 5mg/ml L-glutamine and all cell lines were maintained in a humidified atmosphere of 5% CO_2 / 95% air at 37°C. All cell lines were used at the lowest possible passage number and regularly screened for mycoplasma infection.

2.3 Transformation of *Escherichia coli*

Frozen *Escherichia coli* (TOP10, XL-1 Blue or XL-1 Blue) aliquots were thawed on ice and transferred to chilled eppendorfs. DNA (1-10ng) was gently mixed with the cells and incubated on ice for 30 minutes. Cells were then heat-shocked at 42°C in a thermomixer for 60 seconds and returned to ice for a further 2 minutes. Transformed cells were allowed to grow in antibiotic free SOC media for 60 minutes at 37°C with agitation (500rpm in thermomixer), prior to spreading onto appropriate antibiotic selection plate. Plates were incubated at 37°C overnight in an incubator. Individual colonies were picked into Luria-Bertani (LB) broth containing selection antibiotics

and grown at 37°C overnight, in an incubator with a shaking platform to agitate cultures, for DNA purification and restriction enzyme analysis.

2.4 DNA Purification

Mini-prep (1-10ml) DNA purifications were performed using the Wizard SV Miniprep kit (Promega) as per manufacturers instruction. Large scale (100-500ml) DNA purifications were performed using the Qiagen Endotoxin Free Maxi-prep kit (Qiagen, Crawley, UK) as per manufacturers instruction.

Diagnostic restriction digests were performed on purified DNA with the appropriate restriction enzymes (Promega) and resolved on 1-2% agarose (Seakem, Rockland, Maine, USA) gels containing 0.3µg/ml ethidium bromide to enable UV visualisation. The Pharmacia Biotech Ultraspec 2000 UV spectrophotometer was used to quantify purified DNA.

Where necessary, restriction digest products were gel purified using the Quick Gel extraction kit (Qiagen), as per manufacturer's instruction.

Ethanol precipitation was used to purify DNA products following restriction digests where it was necessary to keep the loss of DNA to a minimum. NaAc was added to the restriction digest at 1/10 total digest volume. EtOH was added at 2X total digest volume and 1µl glycogen was added as a carrier. Samples were spun down and the resulting pellet was washed in 70% (v/v) EtOH before being resuspended in an appropriate volume of dH_2O.

2.5 Cell Transfection

2.5.1 Transient transfections

Transient transfections of $\alpha\beta$-py and CHO-K1 cells were performed with Lipofectamine™ and the Plus reagent (Invitrogen). Cells were seeded at an appropriate density so as to reach 50-70% confluency overnight in 60/100mm tissue culture treated dishes (Corning, High Wycombe, UK). Purified DNA was placed in 5ml BD Falcon tubes (Part No: 352034, Oxford, UK) in a volume ranging 1-20µl. The DNA was pre-complexed with 110µl of the Plus reagent and gently mixed. The

Plus reagent mixture contained Plus reagent 0.25% (v/v) diluted in DMEM containing 1% non-essential amino acids (+AA). Following a 15 minute room temperature incubation, the DNA was complexed with 110µl of the Lipofectamine mixture and gently mixed. The Lipofectamine mixture contained Lipofectamine reagent 0.25% (v/v) diluted in DMEM(+AA). Following a further 15 minute incubation, the transfection mixture was made up to a final volume of 4ml in warmed DMEM(+AA) and placed onto washed cells. Cells were incubated for 5 hours at 37°C and then fed with complete media (4ml). Twenty four hours after transfection, media containing DNA and Lipofectamine was removed and replaced with fresh complete media. For experiments where protein kinase activities were to be assessed, the transfection media was replaced with quiescent media. Forty eight hours post-transfection cells were either lysed for SDS-PAGE analysis or used for integrin affinity analysis.

2.5.2 Production of stable cell lines.

For each plasmid DNA to be stably expressed, CHO-K1 cells were transfected in 100mm dishes using 3µg of plasmid DNA. Forty eight hours post transient transfection, CHO-K1 complete media was supplemented with G418 at 800µg /ml (stable selection media). Stable selection media was replaced frequently as untransfected cells began to die and selected cells grew back to confluency. Once the 100mm plates were fully confluent, cells were trypsinised, washed and resuspended in PBS (w/o ca and mg). The single cell suspension was seeded into 96-well plates at a density of approximately one cell/well. Cells were incubated at 37°C until clonal growth was observed in the wells (colour change). Cells were trypsinised from the wells and plated out in duplicate wells (of 6-well plates) and grown to confluency in selection media. The expression of some gene products is not well tolerated, such that cells which have either low or no protein expression may be preferentially selected. Therefore, it is desirable (and in the case of cells which are not morphologically transformed, critical) to test the selected populations for expression of the gene of interest. This was carried out by SDS page and western blot analysis or by intracellular FACS staining using one set of the duplicate wells, the second well was maintained to grow up gene positive clones.

2.6 Assessment of protein concentration

Protein concentrations were quantified using BCA protein reagent (Pierce, IL, USA). A protein standard curve was generated using bovine serum albumin (Sigma) at a range of 0.1-0.5mg/ml diluted in 1:5 lysis buffer. Samples were diluted 1 in 5 in dH_2O and 10µl incubated with 200µl BCA reagent (30 minutes, 37°C) in 96 well plates. Protein concentration was determined using an automated plate reader (MRX microplate reader, Dynatech, Chantilly VA).

2.7 SDS Page and Western Blotting

2.7.1 Cell Lysis

Transfected cells were washed once with ice-cold PBS and lysed at 4°C in an appropriate volume of lysis buffer. Lysates were shaken for 20 minutes at 4°C and then cleared by centrifugation at 13000rpm for 10 minutes at 4°C, assessed for protein concentration (described in 2.6) and solubilised in 4x sodium dodececyl sulphate polyacrylamide gel electrophoresis (SDS-PAGE) sample buffer at 99°C for 5 minutes. Samples were analysed immediately or stored at -20°C for future analysis.

BUFFERS:

Lysis buffer: 50mM Hepes (Na Salt), 0.3M NaCl, 1.5mM $MgCl_2$, 1.2mM EDTA, 0.5% Triton X-100 (v/v), 20mM β-glycerphosphate, 100mM sodium fluoride, 10mM sodium pyrophosphate, 1mM sodium vanadate and 0.5mM dithiothreitol (DTT). One Complete™ protease inhibitor tablet (Boehringer Manheim, Lewes, UK) was added per 50ml of lysis buffer.

2.7.2 SDS PAGE and Western Immunoblotting

Samples were cooled, or thawed from frozen, and equal amounts of protein (10-100µg) were resolved on SDS polyacrylamide gels using a vertical electrophoresis tank Biorad Protean 3 system (Biorad, Hemel Hempstead, UK). Samples were electrophoresed at 100-150 volts using SDS-Tris-glycine electrophoresis buffer for 1-2 hours alongside pre-stained molecular weight markers (Invitrogen, Paisley, UK).

For optimal separation, 8% gels, 10% and 12% gels were used for analysis of 60-120 kDa proteins, 40-70 kDa proteins and 10-40 kDa proteins respectively.

Proteins were transferred onto Hybond C nitrocellulose membranes (Amersham Pharmacia Biotech, Amersham, UK) in a methanol based transfer buffer at 400 milliamps for 1 hour using a Mini Protean II blotting tank (Biorad, UK). Equal protein loading was confirmed by incubating blots for 5 minutes in Ponceau S staining solution (Sigma). Non-specific protein binding sites on the membranes were blocked by incubation with TBS-Tween 20 containing 5% non-fat dried milk powder for 1 hour at room temperature. Membranes were probed with appropriate primary antibodies (Table 2.1) diluted in TBS-Tween 20 containing 5% non-fat dried milk powder overnight at 4°C. Membranes were washed in TBS-Tween 20 (3 x 10 minute washes) before species appropriate horseradish peroxidase (HRP) conjugated secondary antibody (DAKO, Ely, UK) (diluted in TBS-Tween 20 containing 5% non-fat dried milk powder) was added for 1 hour (Table 2.1). Finally, membranes were washed as above and immunoreactive bands were identified using enhanced chemiluminescence (ECL) (Amersham Pharmacia Biotech, Amersham, UK) as per manufacturer's instructions.

BUFFERS:

4x SDS-PAGE sample buffer: 50mM Tris-HCl, 10% (v/v) glycerol, 2% (v/v) SDS, 0.1% (v/v) bromophenol blue and 10% (v/v) β-mercapoethanol.

SDS polyacrylamide gels: Resolving Gel - 0.375M Tris base (pH8.8), 0.1% (v/v) SDS, 8-12% (v/v) acrylamide (Life Technologies, Paisley, U.K.), 0.1% (v/v) ammonium persulphate and 0.08% (v/v) TEMED.

Stacking Gel – 0.13M Tris Base (pH8.8), 0.15% (v/v) SDS, 4.6% (v/v) acrylamide, 0.13% (v/v) ammonium persulphate and 0.1% (v/v) TEMED.

Gel electrophoresis buffer: 5mM Tris base (pH8.3), 25mM glycine and 0.01% (v/v) SDS.

Transfer buffer: 210mM glycine, 24.7mM Tris base and 20% (v/v) methanol.

TBS-Tween 20 Wash buffer: TBS containing 0.2% (v/v) Tween 20 (Sigma).

Primary Antibody	Dilution	Secondary Antibody	Dilution
Ha Antibody (Y-11)	1:500	Anti-Rabbit HRP	1:1000
Myc Antibody (9E10)	1:1000	Anti-Mouse HRP	1:1000
Phospho-ERK1/2	1:2000	Anti-Mouse HRP	1:1000
ERK2 (C-10)	1:2000	Anti-Rabbit HRP	1:1000
FLAG (M2) monoclonal	1:3000	Anti-Mouse HRP	1:1000
Raf-1 (E-10)	1:1000	Anti-Mouse HRP	1:1000

Table 2.1 Immunoblotting antibody dilutions

2.8 Integrin affinity determination by flow cytometry

2.8.1 Cell Staining

Integrin affinity in transfected cells was analysed by three-colour flow cytometry, forty eight hours post transfection. Cells were transfected with test DNA (0-10μg) together with 0.75μg Tac-α_5 transfection reporter construct (extracellular domain of the IL-2 receptor and the intracellular domain of the α_5 integrin). Single cell suspensions of trypsinised cells were resuspended in a total volume of 50μl containing 0.4% (v/v) PAC1 ascites (gift from S. Shattil, Scripps Institute, La Jolla, USA or purchased from Becton Dickinson, Oxford, UK) (Shattil *et al.*, 1985) for 30 minutes at room temperature in Hepes/NaCl buffer. Internal controls for each sample were performed containing either 5mM EDTA or 100μM $MnCl_2$. Cells were washed with cold PBS (w/o ca and mg) and incubated on ice with 50μl DMEM containing 4% (v/v) anti-mouse IgM-FITC (Biosource, Nivelles, Belgium) for 30 minutes in the dark. Cells were washed with cold PBS and incubated for a further 30 minutes with 50μl DMEM containing 2% (v/v) anti-Tac-R-phycoerythrin (R-PE) (DAKO, Ely, UK). Cells were finally washed and resuspended in cold PBS. Immediately prior to analysis on a FACS-Caliber (Becton Dickinson, Oxford, UK), ToPro3 (Molecular probes, Leiden, Netherland) was added to each sample at a final concentration of 1μM (in PBS).

Hepes/NaCl buffer: 20mM Hepes, 140mM NaCl, 1.8mM $CaCl_2$, 1mM $MgCl_2$ and 2mg/ml Glucose, pH 7.4.

2.8.2 FACS and data analysis

PAC1 binding was determined by gating for live and highly transfected cells (ToPro3 negative and high Tac binding respectively). To obtain numerical estimates of integrin activation, an integrin activation index (AI) was calculated.

$$AI = ((F_N - F_I) / (F_A - F_I)) \times 100 \text{ and Percent Inhibition} = ((AI_0 - AI) / AI_0) \times 100$$

F_N: Geometric mean fluorescence intensity (MFI) of PAC1 binding of the native integrin

F_I: MFI of PAC1 binding in the presence of 5mM EDTA

F_A: MFI of PAC1 binding in the presence of 100µM Mn^{2+}

AI_0: Activation index with the control vector

AI: Activation index with DNA under test

2.9 Stable expression determination by flow cytometry

2.9.1 Intracellular staining

Stable protein expression was analysed by flow cytometry following antibiotic selection. Single cell suspensions of trypsinised cells were fixed in 100µl PBS containing 70% (v/v) ice cold methanol for 20 minutes on ice. Cells were washed with cold FACS Flow (Becton Dickinson, Oxford, UK) and resuspended in 150µl permeabilisation buffer (mixing gently with a pipette) for 10 minutes at room temperature. Cells were washed with FACS Flow and resuspended in a total volume of 50µl permeabilisation buffer containing appropriate primary antibodies for 30 minutes at room temperature. Cells were washed with cold permeabilisation buffer and incubated on ice with 50µl permeabilisation buffer containing appropriate FITC-conjugated secondary antibodies for 20 minutes on ice in the dark. Cells were finally washed and resuspended in cold FACS Flow. Cells were analysed on a FACS-Caliber (Becton Dickinson, Oxford, UK).

Permeabilisation buffer: 0.5% Saponin (Sigma) (v/v) in FACS Flow, pH 7.4.

Primary Antibody	Dilution	Secondary Antibody	Dilution
Ha Antibody (Y-11)	1:50	Anti-Rabbit IgG FITC	1:50
Myc Antibody (9E10)	1:50	Anti-Mouse IgG FITC	1:50
FLAG (M2) monoclonal	1:400	Anti-Mouse IgG FITC	1:50

Table 2.2 Intracellular FACS staining antibody dilutions.

2.9.2 FACS and data analysis

Primary antibody binding was determined by gating for untransfected controls (primary antibody negative), gated labelled M1. Numerical estimates for expression of subsequent samples obtained from the percentage of cells positive for primary antibody, gated labelled M2.

2.10 Gene subcloning

H-Ras G12V and R-Ras G38V genes were obtained from Dr. M. H. Ginsberg (Scripps Research Institute, La Jolla, USA). H-Ras G12V and R-Ras G38V were cloned vectors pDCR and pSG5 respectively. To permit stable cell selection, genes were subcloned into pCDNA3.1(+) (see Appendix I for construct map).

R-Ras G38V was subcloned into pCDNA3.1(+) using a simple EcoRI restriction digest from pSG5, followed by ligation into a pre-cut pCDNA3.1(+) vector. Cells were transformed with the ligation products (see section 2.3). Plasmid DNA positive for a 600bp insert were sent for sequence analysis to check for correct insert orientation.

H-Ras G12V was amplified from pDCR using high-fidelity PCR, with forward and reverse primers designed against H-Ras G12V (see Table 2.3). Following amplification, PCR products were cloned into pGEMT- vector prior to subcloning into pCDNA3.1(+).

2.10.1 High fidelity PCR of genes

Primers were designed flanking the gene of interest. All primers were screened against Genbank databases to check for mismatches or cross-reactivities, none were

found. High fidelity PCR was performed using Pfu Turbo DNA polymerase (Stratagene, Amsterdam, Netherlands). Fifty nanograms of template DNA were amplified in a reaction volume of 50µl containing (1X Pfu reaction buffer (contains 2mM MgSO4), 0.2mM of each dNTP, 0.2µM of each primer and 2.5U of Pfu polymerase). Reactions were performed on a MWG Primus 96 Plus machine (Ebersberg, Germany), with standard cycle conditions (unless otherwise stated) which involved a 1 minute incubation at 95°C followed by 25 cycles at 95°C for 1 minute, 62°C for 1 minute and 72°C for 1 minute. After this, a final step at 72°C for 10 minutes was followed by cooling to 4°C. PCR products were resolved on a 1% agarose gel containing 0.3µg/ml ethidium bromide to enable UV visualisation.

Construct	Primer Sequence
JLHRasHAF	5'-CTAGAAGCTTTATCCTTATGACGTGCCTGAC-3'
EcoHRasR	5'-CCGGAATTCTCAGGAGAGCACACACTTGCAGCT-3'
(F=Forward, R=Reverse)	

Table 2.3 Primers for H-Ras G12V high fidelity PCR

2.10.2 Cloning of genes into pGEMT vector

PCR products were ethanol precipitated and 500ng of the product was used in a poly-A-tail reaction containing 2mM dATP and 2.5U standard Taq polymerase (Promega, Southampton, UK), reactions were performed for 30 minutes at 70°C. Poly-A-tailed PCR products were ligated into the pGEMT vector (Promega) using the Rapid Ligation kit. Ligations were performed as per manufacturers instructions using 50ng of pre-cut pGEMT vector and a 3:1 insert ratio. Following a 2 hour ligation at room temperature, 50% of the ligation mixture was transformed into DH5α *E.Coli* and spread onto LB agar plates containing 50µg/ml ampicillin, 0.5mM isopropylthio-beta-D-galactoside (IPTG) and 80µg/ml 5-Bromo-4-chloro-3-indoyl beta-D-galactopyranoside (X-Gal). White colonies were subsequently amplified and screened for correct insert size by appropriate restriction digests.

Successful ligations were sent for sequencing either at Genetix Genescreen or an in-house sequencing facility using the ABI automated fluorescence sequencing kit. Sequences from clones that matched the template DNA were subsequently used for sub-cloning into the pCDNA3.1 (+) vector.

2.11 Site-directed mutagenesis

Site-directed mutagenesis was carried out using the QuikChange® Multi Site-Directed Mutagenesis Kit (Stratagene) as per manufacturers instructions. In brief: firstly, mutagenic primers (listed in Table 2.4) were used in a high fidelity PCR (see 2.10.1) of template, 50ng of (R-Ras (G38V) in pCDNA3.1 (+)). Secondly, the PCR products are treated with the restriction endonuclease *Dpn*1. DNA isolated from most *E.Coli* strains is dam methylated, the *Dpn1* endonuclease (target sequence 5'-Gm6ATC-3') is specific for methylated and hemimethylated DNA and is used to digest parental DNA template and to select for the newly synthesised DNA, containing the required mutation. In the third step, the reaction mixture, enriched with multiply mutated single strand DNA, is transformed into XL-1 Blue Competent cells (Stratagene, La Jolla, CA, USA) (see section 2.3).

Construct	Primer Sequence
JLsdm1F	5'-GTGCGGGCTGTCCGGAAACACCAGGAACAAGAGCTCCCA-3'
JLsdm1R	5'-TGGGAGCTCTTGTTCCTGGTGTTTCCGGACAGCCCGCAC-3'
JLsdm2F	5'-CGGGCTGTCCGGAAATACAAGGAACAAGAGCTCCCACCG-3'
JLsdm2R	5'-CGGTGGGAGCTCTTGTTCCTTGTATTTCCGGACAGCCCG-3'
JLsdm5F	5'-CGGAAATACCAGGAACAAAAGCTCCCACCGAGCCCTCCC-3'
JLsdm5R	5'-GGGAGGGCTCGGTGGGAGCTTTTGTTCCTGGTATTTCCG-3'
JLsdm5aaF	5'-GCTGTCCGGAAACACAAGCTGCGGAAGCTGCCACCGAGCCCT-3'
JLsdm5aaR	5'-AGGGCTCGGTGGCAGCTTCCGCAGCTTGTGTTTCCGGACAGC-3'
(F=Forward, R=Reverse)	

Table 2.4 Site Directed Mutagenesis Primers

2.12 Splice-overlap Extension by PCR

Splice-overlap extension by PCR was carried out according to Warrens *et al.*, (1997). In brief, high fidelity PCR (see section 2.10.1) was used to generate PCR products in all stages of this method. $MgCl_2$ (BDH) concentrations were optimised for splice-overlap PCR, and a concentration of 3.5mM $MgCl_2$, was found to the most efficient concentration. Reactions were performed in a final volume of either 25 or 50µl. Table 2.5 provides a list of the primers used. See Chapter 5 (figure 5.11) for schematic representation of SOE by PCR.

In all first stage reactions, 50ng of template DNA (R-Ras G38V) and 125ng of each oligonucleotide primer were added. The PCR protocol used at this stage (unless

otherwise stated) involved an initial melting step at 95° for 1 minute, followed by 30 cycles as follows: 92°C for 90s, 55°C for 90s, and 72°C for 1 minute (usually 1 minute per kb of template). After this, a final step at 72°C for 15 minutes was followed by cooling to 4°C. Appropriate PCR controls were performed for each reaction. Following the first stage, the PCR products were gel purified (see section 2.4) and used in the second-stage reaction.

Equimolar amounts of the first stage intermediate products were added to the second stage reaction, along with 125ng of appropriate primers and 3.5mM $MgCl_2$. The PCR protocol used at this stage (unless otherwise stated) involved an initial melting step at 95°for 1 minute followed by 4 cycles at : 95°C for 90s, 58°C for 90s, and 72°C for 2 minutes (usually 1 minute per kb of template), followed by 25 cycles at: 95°C for 90s, 68°C for 90s, and 72°C for 2 minutes. After this, a final step at 72°C for 15 minutes was followed by cooling to 4°C. The final product was gel-purified and cloned into pCDNA3.1(+). Positive clones were verified by sequencing.

Construct	Primer Sequence
PCR1fwdFLAG	5'-CGAGAATTCATGGACTACAAAGATGACGATGACATGAGC AGCGGGGCGGCGTCC-3'
SplicePCR1rev	5'-GTAGAAGGCATCCTCCACTCCCTGCCGGGTCTTGGCCGAG GCCTC-3'
SPLPCR2fwd	5'-ACGTTGGTGCGTGAGATCCGGCAGCACCAGGAACAAGAG CTCCCACCGAGCCCT-3'
splicePCR2rev	5'-CGAAAGCTTCTACAGGAGGACGCAGGGGCAGCC-3'
PCR1fwdFLAGHind	5'-CGAAAGCTTATGGACTACAAAGATGACGATGACATGAGC AGCGGGGCGGCGTCCGGGACA -3'
PCR1RevOvlp	5'-CACCAACGTGTAGAAGGCCTCCACTCCCTGCCGGGTCTTGG CCGAGGCCTC-3'
PCR2FwdOvlp	5'-GAGGCCTTCTACACGTTGGTGCGTGAGATCCGGCAGCACCA GGAACAAGAGCTCCCACCGAGCCCTCCC-3'
splPCR2RevEco	5'- CGAGAATTCCTACAGGAGGACGCAGGGGCAGCC-3'
(F=Forward, R=Reverse	

Table 2.5 Primers for SOE by PCR

2.13 ERK activity assay

Cells were transfected as described in section 2.5.1, and quiesced 24 hours prior to lysis. Samples were lysed on ice as for SDS-PAGE in 0.5ml kinase lysis buffer. Lysates were cleared by centrifugation at 13000rpm for 10 minutes and protein concentration determined (see section 2.6). Protein concentrations were normalised to approximately 1mg/ml and 400µl of each cell lysate was incubated with 2µg of

anti-ERK2 (C-14) antibody (Santa Cruz) for 1 hour at 4°C. Anti-mouse agarose beads (20µl/ sample, Sigma) were added and the samples vortexed for 1 hour at 4°C. Agarose beads were washed 3x in Wash buffer and once in Kinase buffer. Each sample was incubated at 30°C for 20 minutes in 20µl of kinase buffer containing 10µg myelin basic protein, 100µM ATP and 1µCi γ-^{33}P ATP (500Ci/mmol) (Amersham Pharmacia Biotech). Samples were spotted onto Whatman p81 paper (Whatman Inc, new Jersey, USA) and washed extensively in 0.5% phosphoric acid and allowed to dry, radioactivity was quantified by liquid scintillation counting using 'Flo-Scint' IV (Packard, Biosciences, Groningen, Netherlands) and a Packard 1900 TR liquid scintillation counter.

BUFFERS: (all made up with dH_2O, at pH7.4, unless otherwise stated)

Kinase lysis buffer: 25mM Hepes (Na Salt), 0.3M NaCl, 1.5mM $MgCl_2$, 0.2mM EDTA, 0.5% Triton X-100 (v/v), 20mM β-glycerphosphate, 1mM sodium vanadate (pH7.4) and 0.5mM DTT. One Complete™ protease inhibitor tablet (Boehringer Manheim, Lewes, UK) was added per 50ml of lysis buffer).

Wash buffer: 20mM Hepes (Na Salt), 50mM NaCl, 2.5mM $MgCl_2$, 0.1mM EDTA

Kinase buffer: 20mM Hepes (Na Salt), 0.5mM sodium fluoride, 7.5mM $MgCl_2$, 0.2mM EGTA, 10mM β-glycerphosphate, 0.5mM sodium vanadate (pH7.4), 2mM DTT and Complete™ protease inhibitor tablet.

2.14 ERK 1/2 ELISA

ERK 1/2 ELISA [pTpY185/187] carried out as per manufacturers instructions (Biosource International).

In brief: twenty-four hours post transfection cells were quiesced and the following day cells were lysed (as described in 2.7.1). Protein concentrations were normalised (see section 2.6) and cell lysates and standards were added to wells coated with ERK1/2 specific monoclonal antibody and incubated for 2 hours at room temperature. Wells were washed and 100µl of antibody specific for ERK1/2 phosphorylated at threonine 185 and tyrosine 187 was added to the wells for 1 hour at room temperature. Wells were washed and 100µl anti-rabbit IgG-HRP was added for 30 minutes at room temperature. Wells were washed and 100µl of Stabilised

Chromogen was added to each well for 30 minutes at room temperature in the dark. A Stop solution was added and absorbance was read at 450nm. The intensity of this coloured product was directly proportional to the concentration of ERK1/2 [pTpY185/187] present in the original sample.

2.15 2-Step Raf kinase assay

Cells were transfected as described in section 2.5.1, and quiesced 24 hours prior to lysis. Samples were lysed on ice in 0.5ml Barnard lysis buffer. Lysates were cleared by centrifugation at 13000rpm for 10 minutes and protein concentration determined (see section 2.6). Protein concentrations were normalised and 400µl of each cell lysate incubated with 1µg of Raf-1 (E-10) antibody for 1 hour at 4°C. Anti-mouse IgG agarose beads (25µl / sample, Sigma) were added and the samples vortexed for 1 hour at 4°C. Agarose beads were washed 3x in 500µl RIPA buffer and then 2x in 500µl Dilution buffer. Sample volumes were adjusted to 30µl using Dilution buffer.

First step: Sample (10µl) was incubated for 15 minutes at 30°C in 15µl of dilution buffer containing 0.1µg His-tagged MEK-1 (FL, Santa Cruz), 1µg His-tagged ERK p42 (ERK2) (FL, Santa Cruz) and 5µl Mg^{2+}/ATP buffer. The kinase reaction was terminated by addition of 100µl ice cold Assay buffer. Samples were incubated on ice. The remaining Raf IP was retained for western blot analysis to assure equal Raf precipitation.

Second step: Activated ERK2 samples (25µl) were incubated for 15 minutes at 30°C in 25µl reaction mix containing 23µl myelin basic protein (MBP) substrate (0.61µg/ul, Gibco), 2µl Reaction Start Mix (37.5mM $MgCl_2$ and 1.25 mM ATP) and 0.2µl ^{32}P-γ-ATP (3000µCi/mmol). Reactions were terminated by addition of 16.7µl 4x SDS-gel sample buffer. Samples were run on a 12.5% gel, the solvent front was removed (contains free ATP).

Gels were exposed to a Molecular Dynamics phospho-screen and analysed on a Molecular Dynamics Storm™ 860 phospho-imager (Amersham Pharmacia Biotech, Amersham, U.K.). Band density was performed with ImageQuant 5.0 software (Amersham Pharmacia Biotech). Gels were also exposed to Kodak X-Omat film (Sigma), overnight at room temperature, with an intensifying screen.

BUFFERS: (all made up with dH_2O, unless otherwise stated)

Barnard Lysis buffer: 20mM Tris (pH8), 2mM EDTA, 1% Triton X-100 (v/v), 10% glycerol (v/v), 10mM β-glycerphosphate, 2mM sodium fluoride, 2mM sodium pyrophosphate and 5mM sodium vanadate (pH9). One Complete^{TM} protease inhibitor tablet (Boehringer Manheim, Lewes, UK) was added per 50ml of lysis buffer).

RIPA buffer: 20mM TrisHCl (pH7), 150mM NaCl, 1% Triton X-100 (v/v), 0.5% Deoxycholate (w/v) and 0.1% SDS (w/v).

Dilution buffer: 50mM Tris (pH7.5), 75mM NaCl, 5mM EGTA and 5mM $MgCl_2$.

Mg2+/ATP buffer: 50mM $MgCl_2$ and 0.8mM ATP.

Assay buffer: 1mM DTT and 1mM sodium vanadate.

2.16 Immunofluorescence

Transfected cells or stable cell lines were grown on sterile glass cover slips (22 x 22 mm, Fisher, Loughborough, UK) placed within 6-well tissue culture plates (Corning, High Wycombe, UK), and left overnight in complete medium at 37°C.

Cells to be examined live were washed gently with PBS and then non-specific binding sites were blocked with 0.2% (w/v) fish skin gelatin (FSG)/PBS (Sigma) for 20 minutes at room temperature. Cells were probed with appropriate primary antibodies (Table 2.5) diluted in 0.2% FSG for a minimum of 1 hour at room temperature. Cells were washed with PBS (3x 2 minute washes) before species appropriate Alexa-Fluor –conjugated antibodies (Molecular Probes, The Netherlands) was added, diluted in 0.2% FSG for 30 minutes on ice and in the dark. Cover slips were removed from the tissue culture plates, washed in PBS and allowed to dry before mounting on slides using Mowiol mounting medium (Calbiochem, Nottingham, UK).

Where cells could be fixed, cells were washed in PBS and a solution of 3% (w/v) paraformaldehyde (PFA) was added to cells for 20 minutes at room temperature. PFA was removed and 50mM NH_4Cl (made up in dH2O) added to quench aldehyde groups for 10 minutes at room temperature. Cells were washed further with PBS and non-specific binding sites were blocked with 0.2% (w/v) FSG/PBS (Sigma) for 20

minutes at room temperature. Cells were probed with appropriate primary antibodies (Table 2.6) diluted in 0.2% FSG for a minimum of 1 hour at room temperature. Cells were washed with PBS (3x 2 minute washes) before species appropriate Alexa-Fluor –conjugated antibodies (Molecular Probes, The Netherlands) was added, diluted in 0.2% FSG for 30 minutes on ice and in the dark. Cover slips were removed from the tissue culture plates, washed in dH2O and allowed to dry. Cells were mounted on slides using Mowiol.

All cells were visualised using a Leica TCS NT confocal microscope (Leica Microsystems, Heidelburg GmbH) and images captured and analysed using Leica Confocal Software - Lite Version (Leica Microsystems, Heidelburg GmbH).

Primary Antibody	Dilution	Secondary Antibody	Dilution
Ha Antibody (Y-11)	1:100	Alexa 488-conjugated goat anti-rabbit IgG	1:200
Myc Antibody (9E10)	1:100	Alexa 568-conjugated goat anti-mouse IgG	1:200
Myc Antibody (A-14)	1:100	Alexa 568-conjugated goat anti-rabbite IgG	1:200
FLAG (M2) monoclonal	1:250	Alexa 568-conjugated goat anti-mouse IgG	1:200
Rhodamine-conjugated Phallodin	1:50		
Vinculin (hVIN-1) monoclonal	1:400	Alexa 568-conjugated goat anti-mouse IgG	
Rhodamine-conjugated Cholera toxin (B)	1:50	Anti-Cholera toxin	1:100

Table 2.6 Immunofluorescence antibody dilutions

2.17 Incorporation of exogenous GM1 in cell membranes

Incorporation of GM1 was performed as described by Rusnati *et* al., (1999). In brief, CHO-K1 cells were seeded at 5 x 10^5 cells per 100mm plate and left to adhere overnight in complete medium. Cell media was then replaced with medium containing 0.4% (v/v) FCS with 100μM GM1 (Sigma) for a further 96 hours. At the end of incubation, cells were washed with PBS, trypsinised, and used for further experimentations.

Stock solutions of GM1 were prepared in methanol (as per manufacturers' instructions) and stored at -20°C.

2.18 CTB-patch staining

Lipid raft aggregation or patch staining was adapted from Janes *et al.*, (1999). Cells were seeded onto coverslips, in 6-well plates and transfected with appropriate constructs (see section 2.5.1). Cells were quiesced 24 hours prior to treatment. Forty eight hours post transfection; cells were labelled with 10µg/ml rhodamine-conjugated cholera toxin B (List Biological Laboratories, Quadratech, Epsom, UK) made up in PBS with 0.1% BSA, for 1 hour on ice and in the dark. Cells were then washed 3x with PBS. In cross-linking experiments, cells were further incubated with rabbit anti-cholera toxin IgG (Sigma; 1:100 in PBS with 0.1% BSA) for 30 minutes on ice, followed by a 20 minute incubation at 37°C (in the dark). After three washes in PBS, coverslips were mounted onto slides in Mowiol and visualised (see section 2.16).

2.19 Methyl-β-Cyclodextrin (MβCD) membrane disruption

For all cells, transfections were carried out as described in section 2.5.1 and cells quiesced 24 hours prior to treatment. Samples required for flow cytometry were trypsinised and neutralised using Soybean Trypsin inhibitor (Sigma) prior to MβCD-treatment, cells were resuspended in 2ml of quiescent media. Cells required for immunofluorescence were left attached to coverslips inside 6-well plates with 2ml of quiescent media.

Cells were treated with PBS containing MβCD (Sigma) to a final concentration of 1% and incubated for 1 hour at 37°C. Following incubation, MβCD-containing media was removed (by centrifugation for suspended cells) and cells resuspended in 2ml quiescent media. For experiments requiring cholesterol replenishment, 0.5mM cholesterol/ml was added to quiescent media for 1 hour at 37°C in the form of cholesterol-MβCD inclusion complexes. Cholesterol-MβCD inclusion complexes were produced as described by Klein *et al.*, (1995). In brief, a solution of 30mg cholesterol (Sigma) in 400µl of 2:1 (v/v) methanol/chloroform was added drop-wise to a stirred solution of 1g MβCD in 11ml PBS prewarmed in an 80°C waterbath. The solution was stirred at 80°C until a clear solution resulted. The cholesterol-MβCD inclusion complexes were used immediately or aliquoted and lyophilised. For convenience, 375µl (5 x 69.4µl) aliquots of the cholesterol-MβCD inclusion complex

solution were lyophilised. For use, the individual aliquots could be resuspended in 5ml PBS to provide 5 x 1ml treatments (0.5mM cholesterol).

Following treatment, cells were washed in PBS. Cells required for FACS analysis were then stained as described in section 2.8. Cells for immunofluorescence were left attached to coverslips and treated as mentioned in section 2.16.

2.20 Anchorage-independent growth assays (Colony assays)

For each cell line, single cell suspensions were prepared in triplicate at $2x10^3$ cells per well of a 6 well plate, in a 0.3% top agarose suspension, overlaid onto a 0.5% agarose bottom layer, and grown at 37°C for colony formation.

A 50:50 mixture of Seakem agarose (Cambrex Bioproducts, Maine): low melting point agarose (Sigma), was used to prepare 5% and 3% (w/v) (10x) stock solutions of agarose in sterile water, in autoclaved bottles. Solutions were boiled to dissolve the agarose and stored at room temperature. On the day of the assay, stock solutions were melted and maintained at 45°C in a water bath. The 0.5% agarose layer was prepared by diluting the 5% stock solution in warmed growth medium (i.e., DMEM + required serum concentration); 2ml were added to each well of a 6 well plate.

Once the bottom layer had set, a single cell suspension containing $1x10^3$ cells per ml of growth medium (i.e., DMEM + required serum concentration + any required antibiotics) was warmed and the melted 3% agarose stock was added to a final concentration of 0.3%. The cell and agarose suspension was mixed gently by pipetting to resuspend the cells uniformly, then 2ml per well was added to the hardened 0.5% agar base layer and left to set. Plates were covered with tinfoil, to prevent drying-out, and incubated at 37°C in a humidified 10% CO_2 environment.

On days 2, 4 and 6, the number of colonies from five random fields was counted for each replicate. Percentage cloning efficiency was calculated as follows:

$(((Mean / 5^{*}) \times 160^{\int}) / 2000^{\S}) \times 100.$

Mean Total colonies counted for each sample divided by the number of replicates (in this case, n=3).

* Number of fields viewed per well.

$\int$ (Well area/ view area). Multiplying by this figure allows an approximation of the total number of colonies per well to be made.

§ Number of cells seeded

2.21 Adhesion assays

For transiently transfected cells lines, 100mm plates of 40-60% confluent $\alpha\beta$-py cells were co-transfected with test DNA and a GFP-expressing construct. Twenty-four hours post transfection, cells were quiesced in preparation for the adhesion assay. With stable lines, 100mm plates were seeded with cell lines, to reach confluency 24 hours prior to assay. Stable cell lines were also quiesced in preparation for the assay.

Cell adhesion assays were performed using flat bottom tissue culture 96-well plates (Costar, Cambridge, USA). Wells were coated with appropriate matrix for 1 hour at 37°C (wells left uncoated as a negative control; for transiently transfected cells, wells were coated with 10µg/ml fibrinogen and for stably transfected CHO-K1 cells, wells were coated with 20µg/ml fibronectin). All wells were then washed with 200µl PBS and blocked using 100µl of 2% (w/v) BSA (made up in PBS) for 1 hour at room temperature.

Single cell suspensions of each cell line to be tested, were washed thoroughly and resuspended in DMEM (containing no additives) and diluted to $1x10^6$ cells per ml. Cell suspension (200µl) was added to triplicate wells. Each sample was plated out onto plastic (negative control), matrix coated test sample and a matrix coated whole cell control. Cells were incubated for the required time at 37°C. Plates were gently shaken on a thermomixer (800rpm, for 3x10 second intervals) and gently washed with PBS to remove any unadhered cells. Whole cell control wells were incubated until all cells adhered (checked using a microscope) or alternatively, plates were centrifuged for 5 minutes at 3000rpm. Transiently transfected cell (co-transfected

with GFP-construct) adhesion was determined using a fluorescent plate reader (Wallac Victor^2, 1420 Multi-label).

For stable cell lines, following the PBS wash of plastic negative controls and matrix coated wells, cells were fixed using 200µl of 3% paraformaldehyde (PFA) per well for 20 minutes. At this stage, whole cell controls were allowed to fully adhere naturally or they were 'splattered' by centrifuging the plate at 1000rpm for 5 minutes. Whole cell wells were then also fixed. Following fixation, wells were allowed to air-dry and cells stained using 100µl of 1% (w/v) methylene blue (made up in dH_2O) per well for 20 minutes. Plates were washed with tap water and then allowed to air-dry before the colour was eluted by the addition of 100µl of 0.1M HCl per well. Adhesion of stably transfected cells was determined using an automated plate reader (MRX microplate reader, Dynatech, Chantilly VA) at 630nm.

2.22 Migration assays

For transiently transfected cells lines, 100mm plates of 40-60% confluent $\alpha\beta$-py cells were co-transfected with a test DNA and a GFP-expressing construct (to serve as a positive control for transfection). Twenty-four hours post transfection, cells were quiesced in preparation for migration assay. With stable lines, 100mm plates were seeded with cell lines, to reach confluency 24 hours prior to assay. Stable cell lines were also quiesced in preparation for assay.

Cell migration assays were performed using Millipore Multiscreen Assay System 96-well filtration plates (Millipore). Where required, wells were coated on the underside only, (as per manufacturers instructions) with appropriate matrix for 1 hour at 37°C (for transiently transfected cells, wells were coated with 10µg/ml fibrinogen and for stably transfected CHO-K1 cells, wells were coated with 20µg/ml fibronectin). All wells were then washed with PBS and blocked using 2% (w/v) BSA (made up in PBS) for 1 hour at room temperature. Teardrop plates were washed and appropriate media conditions applied (150µl per teardrop well). A single cell suspension of each cell line to be tested was diluted in DMEM (containing no additives) to $5x10^5$ cells per ml and 100µl of cell suspension was added to appropriate wells. Each sample was plated out in triplicate and incubated for the required time at 37°C. Following incubation, the supernatant was removed from all wells and a cotton swap was used

to remove cells adhered to the upper surface of all wells excluding the whole cell controls.

Migration of transiently transfected cells (co-transfected with GFP-construct) was determined using a fluorescent plate reader (Wallac Victor^2, 1420 Multi-label). Stable cell lines were fixed using ice-cold 70% methanol and stained using the Diff-Quick system. Plates were washed with tap water and allowed to air-dry before eluting the colour by addition of 100µl of 0.1M HCl per well. Adhesion of stably transfected cells was determined using an automated plate reader (MRX microplate reader, Dynatech, Chantilly VA) at 630nm.

2.23 Wound assays

Freshly trypsinised cells ($0.5x10^6$) were seeded into 6-well plates in growth medium containing 10% serum and incubated overnight at 37°C to allow a confluent monolayer to form. At time point 0 hours, a p200 pipette tip was used to scrape a small wound through the centre of the cell monolayer. Wells were washed with sterile PBS to remove any dead or floating cells. Quiescent growth media was added to the cells. Cells were visualised on a Carl-Zeiss Axiovert 5100 microscope (Jena, Germany) and an image of an identified stretch of the wound captured using a Coolsnap cooled CCD camera and Openlab 3.01 software (Improvision, Lexington, USA). Cells were maintained in quiescent media at 37°C. At time points 24 hours and 48 hours post-wounding, wells were washed with PBS and following the addition of fresh quiescent media, images of the identified stretch of wound were re-captured.

2.24 Proliferation assays

Freshly trypsinised cells ($2x10^4$) were seeded into 100mm plates in growth medium containing 10% serum with one plate per day per cell line. The cells were incubated at 37°C and growth medium was refreshed every 2-3 days. For 8-10 consecutive days post-seeding, one plate per cell line was counted. Plates were washed with PBS to remove any dead or floating cells and the remaining adhered cells were trypsinised and resuspended in growth medium. An aliquot of cell suspension was removed for each sample and cell number was determined using a Coulter counter (Epics).

2.25 Statistical Analysis

Results are reported as pooled data from a series of n separate experiments and presented as mean ± S.E.M. Statistical significance was analysed by one-way analysis of variance (ANOVA) with comparisons between groups made using the Bonferroni Multiple Comparison Test (Prism software).

Statistical significance was assigned to data returning a P value of less than 0.05.

Appendix I

pCDNA3.1 (+) construct map

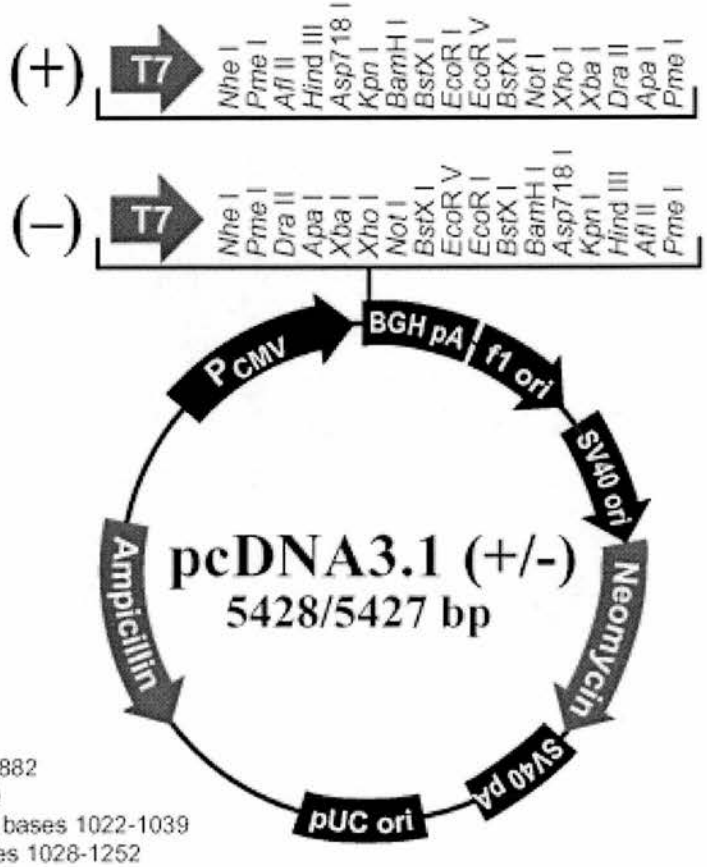

Comments for pcDNA3.1 (+)
5428 nucleotides

CMV promoter: bases 232-819
T7 promoter/priming site: bases 863-882
Multiple cloning site: bases 895-1010
pcDNA3.1/BGH reverse priming site: bases 1022-1039
BGH polyadenylation sequence: bases 1028-1252
f1 origin: bases 1298-1726
SV40 early promoter and origin: bases 1731-2074
Neomycin resistance gene (ORF): bases 2136-2930
SV40 early polyadenylation signal: bases 3104-3234
pUC origin: bases 3617-4287 (complementary strand)
Ampicillin resistance gene (*bla*): bases 4432-5428 (complementary strand)
ORF: bases 4432-5292 (complementary strand)
Ribosome binding site: bases 5300-5304 (complementary strand)
bla promoter (P3): bases 5327-5333 (complementary strand)

p-EGFP construct map

pEGFP-C3 Vector Information PT3052-5

GenBank Accession #: U57607 Catalog #6082-1

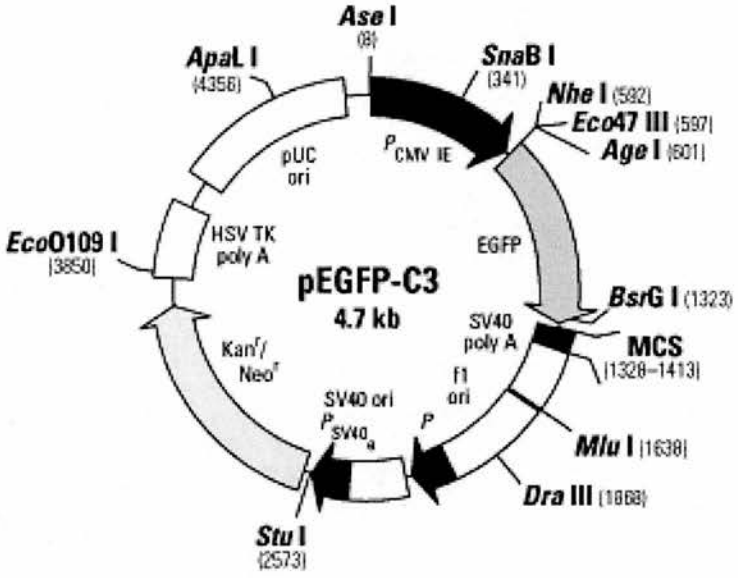

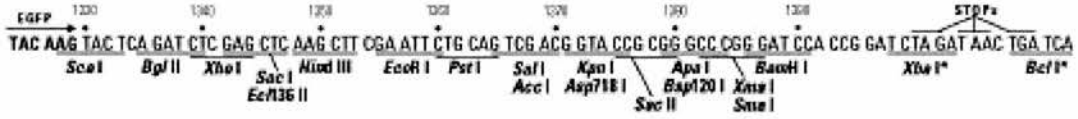

Restriction Map and Multiple Cloning Site (MCS) of pEGFP-C3. All restriction sites shown are unique. The *Bcl* I site cannot be used for fusions since it contains an in-frame stop codon. The *Xba* I and *Bcl* I sites (*) are methylated in the DNA provided by BD Biosciences Clontech. If you wish to digest the vector with these enzymes, you will need to transform the vector into a *dam*⁻ host and make fresh DNA.

Chapter 3

Integrin affinity modulation by H-Ras and R-Ras

3.1 Introduction

A central property of the integrin family of cell adhesion receptors is the capacity to rapidly modulate their ability to bind ligands. Integrins can use both affinity ('conformation change') and avidity (clustering of integrins) modulation to regulate ligand-binding strength.

Integrin affinity modulation is proposed to involve the propagation of conformational changes from the cytoplasmic tails to the extracellular ligand-binding sites, leading to a direct change in ligand-binding affinity (Hughes and Pfaff, 1998). One of the best-documented examples of integrin affinity modulation involves the binding of fibrinogen to platelets via the $\alpha_{IIb}\beta_3$ fibrinogen receptor. The affinity of $\alpha_{IIb}\beta_3$ is tightly regulated and modulated from within platelets by a phenomenon that has been referred to as 'inside-out' signalling (Ginsberg *et al.,* 1992). Following fibrinogen binding to $\alpha_{IIb}\beta_3$, clustering of integrin can cause tyrosine phosphorylation of specific platelet proteins resulting in 'outside-in' signalling to the cell (Haimovich *et al.*, 1993). Platelets have provided a useful model for examining integrin-affinity modulation. The PAC1 monoclonal (IgM isotype) antibody specifically recognises the activated $\alpha_{IIb}\beta_3$ integrin, by mimicking the binding characteristics of fibrinogen (Shattil *et al.*, 1985). The binding of PAC1 to platelets is stimulated by physiological agonists, such as ADP and thrombin, which are dependent upon divalent cations. The binding of fibrinogen to activated platelets can be inhibited by addition of EDTA (which chelates Ca^{2+}/Mg^{2+}) or stimulated by Mn^{2+}, which has often been used as an activator of ligand binding to integrins (Abrams *et al.*, 1994).

At present, the cytoplasmic signalling pathways regulating integrin affinity are poorly understood. A model system in Chinese Hamster Ovary (CHO) cells was developed to allow genetic and pharmacological study of integrin affinity modulation (O'Toole *et al.*, 1990). CHO cells were selected for this model due to their simple

maintenance and ease of transfection (Hughes *et al.*, 1997). CHO cells expressing $\alpha_{IIb}\beta_3$ fail to bind PAC1, even in the presence of $\alpha_{IIb}\beta_3$-activating stimuli including ADP, thrombin and phorbol esters (O'Toole *et al.*, 1990). Chimeric integrins, in which the extracellular and transmembrane domains of the α_{IIb} and β_3 are joined to the cytoplasmic domains of α_5, α_{6A}, α_{6B} and β_1 respectively, are constitutively active in CHO cells and restore PAC1 binding (O'Toole *et al.*, 1994). The combined properties of the active chimera and the activation-dependent PAC1 antibody, permit the use of the extracellular domain of $\alpha_{IIb}\beta_3$ as a reporter for cytoplasmic signalling events involved in integrin activation (Hughes *et al.*, 1997).

Using a CHO cell line stably expressing the chimeric integrin $\alpha_{IIb}\alpha_{6A}\beta_3\beta_1$ ($\alpha\beta$-py cells), complementary DNAs were screened for their ability to inhibit PAC1 integrin-binding. An active variant of the small GTP-binding protein, H-Ras, and its effector kinase, Raf-1, were capable of inhibiting PAC1 binding in a MAP kinase-dependent manner (Hughes *et al.*, 1997). Furthermore R-Ras, a small GTP-binding protein related to H-Ras, antagonises the Ras/Raf-initiated integrin suppression pathway (Sethi *et al.*, 1999). The changes in integrin affinity modulation by H-Ras and R-Ras appear to be both integrin- and cell type-specific.

In order to gain further understanding of the mechanisms of H-Ras- and R-Ras-mediated integrin affinity modulation, the $\alpha\beta$-py model system was employed for this thesis. The aim of this preliminary results chapter was to investigate whether the previous observations made by Sethi *et al.*, (1999), that H-Ras G12V mediated integrin suppression and that R-Ras G38V reverses H-Ras-mediated suppression, could be reproduced in this laboratory.

3.2 The αβ-py transfection system and detection of integrin affinity modulation

The αβ-py model system makes use of a stably expressed chimeric integrin on the cell surface which can be used, in conjunction with the PAC1 monoclonal antibody, as a reporter for integrin affinity modulation (Hughes *et al.*, 1997). The binding of the PAC1 antibody was detected by flow cytometry using a secondary anti-mouse IgM-FITC (fluorescein isothiocyanate) antibody.

A cell surface marker encoding the extracellular domain of the IL-2 receptor, known as Tac, and the intracellular domain of the α_5 integrin (Tac-α_5) was used as a marker for transfection efficiency. Transfection efficiency of αβ-py cells was detected by flow cytometry using an antibody against the IL-2 receptor, Tac-R-PE (R-phycoerythrin). The reporter construct Tac-α_5 has previously been titrated for maximal expression in αβ-py cells. It was found that transfection of 0.75μg of the construct, in 60mm plates, was sufficient to obtain a high degree of Tac-PE positive cells, without interfering with constructs under test.

Previous work in this laboratory has optimised transfection efficiency of αβ-py cells using Invitrogen's transfection reagent, Lipofectamine, in conjunction with their Plus reagent. All subsequent transfections have been performed with Lipofectamine in combination with the Plus reagent.

3.2.1 PAC1 antibody binding to αβ-py cells

Both the primary PAC1 mouse monoclonal antibody and the secondary anti-mouse IgM-FITC antibody have been previously titrated for maximal binding to the αβ-py cells. Figure 3.1 shows a representative histogram of FL-1 PAC1 binding in the FL1 channel. Compared to the IgM isotype control, the PAC1 antibody displayed a rightward shift in the FL1 channel with the mean fluorescence intensity increasing from 60.1 arbitrary units (AU) to 130.2 AU.

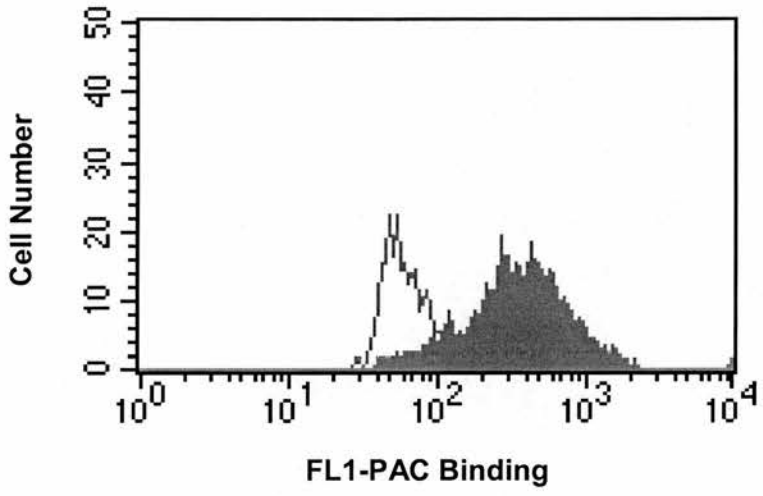

Figure 3.1 PAC1 antibody binding to $\alpha\beta$-py cells.

PAC1 antibody binding to $\alpha\beta$-py cells was determined by flow cytometry.
PAC1 antibody binding to $\alpha\beta$-py cells (solid grey) and IgM isotype matched control antibody (grey line). Histogram is representative of three experiments.

3.2.2 External control factors can modulate integrin affinity

To demonstrate integrin modulation by external factors, PAC1 binding was determined in the native integrin and in the presence of 5mM EDTA or 100μM Mn^{2+}. Figure 3.2A shows a representative histogram of three experiments of PAC1 binding in the presence of EDTA or Mn^{2+}. In the absence of any exogenous mediators, the mean fluorescence intensity of the native integrin was 97.4 ± 17.7 AU. Addition of EDTA led to a reduction in PAC1 binding which correlated with a drop in the mean fluorescence intensity (19.7 ± 3.4 AU). An increase in antibody binding was observed with addition of Mn^{2+} , the corresponding mean fluorescence intensity; 118.8 ± 21.4 AU.

Dot plots display PAC1 binding on the x-axis and Tac-PE antibody binding (transfection efficiency) on the y-axis. The quadrant markers on the dot blots distinguish between high and low integrin affinity status on the x-axis, as a measure of PAC1 binding and on the y-axis, highly transfected cells (red) against those of a lower transfection efficiency (blue). The quadrant marker separating highly transfected cells was set for each individual experiment to denote the top 20-25% of Tac-positive cells.

Figure 3.2B shows representative dot plots of cells transfected with control vector and Tac-α_5. In the native state, the majority of the highly transfected cells are in the upper right quadrant (67%). Addition of 5mM EDTA results in a leftward shift in the cell population, indicative of a loss of PAC1 binding, with the majority of the highly transfected cells moving towards the upper left quadrant (99.5%). Addition of 100μM Mn^{2+} leads to a rightward shift in the cell population. In the presence of this activating stimulus, the percentage of highly transfected cells in the high PAC binding upper right quadrant is increased to 77%. This demonstrates not only that $\alpha\beta$-py cells constitutively express the chimeric integrin $\alpha_{IIb}\alpha_{6A}\beta_3\beta_1$ in an active state but that the integrin can be modulated by external factors. The addition of 5mM EDTA or 100μM Mn^{2+} act as internal controls for each transfection representing a minimum and maximum of PAC1 binding within these cells. The mean fluorescence of PAC1 binding in the native, inactive and active states allow a numerical estimate of integrin activation to be calculated as an activation index (AI) as described in the

Materials and Methods (section 2.8.2) whereby 0 units represent an inactive integrin (+EDTA) and 100 units represents an active integrin (+Mn^{2+}).

3.2.3 The $\alpha_{IIb}\beta_3$ ligand, fibrinogen, binds to $\alpha\beta$-py cells

To demonstrate that the changes in affinity modulation undergone by the chimeric integrin are not an artefact of PAC1 antibody binding, affinity modulation was observed using Alexa-488-conjugated fibrinogen. Cells were treated using the same external factors i.e. 5mM EDTA and 100μM Mn^{2+} as those used in PAC1 binding experiments. Figure 3.3 shows representative dot blots from cells transfected with control vector. In the native state, 29% of the highly transfected cells are in the upper right quadrant. Addition of 5mM EDTA results in a leftward shift in the cell population, indicative of a loss of PAC1 binding, with the majority of the highly transfected cells moving towards the upper left quadrant (98%). Addition of 100μM Mn^{2+} leads to a rightward shift in the cell population. In the presence of activating Mn^{2+} , the percentage of highly transfected cells in the high PAC1 binding upper right quadrant is increased to 66%.

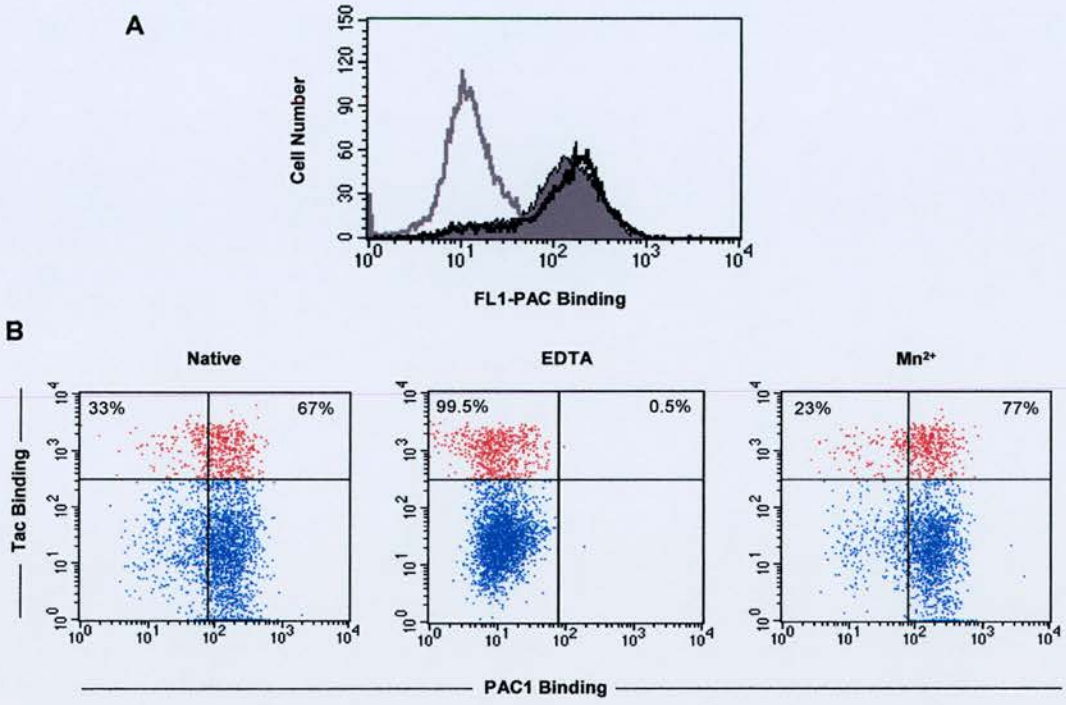

Figure 3.2 Integrin Affinity Modulation by External Control Factors as Determined by PAC1 binding.

Flow cytometry was performed on control vector (1μg) transfected cells to determine integrin affinity.
(A) PAC1 binding in the presence of external factors, untreated (solid grey), 5mM EDTA (grey line) or 100μM Mn^{2+} (black line).
(B) Representative dot blots show PAC1 binding versus Tac binding, high Tac binding cells are shown in red. PAC1 binding was determined in the native integrin and in the presence of 5mM EDTA or 100μM Mn^{2+}. Quadrant markers distinguish between high and low Tac and PAC1 binding cells. The percentage of high Tac binding cells in the upper left- and right- hand quadrants are shown for each dot blot. Histogram and dot plots are representative of three experiments.

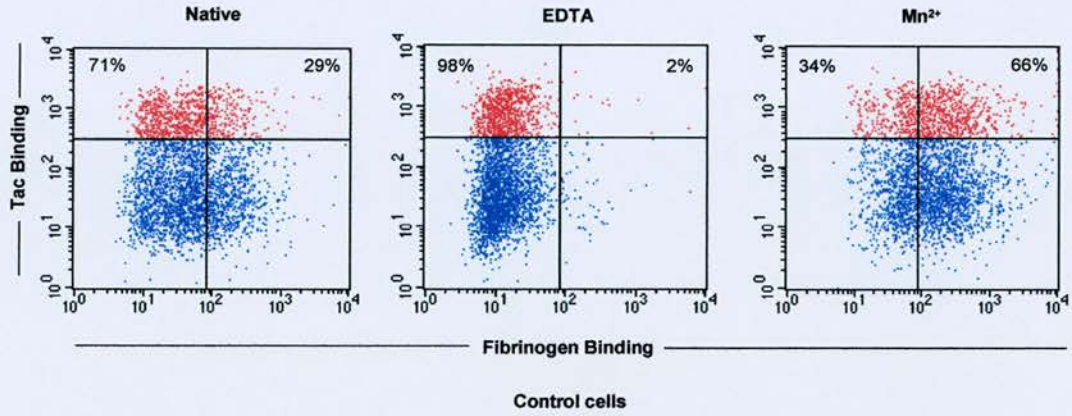

Figure 3.3 Integrin Affinity Modulation by External Control Factors as Determined by Alexa-488-Conjugated Fibrinogen Binding.

Flow cytometry was performed on control vector (1μg) transfected cells to determine integrin affinity. Representative dot blots show Alexa-488-conjugated fibrinogen binding versus Tac binding, high Tac binding cells are shown in red. Fibrinogen binding was determined in the native integrin and in the presence of 5mM EDTA or 100μM Mn^{2+}. Quadrant markers distinguish between high and low Tac and fibrinogen binding cells. The percentage of high Tac binding cells in the upper left- and right- hand quadrants are shown for each dot blot.

3.3 H-Ras- and R-Ras-mediated integrin affinity

3.3.1 H-Ras G12V -Mediated Integrin Suppression is reversed by R-Ras G38V.

Integrin affinity status in transfected cells was determined as described in Materials and Methods (2.8.2). Figure 3.4 shows representative dot plots of cells transfected with control vector ± H-Ras G12V and R-Ras G38V ± H-Ras G12V. Compared with control vector transfected cells, transfection of H-Ras G12V into $\alpha\beta$-py cells (Figure 3.4) results in a decrease in PAC1 binding with 77% of the highly transfected cells (shown in red) found in the upper left hand quadrant compared with 50% in control cells. Transfection with R-Ras G38V results in the majority of the highly transfected cells being found in the upper right hand quadrant (62%). Co-transfection of $\alpha\beta$-py cells with R-Ras G38V and H-Ras G12V returns the highly transfected cell distribution to that resembling the control vector cells with 45% of the highly transfected cells located in the upper right hand quadrant.

Using the activation index calculated for the cells, percentage inhibition relative to the control cell activation index was calculated as described in the materials and methods. Figure 3.5A shows that transfection with H-Ras G12V results in a highly significant suppression 58.2 ± 4.5 of the integrin ($P<0.001$) as compared with control vector alone. Transfection with R-Ras G38V resulted in a slight activation of the integrin -34.7 ± 8.6 ($P<0.05$) compared with the control vector alone. Co-transfection of $\alpha\beta$-py cells with both the R-Ras G38V and H-Ras G12V constructs resulted in a reversal of H-Ras G12V mediated integrin suppression with the resulting state of the integrin 4.9 ± 2 showing no significant difference to that of control cells.

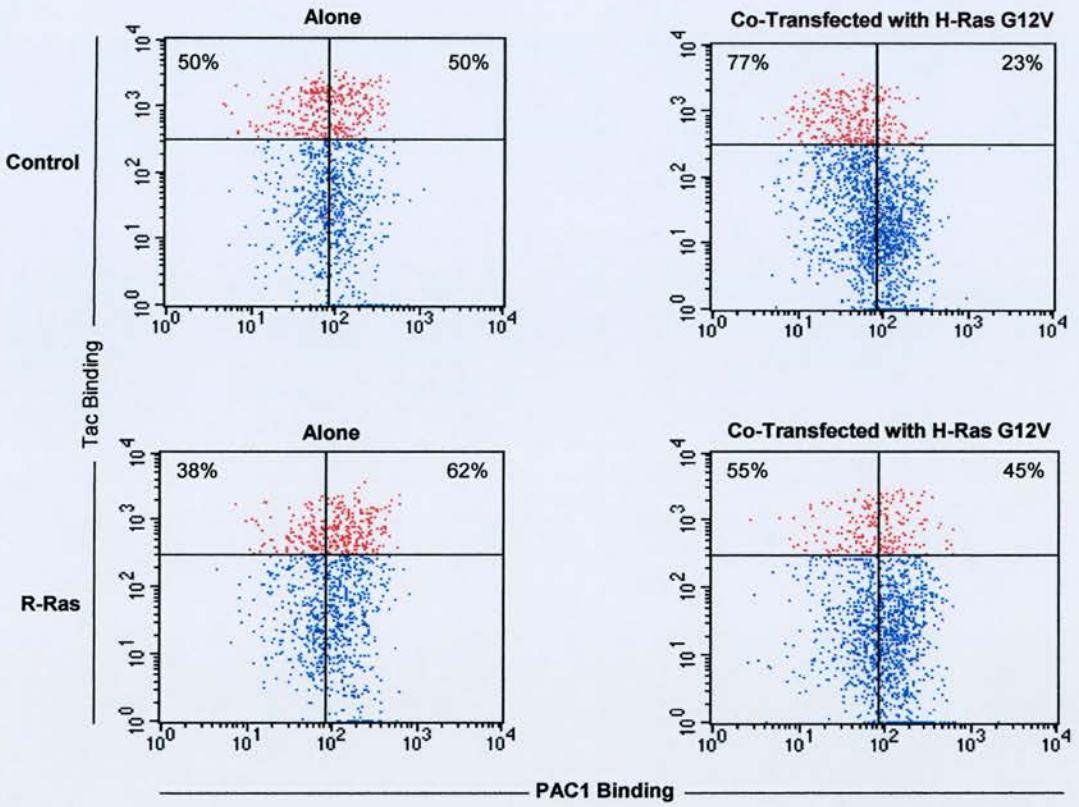

Figure 3.4 H-Ras G12V Mediated Integrin Suppression is reversed by R-Ras G38V.

Flow cytometry was performed on control vector ± H-Ras G12V (1μg), and R-Ras G38V ± H-Ras G12V (1μg) transfected cells. In each assay, total DNA content was standardised to 2μg using control vector. Representative dot blots show PAC1 binding in the native integrin versus Tac binding, high Tac binding cells are shown in red. Quadrant markers distinguish between high and low Tac and PAC1 binding. The percentage of high Tac binding cells in the upper left- and right- hand quadrants are shown for each dot blot. The dot blots are representative of three experiments.

3.3.2 H-Ras G12V expression leads to ERK1/2 activation

Importantly, Figures 3.5B and C show that levels of H-Ras G12V and R-Ras G38V expression are unaffected by co-expressing the two constructs together in $\alpha\beta$-py cells. In cells transfected with control vector ± H-Ras G12V and cells transfected with R-Ras G38V± H-Ras G12V, activation of the classical Ras-ERK pathway was determined with phospho-specific ERK1/2 antibody that recognises the dual phosphorylated ERK1 and 2. Figure 3.5D shows that in cells quiesced overnight there was an increase in ERK1/2 phosphorylation in H-Ras G12V cells compared to control vector transfected cells. Interestingly, co-transfection of cells with H-Ras G12V and R-Ras G38V show no reduction in ERK1/2 phosphorylation compared to control vector + H-Ras G12V. Total ERK2 levels in all samples were similar and remain unaffected by construct expression in these cells (Figure 3.5E).

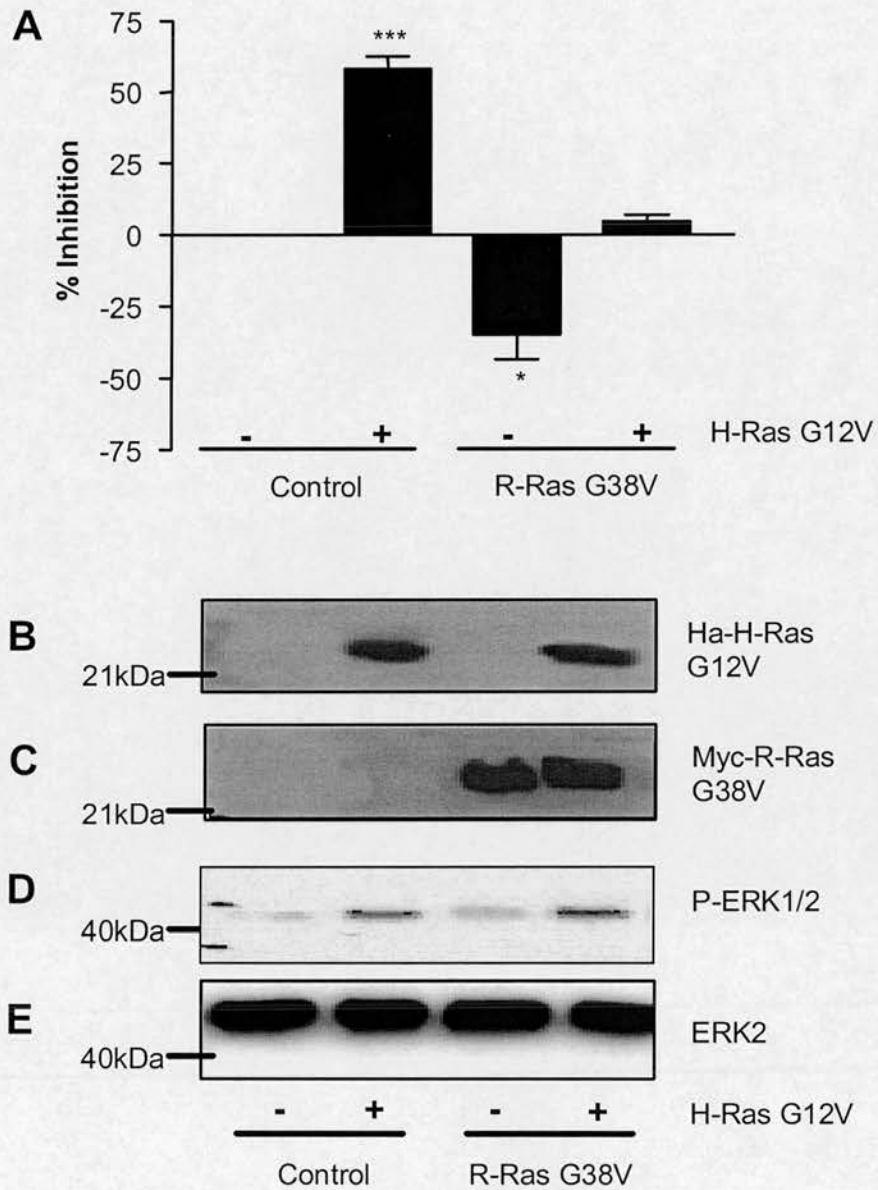

Figure 3.5 R-Ras G38V Reversal of H-Ras G12V Mediated Integrin Suppression does not affect activation of ERK 1/2.

(A) Suppression of integrin activation was determined in control vector ± H-Ras G12V (1µg), and R-Ras G38V ± H-Ras G12V (1µg) transfected cells. In each assay, total DNA content was standardised to 2µg using control vector. The results shown are the mean ± SEM of 3 independent experiments. Statisical analysis was performed by one-way ANOVA test. * = $P<0.05$ and *** = $P<0.001$, compared with 'Control'. A duplicate set of transfected cell lysates were probed with (B) the anti-Ha antibody, (C) the anti-Myc antibody, (D) the phospho-specific ERK1/2 antibody and (E) the ERK2 antibody. Western blots are representative of three experiments.

3.4 Discussion

The $\alpha\beta$-py transfection and flow cytometry system, developed by Dr. M. Ginsberg and colleagues (Scripps Research Institute, La Jolla, USA), was employed in this project to enable the examination of the roles of H-Ras and R-Ras, together with ERK1/2 activation, in modulating integrin affinity.

PAC1 is a pentameric IgM antibody that binds to agonist-stimulated platelets. The PAC1 monoclonal antibody specifically binds to the activated $\alpha_{IIb}\beta_3$ integrin, mimicking the binding characteristics of fibrinogen (Shattil *et al.*, 1985). The ability of PAC1 to bind to the chimeric $\alpha_{IIb}\alpha_{6A}\beta_3\beta_1$ integrin present on $\alpha\beta$-py cells is in accordance with a previous report that this integrin is constitutively active in $\alpha\beta$-py CHO-K1 cells (Hughes *et al.*, 1997). Expression of full length $\alpha_{IIb}\beta_3$ in CHO-K1 cells does not permit PAC1 binding, as the integrin is in a low affinity state. Inside-out signalling, directed at the $\alpha_{6A}\beta_1$ cytoplasmic domains of the chimeric integrin, must therefore induce a conformational change in the integrin to a high affinity state.

The affinity status of the $\alpha_{IIb}\alpha_{6A}\beta_3\beta_1$ integrin was successfully modulated through exogenous factors, as shown by Figure 3.2. Addition of EDTA at 20-22°C, which results in chelation of Ca^{2+} and Mg^{2+} ions, induced a low integrin affinity state (suppressed integrin). Conversely, addition of Mn^{2+} increased the activation index of the integrin. This demonstrates that the internal controls used for each transfection, representing a minimum and maximum of PAC1 binding within these cells, can be utilised with this chimeric integrin.

PAC1 is a ligand-mimetic antibody. Using the natural ligand for $\alpha_{IIb}\beta_3$ we hypothesised that Alexa-488 labelled fibrinogen would act in a similar fashion to that of PAC1 binding in response to exogenous factors. Figure 3.3 shows that, with addition of the same exogenous factors as used in the PAC1 controls, the integrin affinity state of cells stained using an Alexa-488-conjugated fibrinogen responded in a similar fashion. These results helped to confirm that results obtained using PAC1 as a reporter of integrin affinity state could be related back to the binding of the natural ligand.

Hughes *et al.*, (1997) have shown previously that an activated variant of the small GTP-binding protein H-Ras can suppress the chimeric integrin in $\alpha\beta$-py CHO-K1

cells. The results shown in Figure 3.4 are in agreement with Hughes *et al.* (1997), as transfection of $\alpha\beta$-py cells with the activated mutant H-Ras G12V resulted in a reduction in PAC1 binding. This effect was cell-autonomous as untransfected cells (Tac negative) did not show a decrease in PAC1 binding. H-Ras G12V-mediated suppression is not restricted to β_1 and α_{6A} cytoplasmic domains since chimeras composed of the cytoplasmic domains of α_{6B} or α_5 fused to α_{IIb}, co-expressed with either native β_3 or a $\beta_3\beta_1$ chimera could also suppress PAC1 binding (Hughes *et al.*, 1997).

Affinity modulation of integrins by H-Ras G12V has been described by several groups. Purified osteoblasts highly express integrins β_1, α_4, α_5, α_6 and the activation epitope of β_1 (Tanaka *et al.*, 2002). H-Ras signals inhibit the ligand-binding activation epitope of β_1 on the surface of osteoblasts and subsequent β_1-mediated osteoblast adhesion to matrix proteins (Tanaka *et al.*, 2002). In contrast, H-Ras G12V has also been shown to activate $\alpha_5\beta_1$ in bone-marrow derived mast cells and also to aid interleukin-3 (IL-3)-induced cell adhesion to fibronectin by the murine hematopoietic cell line, Baf3, through activation of $\alpha_4\beta_1$ and $\alpha_5\beta_1$ (Kinashi *et al.*, 2000; Shibayama *et al.*, 1999). The conflicting evidence of the effect active H-Ras has upon integrins demonstrates that modulation of integrin affinity by H-Ras appears to cell type-specific. H-Ras probably varies its utilisation of protein partners in a cell-type-specific manner to effect its regulation of integrins (Kinbara *et al.*, 2003).

Hughes *et al.*, (1997) found that the expression of H-Ras G12V, and its kinase effector Raf-1, blocks integrin activation and that this suppressive activity correlates with activation of the ERK MAP kinase pathway. Results shown in Figures 3.5A and 3.5D concur with the findings of Hughes *et al.*, (1997), showing that expression of H-Ras G12V increased ERK1/2 phosphorylation in $\alpha\beta$-py cells.

MAP kinase phosphatase 1 (MKP-1) prevents the accumulation of active ERK1/2 in the cell by dephosphorylation of ERK1/2 (Alessi *et al.*, 1993). Since levels of H-Ras/Raf mediated suppression can be reduced by treatment with MKP-1, it has been suggested that suppression appears to be mediated by ERK1/2 (Hughes *et al.*, 1997). However, other more recent studies have indicated that ERK/MAPKs are not

required for H-Ras to suppress integrins (Hughes *et al.*, 2002; Hansen *et al.*, 2002). These reports suggest the possibility of an ERK1/2-independent integrin suppression pathway. This hypothesis will be addressed in Chapter 4 of this thesis.

In contrast to H-Ras, the closely related small GTP-binding protein R-Ras has been reported to 'activate' integrins. Zhang *et al.* (1996) showed, using a CHO cell line expressing the native $\alpha_{IIb}\beta_3$ integrin in a low affinity state, that expression of a constitutively active R-Ras (R-Ras G38V) enhanced ligand-binding activity of $\alpha_{IIb}\beta_3$ present on the cell surface, shown by PAC1 binding. R-Ras G38V was shown to have strong stimulatory effects on adhesion and ligand binding activity of $\alpha_5\beta_1$ to fibronectin in bone marrow-derived mast cells (Kinashi *et al.*, 2000).

While R-Ras G38V greatly enhanced the ligand-binding activity of CHO cells expressing the native $\alpha_{IIb}\beta_3$ integrin (Zhang *et al.*, 1996), Sethi *et al.* (1999) demonstrated that R-Ras G38V does not directly increase PAC1 binding when transfected into CHO cells stably expressing the chimeric integrin $\alpha_{IIb}\alpha_{6A}\beta_3\beta_1$ ($\alpha\beta$-py cells). The data in Figure 3.5A shows only a slightly significant increase in PAC1 binding of $\alpha\beta$-py cells transfected with R-Ras G38V. The reason why R-Ras G38V has a less obvious activating effect on the $\alpha\beta$-py cells expressing the chimeric integrin compared with CHO cells expressing the native $\alpha_{IIb}\beta_3$ integrin (Zhang *et al.*, 1996), may simply be because the chimeric integrin is basally active.

Sethi *et al.*, (1999) hypothesised that the 'activating' effects of R-Ras in CHO cells might be attributable to it antagonising the suppressive effect of H-Ras. Figures 3.4 and 3.5A show that $\alpha\beta$-py cells transfected with H-Ras G12V alone cause a highly significant decrease in PAC1 binding; however, co-transfection with active R-Ras G38V completely restored PAC1 binding (Figures 3.4 and 3.5A). Western blot analysis showed that co-transfection with R-Ras G38V had no effect on H-Ras G12V expression (Figures 3.5B and 3.5C). Therefore the reversal of suppression observed with R-Ras is not a consequence of reduced levels of H-Ras expression.

As previously mentioned, H-Ras/Raf-mediated suppression correlates with the activation of the ERK1/2 kinase pathway. Reports suggest that levels of H-Ras/Raf-mediated suppression can be reduced by treatment with MKP-1 (Hughes *et al.*, 1997). Therefore, it is not unreasonable to assume that activated R-Ras could rescue

suppression by affecting the capability of H-Ras and Raf-1 to activate ERK1/2. However, in agreement with Sethi *et al.*, (1999), coexpression of R-Ras G38V with H-Ras G12V did not influence the ability of H-Ras to activate ERK1/2 (Figure 3.5D). This suggests that the ability of R-Ras G38V to reverse H-Ras G12V-mediated suppression is not caused by the inactivation of the ERK1/2 kinase pathway but at a point down stream of ERK1/2 activation (Oertli *et al.*, 2000; Sethi *et al.*, 1999).

3.4.1 Summary

The $\alpha\beta$-py integrin affinity detection and transfection system successfully reproduced the initial findings that, despite high sequence homology, activated H-Ras-mediated integrin suppression, while activated R-Ras reversed H-RasG12V-mediated integrin suppression in $\alpha\beta$-py cells.

H-Ras G12V-mediated integrin suppression correlated with an increase in ERK1/2 phosphorylation. H-Ras/Raf-mediated ERK1/2 phosphorylation was not affected by co-expression of R-Ras G38V.

Chapter 4

Characterisation of H-and R-Ras Chimeras

4.1 Introduction

R-Ras was originally identified by low stringency hybridisation with an H-Ras probe, as its sequence is 55% identical in the region of overlap with H-Ras (Lowe *et al.*, 1987).

H-Ras and R-Ras are GTP-binding proteins which cycle between an inactive GDP-bound state and an active GTP-bound state. Mutation and deletion studies have demonstrated that the intrinsic GTPase activity is contained within the conserved N-terminal 166 amino acids of the Ras proteins (Lowy and Willumsen, 1993). Mutation of residues Gly^{12} or Glu^{61} of H-Ras disrupts the rate of GTP hydrolysis resulting in constitutively active mutants (Barbacid *et al.*, 1987; Sweet *et al.*, 1984). This project makes use of the activated mutant of H-Ras which contains a glycine- to- valine substitution at codon 12 (H-Ras G12V).

The intrinsic GTPase activity of R-Ras containing a glycine- to- valine substitution at codon 38 (equivalent to codon 12 in Ras proteins) is insensitive to stimulation by GAPs and this mutant is therefore constitutively active (Rey *et al.*, 1994). The constitutively active R-Ras (G38V) has been used in this project.

H-Ras and R-Ras contain conserved sequences in their minimal effector binding domains and bind to common downstream effectors when in the GTP bound state. Both H-Ras and R-Ras interact with the p110 catalytic subunit of PI 3-kinase *in vitro*, and induce elevation of PI 3-kinase lipid products *in vivo* (Rodriguez-Viciana *et al.*, 1994; Marte *et al.*, 1997). Like H-Ras, R-Ras interacts with the Raf serine/threonine kinases *in vitro* (Rey *et al.*, 1994; Spaargaren *et al.*, 1994). However, in contrast to H-Ras, R-Ras does not markedly activate Raf, or the ERK1/2 family of MAP kinases (Marte *et al.*, 1997; Sethi *et al.*, 1999).

Despite the sequence similarity between H-Ras and R-Ras, activated variants of these proteins confer distinct biological properties when expressed in mammalian

cells. In contrast to activated H-Ras, analogous R-Ras mutants do not contribute to focus formation or soft-agar growth by rat fibroblasts, indicative of cellular transformation (Lowe and Goeddel, 1987). When activated, H-Ras or R-Ras were injected into Swiss 3T3 cells, only H-Ras was capable of inducing DNA synthesis (Rey *et al.*, 1994). R-Ras was capable of inducing malignant, but not morphologic, transformation of NIH3T3 cells (Cox *et al.*, 1994).

In the previous chapter, expression of the active mutant of H-Ras, H-Ras G12V, was shown to mediate a suppressive effect on integrin activation. Co-expression of the active mutant form of R-Ras, R-Ras G38V, demonstrated an ability to reverse H-Ras mediated integrin suppression. The divergent effects of these two proteins on integrin affinity is surprising as there is a high degree of sequence similarity between H-Ras and R-Ras with approximately 71% amino acid sequence conservation over the first 120 amino acids of H-Ras. The main areas of sequence divergence between the two proteins include the 26 additional N-terminal amino acids of R-Ras compared to H-Ras; the extended effector region, (amino acids 23-46 of H-Ras); and the hypervariable C-terminal domain which encompasses the hypervariable linker domain and the C-terminal binding domain.

The aim of this chapter is to further characterise H-Ras and R-Ras to determine what role, if any, the sequence variations in H-Ras and R-Ras may play in their differing properties with respect to integrin affinity modulation and activation of ERK1/2 MAP kinases. For the purposes of this chapter, H-Ras G12V and R-Ras G38V were both cloned out of their original vectors and into pCDNA3.1 (+), along with their N-terminal HA- and Myc- tags respectively (see Appendix I for sequence verification). Section 2.10 of the Materials and Methods section describes the subcloning of H-Ras and R-Ras into pCDNA3.1(+). The subcloning of the H-Ras G12V and R-Ras G38V genes into pCDNA3.1(+) was considered necessary for them to act as appropriate controls for H-and R-Ras chimeras, which are also cloned into pCDNA3.1(+). These H-and R-Ras chimeras were utilised to help gain insight into the regions responsible for the contrasting effects H-Ras and R-Ras have on integrin function.

4.2 Introducing the H-and R-Ras Chimeras

The H-and R-Ras chimeras were provided as a gift by Dr. Mark Ginsberg (Division of Vascular Biology, The Scripps Research Institute). The chimeras were constructed using splice overlap PCR mutagenesis with pSG5-R-Ras(G38V) and pcDR-H-Ras(G12V) as templates. The amplified DNA was ligated into the *Eco*RI site of pCDNA 3.1 (+) with an N-terminal FLAG tag sequence. Upon receipt all constructs were verified by DNA sequencing (see Appendix II for full chimera sequences, aligned with H-Ras and R-Ras. Areas highlighted in red indicate where exchanges were made to generate the chimera). Figure 4.1 is a schematic representation of the chimeras indicating the main areas of sequence divergence between H-Ras and R-Ras. Chimeras CH3, CH6, H197 and H201 contain the N-terminus of H-Ras G12V while, reciprocal chimeras CH1, CH5, R197 and R201 contain the N-terminus of R-Ras G38V. A brief description of these inverted pairs follows:

CH1 (R-Ras 1-85; H-Ras 60-198) and CH3 (H-Ras 1-59; R-Ras 86-219) substitute the N-terminal regions of the H-Ras and R-Ras proteins, to include the N-terminal minimal and extended effector binding regions and switch I region.

CH5 (R-Ras 1-174; H-Ras 149-198) and CH6 (H-Ras 1-146; R-Ras 175-219), substitute the N-terminal regions of the H-Ras and R-Ras proteins. This pair extend the N-terminal to encompass the switch II domain.

H197 (H-Ras 1-171; R-Ras 199-219) and R197 (R-Ras 1-198; H-Ras 172-198) substitute the N-terminal regions of the H-Ras and R-Ras proteins extending into the hypervariable linker domain at the C-terminus.

H201 (H-Ras 174; R-Ras 204-219) and R201 (R-Ras 203; H-Ras 175-198) substitute the C-terminal binding domains of H-Ras and R-Ras.

At this point, it is worth noting that it may be of advantage to the reader to keep to hand a copy of the schematic diagram of the chimeras (Figure 4.1), as this may aid understanding of the following results section.

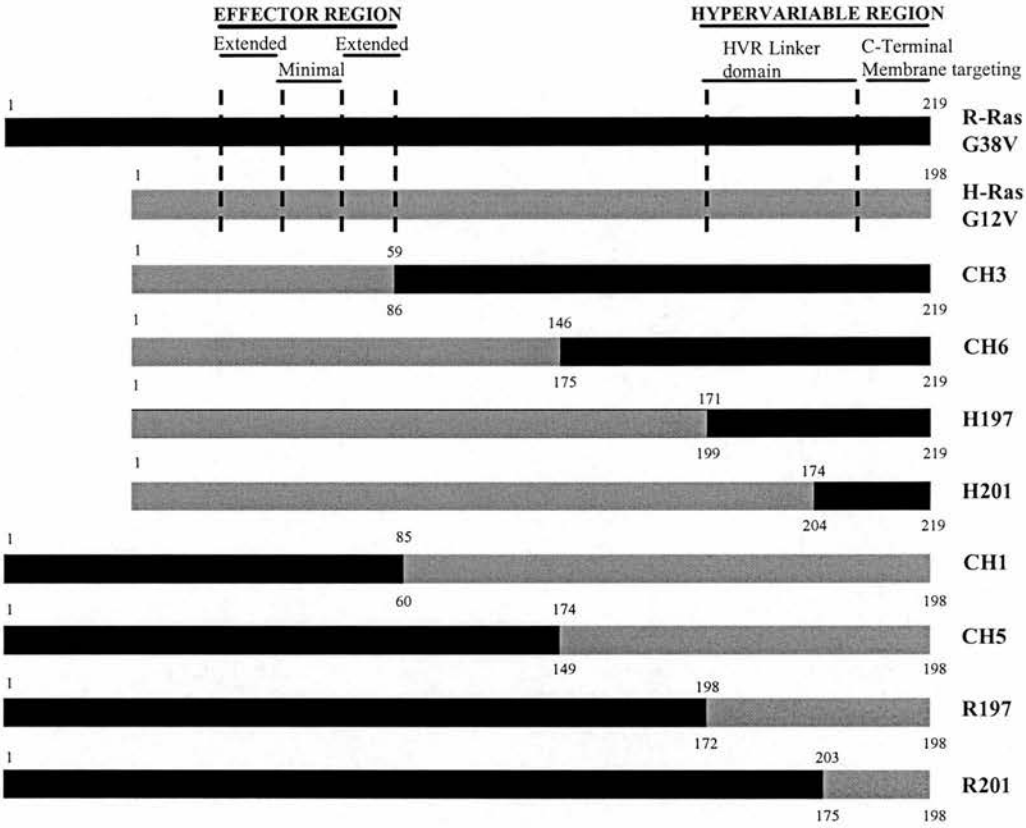

Figure 4.1 Schematic representation of H-Ras G12V and R-Ras G38V chimeras.

Schematic represents H-Ras G12V (grey) and R-Ras G38V (black) chimeras.
Amino acid numbers above the box represent the N-terminal segment and those below denote the C-terminal segment of the chimera.
All chimeras are FLAG-tagged and subcloned into pCDNA3.1(+).

4.3 The effect of H-/R-Ras chimeras on integrin affinity.

It has previously been described that H-Ras G12V transfection of $\alpha\beta$-py cells mediates integrin suppression. H-Ras-mediated integrin suppression seems to correlate with increased ERK1/2 activity. Transfection with R-Ras G38V results in a slightly higher activation state of the $\alpha_{IIb}\alpha_{6A}\beta_3\beta_1$ chimeric integrin compared with control cells. R-Ras G38V is capable of reversing H-Ras G12V-mediated integrin suppression, without affecting levels of ERK1/2 activation. The H/R-Ras chimeras provide us the opportunity to examine whether specific sequences within H-Ras G12V and R-Ras G38V are required for their contrasting effects on integrin affinity and ERK1/2 activation.

4.3.1 Modulation of integrin affinity by H-and R-Ras chimeras

PAC1 binding was assessed in $\alpha\beta$-py cells transfected with the H-and R-Ras chimeras. The percentage inhibition relative to the control cell activation index was calculated for each of the chimeras (Figure 4.2).

Transfection with full-length H-Ras G12V resulted in suppression 53.3 ± 9.8% of the active chimeric integrin, while R-Ras G38V demonstrated a slight activation of the integrin -32.1 ± 18.7%.

Each of the inverted pairs of chimeras had opposite effects on integrin affinity, except for chimeras H197 and R197 which appeared to have very little overall effect on the affinity state of the integrin, compared to control.

Like H-Ras G12V, the chimeras CH1 (13.65 ± 5.1%), CH5 (40.8 ± 9.2%) and H201 (21.1 ± 5.9%) each mediated integrin suppression. The respective inverted pair of each of the suppressing chimeras was capable of activating the integrin in a manner similar to R-Ras G38V, CH3 (-12.9 ± 7.8%), CH6 (-17.3 ± 4.9%) and R201 (-27.7 ± 8.9%).

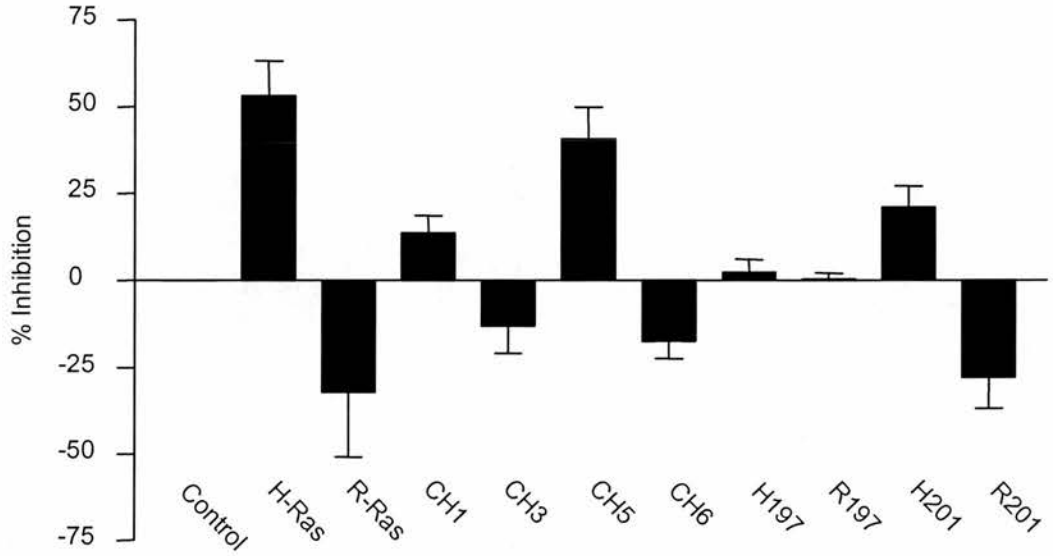

Figure 4.2 Effects of H-and R-Ras Chimeras on Integrin Affinity.

Integrin affinity was determined in $\alpha\beta$-py cells transfected with H- and R-Ras chimeras (1μg). H-Ras G12V (1μg) and R-Ras G38V (1μg) transfected cells were used as controls. Percentage inhibition was calculated by comparing the activation index in the presence of the test DNA to that of the control vector. The results shown are the mean ± SEM of three independent experiments.

4.3.2 Suppression of integrin activation does not correlate with ERK1/2 activation

As the integrin suppression mediated by H-Ras G12V correlates with activation of ERK1/2 (Figure 3.5D), it was decided that it would be of interest to see if any of the chimeras had a similar effect on ERK1/2 activation. Of particular interest were the chimeras which caused integrin suppression, CH1, CH5 and H201. The CH1 and CH5 chimeras, despite acting like H-Ras G12V in terms of their ability to suppress integrin affinity, are lacking in N-terminal H-Ras G12V sequences including the effector region, and it was hypothesised that this may affect their ability to cause ERK1/2 activation.

The FLAG-tagged H/R-Ras chimeras were transfected into $\alpha\beta$-py cells and Figure 4.3A shows that they were all expressed at similar levels. Those chimeras containing the R-Ras G38V N-terminus (CH1, CH5, R197 and R201) were approximately 23kDa and those containing the H-Ras G12V N-terminus (CH3, CH6, H197 and H201) were approximately 21kDa.

The ability of the chimeras to mediate the phosphorylation of ERK1/2 was assessed using a phospho-specific ERK1/2 antibody. Transfection with H-Ras G12V showed an increase in ERK1/2 phosphorylation (Figure 4.3B), which is consistent with results from Chapter 3 (Figure 3.5D). The serum stimulated, positive control, cells also resulted in an increase in ERK1/2 phosphorylation. H201 mediated a slight increase in ERK1/2 phosphorylation, however none of the other H/R-Ras chimeras were capable of mediating ERK1/2 phosphorylation above control levels (Figure 4.3B). Total ERK2 levels, used as a control for equal protein loading, remained unchanged in transfected cells (Figure 4.3C).

As phospho-specific ERK1/2 blots can only provide a qualitative measure of ERK1/2 phosphorylation state, it was decided to further investigate the effects of the chimeras on ERK1/2 phosphorylation and subsequent activation using more quantitative approaches.

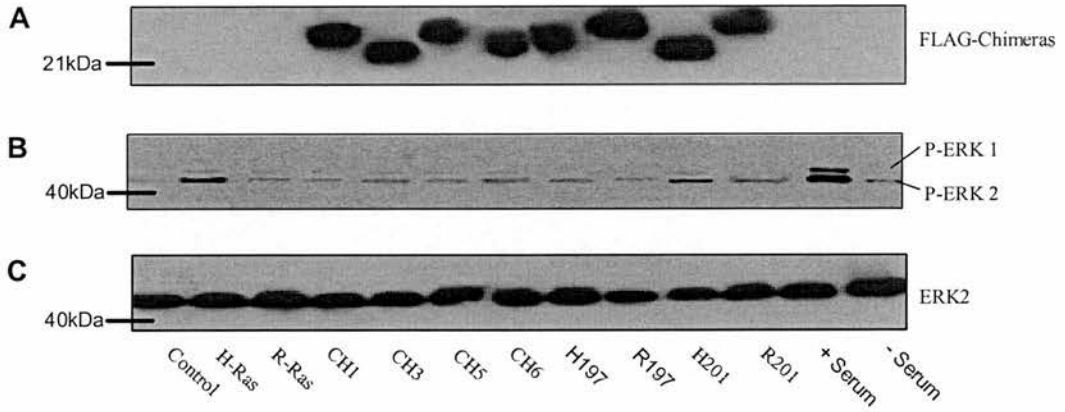

Figure 4.3 Effects of H-and R-Ras Chimera Expression on ERK1/2 Phosphorylation.

Cell lysates from chimera (1μg) transfected cells were probed for chimera expression with (A) the anti-FLAG monoclonal antibody. Lysates were also probed with (B) a phospho-specific ERK1/2 antibody and (C) ERK2 antibody. H-Ras G12V (1μg) transfected cells and serum stimulated cells used as positive controls for ERK1/2 phosphorylation. Western blots are representative of three experiments.

The ERK1/2 [pTpY185/187] ELISA is designed to detect and quantify the level of dual-phosphorylated ERK1 and 2 at Thr^{202}, Tyr^{204} and Thr^{185}, Tyr^{187} respectively. The dual phosphorylation is required for full enzyme activity of ERK1 and ERK2. The level of phosphorylation of ERK1/2 can be an indirect indication of the level of ERK1/2 activity and also indicative of the activity of upstream kinases of ERK1/2. Figure 4.4A shows ERK1/2 activation represented as a fold increase above control vector. Stimulation of untransfected cells with serum resulted in a significant 3-fold increase ($p<0.05$) in ERK1/2 activity compared with control. Transfection with H-Ras G12V also caused a significant 2.5-fold increase in ERK1/2 activity ($P<0.05$). Transfection of $\alpha\beta$-py cells with R-Ras G38V and the H/R-Ras chimeras did not give rise to any significant activation of ERK1/2, compared to control. Representative western blots run using the remaining lysates from the ERK1/2 ELISA showed that the chimeras were all expressed at similar levels (Figure 4.4B). Total ERK2 levels remained unchanged in the transfected cells (Figure 4.5C).

ERK2 activity was also measured by an in-vitro kinase assay, whereby ERK2 activity was assayed by immunoprecipitating ERK2 from transfected cell lysates with agarose-conjugated ERK2 phospho-antibody and phosphorylating the substrate myelin basic protein (MBP) in the presence of ^{32}P-ATP. Figure 4.5A shows a representative graph illustrating the general trend observed in three independent experiments. MBP phosphorylation is represented as a fold increase above control vector. H-Ras G12V and untransfected, serum-stimulated cells both resulted in a 3 fold increase in MBP phosphorylation compared to control. Transfection with chimera H201 resulted in a 2-fold increase in MBP phosphorylation levels, compared to control. All other chimeras failed to increase MBP phosphorylation above 1.5-fold. Cell lysates taken from the assay showed that expression levels were similar for all the chimeras (Figure 4.5B). Total ERK2 levels remained unchanged in the transfected cells (Figure 4.5C).

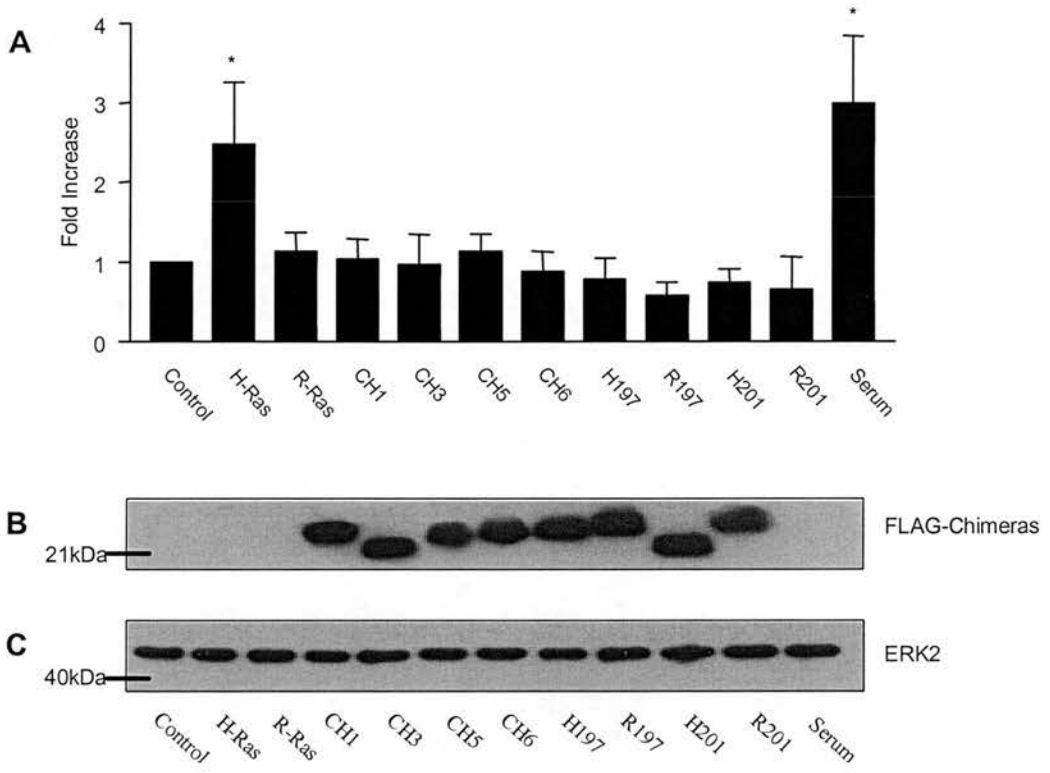

Figure 4.4 H-and R-Ras Chimeras have no significant effect on the levels of ERK1/2 phosphorylation.

Lysates from cells transfected with chimeras (1μg) were (A) analysed by ERK1/2 ELISA. Fold increase was calculated where 'Control'=1. Values represent mean ± SEM of three experiments, each performed in triplicate. H-Ras G12V (1μg) transfected and serum stimulated cells were used as positive controls for ERK1/2 activation. * = significant difference ,$p<0.05$, compared with 'Control'.
Lysates were also run on western blots and probed for chimera expression with (B) the anti-FLAG monoclonal antibody. Total ERK2 (C) was measured as a control for equal loading.

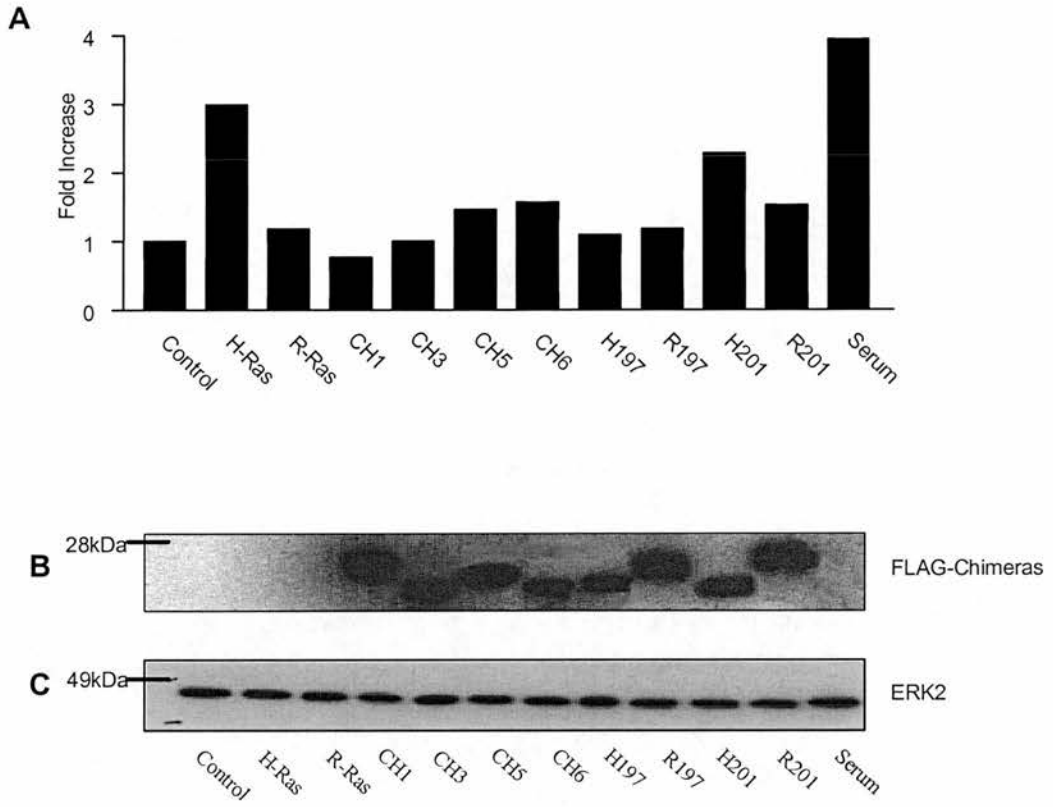

Figure 4.5 Representative in-vitro ERK2 kinase assay.

Lysates from cells transfected with chimeras (1μg) were (A) subjected to an in-vitro ERK2 kinase assay using MBP as a substrate. The graph is representative of three independent experiments carried out in duplicate with results normalised against control values.

Cell lysates were also probed for chimera expression (B) using the anti-FLAG monoclonal antibody and total ERK2 (C) was measured using an ERK2 antibody, as a control for equal protein loading.

The 2-Step Raf kinase assay is routinely used to measure Raf activity in cells, with Raf phosphorylating and activating MEK, which in turn activates ERK1/2, leading to MBP phosphorylation. Endogenous Raf-1 was immunoprecipitated from cell lysates with an anti-Raf-1 monoclonal antibody in conjunction with anti-mouse IgG agarose beads. Following the addition of His-tagged MEK-1 and His-tagged ERK2, Raf activity was assessed as a measure of MBP phosphorylation. Samples were run on a 12.5% SDS-PAGE gel and exposed to a phosphoimager for analysis. Raf-BXB was used as a positive control for the 2-Step Raf kinase assay. Raf-BXB is a constitutively active variant of Raf (Stanton *et al.*, 1989), which does not contain a Ras binding domain.

Figure 4.6A shows a representative graph illustrating the general trend observed in three independent experiments. MBP phosphorylation is represented as a fold increase above control vector. Stimulation with serum resulted in a 2-fold increase in Raf activity, while transfections with H-Ras G12V and Raf-BxB both resulted in a 1.5-fold increase in Raf activity.

None of the H- and R-Ras chimeras showed Raf activity levels much beyond that observed with control. The Raf activity autoradiograph (Figure 4.6B), used to get a quantitative reading from the phosphoimager, provided a qualitative representation of activity levels. The Raf immunoprecipitation blot (Figure 4.6C) confirmed equal loading of samples.

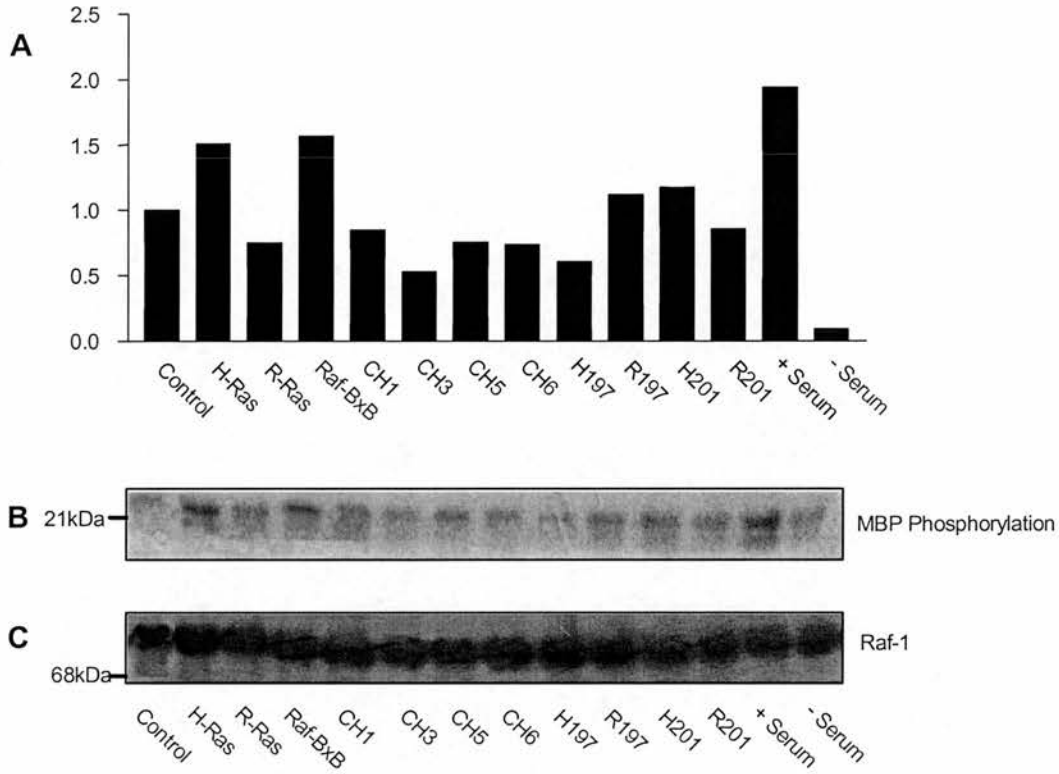

Figure 4.6 Representative 2-Step Raf Kinase Assay.

Lysates from cells transfected with constructs under test (1µg) were (A) analysed by 2-Step Raf Kinase Assay. The kinase activity was assessed by MBP phosphorylation. H-Ras G12V (1µg) and Raf-BxB (1µg) transfected as well as serum stimulated cells used as positive controls for MBP phosphorylation. The results are expressed as fold increase normalised against control cells. The graph represents the trend observed in three independent experiments carried out in duplicate.
(B) is a representative gel showing the phosphorylation levels of MBP as detected by exposure to a phosphoimager. Lysates were also probed with Raf-1 antibody (C) to detect equal Raf immunoprecipitation

4.4 C-terminal sequences are sufficient to confer differing properties of H-Ras and R-Ras

It has been well established that the Ras related protein, R-Ras, has the ability to reverse H-Ras mediated integrin suppression (Sethi *et al.*, 1999). This reversal does not affect levels of H-Ras G12V-mediated ERK1/2 activation (Figure 3.5D). The H/R-Ras chimeras will allow us to determine whether specific sequences of H-Ras and R-Ras are required for their opposing effects on integrin affinity in CHO cells.

4.4.1 Residues 149-174 of H-Ras are required for suppression of integrin activation.

Like H-Ras G12V, chimeras CH1, CH5 and H201 all demonstrated an ability to suppress integrin affinity (see Figure 4.2). As chimera H197 contains predominantly H-Ras N-terminal sequences, like H201, it was decided that these four chimeras should be grouped together for analysis. Integrin affinity was determined in cells transfected with the CH1, CH5, H197 and H201 chimeras ± H-Ras G12V, see Figure 4.7.

As a positive control, full length R-Ras G38V was used to reverse H-Ras G12V-mediated suppression. Percentage inhibition fell significantly from 58.2 ± 4.5% to 4.93 ± 2% ($P<0.001$) in R-Ras G38V co-transfectants. Chimeras CH1, CH5 and H201 had no significant effect on the level of integrin suppression when co-transfected with H-Ras G12V ($P>0.05$). In contrast, H197 failed to suppress integrin affinity (-0.45 ± 4%) and co-transfection with H-Ras G12V showed significant reversal of integrin suppression (58.2 ± 4.5% to 19.5 ± 3.2%) ($P<0.05$).

Figures 4.8A and 4.8B show that co-transfection of chimeras CH1, CH5, H197 and H201 with H-Ras G12V did not affect the expression levels of the H- and R-Ras chimeras or H-Ras G12V. Total ERK2 remained similar in all transfected cells (Figure 4.8C).

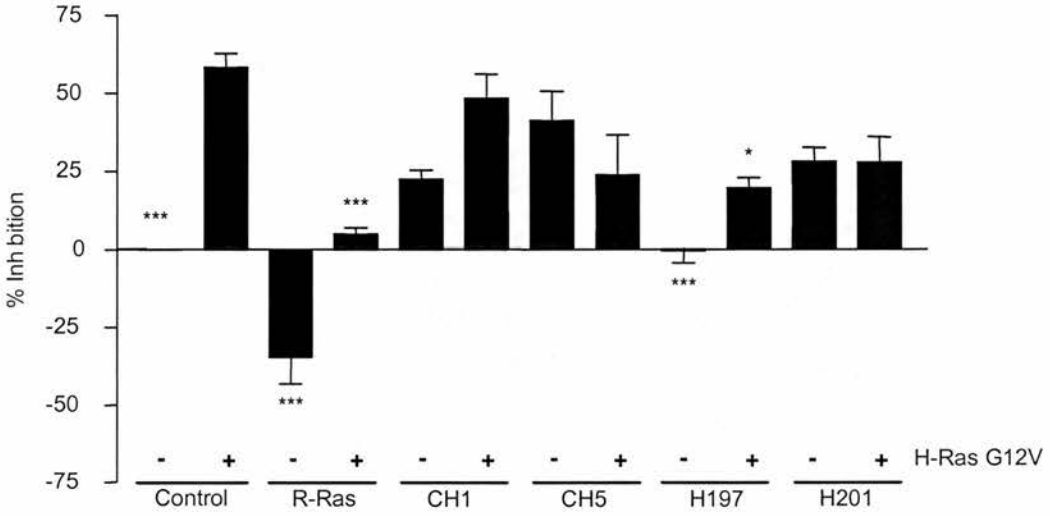

Figure 4.7 Chimeras CH1, CH5 and H201 mediate integrin suppression

Integrin affinity was determined in cells transfected with 1μg of chimera CH1,CH5, H197 or H201 ± H-Ras G12V (1μg). In each transfection, total DNA content was standardised to 2μg using control vector. Percentage inhibition was calculated in reference to control vector alone. The values represent mean ± SEM of 3-5 experiments. Statistical analysis was performed by one-way ANOVA test compared with 'Control + H-Ras G12V'; *, ** and *** denoting $P<0.05$, $p<0.01$ and $P<0.001$ respectively.

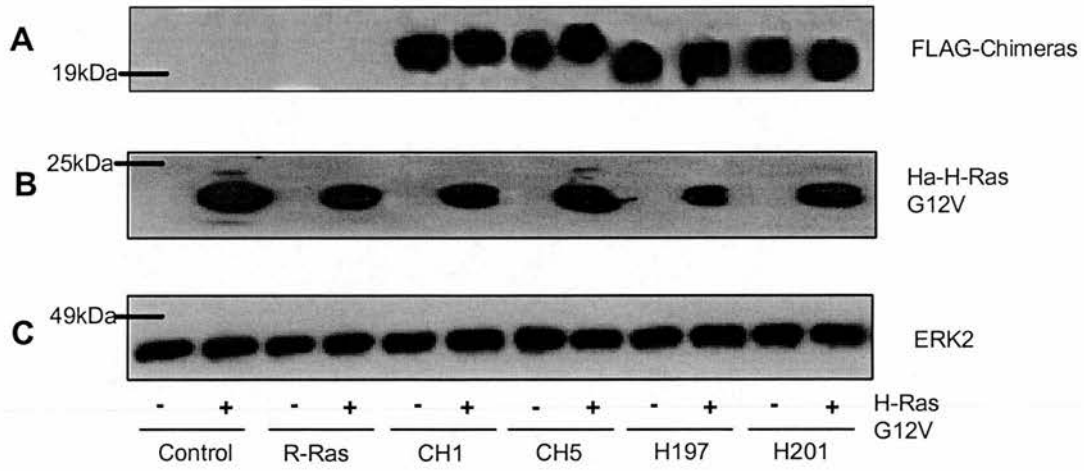

Figure 4.8 Co-transfecting chimeras CH1, CH5, H197 and H201 with H-Ras G12V does not affect expression levels.

Cell lysates were prepared from cells transfected with 1μg of chimera CH1, CH5, H197 or H201 ± H-Ras G12V (1μg). In each transfection, total DNA content was standardised to 2μg using control vector. Cell lysates were probed for chimera expression using the anti-FLAG monoclonal antibody (A). H-Ras G12V expression was checked for using anti-Ha antibody (B). Total ERK2 was probed for using an anti-ERK2 antibody (C).

4.4.2 Residues 175-203 of R-Ras are sufficient to reverse H-Ras-mediated integrin suppression.

Like R-Ras G38V, chimeras CH3, CH6 and R201 all demonstrated an ability to activate integrin affinity (see Figure 4.2). As chimera R197 contains predominantly R-Ras N-terminal sequences, like R201, it was decided that these four chimeras should be grouped together for analysis. Integrin affinity was determined in cells transfected with the CH3, CH6, R197 and R201 chimeras ± H-Ras G12V, see Figure 4.9.

As a positive control, full length R-Ras G38V was used to reverse H-Ras G12V-mediated suppression. Percentage inhibition fell significantly from 58.2 ± 4.5% to 4.93 ± 2% ($P<0.001$) in R-Ras G38V co-transfectants. Chimeras CH3, CH6, and R201 all significantly reversed H-Ras-mediated integrin suppression from 58.2 ± 4.5% to 2.7 ± 2%, -2.8 ± 10%, and -20.43 ± 8.7% respectively ($P<0.001$). Chimera, R197, was capable of reversing H-Ras-mediated integrin suppression from 58.2 ± 4.5% to 20.2 ± 5% ($P<0.05$) but this reversal was not as highly significant as that observed with chimeras CH3, CH6 and R201.

Figures 4.10A and 4.10B show that co-transfection of chimeras CH3, CH6, R197 and R201 with H-Ras G12V did not affect the expression levels of the H- and R-Ras chimeras or H-Ras G12V. Total ERK2 remained similar in all transfected cells (Figure 4.10C).

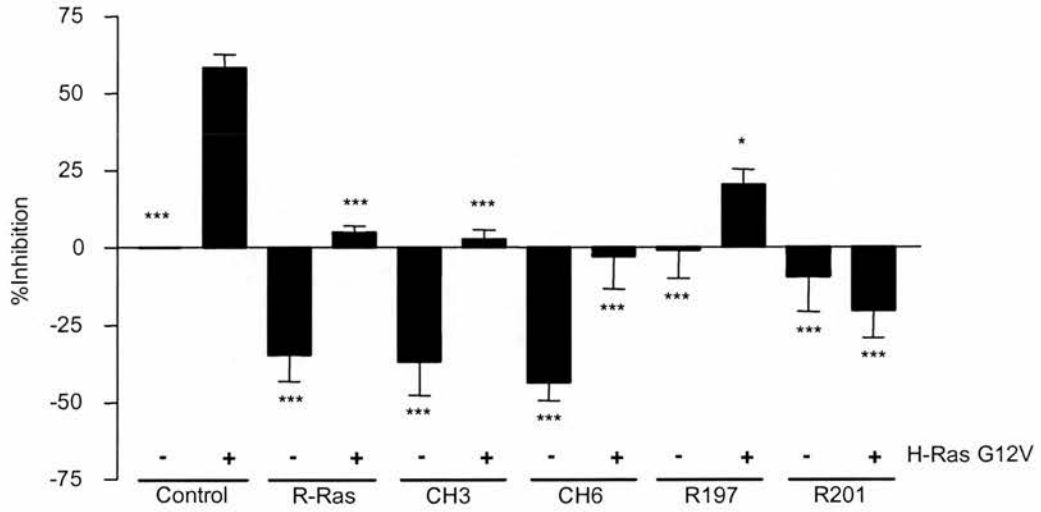

Figure 4.9 Chimeras CH3, CH6 and R201 show reversal of H-Ras G12V-mediated integrin suppression

Integrin affinity was determined in cells transfected with 1μg of chimera CH3, CH6, R197 or R201 ± H-Ras G12V (1μg). In each transfection, total DNA content was standardised to 2μg using control vector. Percentage inhibition was calculated in reference to control vector alone. The values represent mean ± SEM of 3-5 experiments. Statistical analysis was performed by one-way ANOVA test compared with 'Control + H-Ras G12V'; *, ** and *** denoting $P<0.05$, $p<0.01$ and $P<0.001$ respectively.

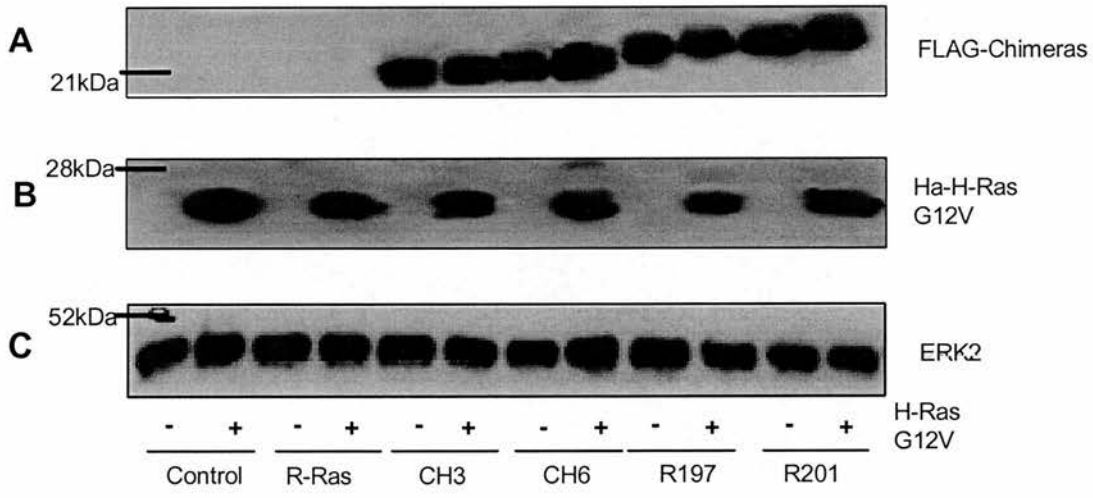

Figure 4.10 Co-transfecting chimeras CH3, CH6, R197 and R201 with H-Ras G12V does not affect expression levels.

Cell lysates were prepared from cells transfected with 1μg of chimera CH3, CH6, R197 or R201 ± H-Ras G12V (1μg). In each transfection, total DNA content was standardised to 2μg using control vector. Cell lysates were probed for chimera expression using the anti-FLAG monoclonal antibody (A). H-Ras G12V expression was checked for using anti-Ha antibody (B). Total ERK2 was probed for using an anti-ERK2 antibody (C).

4.5 Integrin suppression by Raf-BxB CAAX

One of the main concerns from section 4.4 was that the H-and R-Ras chimeras, in particular CH3, CH6 and R201, may have been acting as dominant-negative proteins. This would mean that their reversal of H-Ras G12V-mediated integrin suppression would only be as a consequence of their sequestering Ras effectors and thus distorting the normal signalling pathways. Raf-1 is one of the main downstream effectors of Ras. Cells transfected with the constitutively active Raf mutant, Raf-BxB CAAX, display a loss in PAC1 binding and suppression of the integrin (Sethi *et al.*, 1999). The constitutively active Raf-BxB CAAX mutant does not contain a Ras-binding domain and therefore it would not be capable of binding to the H-and R-Ras chimeras. An ability to reverse Raf-BxB CAAX-mediated integrin suppression would discount a dominant-negative effect of the H/R-Ras chimeras on the Ras-Raf initiated suppression pathway.

4.5.1 R-Ras residues 199-204 may influence the reversal of Raf-BxB CAAX-mediated integrin suppression

Integrin affinity was determined in cells transfected with the CH1, CH5, H197 and H201 chimeras ± Raf-BxB CAAX. Figure 4.11 shows that levels of integrin suppression mediated by Raf-BxB CAAX were 67.8 ± 5.7%. Chimeras CH1, CH5 and H201 had no significant effect on the level of integrin suppression when co-transfected with Raf-BxB CAAX ($P>0.05$) (Figure 4.11). As with previous results, H197 failed to suppress integrins (-2.8 ± 3.4%). Co-transfection of H197 with Raf-BxB CAAX showed a significant reversal of Raf-BxB CAAX mediated integrin suppression from 67.8 ± 5.7% to 18.5 ± 12.7% ($P<0.05$).

Analysis of the chimera sequences (see Figure 4.1) indicate that the sequence peculiar to the suppressing chimeras and H197, which is capable of reversing Raf-BxB CAAX mediated suppression, is R-Ras 199-204.

Figures 4.12Aand 4.12B show that co-transfection with chimeras CH1, CH5, H197 and H201 with Raf-BxB CAAX did not affect the expression levels of any of the constructs. Total ERK2 remained similar in all transfected cells (Figure 4.12C).

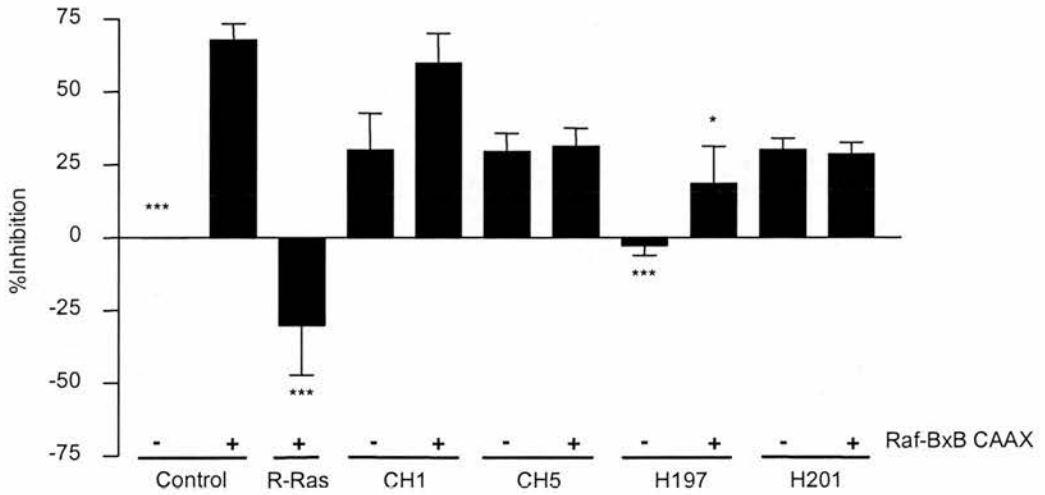

Figure 4.11 Chimeras CH1, CH5 and H201 display integrin suppression.

Integrin affinity was determined in cells transfected with 1μg of chimera CH1,CH5, H197 or H201 ± constitutively active Raf-BxB CAAX (1μg). In each transfection, total DNA content was standardised to 2μg using control vector. Percentage inhibition was calculated in reference to control vector alone. The values represent mean ± SEM of 3-5 experiments. Statistical analysis was performed by one-way ANOVA test compared with Control + Raf BxB CAAX; *, ** and *** denoting $P<0.05$, $p<0.01$ and $P<0.001$ respectively.

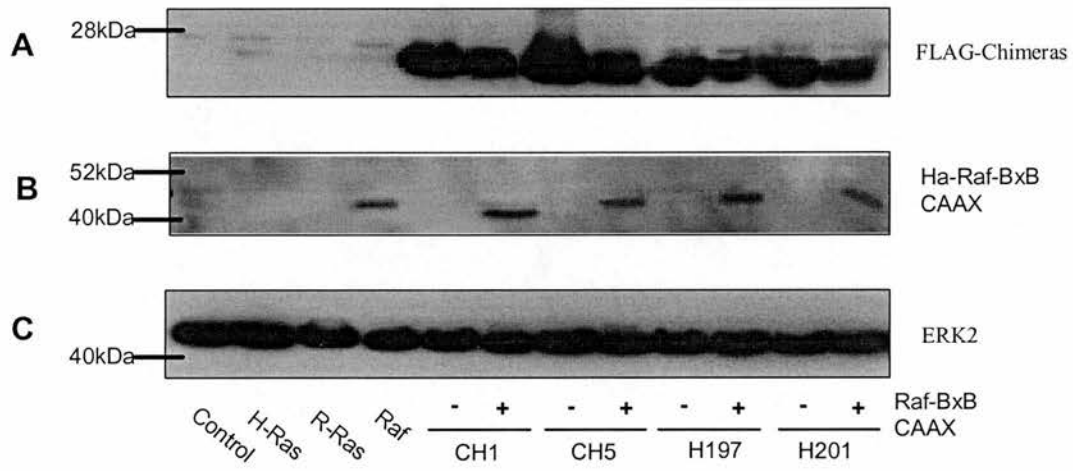

Figure 4.12 Co-expressing chimeras CH1, CH5, H197 and H201 with Raf-BxB CAAX has no effect on expression levels.

Cell lysates were prepared from cells transfected with 1μg of chimera CH1, CH5, H197 or H201 ± Raf-BxB CAAX (1μg). In each transfection, total DNA content was standardised to 2μg using control vector. Cell lysates were run on western blots and probed for chimera expression (A) using the anti-FLAG monoclonal antibody, Raf-BXB CAAX expression was checked for using (B) anti-Ha antibody. Total ERK2 (C) was measured as a control for equal loading of sample.

4.5.2 R-Ras like chimeras do not act as dominant negative proteins on the Ras-Raf initiated integrin suppression pathway

Integrin affinity was determined in cells transfected with the CH3, CH6, R197 and R201 chimeras ± Raf-BxB CAAX. Figure 4.13 shows that the level of integrin suppression mediated by Raf-BxB CAAX was 67.8 ± 5.7%. Chimeras CH3, CH6 and R201 all significantly reversed Raf BxB CAAX mediated suppression from 67.8 ± 5.7% to -1.2 ± 2.3%, –4.5 ± 4%, and -12.3 ±7.5% respectively ($P<0.001$). Co-transfection with R197 did not have any significant effect on Raf-BxB CAAX mediated integrin suppression.

That chimeras CH3, CH6 and R201 can reverse constitutively active Raf-BxB CAAX-mediated integrin suppression, rules out a dominant negative effect. Analysis of these results with reference to the chimera sequences (see Figure 4.1) indicate that the sequence residues peculiar to the chimeras capable of reversing Raf-BxB CAAX-mediated suppression and R197, which is incapable of reversing Raf-BxB CAAX-mediated suppression, are H-Ras residues 172-175.

Figures 4.14A and 4.14B reveal that co-transfection of Raf-BxB CAAX with the chimeras CH3, CH6, R197 and R202 did not affect the expression levels of the constructs. Total ERK2 remained similar in all transfected cells (Figure 4.14C).

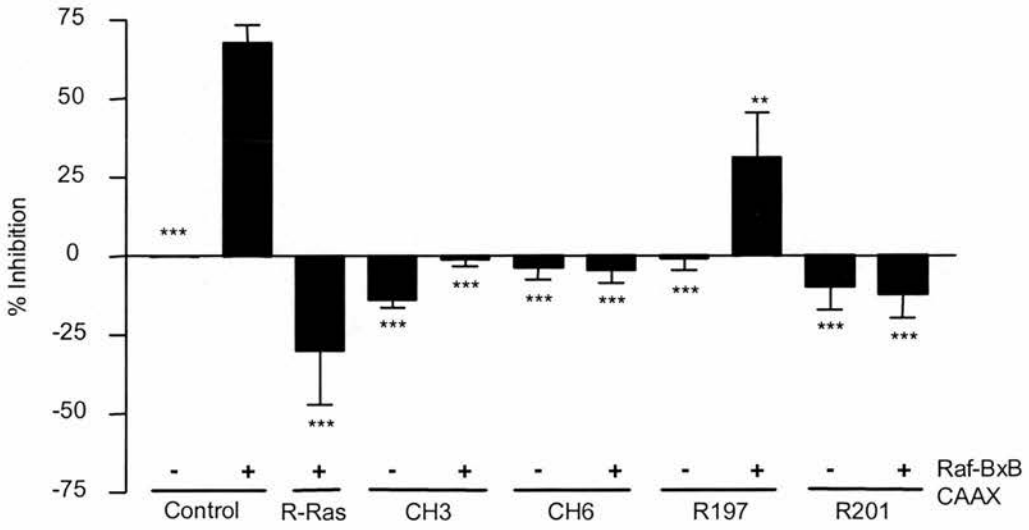

Figure 4.13 Chimeras CH3, CH6 and R201 reverse Raf-BxB CAAX-mediated-integrin suppression.

Integrin affinity was determined in cells transfected with 1μg of chimera CH3, CH6, R197 or R201 ± constitutively active Raf-BxB CAAX (1μg). In each transfection, total DNA content was standardised to 2μg using control vector. Percentage inhibition was calculated in reference to control vector alone. The values represent mean ± SEM of 3-5 experiments. Statistical analysis was performed by one-way ANOVA test. **, *** = significant difference, $P<0.01$ and $P<0.001$ respectively, compared to 'Control+ Raf-BxB CAAX.

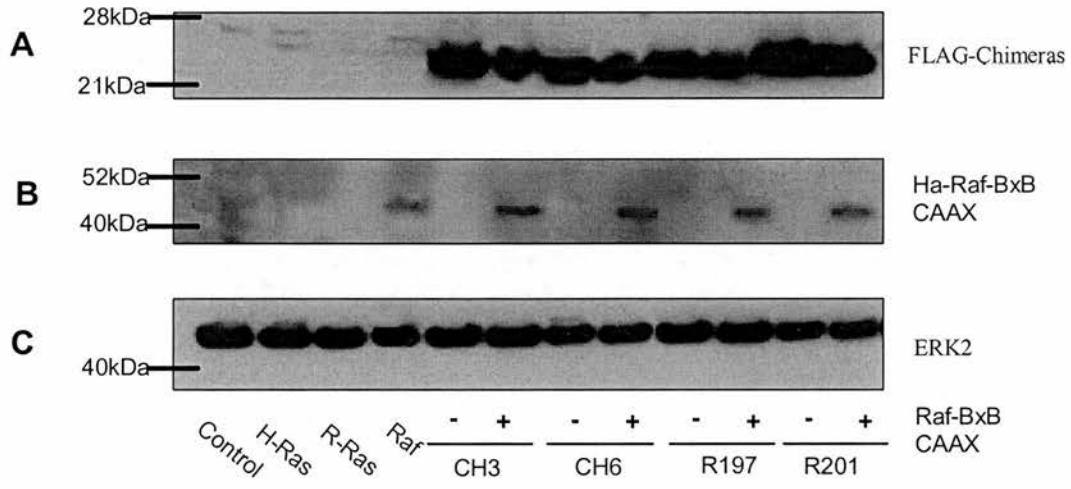

Figure 4.14 Co-expressing chimeras CH3, CH6, R197 and R201 with Raf-BxB CAAX has no effect on expression levels.

Cell lysates were prepared from cells transfected with 1μg of chimera CH3, CH6, R197 or R201 ± Raf-BxB CAAX (1μg). In each transfection, total DNA content was standardised to 2μg using control vector. Cell lysates were run on western blots and probed for chimera expression (A) using the anti-FLAG monoclonal antibody, Raf-BXB CAAX expression was checked for using (B) anti-Ha antibody. Total ERK2 (C) was measured as a control for equal loading of sample.

4.6 Discussion

The suppression of integrin activation by H-Ras and its downstream effector kinase Raf-1 can control cell morphology, migration and assembly of the extracellular matrix (Hughes *et al.*, 1997; Brenner *et al.*, 2000). In contrast, the small GTP-binding protein R-Ras lacks this activity; R-Ras has the ability to promote rather than suppress integrin activation (Zhang *et al.*, 1996; Sethi *et al.*, 1999; Kinashi *et al.*, 2000). Consistent with a role for R-Ras in activating integrins, R-Ras stimulates $\alpha_2\beta_1$-dependent cell migration of breast epithelial cells (Keely *et al.*, 1999). Activated R-Ras can also induce the adhesion of bone-marrow-derived mast cells to fibronectin through activation of $\alpha_5\beta_1$ (Kinashi *et al.*, 2000).

Recently there have been studies carried out on H-Ras and R-Ras to try and define variable and essential regions of each of these proteins. In particular, two separate studies have been published by Hansen *et al.*, (2002) and Hughes *et al.*, (2002) during the course of the investigations described in this thesis. While overlap between this work and the two specified studies is regrettable, this discussion will focus mainly on the findings obtained during this research, with appropriate reference made to the aforementioned studies.

With the aim of mapping the regions of H-Ras and R-Ras responsible for conferring their differing effects on integrin affinity, a series of chimeric proteins composed of portions of the N-terminus of H-Ras fused to the C-terminus of R-Ras and the reciprocal chimeras composed of the N-terminus of R-Ras fused to the C-terminus of H-Ras were utilised. The major findings of this chapter are as follows: First, a 25-amino acid stretch of H-Ras (149-174) is required for integrin suppression. Second, a 28-amino acid stretch of R-Ras (175-203) is sufficient to reverse H-Ras mediated integrin suppression. Third, several of the suppressive chimeras had little significant effect on ERK1 and ERK2 MAP kinase phosphorylation, suggesting that Ras-induced integrin suppression may be independent of the bulk activation of ERK1/2.

In an attempt to ease the discussion of the relevance of the results obtained in this chapter, I am going to concentrate first on the affects on integrin affinity modulation determined by transfection with the H/R-Ras chimeras as compared to H-Ras G12V and R-Ras G38V. Following this, I will discuss the effects on ERK1 and ERK2 MAP

kinase phosphorylation. Please refer to the schematic representation of the chimeras (Figure 4.1) during the following discussion.

4.6.1 Integrin affinity modulation by H/R-Ras chimeras

Using the $\alpha\beta$-py transfection system, results here indicate that a 25-amino-acid stretch of H-Ras, comprising residues 149-174, is required for its ability to suppress integrin activation. This conclusion was drawn from two observations; first, that a chimera, CH5, comprising H-Ras sequences C-terminal of Lys^{149}, (R-Ras 174; H-Ras 149-198), was sufficient to convey suppressive activity to R-Ras. Second, that chimera H201, that contains H-Ras residues N-terminal of Pro^{174} (H-Ras 174; R-Ras 204-219) was able to suppress integrin activation (see Figures 4.1 and 4.2). This is in accordance with the recently published paper by Hughes *et al.* (2002), where it was established that a 35-amino acid stretch of H-Ras, encompassing residues 149-174, was required for its ability to suppress integrin activation.

It would therefore be expected that those chimeras which contain this 25-amino-acid stretch would confer suppressive effects comparable to H-Ras. Figure 4.6 illustrates that chimeras CH1, CH5 and H201 have the ability to suppress the integrin to levels not dissimilar to H-Ras. It was somewhat unexpected to find that despite consisting of H-Ras residues 1-171, H197 showed a significant reversal of H-Ras-mediated integrin suppression. This suggests that the H-Ras C-terminal residues 171-174 (the area of divergence between chimeras H197 and H201) may be required for full suppressive potential of H-Ras. The possible relevance of these C-terminal residues will be discussed further on.

Results here show that a 28-amino-acid stretch of R-Ras, comprising residues 175-203, is sufficient for its ability to promote an activated state of integrin. This conclusion was drawn from the following observations; first, that a chimera, CH6, comprising R-Ras sequences C-terminal of Leu^{175}, (H-Ras 146; R-Ras 175-219), was sufficient to convey activation activity to H-Ras. Second, that chimera R201, which contains R-Ras residues N-terminal of Pro^{203} (R-Ras 203; H-Ras 175-198) was able to activate the integrin (see Figure 4.2). These results are in accordance with the recently published paper by Hansen *et al.*, (2002) who demonstrated that the C-

terminal 53 amino acids of R-Ras, encompassing residues 175-203, were necessary and sufficient to confer R-Ras specificity to H-Ras

The 28-amino-acid stretch of R-Ras, comprising residues 175-203, is sufficient for its ability to promote an activated state of integrin. Full length R-Ras has been shown to completely reverse H-Ras/Raf mediated integrin suppression, see Figure 3.5A (Sethi *et al.*, 1999). Therefore, it was investigated to see if this 28-amino acid stretch was sufficient to impart the reversing effect of R-Ras. Figure 4.9 shows that chimeras CH3, CH6 and R201 all significantly ($P<0.001$) reverse H-Ras mediated integrin suppression, and that this reversal is not due to a reduction in the level of H-Ras expression (Figure 4.10B). Unlike the rest of the 'reversing' chimeras, the effect by R197 was less significant ($P<0.05$) (Figure 4.9). This would imply that the area of divergence between chimeras R197 and R201, R-Ras C-terminal residues 198-203, affect its ability to fully promote an activated integrin state.

The requirement for Ras in Raf activation can be overcome by targeting Raf to the plasma membrane (Leevers *et al.*, 1994). Leevers *et al.*, (1994), describe a Raf protein (Raf CAAX) with a C terminus comprising the C-terminal 20 amino acids of K-Ras (4B), including the CAAX box required for post-translational modification and the polybasic domain required for plasma membrane localisation. Raf-CAAX is constitutively active and this activity is independent of cellular Ras, kinase activity is not inhibited by dominant-negative N17Ras (Leevers *et al.*, 1994). A variant of the activated Raf-CAAX, Raf-BxB CAAX, does not contain a Ras-binding domain (Hughes *et al.*, 1997). Transfection of $\alpha\beta$-py cells with Raf-BxB CAAX results in a suppression of integrin activity (Figures 4.11 and 4.13), this is in agreement with several publications (Hughes *et al.*, 1997; Sethi *et al.*, 1999; Hughes *et al.*, 2002). As Raf-BxB CAAX does not contain a Ras-binding domain, it would not be able to be bound to and sequestered by the H-and R-Ras chimeras in a dominant negative manner. Therefore, reversal of Raf-BxB CAAX-mediated suppression would rule out a dominant negative effect by the H/R-Ras chimeras on the Ras-Raf pathway.

Figure 4.11 shows that chimeras CH1, CH5 and H201 have the ability to suppress the integrin to levels comparable to Raf-BxB CAAX transfected cells. H197 shows a significant ($P<0.05$) reversal of Raf-BxB CAAX mediated integrin suppression. This

observation supports the proposal that H-Ras C-terminal residues 171-174 (the area of divergence between chimeras H197 and H201) affect the full suppressive potential of H-Ras.

R-Ras has been shown to completely reverse the suppressive effect mediated by Raf-BxB CAAX (Sethi *et al.*, 1999). This suggests that the R-Ras reversal of H-Ras induced suppression is not caused by competition for the common effector Raf-1 (since Raf-BxB CAAX does not contain a Ras binding domain) or by a dominant negative effect (Sethi *et al.*, 1999). Like R-Ras G38V, chimeras CH3, CH6 and R201 are capable of fully reversing Raf-BxB CAAX-mediated suppression (Figure 4.13). This reversal was not as a consequence of reduced Raf-BxB CAAX expression levels (Figure 4.14 B). Although R197 was able to reduce Raf-BxB CAAX-mediated integrin suppression, it was not able to fully reverse integrin suppression. This observation draws attention, once again, to the area of divergence between chimeras R197 and R201. It would appear that R-Ras C-terminal residues 198-203 are necessary for it to be fully capable of reversing Raf-BxB CAAX-mediated suppression.

The molecular basis for the dependence on H-Ras (149-174) and R-Ras (175-203) on integrin modulation is not immediately obvious. Prior to the work carried out for this thesis, and the recent studies by Hansen *et al.*, (2002) and Hughes *et al.*, (2002), previous analyses of H-Ras and R-Ras have not implicated these regions as critical for specifying interactions with downstream effectors.

The main sequence variation between H-Ras and R-Ras is the N-terminal 26-amino acid extension of R-Ras. However, the ability of chimeras CH1 and CH5, which contain this 26-amino acid stretch of R-Ras, to still induce a suppressive effect on integrins discounts the importance of this 26-amino acid extension with respect to integrin affinity modulation. A previous study demonstrated the null effect of substituting the first 30-amino acids of R-Ras for the first 4-amino acids of H-Ras on the biological activity of H-Ras G12V, strongly suggesting that the N-terminal of R-Ras does not interfere with the effector function of H-Ras (Lowe *et al.*, 1988).

Extensive analysis of both H-Ras point mutations and H-Ras/Rap1 chimeras has suggested that the critical sequences involved in determining effector binding and

activation are amino-acids 20-48 and amino-acids 60-76, which comprise the switch I (within the effector binding domain) and switch II regions, respectively (Marshall *et al.*, 1991; Marshall *et al.*, 1996; Campbell *et al.*, 1998). However, in this study, the substitution of these regions between H-Ras and R-Ras (demonstrated with chimeras CH1, CH3, CH5 and CH6) had only minimal effects on integrin modulation. This may be due to the high degree of sequence similarity between H-Ras and R-Ras effector binding regions, which means that despite swapping the effector regions they can bind to common effectors such as Raf-1 and PI 3-kinase. Results here indicate that residues important for integrin affinity modulation, located in the C-terminal regions of H-Ras and R-Ras, could also be responsible for the regulation of the activation of bound effectors.

The main sequence divergence between the three Ras isoforms, H, N and K (which exhibit biologically significant differences despite their high degree of sequence homology) is confined to 23-amino acids of the carboxy-terminal hypervariable region (HVR) (Prior *et al.*, 2001). This hypervariable domain can be divided into two distinct areas, the HVR linker domain (H-Ras 166-179) and the C-terminal targeting domain (H-Ras 180-189) (Prior *et al.*, 2001). The latter C-terminal targeting domain contains the –CAAX box, common to all Ras proteins (Hancock *et al.*, 1989). The targeting of Ras to the plasma membrane is essential for its correct biological activity (Williumsen *et al.*, 1984).

Results here show that substitution of the C-terminal targeting domains of H-Ras with R-Ras (chimera H201) was not sufficient to convey the integrin activating properties of R-Ras (Figures 4.2, 4.7 and 4.11). Consistent with this, substitution of the C-terminal targeting domains of R-Ras with H-Ras (chimera R201) was not sufficient to convey suppressive activity (Figures 4.2, 4.9 and 4.13). This demonstrates that the C-terminal targeting domain alone is not sufficient to mediate the differing integrin modulating properties of H-Ras and R-Ras, these findings concur with the recent publication by Hughes *et al.*, (2002).

There have been a number of recent investigations to determine the specific functions of the HVR linker domain. Prior *et al.*, (2001) showed that palmitolyation and farnesylation targets H-Ras to lipid rafts and caveolae within the plasma

membrane; subsequent GTP-loading redistributes H-Ras from rafts into the bulk plasma membrane and the H-Ras HVR linker domain is necessary for GTP-dependent release of H-Ras from the lipid rafts and for biological activity. The importance of the HVR linker domain was further supported by Jaumont *et al.*, (2002) who used deletion analysis to show that removal of the N-terminal amino acids of the HVR linker domain, H-Ras residues 166-172, compromised the normal raft/non-raft equilibrium and effector function of H-Ras. The remaining C-terminal 7-amino acids of the linker domain have been described as an essential spacer element of the HVR linker domain (Jaumont *et al.*, 2002). While alanine replacement of residues 166-172 abrogated Raf-1 activity similar to that seen with deletion of the entire linker domain, alanine replacement of residues 173-179 resulted in activation of Raf-1 as efficiently as full-length H-Ras G12V (Jaumont *et al.*, 2002).

The H-Ras (149-174) and R-Ras (175-203) residues identified in this study as having influence over integrin affinity modulation by H-Ras and R-Ras overlap with the proteins' HVR linker domains. Therefore, investigations here draw attention to the importance of the HVR linker domain in the modulation of integrin affinity.

The H/R-Ras chimera, H197 (H-Ras 171; R-Ras 199-219), despite comprising of >85% H-Ras N-terminal sequence, has a compromised ability to suppress integrins. Moreover, H197 demonstrates significant ($P<0.05$) reversal of both H-Ras G12V- and Raf-BxB CAAX-mediated integrin suppression. That H197 does not contain the specific amino acids of the essential spacer element of H-Ras would not explain its lack of suppressive ability. As demonstrated by Jaumont *et al.*, (2002), alanine substitution of these amino acids preserves H-Ras G12V properties.

Likewise, the H/R-Ras chimera R197 (R-Ras 198; H-Ras 172-198), despite being comprised of ~90% R-Ras N-terminal sequence, has a limited ability to reverse H-Ras G12V and Raf-BxB CAAX mediated integrin suppression.

Since substitution of the C-terminal binding domain of the HVR of H-Ras and R-Ras, demonstrated by chimeras H201 and R201, does not affect their abilities to modulate integrin affinity, we can look to see if the areas of sequence divergence between H197 and H201 (H-Ras C-terminal residues 171-174) and the equivalent

area of sequence divergence between R197 and R201 (R-Ras C-terminal residues 198-203) hold any significance.

R-Ras differs from Ras and most other members of the Ras super family of small GTPases in that it possesses a distinct proline rich site (Wang *et al.*, 2000). This proline rich site is located within the HVR linker domain (R-Ras residues Pro^{199} to Pro^{206}) and overlaps with the area of sequence divergence between R197 and R201; R-Ras C-terminal residues 198-203.

The proline-rich motif of R-Ras resembles Src Homology 3 (SH3) domain binding sites (PXXP motifs, where X represents any amino acid) (Wang *et al.,* 2000). Molecules that contain Src Homology 2 (SH2) and SH3 domains provide one of the principle ways by which signals are transduced in cells using protein-protein interactions between proline-rich domains and SH3 domains and induced interactions between phosphotyrosine residues and SH2 domains (Birge *et al.*, 1996). Wang *et al.*, (2000) have recently demonstrated that the adaptor protein Nck (SH3-domain containing protein) interacted strongly with the R-Ras proline-rich sequence, independent of whether R-Ras was in its GDP or GTP form. Proline to alanine point mutations to alter the PXXP motifs (P202A, P203A) reduced Nck binding showing that the proline-rich domain is required for binding to Nck domains (Wang *et al.*, 2000).

It has been suggested that the adaptor protein, Nck, is required to recruit R-Ras effectors that are then employed by R-Ras to augment integrin affinity (Kinbara *et al.*, 2003). Nck could mediate a cross talk between R-Ras and Rac1, as it binds to PAK, which is known to interact with Rac1A (Manser *et al.*, 1994; Manser *et al.*, 1997). Furuhjelm and Peranen, (2003) showed that R-Ras and Rac1 colocalise to focal adhesions. The possible cross talk between these two proteins, within focal adhesions, could help to amplify signals which mediate cell adhesion and spreading. Nck has also been shown to interact through its SH2 domain with $p130^{cas}$ (Barbacid, 1987). $P130^{cas}$ is a docking protein that accumulates in focal adhesions (Holland *et al.*, 1998; Hanks and Polte, 1996). Thus, Nck could, by binding R-Ras, via its SH3 domain, and $p130^{cas}$, via its SH2 domain, allow cross talk between these two proteins

within focal adhesions. In fact a recent study has shown that R-Ras can enhance the phosphorylation of $p130^{cas}$ (Kwong *et al.*, 2003).

Expression of constitutively active R-Ras G38V enhanced cell adhesion to extracellular matrix substrates by enhancing integrin ligand-binding activity in a CHO cell line (Zhang *et al.*, 1996). Wang *et al.*, (2000) show that 32D mouse monocytic cells, which grow in suspension, when transfected with R-Ras G38V adhered to fibronectin however, clones expressing the R-Ras G38V (P202A, P203A) mutant showed reduced cell attachment to fibronectin. The importance of the proline-rich domain in contributing to the integrin activating function of R-Ras may help to explain the effects of chimeras H197 and R197 on integrin affinity. It may be that the significant ($P<0.05$) reversal of both H-Ras G12V and Raf-BxB CAAX mediated integrin suppression by H197 (H-Ras 171; R-Ras 199-219), despite comprising of >85% H-Ras N-terminal sequence, may be due to the fact that this chimera contains the proline-rich motifs of R-Ras (R-Ras residues 199-206) which may help promote integrin activation. The limited ability of R197 (R-Ras 198; H-Ras 172-198) to reverse H-Ras G12V and Raf-BxB CAAX mediated integrin suppression, despite being comprised of ~ 90% R-Ras N-terminal sequence, may be due to it lacking the proline-rich motifs of R-Ras, which begins with R-Ras Pro^{199}.

Further investigations into the proline-rich domain of R-Ras would help to resolve the role, if any, for this sequence in mediating R-Ras's effect on integrin affinity.

4.6.2 Phosphorylation of ERK1/2 by H/R-Ras chimeras.

The Ras proteins function as molecular switches that are controlled by a GDP/GTP binding cycle, coupling to and activating downstream effectors when in the activated GTP-bound conformation (Bos *et al.*, 1998). Both H-Ras and R-Ras have similar core-effector binding domains, and bind to common downstream effectors when in the GTP-bound state. The major downstream effector of H-Ras is Raf-1 and in its active (GTP-bound) state, H-Ras recruits Raf-1 to the plasma membrane and stimulates its kinase activity (Leevers *et al.*, 1994). Following on from this, Raf-1 activates the ERK1/2 MAP kinase cascade and eventually leads to changes in transcription (Leevers *et al.*, 1994). R-Ras interacts with the Raf serine/threonine kinases (Spaargaren *et al.*, 1994; Rey *et al.*, 1994). However, R-Ras has not been

reported to activate Raf or the ERK1/2 family of MAP kinases (Sethi *et al.*, 1999). It has been described that expression of H-Ras G12V and its kinase effector, Raf-1, mediates integrin suppression and that this correlates with increased ERK1/2 activity (Hughes *et al.*, 1997). Constitutively active R-Ras (G38V) has been shown to antagonise the Ras/Raf initiated integrin suppression pathway furthermore, this reversal of suppression does not affect ERK2 activation induced by H-Ras or Raf (Sethi *et al.*, 1999).

Using the H-and R-Ras chimeras the relationship between H-Ras and R-Ras in modulating integrin affinity, and their ability to influence MAP kinase activation was further investigated.

The effect of H/R-Ras chimera expression on ERK 1/2 phosphorylation and activation was observed using a variety of methods. A decision was made to employ several methods to provide both quantitative and qualitative results, as it was obvious from preliminary experiments that there was little qualitative difference between the levels of ERK1/2 activation by the individual chimeras. The central aim was to try and determine the specific sequences of H- and R-Ras which may affect their ability to activate ERK1/2. As positive controls for each of the methods employed, cells transfected with H-Ras G12V and serum stimulation of quiesced cells were used.

In contrast to an initial report by Hughes *et al.*, (1997), who suggested that integrin suppression was a novel function of the Ras/Raf-initiated pathway, results here demonstrate that the activation of ERK1/2 might not be necessary for suppression of integrins. This is in agreement with several recent studies by Hughes *et al.*, (2002) and Hansen *et al.*, (2002). The chimeras, CH1; CH5 and H201, which have demonstrated suppressive effects on integrins similar to H-Ras G12V (Figures 4.2, 4.7 and 4.11), did not activate ERK1/2 to any significant level (see Figure 4.4). Hughes *et al.*, (2002) also showed that H-and R-Ras chimeras very similar to those employed in this study, which had a suppressive effect on integrin-affinity, were poor activators of ERK1/2. Hughes *et al.*, (2002) further investigated this finding by inhibiting bulk ERK1/2 activation by: co-expressing MAP kinase phosphatase 3 (MKP3), a phosphatase which specifically binds and dephosphorylates ERK1 and ERK2 (Muda *et al.*, 1996; Keyse *et al.*, 2000); and using MEK kinase inhibitor,

U0126 (Favata *et al.*, 1998), neither of which affected the ability of H-Ras or Raf-1 to suppress integrin activation. Additionally, it was found that activation of ERK1/2 alone, using a constitutively active mutant of MEK1, was not sufficient for integrin suppression (Hughes *et al.*, 2002). Using H/R-Ras chimeras similar to those used in the investigations for this project and those used by Hughes *et al.*, (2002), Hansen *et al.*, (2002) further verify the conclusion that integrin suppression does not necessarily correlate with the activation of the ERK1/2 pathway.

Hansen *et al.*, (2002) reported that ERK1/2 activity, as determined using a phospho-specific ERK1/2 antibody, correlated with the presence of H-Ras N-terminal sequences. Their study revealed that H-and R-Ras chimeras which contained H-Ras sequences N-terminal of Ala^{121} were capable of activating ERK1/2 to levels comparable to H-Ras G12V (Hansen *et al.*, 2002). Results here conflict with this account. Figures 4.3B and 4.4A show the phosphorylation state of ERK1/2 using a western blot probed with a phospho-specific ERK1/2 antibody and an ERK1/2 ELISA respectively. Results suggest that none of the H/R-Ras chimeras, whether they contain H-Ras N-terminal sequences or not, exhibited the ability to activate ERK1/2, to levels similar to H-Ras G12V. The H201 chimera, which contains the H-Ras sequences 1 to 174, did increased the phosphorylation state of ERK1/2, but not to the levels observed with H-Ras G12V.

One hypothesis that may be drawn from the overall null effect of the H-and R-Ras chimeras on levels of ERK1/2 phosphorylation may be that, in order for H-Ras to interrelate with and stimulate the kinase activity of its down stream effector kinase Raf-1 it must first of all be targeted to the correct membrane microdomain by the C-terminal farnesyl group. H-Ras Ser^{186} (which lacked the cysteine residue to be farnesylated) had almost negligible activity, indicating that the post-translational modifications of H-Ras, especially the farnesylation step, are critical for normal activation of Raf (Okada *et al.*, 1996).

The above hypothesis may explain why H201 is incapable of phosphorylating ERK1/2 to similar levels of H-Ras G12V, despite possessing >85% H-Ras sequence. As H201 comprises the C-terminal targeting domain of R-Ras, it is likely be to be targeted to an alternative plasma membrane domain where it may not be as proficient

at interacting with Raf sufficiently to induce its kinase activity. Alternatively, it may be that the chimeric 3-D structure (determined by post-translational modifications) of H201 may disrupt the ability of the chimera to target the correct microdomain or affect its ability to interact with Raf. Cell passage number (age) may also affect the cell's ability to activate ERK1/2.

The use of the phospho-specific ERK1/2 antibody and an ERK1/2 ELISA allowed us to determine the phosphorylation of ERK1/2, as an indicator of the activation state. The kinase assays, Figures 4.5 and 4.6, were performed to allow us to quantify the effect the chimeras had on levels of kinase activity, for ERK1/2 and Raf respectively. However, a number of problems encountered while performing the kinase assays, concerning kinase assay sensitivity, limited the value of performing statistical analyses on the data. The above-mentioned problems included: inaccurate pipetting, resulting from the use of agarose beads; radioactive decay; deterioration of substrate activity and washing techniques. Despite taking appropriate steps to rule out some of the problems encountered with the kinase assays, the discrepancy of scintillation counts and phospho-imager readings caused by biological variations between experiments meant that collating data from several experiments would lead to increased error and a lack of statistical significance. Therefore, it was decided to use representative graphs to display the general trend observed within each individual kinase assay.

As expected, H-Ras G12V and serum stimulation induced the greatest increase in MAPK and Raf kinase activity. The H201 chimera also increased the kinase activity of Raf1 and ERK1/2, but not to the same extent as observed with H-Ras G12V transfection and serum stimulation (Figure 4.5). The other H/R-Ras chimeras were incapable of inducing kinase activities to levels beyond those observed with control vector alone.

Although the H201 chimera was capable of inducing phosphorylation of ERK1/2 (Figures 4.3B and 4.4A), perhaps the lack of the H-Ras C-terminal domain diminished the ability of the chimera to increase the phosphorylation state of ERK1/2 to the levels required for full ERK1/2 kinase activity (4.5A). This would suggest that for maximal stimulation of ERK1/2 kinase activity (i.e. dual phosphorylation of the

relevant ERK1/2 Thr and Tyr residues) the full-length sequence of H-Ras is necessary.

4.6.3 Summary

The H/R-Ras chimeras imply that the C-terminal sequences of H-Ras and R-Ras are critical to determining their different effects on integrin affinity. More specifically, a 25-amino acid stretch of H-Ras (Arg^{149} to Pro^{174}) is required for integrin suppression, and a 28-amino acid stretch of R-Ras (Leu^{175} to Pro^{203}) is sufficient to reverse H-Ras mediated integrin suppression.

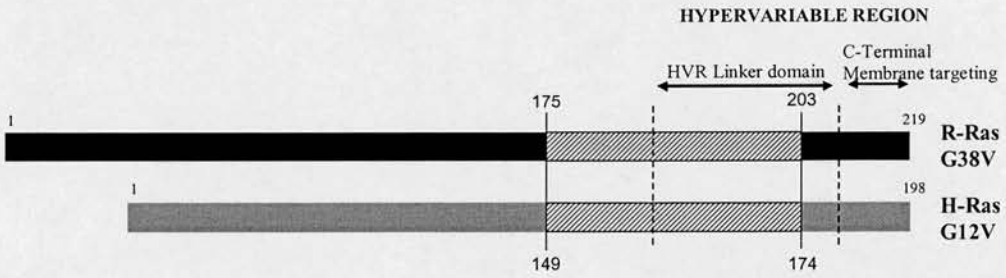

The areas of H-Ras and R-Ras identified as being important for determining their different effects on integrin affinity are shown as a hatched effect on the above schematic. The sequences are shown to be in the same place for each of the proteins, in a C-terminal position which overlaps with the HVR.

The proline-rich domain of R-Ras (residues Pro^{199} to Pro^{206}) may be important in conferring R-Ras's ability to fully reverse H-Ras G12V-mediated integrin suppression.

Like H-Ras G12V, chimeras CH1, CH5 and H201, all suppressed integrin affinity. However, only H201 induced integrin suppression correlated with ERK1/2 activation, which suggests that Ras-induced integrin suppression may be independent of the bulk activation of ERK1/2. Results indicate the presence of a possible integrin suppression pathway that is independent of ERK1/2.

Further analysis of the effect of the H-and R-Ras chimeras on ERK1/2 kinase activity suggests that the full-length H-Ras sequence is required for maximal activation of ERK1/2.

See below for a summary table showing all the observations made for each chimera in this chapter; refer to Figure 4.1 for schematic representation of chimeric sequences.

Chimera	Integrin affinity	Reversal of H-Ras suppression	Reversal of Raf-BxB CAAX suppression	ERK1/2 activation
R-RAS	Activated	***	***	+
H-RAS	Suppressed	N/A	N/A	+++
CH3	Activated	***	***	+
CH6	Activated	***	***	+
H197	Little effect	*	*	+
H201	Suppressed	N/A	N/A	++
CH1	Suppressed	N/A	N/A	+
CH5	Suppressed	N/A	N/A	+
R197	Little effect	*	*	+
R201	Activated	***	***	+

Key: Influence on the reversal of suppression of H-Ras G12V and Raf-BxB CAAX shown with asterisks, where * = small reversal and *** = highly significant reversal. Effect on ERK1/2 activation shown using crosses, where + = control level activation, ++ = slight increase in activation and +++ = significant increase in activation.

APPENDIX I

H-Ras G12V sequence in pCDNA3.1(+)

```
Page 1.1
          1              15 16              30 31              45 46              60 61              75 76              90
1 HRAS    ATGACGGAATATAAG CTGGTGGTGGTGGGC GCCGGCGGTGTGGGC AAGAGTGCGCTGACC ATCCAGCTGATCCAG AACCATTTT-GTGGA   89
2 HRASSP6 ATAACGGAATATAAG NTGGTGGTGGTGGGC GCCGTCGGTGTGGGC AAGAGTGCGCTGACC ATCCAGCTGATCCAG AACCATTTTTGTGNN   90

Page 2.1
          91             105 106             120 121             135 136             150 151             165 166             180
1 HRAS    CGAATACGACCCCAC TATAGAGGATTCCTA CCGGAAGCAGGTGGT CATTGATGGGGAGAC GTGCCTGTTGGACAT CCTGGATACCGCCGG  179
2 HRASSP6 CGAATACGACCCCAC TATAGAGGATTCCTA CCGGAAGCAGGTGGT CATTGATGGGGAGAC GTGCCTGTTGGACAT CCTGGATACCGCCGG  180

Page 3.1
          181            195 196            210 211            225 226            240 241            255 256            270
1 HRAS    CCAGGAGGAGTACAG CGCCATGCGGGACCA GTACATGCGCACCGG GGAGGGCTTCCTGTG TGTGTTTGCCATCAA CAACACCAAGTCTTT  269
2 HRASSP6 CCAGGAGGAGTACAG CGCCATGCGGGACCA GTACATGCGCACCGG GGAGGGCTTCCTGTG TGTGTTTGCCATCAA CAACACCAAGTCTTT  270

Page 4.1
          271            285 286            300 301            315 316            330 331            345 346            360
1 HRAS    TGAGGACATCCACCA GTACAGGGAGCAGAT CAAACGGGTGAAG-G ACTCGGATGACGTGC CCATGGTGCTGGTGG GGAACAAGTGTGACC  358
2 HRASSP6 TGAGGACATCCACCA GTACAGGGAGCAGAT CAAACGGGTGAAGAG ACTCGGATGACGTGC CCATGGTGCTGGTGG GGAACAAGTGTGACC  360

Page 5.1
          361            375 376            390 391            405 406            420 421            435 436            450
1 HRAS    TGGCTGCACGCACTG TGGAATCTCGGCAGG CTCAGGACCTCGCCC GAAGCTACGGCATCC CCTACATCGAGACCT CGGCCAAGACCCGGC  448
2 HRASSP6 TGGCTGCACGCACTG TGGAATCTCGGCAGG CTCAGGACCTCGCCC GAAGCTACGGCATCC CCTACATCGAGACCT CGGCCAAGACCCGGC  450

Page 6.1
          451            465 466            480 481            495 496            510 511            525 526            540
1 HRAS    AGGGAGTGGAGGATG CCTTCTACACGTTGG TGCGTGAGATCCGGC AGCACAAGCTGCGGA AGCTGAACCCTCCTG ATGAGAGTGGCCCCG  538
2 HRASSP6 AGGGAGTGGAGGATG CCTTCTACACGTTGG TGCGTGAGATCCGGC AGCACAAGCTGCGGA AGCTGAACCCTCCTG ATGAGAGTGGCCCCG  540

Page 7.1
          541            555 556            570 571            585 586            600 601            615 616            630
1 HRAS    GCTGCATGAGCTGCA AGTGTGTGCTCTCCT GA    570
2 HRASSP6 GCTGCATGAGCTGCA AGTGTGTGCTCTCCT GA    572
```

R-Ras G38V sequence in pCDNA3.1 (+)

```
Page 1.1
          1              15 16              30 31              45 46              60 61              75 76              90
1 RRAS  ATGAGCAGCGGGGCG GCGTCCGGGACAGGG CGGGGGCGGCCCCGG GGCGGGGGACCTGGG CCCGGGGACCCCCCG CCCAGCGAGACACAC     90
2 RRASb ATGAGCTCTGGTGCT GCTTCTGGTACAGGT CGTGGTCGTCCACGT GGTGGAGGTCCAGGT CCCGGGGACCCTCCG CCTAGCGAGACACAC     90

Page 2.1
          91             105 106             120 121             135 136             150 151             165 166             180
1 RRAS  AAGCTGGTGGTCGTG GGCGGCGGCGGCGTG GGCAAGAGCGCGCTG ACCATCCAGTTCATC CAGTCCTACTTCGTG TCTGACTACGACCCC  180
2 RRASb AAGCTTGTGGTCGTG GGTGGTGTCGGCGTG GGCAAGAGCGCGCTG ACCATCCAGTTCATC CAGTCCTACTTCGTG TCTGACTACGACCCC  180

Page 3.1
          181            195 196            210 211            225 226            240 241            255 256            270
1 RRAS  ACTATTGAGGACTCC TACACGAAGATCTGC AGTGTGGATGGCATC CCAGCCCGGCTGGAC ATCCTGGACACCGC- ----GGGCCAGGAAG  265
2 RRASb ACTATTGAGGACTCC TACACGAAGATCTGC AGTGTGGATGGCATC CCAGCCCGGCTGGAC ATCCTGGACATCTCT NGTCGGGCCAGGAAG  270

Page 4.1
          271            285 286            300 301            315 316            330 331            345 346            360
1 RRAS  AGTTCGGGGCCATGA GAGAGCAGTACATGC GTGCTGGCCACGGCT TCCTGCTGGTGTTCG CCATTAATGACCGGC AGAGTTTCAACGAGG  355
2 RRASb AGTTCGGGGCCATGA GAGAGCAGTACATGC GTGCTGGCCACGGCT TCCTGCTGGTGTTCG CCATTAATGACCGGC AGAGTTTCAACGAGG  360

Page 5.1
          361            375 376            390 391            405 406            420 421            435 436            450
1 RRAS  TGGGCAAGCTCTTCA CGCAGATTCTGCGGG TCAAGGACCGCGACG ACTTCCCCGTTGTGT TGGTCGGGAACAAGG CAGATCTGGAGTCAC  445
2 RRASb TGGGCAAGCTCTTCA CGCAGATTCTGCGGG TCAAGGACCGCGACG ACTTCCCCGTTGTGT TGGTCGGGAACAAGG CAGATCTGGAGTCAC  450

Page 6.1
          451            465 466            480 481            495 496            510 511            525 526            540
1 RRAS  AGCGCCAGGTCCCCC GATCAGAAGCCTCTG CC-TTCGGCGCCTCC CACCACGTGGCCTAC TTTGAGGCCTCGGCC AAACTGCGTCTCAAC  534
2 RRASb AGCGCCAGGTCCCCC GATCAGAANCCTCTG CCCTTCGGCGCCTCC CACCACGTGGCCTAC TTTGAGGCCTCGGCC AAACTGCGTCTCAAC  540

Page 7.1
          541            555 556            570 571            585 586            600 601            615 616            630
1 RRAS  GTGGACGAGGCTTTT GAGCAGCTGGTGCGG GCTGTCCGGAAATAC CAGGAACAAGAGCTC CCACCGAGCCCTCCC AGTGCCCCCAGGAAG  624
2 RRASb GTGGACCANGCTTTT GAGCAGCTGGTGCGG GCTGTCCGGAAATAC CAGGAACAAGAGCTC CCACCGAGCCCTCCC AGTGCCCCCAGGAAG  554

Page 8.1
          631            645 646            660 661            675 676            690 691            705 706            720
1 RRAS  AAGGGCGGGGGCTGC CCCTGCGTCCTCCTG TAG    657
2 RRASb AAGGGCGGGGGCTGC CCCTGCGTCCTCCTG TAG    554
```

APPENDIX II

Chimera CH1 alignment sequence

```
        1           15 16          30 31          45 46          60 61          75 76          90
1  CH1  AAGAGCTCTGGTGCT GCTTCTGGTACAGGT CGTGGTCGTCCACGT GGTGGAGGTCCAGGT CCCGGGGACCCTCCG CCTAGCGAGACACAC    90
2 HRAS  --------------- --------------- --------------- --------------- --------------- -ATGACG-GA-ATAT    12
3 RRAS  ATGAGCAGCGGGGCG GCGTCCGGGACAGGG CGGGGGCGGCCCCGG GGCGGGGGACCTGGG CCCGGGGACCCCCCG CCCAGCGAGACACAC    90

Page 2.1
        91          105 106         120 121         135 136         150 151         165 166         180
1 CH1con AAGCTTGTGGTCGTG GGTGGTGTCGGCGTG GGCAAGAGCGCGCTG ACCATCCAGTTCATC CAGTCCTACTTCGTG TCTGACTACGACCCC  180
2 HRAS  AAGCTGGTGGTGGTG GGCGCCGGCGGTGTG GGCAAGAGTGCGCTG ACCATCCAGCTGATC CAGAACCATTTTGTG GACGAATACGACCCC  102
3 RRAS  AAGCTGGTGGTCGTG GGCGGCGGCGGCGTG GGCAAGAGCGCGCTG ACCATCCAGTTCATC CAGTCCTACTTCGTG TCTGACTACGACCCC  180

Page 3.1
        181         195 196         210 211         225 226         240 241         255 256         270
1 CH1con ACTATTGAGGACTCC TACACGAAG-ATCTG CAGTG-TGGATGGCA TCCCAGCCCGGCTGG ACATCCTGGACACCG CGGGCCATGAGGAGT  268
2 HRAS  ACTATAGAGGATTCC TACCGGAAGCAGGTG --GTCATTGATGGGG AGACGTGCCTGTTGG ACATCCTGGATACCG CCGGCCAGGAGGAGT  190
3 RRAS  ACTATTGAGGACTCC TACACGAAG-ATCTG CAGTG-TGGATGGCA TCCCAGCCCGGCTGG ACATCCTGGACACCG CGGGCCAGGAAGAGT  268

Page 4.1
        271         285 286         300 301         315 316         330 331         345 346         360
1 CH1con ACAGCGCCATGCGGG ACCAGTACATGCGCA CCGGGGAGGGCTTCC TGTGTGTGTTTGCCA TCAACAACACCAAGT CTTTTGAGGACATCC  358
2 HRAS  ACAGCGCCATGCGGG ACCAGTACATGCGCA CCGGGGAGGGCTTCC TGTGTGTGTTTGCCA TCAACAACACCAAGT CTTTTGAGGACATCC  280
3 RRAS  TCGGGGCCATGAGAG AGCAGTACATGCGTG CTGGCCACGGCTTCC TGCTGGTGTTCGCCA TTAATGACCGGCAGA GTTTCAACGAGGTGG  358

Page 5.1
        361         375 376         390 391         405 406         420 421         435 436         450
1 CH1con ACCAGTACAGGGAGC AGATCAAACGGGTGA AGGACTCGGATGACG TGCCCATGGTGCTGG TGGGGAACAAGTGTG ACCTGGGCTGCAC-G  447
2 HRAS  ACCAGTACAGGGAGC AGATCAAACGGGTGA AGGACTCGGATGACG TGCCCATGGTGCTGG TGGGGAACAAGTGTG ACCTGG-CTGCAC-G  368
3 RRAS  GCAAGCTCTTCACGC AGATTCTGCGGGTCA AGGACCGCGACGACT TCCCCGTTGTGTTGG TCGGGAACAAGGCAG ATCTGGAGT-CACAG  447

Page 6.1
        451         465 466         480 481         495 496         510 511         525 526         540
1 CH1con CACTGTGGAATC--- TCGGCAGGCTCAGGA CCTCGCCCGAAGCTA CGGCATCCCCTACAT CGAGACCTCGGCCAA GACCCGGCAGGGAGT  534
2 HRAS  CACTGTGGAATC--- TCGGCAGGCTCAGGA CCTCGCCCGAAGCTA CGGCATCCCCTACAT CGAGACCTCGGCCAA GACCCGGCAGGGAGT  455
3 RRAS  CGCCAGGTCCCCCGA TCAGAAGCCTCTGC- CTTCGGCGCCTCCCA CCACGTGGCCTACTT TGAGGCCTCGGCCAA ACTGCGTCTCAACGT  536

Page 7.1
        541         555 556         570 571         585 586         600 601         615 616         630
1 CH1con GGAGGATGCCCTTCT ACNCNTNGGGTGCTT GAAATCCNGCAGCAC AANCTGCGGAACCNN ACCCCTCCCTGA--T TANATTGNCCCCGGC  622
3 RRAS  GGACGAGGCT-TTTG AGCAGCTGG-TGCGG GCTGTCCGGAAATAC CAGGAACAAGAGCT- --CCCACCGAGCCCT CCCAGTGCCCCCAGG  621

Page 8.1
        631         645 646         660 661         675 676         690 691         705 706         720
1 CH1con T------GCTTTANC TGCAATTNTNTGCTC TCCTGA--    652
2 HRAS  T------GCATGAGC TGCAAGTGTGTGCTC TCCTGA--    570
3 RRAS  AAGAAGGGCGGGGGC TGCCCCTGCGTCCTC --CTGTAG    6
```

Chimera CH3 alignment sequence

```
Page 1.1
       1              15 16              30 31              45 46              60 61              75 76              90
1 CH3  --------------- --------------- --------------- --------------- --------------- ---ATGACGGAATAT      12
2 RRAS ATGAGCAGCGGGGCG GCGTCCGGGACAGGG CGGGGGCGGCCCCGG GGCGGGGGACCTGGG CCCGGGGACCCCCCG CCCAGCGAGACACAC      90
3 HKAS --------------- --------------- --------------- --------------- --------------- ---ATGACGGAATAT      12

Page 2.1
       91          105 106         120 121         135 136         150 151         165 166         180
1 CH3  AAGCTGGTGGTGGTG GGCGCCGTCGGTGTG GGCAAGAGTGCGCTG ACCATCCAGCTGATC CAGAACCATTTTGTG GACGAATACGACCCC     102
2 RRAS AAGCTGGTGGTCGTG GGCGGCGGCGGCGTG GGCAAGAGCGCGCTG ACCATCCAGTTCATC CAGTCCTACTTCGTG TCTGACTACGACCCC     180
3 HRAS AAGCTGGTGGTGGTG GGCGCCGGCGGTGTG GGCAAGAGTGCGCTG ACCATCCAGCTGATC CAGAACCATTTTGTG GACGAATACGACCCC     102

Page 3.1
       181         195 196         210 211         225 226         240 241         255 256         270
1 CH3  ACTATAGAGGATTCC TACCGGAAGCAGGTG --GTCATTGATGGGG AGACGTGCCTGTTGG ACATCCTGGATACCG CCGGCCAGGAAGAGT     190
2 RRAS ACTATTGAGGACTCC TACACGAAG-ATCTG CAGTG-TGGATGGCA TCCCAGCCCGGCTGG ACATCCTGGACACCG CGGGCCAGGAAGAGT     268
3 HRAS ACTATAGAGGATTCC TACCGGAAGCAGGTG --GTCATTGATGGGG AGACGTGCCTGTTGG ACATCCTGGATACCG CCGGCCAGGAGGAGT     190

Page 4.1
       271         285 286         300 301         315 316         330 331         345 346         360
1 CH3  TCGGGGCCATGAGAG AGCAGTACATGCGTG CTGGCCACGGCTTCC TGCTGGTGTTCGCCA TTAATGACCGGCAGA GTTTCAACGAGGTGG     280
2 RRAS TCGGGGCCATGAGAG AGCAGTACATGCGTG CTGGCCACGGCTTCC TGCTGGTGTTCGCCA TTAATGACCGGCAGA GTTTCAACGAGGTGG     358
3 HRAS ACAGCGCCATGCGGG ACCAGTACATGCGCA CCGGGGAGGGCTTCC TGTGTGTGTTTGCCA TCAACAACACCAAGT CTTTTGAGGACATCC     280

Page 5.1
       361         375 376         390 391         405 406         420 421         435 436         450
1 CH3  GCAAGCTCTTCACGC AGATTCTGCGGGTCA AGGACCGCGACGACT TCCCCGTTGTGTTGG TCGGGAACAAGGCAG ATCTGGAGTCACAGC     370
2 RRAS GCAAGCTCTTCACGC AGATTCTGCGGGTCA AGGACCGCGACGACT TCCCCGTTGTGTTGG TCGGGAACAAGGCAG ATCTGGAGTCACAGC     448
3 HRAS ACCAGTACAGGGAGC AGATCAAACGGGTGA AGGACTCGGATGACG TGCCCATGGTGCTGG TGGGGAACAAGTGTG ACCTGGCTGCAC-GC     369

Page 6.1
       451         465 466         480 481         495 496         510 511         525 526         540
1 CH3  GCCAGGTCCCCCGAT CAGAAGCCTCTGC-C TTCGGCGCCTCCCAC CACGTGGCCTACTTT GAGGCCTCGGCCAAA CTGCGTCTCAACGTG     459
2 RRAS GCCAGGTCCCCCGAT CAGAAGCCTCTGC-C TTCGGCGCCTCCCAC CACGTGGCCTACTTT GAGGCCTCGGCCAAA CTGCGTCTCAACGTG     537
3 HRAS ACTGTGGAATC---T CGGCAGGCTCAGGAC CTCGCCCGAAGCTAC GGCATCCCCTACATC GAGACCTCGGCCAAG ACCCGGCAGGGAGTG     456

Page 7.1
       541         555 556         570 571         585 586         600 601         615 616         630
1 CH3  GACGAGGCTTTTGAG CAGCTGGTGCGGGCT GTCCGGAAATACCAG GAACAAGAGCTCCCA CCGAGCCCTCCCAGT GCCCCCAGGAAGAAG     549
2 RRAS GACGAGGCTTTTGAG CAGCTGGTGCGGGCT GTCCGGAAATACCAG GAACAAGAGCTCCCA CCGAGCCCTCCCAGT GCCCCCAGGAAGAAG     627
3 HRAS GAGGATGCCTTCTAC ACGTTGGTGCGTGAG ATCCGGCAGCACAAG CTGCGGAAGCTGAAC CCTCCTGATGAGAGT GGCCCCGGCT-----     541

Page 8.1
       631         645 646         660 661         675 676         690 691         705 706         720
1 CH3  GGCGGGGGCTGCCCC TGCGTC---TCCTGT AG    578
2 RRAS GGCGGGGGCTGCCCC TGCGTCC--TCCTGT AG    657
3 HRAS -GCATGAGCTGCAAG TGTGTGCTCTCCTGA --    570
```

Chimera CH5 alignment sequence

```
Page 1.1
       1            15 16           30 31           45 46           60 61           75 76           90
1 CH5  ATGAGCTCTGGTGCT GCTTCTGGTACAGGT CGTGGTCGTCCACGT GGTGGAGGTCCAGGT CCCGGGGACCCTCCG CCTAGCGAGACACAC     90
2 RRAS ATGAGCAGCGGGGCG GCGTCCGGGACAGGG CGGGGGCGGCCCCGG GGCGGGGGACCTGGG CCCGGGGACCCCCCG CCCAGCGAGACACAC     90
3 HRAS ---------------- ---------------- ---------------- ---------------- ---------------- ---ATGACGGAATAT     12

Page 2.1
       91          105 106          120 121          135 136          150 151          165 166          180
1 CH5  AAGCTTGTGGTCGTG GGTGGTGTCGGCGTG GGCAAGAGCGCGCTG ACCATCCAGTTCATC CAGTCCTACTTCGTG TCTGACTACGACCCC    180
2 RRAS AAGCTGGTGGTCGTG GGCGGCGGCGGCGTG GGCAAGAGCGCGCTG ACCATCCAGTTCATC CAGTCCTACTTCGTG TCTGACTACGACCCC    180
3 HRAS AAGCTGGTGGTGGTG GGCGCCGGCGGTGTG GGCAAGAGTGCGCTG ACCATCCAGCTGATC CAGAACCATTTTGTG GACGAATACGACCCC    102

Page 3.1
       181         195 196          210 211          225 226          240 241          255 256          270
1 CH5  ACTATTGAGGACTCC TACACGAAG-ATCTG CAGTG-TGGATGGCA TCCCAGCCCGGCTGG ACATCCTGGACACCG CGGGCCAGGAAGAGT    268
2 RRAS ACTATTGAGGACTCC TACACGAAG-ATCTG CAGTG-TGGATGGCA TCCCAGCCCGGCTGG ACATCCTGGACACCG CGGGCCAGGAAGAGT    268
3 HRAS ACTATAGAGGATTCC TACCGGAAGCAGGTG --GTCATTGATGGGG AGACGTGCCTGTTGG ACATCCTGGATACCG CCGGCCAGGAGGAGT    190

Page 4.1
       271         285 286          300 301          315 316          330 331          345 346          360
1 CH5  TCGGGGCCATGAGAG AGCAGTACATGCGTG CTGGCCACGGCTTCC TGCTGGTGTTCGCCA TTAATGACCGGCAGA GTTTCAACGAGGTGG    358
2 RRAS TCGGGGCCATGAGAG AGCAGTACATGCGTG CTGGCCACGGCTTCC TGCTGGTGTTCGCCA TTAATGACCGGCAGA GTTTCAACGAGGTGG    358
3 HRAS ACAGCGCCATGCGGG ACCAGTACATGCGCA CCGGGGAGGGCTTCC TGTGTGTGTTTGCCA TCAACAACACCAAGT CTTTTGAGGACATCC    280

Page 5.1
       361         375 376          390 391          405 406          420 421          435 436          450
1 CH5  GCAAGCTCTTCACGC AGATTCTGCGGGTCA AGGACCGCGACGACT TCCCCGTTGTGTTGG TCGGGAACAAGGCAG ATCTGGAGTCACAGC    448
2 RRAS GCAAGCTCTTCACGC AGATTCTGCGGGTCA AGGACCGCGACGACT TCCCCGTTGTGTTGG TCGGGAACAAGGCAG ATCTGGAGTCACAGC    448
3 HRAS ACCAGTACAGGGAGC AGATCAAACGGGTGA AGGACTCGGATGACG TGCCCATGGTGCTGG TGGGGAACAAGTGTG ACCTGGCTGCAC-GC    369

Page 6.1
       451         465 466          480 481          495 496          510 511          525 526          540
1 CH5  GCCAGGTCCCCCGAT CAGAAGCCTCTGC-C TTCGGCGCCTCCCAC CACGTGGCCTACTTT GAGGCCTCGGCCAAG ACCCGGCAGGGAGTG    537
2 RRAS GCCAGGTCCCCCGAT CAGAAGCCTCTGC-C TTCGGCGCCTCCCAC CACGTGGCCTACTTT GAGGCCTCGGCCAAA CTGCGTCTCAACGTG    537
3 HRAS ACTGTGGAATC---T CGGCAGGCTCAGGAC CTCGCCCGAAGCTAC GGCATCCCCTACATC GAGACCTCGGCCAAG ACCCGGCAGGGAGTG    456

Page 7.1
       541         555 556          570 571          585 586          600 601          615 616          630
1 CH5  GAGGATGCCTTCTAC ACGTGGGTGCGTGAG ATCCGGCAGCACAAG CTGCGGAAGCTGACC CCTCCTGATGAGAGT GGCCCGG-CTGCATG    626
2 RRAS GACGAGGCTTTTGAG CAGCTGGTGCGGGCT GTCCGGAAATACCAG GAACAAGAGCTCCCA CCGAGCCCTCCCAGT GCCCC---CAGGAAG    624
3 HRAS GAGGATGCCTTCTAC ACGTTGGTGCGTGAG ATCCGGCAGCACAAG CTGCGGAAGCTGAAC CCTCCTGATGAGAGT GGCCCCGGCTGCATG    546

Page 8.1
       631         645 646          660 661          675 676          690 691          705 706          720
1 CH5  AACTGCAAGTG---- ---TGTGCTCTCCTG A--    650
2 RRAS AAGGGCGGGGGCTGC CCCTGCGTCCTCCTG TAG    657
3 HRAS AGCTGCAAGTG---- ---TGTGCTCTCCTG A--    570
```

Chimera CH6 alignment sequence

```
Page 1.1
       1              15 16              30 31              45 46              60 61              75 76              90
1 HRAS ---------------- ---------------- ---------------- ---------------- ---------------- ----------ATGACGGAATAT     12
2 CH6  ---------------- ---------------- ---------------- ---------------- ---------------- ----------ATGACGGAATAT     12
3 RRAS ATGAGCAGCGGGGCG GCGTCCGGGACAGGG CGGGGGCGGCCCCGG GGCGGGGGACCTGGG CCCGGGGACCCCCCG CCCAGCGAGACACAC     90

Page 2.1
       91            105 106            120 121            135 136            150 151            165 166            180
1 HRAS AAGCTGGTGGTGGTG GGCGCCGGCGGTGTG GGCAAGAGTGCGCTG ACCATCCAGCTGATC CAGAACCATTTTGTG GACGAATACGACCCC     102
2 CH6  AAGCTGGTGGTGGTG GGCGCCGTCGGTGTG GGCAAGAGTGCGCTG ACCATCCAGCTGATC CAGAACCATTTTGTG GACGAATACGACCCC     102
3 RRAS AAGCTGGTGGTCGTG GGCGGCGGCGGCGTG GGCAAGAGCGCGCTG ACCATCCAGTTCATC CAGTCCTACTTCGTG TCTGACTACGACCCC     180

Page 3.1
       181           195 196           210 211           225 226           240 241           255 256           270
1 HRAS ACTATAGAGGATTCC TACCGGAAGCAGGTG --GTCATTGATGGGG AGACGTGCCTGTTGG ACATCCTGGATACCG CCGGCCAGGAGGAGT     190
2 CH6  ACTATAGAGGATTCC TACCGGAAGCAGGTG --GTCATTGATGGGG AGACGTGCCTGTTGG ACATCCTGGATACCG CCGGCCAGGAGGAGT     190
3 RRAS ACTATTGAGGACTCC TACACGAAG-ATCTG CAGTG-TGGATGGCA TCCCAGCCCGGCTGG ACATCCTGGACACCG CGGGCCAGGAAGAGT     268

Page 4.1
       271           285 286           300 301           315 316           330 331           345 346           360
1 HRAS ACAGCGCCATGCGGG ACCAGTACATGCGCA CCGGGGAGGGCTTCC TGTGTGTGTTTGCCA TCAACAACACCAAGT CTTTTGAGGACATCC     280
2 CH6  ACAGCGCCATGCGGG ACCAGTACATGCGCA CCGGGGAGGGCTTCC TGTGTGTGTTTGCCA TCAACAACACCAAGT CTTTTGAGGACATCC     280
3 RRAS TCGGGGCCATGAGAG AGCAGTACATGCGTG CTGGCCACGGCTTCC TGCTGGTGTTCGCCA TTAATGACCGGCAGA GTTTCAACGAGGTGG     358

Page 5.1
       361           375 376           390 391           405 406           420 421           435 436           450
1 HRAS ACCAGTACAGGGAGC AGATCAAACGGGTGA AGGACTCGGATGACG TGCCCATGGTGCTGG TGGGGAACAAGTGTG ACCTGGCTGCAC-GC     369
2 CH6  ACCAGTACAGGGAGC AGATCAAACGGGTGA AGGACTCGGATGACG TGCCCATGGTGCTGG TGGGGAACAAGTGTG ACCTGGCTGCAC-GC     369
3 RRAS GCAAGCTCTTCACGC AGATTCTGCGGGTCA AGGACCGCGACGACT TCCCCGTTGTGTTGG TCGGGAACAAGGCAG ATCTGGAGTCACAGC     448

Page 6.1
       451           465 466           480 481           495 496           510 511           525 526           540
1 HRAS ACTGTGGAATC---T CGGCAGGCTCAGGAC CTCGCCCGAAGCTAC GGCATCCCCTACATC GAGACCTCGGCCAAG ACCCGGCAGGGAGTG     456
2 CH6  ACTGTGGAATC---T CGGCAGGCTCAGGAC CTCGCCCGAAGCTAC GGCATCCCCTACATC GAGACCTCGGCCAAA CTGCGTCTCAACGTG     456
3 RRAS GCCAGGTCCCCCGAT CAGAAGCCTCTGC-C TTCGGCGCCTCCCAC CACGTGGCCTACTTT GAGGCCTCGGCCAAA CTGCGTCTCAACGTG     537

Page 7.1
       541           555 556           570 571           585 586           600 601           615 616           630
1 HRAS GAGGATGCCTTCTAC ACGTTGGTGCGTGAG ATCCGGCAGCACAAG CTGCGGAAGCTGAAC CCTCCTGATGAGAGT GGCCCCGGCTGCATG     546
2 CH6  GACGAGGCTTTTGAG CAGCTGGTGCGGGCT GTCCGGAAATACCAG GANCAAGAGCTCCCA CCGAGCCCTCCCAGT GCCCCCAGGAAGAAG     546
3 RRAS GACGAGGCTTTTGAG CAGCTGGTGCGGGCT GTCCGGAAATACCAG GAACAAGAGCTCCCA CCGAGCCCTCCCAGT GCCCCCAGGAAGAAG     627

Page 8.1
       631           645 646           660 661           675 676           690 691           705 706           720
1 HRAS AGCTGCAAGTG---- TGTGCTCTCCTGA--    570
2 CH6  GGCGGGGGCTGCCCC TGCGTCCTCCTGTAG    576
3 RRAS GGCGGGGGCTGCCCC TGCGTCCTCCTGTAG    657
```

Chimera H197 alignment sequence

```
Page 1.1
       1              15 16             30 31             45 46             60 61             75 76             90
1 HRAS ---------------- ---------------- ---------------- ---------------- ---------------- ---ATGACGGAATAT     12
2 H197 ---------------- ---------------- ---------------- ---------------- ---------------- ---ATGACGGAATAT     12
3 RRAS ATGAGCAGCGGGGCG GCGTCCGGGACAGGG CGGGGGCGGCCCCGG GGCGGGGGACCTGGG CCCGGGGACCCCCCG CCCAGCGAGACACAC     90

Page 2.1
       91          105 106          120 121          135 136          150 151          165 166          180
1 HRAS AAGCTGGTGGTGGTG GGCGCCGGCGGTGTG GGCAAGAGTGCGCTG ACCATCCAGCTGATC CAGAACCATTTTGTG GACGAATACGACCCC     102
2 H197 AAGCTGGTGGTGGTG GGCGCCGTCGGTGTG GGCAAGAGTGCGCTG ACCATCCAGCTGATC CAGAACCATTTTGTG GACGAATACGACCCC     102
3 RRAS AAGCTGGTGGTCGTG GGCGGCGGCGGCGTG GGCAAGAGCGCGCTG ACCATCCAGTTCATC CAGTCCTACTTCGTG TCTGACTACGACCCC     180

Page 3.1
       181         195 196         210 211         225 226         240 241         255 256         270
1 HRAS ACTATAGAGGATTCC TACCGGAAGCAGGTG --GTCATTGATGGGG AGACGTGCCTGTTGG ACATCCTGGATACCG CCGGCCAGGAGGAGT     190
2 H197 ACTATAGAGGATTCC TACCGGAAGCAGGTG --GTCATTGATGGGG AGACGTGCCTGTTGG ACATCCTGGATACCG CCGGCCAGGAGGAGT     190
3 RRAS ACTATTGAGGACTCC TACACGAAG-ATCTG CAGTG-TGGATGGCA TCCCAGCCCGGCTGG ACATCCTGGACACCG CGGGCCAGGAAGAGT     268

Page 4.1
       271         285 286         300 301         315 316         330 331         345 346         360
1 HRAS ACAGCGCCATGCGGG ACCAGTACATGCGCA CCGGGGAGGGCTTCC TGTGTGTGTTTGCCA TCAACAACACCAAGT CTTTTGAGGACATCC     280
2 H197 ACAGCGCCATGCGGG ACCAGTACATGCGCA CCGGGGAGGGCTTCC TGTGTGTGTTTGCCA TCAACAACACCAAGT CTTTTGAGGACATCC     280
3 RRAS TCGGGGCCATGAGAG AGCAGTACATGCGTG CTGGCCACGGCTTCC TGCTGGTGTTCGCCA TTAATGACCGGCAGA GTTTCAACGAGGTGG     358

Page 5.1
       361         375 376         390 391         405 406         420 421         435 436         450
1 HRAS ACCAGTACAGGGAGC AGATCAAACGGGTGA AGGACTCGGATGACG TGCCCATGGTGCTGG TGGGGAACAAGTGTG ACCTGGCTGCAC-GC     369
2 H197 ACCAGTACAGGGAGC AGATCAAACGGGTGA AGGACTCGGATGACG TGCCCATGGTGCTGG TGGGGAACAAGTGTG ACCTGGCTGCAC-GC     369
3 RRAS GCAAGCTCTTCACGC AGATTCTGCGGGTCA AGGACCGCGACGACT TCCCCGTTGTGTTGG TCGGGAACAAGGCAG ATCTGGAGTCACAGC     448

Page 6.1
       451         465 466         480 481         495 496         510 511         525 526         540
1 HRAS ACTGTGGAATC---T CGGCAGGCTCAGGAC CTCGCCCGAAGCTAC GGCATCCCC-TACAT CGAGACCTCGGCCAA GACCCGGCAGGGAGT     455
2 H197 ACTGTGGAATC---T CGGCAGGCTCAGGAC CTCGCCCGAAGCTAC GGCATCCCCCTACAT CGAGACCTCGGCCAA GACCCGGCAGGGAGT     456
3 RRAS GCCAGGTCCCCCGAT CAGAAGCCTCTGC-C TTCGGCGCCTCCCAC CACGTGGCC-TACTT TGAGGCCTCGGCCAA ACTGCGTCTCAACGT     536

Page 7.1
       541         555 556         570 571         585 586         600 601         615 616         630
1 HRAS GGAGGATGCCTTCTA CACGTTGGTGCGTGA GATCCGGCAGCACAA GCTGCGGAAGCTGAA CCCTCCTGATGAGAG TGGCCCCGGCTGCAT     545
2 H197 GGAGGATGCCTTCTA CACGTTGGTGCGTGA GATCCGGCAGCACAA GCTGCGGAAGCTGCC ACCGAGCCCTCCCAG TGCCCCCANNAAGAA     546
3 RRAS GGACGAGGCTTTTGA GCAGCTGGTGCGGGC TGTCCGGAAATACCA GGAACAAGAGCTCCC ACCGAGCCCTCCCAG TGCCCCCAGGAAGAA     626

Page 8.1
       631         645 646         660 661         675 676         690 691         705 706         720
1 HRAS GAGCTGCAAGTG--- -TGTGCTCTCCTGA- -    570
2 H197 GGGCNGGGGCTGCCC CTGCGTCCTCCTGTA G    577
3 RRAS GGGCGGGGGCTGCCC CTGCGTCCTCCTGTA G    657
```

Chimera R197 alignment sequence

```
Page 1.1
       1              15 16              30 31              45 46              60 61              75 76              90
1 R197 CTGAGCTCTGGTGCT GCTTCTGGTACAGGT CGTGGTCGTCCACGT GGTGGAGGTCCAGGT CCCGGGGACCCTCCG CCTAGCGAGACACAC      90
2 RRAS ATGAGCAGCGGGGCG GCGTCCGGGACAGGG CGGGGGCGGCCCCGG GGCGGGGGACCTGGG CCCGGGGACCCCCCG CCCAGCGAGACACAC      90
3 HRAS ---------------- ---------------- ---------------- ---------------- ---------------- ---ATGACGGAATAT      12

Page 2.1
      91             105 106             120 121             135 136             150 151             165 166             180
1 R197 AAGCTTGTGGTCGTG GGTGGTGTCGGCGTG GGCAAGAGCGCGCTG ACCATCCAGTTCATC CAGTCCTACTTCGTG TCTGACTACGACCCC     180
2 RRAS AAGCTGGTGGTCGTG GGCGGCGGCGGCGTG GGCAAGAGCGCGCTG ACCATCCAGTTCATC CAGTCCTACTTCGTG TCTGACTACGACCCC     180
3 HRAS AAGCTGGTGGTGGTG GGCGCCGGCGGTGTG GGCAAGAGTGCGCTG ACCATCCAGCTGATC CAGAACCATTTTGTG GACGAATACGACCCC     102

Page 3.1
      181             195 196             210 211             225 226             240 241             255 256             270
1 R197 ACTATTGAGGACTCC TACACGAAG-ATCTG CAGTG-TGGATGGCA TCCCAGCCCGGCTGG ACATCCTGGACACCG CGGGCCAGGAAGAGT     268
2 RRAS ACTATTGAGGACTCC TACACGAAG-ATCTG CAGTG-TGGATGGCA TCCCAGCCCGGCTGG ACATCCTGGACACCG CGGGCCAGGAAGAGT     268
3 HRAS ACTATAGAGGATTCC TACCGGAAGCAGGTG --GTCATTGATGGGG AGACGTGCCTGTTGG ACATCCTGGATACCG CCGGCCAGGAGGAGT     190

Page 4.1
      271             285 286             300 301             315 316             330 331             345 346             360
1 R197 TCGGGGCCATGAGAG AGCAGTACATGCGTG CTGGCCACGGCTTCC TGCTGGTGTTCGCCA TTAATGACCGGCAGA GTTTCAACGAGGTGG     358
2 RRAS TCGGGGCCATGAGAG AGCAGTACATGCGTG CTGGCCACGGCTTCC TGCTGGTGTTCGCCA TTAATGACCGGCAGA GTTTCAACGAGGTGG     358
3 HRAS ACAGCGCCATGCGGG ACCAGTACATGCGCA CCGGGGAGGGCTTCC TGTGTGTGTTTGCCA TCAACAACACCAAGT CTTTTGAGGACATCC     280

Page 5.1
      361             375 376             390 391             405 406             420 421             435 436             450
1 R197 GCAAGCTCTTCACGC AGATTCTGCGGGTCA AGGACCGCGACGACT TCCCCGTTGTGTTGG TCGGGAACAAGGCAG ATCTGGAGTCACAGC     448
2 RRAS GCAAGCTCTTCACGC AGATTCTGCGGGTCA AGGACCGCGACGACT TCCCCGTTGTGTTGG TCGGGAACAAGGCAG ATCTGGAGTCACAGC     448
3 HRAS ACCAGTACAGGGAGC AGATCAAACGGGTGA AGGACTCGGATGACG TGCCCATGGTGCTGG TGGGGAACAAGTGTG ACCTGGCTGCAC-GC     369

Page 6.1
      451             465 466             480 481             495 496             510 511             525 526             540
1 R197 GCCAGGTCCCCCGAT CAGAAGCCTCTGC-C TTCGGCGCCTCCCAC CACGTGGCCTACTTT GAGGCCTCGGCCAAA CTGCGTCTCAACGTG     537
2 RRAS GCCAGGTCCCCCGAT CAGAAGCCTCTGC-C TTCGGCGCCTCCCAC CACGTGGCCTACTTT GAGGCCTCGGCCAAA CTGCGTCTCAACGTG     537
3 HRAS ACTGTGGAATC---T CGGCAGGCTCAGGAC CTCGCCCGAAGCTAC GGCATCCCCTACATC GAGACCTCGGCCAAG ACCCGGCAGGGAGTG     456

Page 7.1
      541             555 556             570 571             585 586             600 601             615 616             630
1 R197 GACGAGGCTTTTGAG CAGCTGGTGCGGGCT GTCCGGAAATACCAG GAACAAGAGCTCAAC CCTCCTGATGAGAGT GGCCCN-GCTGCATG     626
2 RRAS GACGAGGCTTTTGAG CAGCTGGTGCGGGCT GTCCGGAAATACCAG GAACAAGAGCTCCCA CCGAGCCCTCCCAGT GCCCCCAGGAAGAAG     627
3 HRAS GAGGATGCCTTCTAC ACGTTGGTGCGTGAG ATCCGGCAGCACAAG CTGCGGAAGCTGAAC CCTCCTGATGAGAGT GGCCCCGGCTGCATG     546

Page 8.1
      631             645 646             660 661             675 676             690 691             705 706             720
1 R197 AGCTGCAAGTG---- TGTGCTCTCCTGA--    650
2 RRAS GGCGGGGGCTGCCCC TGCGTCCTCCTGTAG    657
3 HRAS AGCTGCAAGTG---- TGTGCTCTCCTGA--    570
```

Chimera H201 alignment sequence

```
Page 1.1
       1              15 16              30 31              45 46              60 61              75 76              90
1 HRAS ---------------- ---------------- ---------------- ---------------- ---------------- ---------------- ----------   0
2 H201 ---------------- ---------------- ---------------- ---------------- ---------------- ---------------- ----------   0
3 RRAS GAATTCATGGAACAA AAACTAATATCGGAA GAAGATCTAATGAGC AGCGGGGCGGCGTCC GGGACAGGGCGGGGG CGGCCCCGGGGCGGG    90

Page 2.1
       91            105 106            120 121            135 136            150 151            165 166            180
1 HRAS ---------------- -----------ATGA CGGA-ATATAAGCTG GTGGTGGTGGGCGCC GGCGGTGTGGGCAAG AGTGCGCTGACCATC     63
2 H201 ---------------- -----------AAGA CGGA-ATATAAGCTG GTGGTGGTGGGCGCC GTCGGTGTGGGCAAG AGTGCGCTGACCATC     63
3 RRAS GGACCTGGGCCCGGG GACCCCCCGCCCAGC GAGACACACAAGCTG GTGGTCGTGGGCGGC GGCGGCGTGGGCAAG AGCGCGCTGACCATC    180

Page 3.1
       181            195 196            210 211            225 226            240 241            255 256            270
1 HRAS CAGCTGATCCAGAAC CATTTTGTGGACGAA TACGACCCCACTATA GAGGATTCCTACCGG AAGCAGGTG--GTCA TTGATGGGGAGACGT    151
2 H201 CAGCTGATCCAGAAC CATTTTGTGGACGAA TACGACCCCACTATA GAGGATTCCTACCGG AAGCAGGTG--GTCA TTGATGGGGAGACGT    151
3 RRAS CAGTTCATCCAGTCC TACTTCGTGTCTGAC TACGACCCCACTATT GAGGACTCCTACACG AAG-ATCTGCAGTG- TGGATGGCATCCCAG    268

Page 4.1
       271            285 286            300 301            315 316            330 331            345 346            360
1 HRAS GCCTGTTGGACATCC TGGATACCGCCGGCC AGGAGGAGTACAGCG CCATGCGGGACCAGT ACATGCGCACCGGGG AGGGCTTCCTGTGTG    241
2 H201 GCCTGTTGGACATCC TGGATACCGCCGGCC AGGAGGAGTACAGCG CCATGCGGGACCAGT ACATGCGCACCGGGG AGGGCTTCCTGTGTG    241
3 RRAS CCCGGCTGGACATCC TGGACACCGCGGGCC AGGAAGAGTTCGGGG CCATGAGAGAGCAGT ACATGCGTGCTGGCC ACGGCTTCCTGCTGG    358

Page 5.1
       361            375 376            390 391            405 406            420 421            435 436            450
1 HRAS TGTTTGCCATCAACA ACACCAAGTCTTTTG AGGACATCCACCAGT ACAGGGAGCAGATCA AACGGGTGAAGGACT CGGATGACGTGCCCA    331
2 H201 TGTTTGCCATCAACA ACACCAAGTCTTTTG AGGACATCCACCAGT ACAGGGAGCAGATCA AACGGGTGAAGGACT CGGATGACGTGCCCA    331
3 RRAS TGTTCGCCATTAATG ACCGGCAGAGTTTCA ACGAGGTGGGCAAGC TCTTCACGCAGATTC TGCGGGTCAAGGACC GCGACGACTTCCCCG    448

Page 6.1
       451            465 466            480 481            495 496            510 511            525 526            540
1 HRAS TGGTGCTGGTGGGGA ACAAGTGTGACCTGG CTGCAC-GCACTGTG GAATC---TCGGCAG GCTCAGGACCTCGCC CGAAGCTACGGCATC    417
2 H201 TGGTGCTGGTGGGGA ACAAGTGTGACCTGG CTGCAC-GCACTGTG GAATC---TCGGCAG GCTCAGGACCTCGCC CGAAGCTACGGCATC    417
3 RRAS TTGTGTTGGTCGGGA ACAAGGCAGATCTGG AGTCACAGCGCCAGG TCCCCCGATCAGAAG CCTCTGC-CTTCGGC GCCTCCCACCACGTG    537

Page 7.1
       541            555 556            570 571            585 586            600 601            615 616            630
1 HRAS CCCTACATCGAGACC TCGGCCAAGACCCGG CAGGGAGTGGAGGAT GCCTTCTACACGTTG GTGCGTGAGATCCGG CAGCACAAGCTGCGG    507
2 H201 CCCTACATCGAGACC TCGGCCAAGACCCGG CAGGGAGTGGAGGAT GCCTTCTACACGTTG GTGCGTGAGATCCGG CAGCACAAGCTGCGG    507
3 RRAS GCCTACTTTGAGGCC TCGGCCAAACTGCGT CTCAACGTGGACGAG GCTTTTGAGCAGCTG GTGCGGGCTGTCCGG AAATACCAGGAACAA    627

Page 8.1
       631            645 646            660 661            675 676            690 691            705 706            720
1 HRAS AAGCT------GAAC CCTCCTGATGAGAGT GGCCCCGGCTGCATG AGCTGCAAGTG---- TGTGCTCTCCTGA--    570
2 H201 AAGCT------GAAC CCTCCCGAT-AG--T GCCCCAGGAAAAAG GGCGGGGGCTGCCCC TGCGTCCTCCTGTAG    570
3 RRAS GAGCTCCCACCGAGC CCTCCC----AG--T GCCCCAGGAAGAAG GGCGGGGGCTGCCCC TGCGTCCTCCTGTAG    696
```

Chimera R201 alignment sequence

```
Page 1.1
       1              15 16             30 31             45 46             60 61             75 76             90
1 R210 ATGAGCTCTGGTGCT GCTTCTGGTACAGGT CGTGGTCGTCCACGT GGTGGAGGTCCAGGT CCCGGGGACCCTCCG CCTAGCGAGACACAC      90
2 RRAS ATGAGCAGCGGGGCG GCGTCCGGGACAGGG CGGGGGCGGCCCCGG GGCGGGGGACCTGGG CCCGGGGACCCCCCG CCCAGCGAGACACAC      90
3 HRAS ---------------- ---------------- ---------------- ---------------- ---------------- ---ATGACGGAATAT      12

Page 2.1
       91            105 106            120 121            135 136            150 151            165 166            180
1 R210 AAGCTTGTGGTCGTG GGTGGTGTCGGCGTG GGCAAGAGCGCGCTG ACCATCCAGTTCATC CAGTCCTACTTCGTG TCTGACTACGACCCC     180
2 RRAS AAGCTGGTGGTCGTG GGCGGCGGCGGCGTG GGCAAGAGCGCGCTG ACCATCCAGTTCATC CAGTCCTACTTCGTG TCTGACTACGACCCC     180
3 HRAS AAGCTGGTGGTGGTG GGCGCCGGCGGTGTG GGCAAGAGTGCGCTG ACCATCCAGCTGATC CAGAACCATTTTGTG GACGAATACGACCCC     102

Page 3.1
       181            195 196            210 211            225 226            240 241            255 256            270
1 R210 ACTATTGAGGACTCC TACACGAAG-ATCTG CAGTG-TGGATGGCA TCCCAGCCCGGCTGG ACATCCTGGACACCG CGGGCCAGGAAGAGT     268
2 RRAS ACTATTGAGGACTCC TACACGAAG-ATCTG CAGTG-TGGATGGCA TCCCAGCCCGGCTGG ACATCCTGGACACCG CGGGCCAGGAAGAGT     268
3 HRAS ACTATAGAGGATTCC TACCGGAAGCAGGTG --GTCATTGATGGGG AGACGTGCCTGTTGG ACATCCTGGATACCG CCGGCCAGGAGGAGT     190

Page 4.1
       271            285 286            300 301            315 316            330 331            345 346            360
1 R210 TCGGGGCCATGAGAG AGCAGTACATGCGTG CTGGCCACGGCTTCC TGCTGGTGTTCGCCA TTAATGACCGGCAGA GTTTCAACGAGGTGG     358
2 RRAS TCGGGGCCATGAGAG AGCAGTACATGCGTG CTGGCCACGGCTTCC TGCTGGTGTTCGCCA TTAATGACCGGCAGA GTTTCAACGAGGTGG     358
3 HRAS ACAGCGCCATGCGGG ACCAGTACATGCGCA CCGGGGAGGGCTTCC TGTGTGTGTTTGCCA TCAACAACACCAAGT CTTTTGAGGACATCC     280

Page 5.1
       361            375 376            390 391            405 406            420 421            435 436            450
1 R210 GCAAGCTCTTCACGC AGATTCTGCGGGTCA AGGACCGCGACGACT TCCCCGTTGTGTTGG TCGGGAACAAGGCAG ATCTGGAGTCACAGC     448
2 RRAS GCAAGCTCTTCACGC AGATTCTGCGGGTCA AGGACCGCGACGACT TCCCCGTTGTGTTGG TCGGGAACAAGGCAG ATCTGGAGTCACAGC     448
3 HRAS ACCAGTACAGGGAGC AGATCAAACGGGTGA AGGACTCGGATGACG TGCCCATGGTGCTGG TGGGGAACAAGTGTG ACCTGGCTGCAC-GC     369

Page 6.1
       451            465 466            480 481            495 496            510 511            525 526            540
1 R210 GCCAGGTCCCCCGAT CAGAAGCCTCTGC-C TTCGGCGCCTCCCAC CACGTGGCCTACTTT GAGGCCTCGGCCAAA CTGCGTCTCAACGTG     537
2 RRAS GCCAGGTCCCCCGAT CAGAAGCCTCTGC-C TTCGGCGCCTCCCAC CACGTGGCCTACTTT GAGGCCTCGGCCAAA CTGCGTCTCAACGTG     537
3 HRAS ACTGTGGAATC---T CGGCAGGCTCAGGAC CTCGCCCGAAGCTAC GGCATCCCCTACATC GAGACCTCGGCCAAG ACCCGGCAGGGAGTG     456

Page 7.1
       541            555 556            570 571            585 586            600 601            615 616            630
1 R210 GACGAGGCTNTTGAG CAGCTGGTGCGGGCT GTCCGGAAATACCAG GAACAAGAGCTTC-A CCGAGCCCTGAGAGT GGCCCCGGCTGCATG     624
2 RRAS GACGAGGCTTTTGAG CAGCTGGTGCGGGCT GTCCGGAAATACCAG GAACAAGAGCTCCCA CCGAGCCCTCCCAGT GCCCCCAGGAAGAAG     627
3 HRAS GAGGATGCCTTCTAC ACGTTGGTGCGTGAG ATCCGGCAGCACAAG CTGCGGAAGCTGAAC CCTCCTGATGAGAGT GGCCCCGGCTGCATG     546

Page 8.1
       631            645 646            660 661            675 676            690 691            705 706            720
1 R210 ANCTGCAAG TGTGTGCTCTCCTGA ------------    652
2 RRAS GGCG-G GGGCTGC-C-CCTGC GTCCTCCTGTAG       657
3 HRAS AGCTGCAAG TGTGTGCTCTCCTGA ------------    570
```

Chapter 5

Analysis of H-Ras and R-Ras C-terminal domains

5.1 Introduction

Results from Chapter 4 indicated that the C-terminal sequences of H-Ras and R-Ras are critical in determining their effects on integrin affinity modulation. It was shown that H-Ras amino acids Arg^{149} to Pro^{174} are required for integrin suppression, and that R-Ras amino acids Leu^{175} to Pro^{203} are sufficient to reverse H-Ras-mediated integrin suppression.

Recently, the main area of study of the H-Ras and R-Ras structures has been the hypervariable region (HVR), which comprises H-Ras His^{166} to Pro^{179} and R-Ras Tyr^{193} to Pro^{206}. Most of the areas of importance indicated by these new studies correlate to the specific C-terminal regions highlighted in Chapter 4. A study by Hansen *et al.*, (2002) showed, using H-and R-Ras chimeras, that the C-terminal 26 amino acids of R-Ras G38V (which include the full-length HVR) were specific for directing an R-Ras specific antagonism of H-Ras-mediated integrin suppression. Another study by Jaumot *et al.*, (2002) demonstrated that the HVR linker domain (H-Ras amino acids His^{166} to Asn^{172}), in association with C-terminal spacer sequences (H-Ras amino acids Pro^{173} to Pro^{179}) were necessary for H-Ras function.

With an aim to further investigate the relevance of these specific C-terminal regions of H-Ras and R-Ras, amino acids within the C-terminal regions were manipulated using several techniques. Early work presented in this chapter relies on site-directed mutagenesis to mutate smaller sections of amino acids. The resulting mutants were analysed using the $\alpha\beta$-py transfection system to determine their effects on integrin affinity modulation. Later work concentrates on the generation of a new H-and R-Ras chimera. This chimera was designed to exchange R-Ras G38V amino acids Ser^{172} to Tyr^{193} for the equivalent H-Ras amino acids Ser^{145} to His^{166}. It was hypothesised that substitution of the C-terminal R-Ras G38V sequences for H-Ras G12V sequences may confer the ability to suppress integrin affinity modulation.

5.2 Site-directed mutagenesis of R-Ras G38V C-terminal amino acids

5.2.1 High fidelity PCR generation of site-directed mutagenesis products

Site-directed mutagenesis was performed on R-Ras G38V using the QuikChange® Multi Site-Directed Mutagenesis Kit. Primers were designed to introduce a single base pair mutation into the R-Ras G38V sequence converting the selected R-Ras G38V amino acid into the equivalent H-Ras G12V amino acid. PCR cycle conditions were optimised (see Materials and Methods Table 2.4 for primer sequence details and section 2.10.1 for PCR cycle protocol). Figure 5.1 shows the amino acid alignment of H-Ras and R-Ras, the area highlighted in red identifies the specific R-Ras sequences targeted by the site-directed mutagenesis and the equivalent H-Ras sequences.

Primers JLsdm1F and JLsdm1R were used to mutate R-Ras G38V Tyr^{193} into the equivalent H-Ras amino acid histidine (base pair mutation from **T**AC to **C**AC). The resulting product, R-Ras (G38V/Y193H), was termed R-RasSDM1.

Primers JLsdm2F and JLsdm2R were used to mutate R-Ras G38V Gln^{194} into the equivalent H-Ras amino acid lysine (base pair mutation from **C**AG to **A**AG). The resulting product, R-Ras (G38V/Q194K), was termed R-RasSDM2.

Primers JLsdm5F and JLsdm5R were used to mutate R-Ras G38V Glu^{197} into the equivalent H-Ras amino acid lysine (base pair mutation from **G**AG to **A**AG). The resulting product, R-Ras (G38V/E197K), was termed R-RasSDM5.

Site-directed products were amplified as shown in Figure 5.2. Since the R-Ras G38V template used for site-directed mutagenesis was still in the pCDNA3.1(+) vector, R-RasSDM1, R-RasSDM2 and R-RasSDM5 were amplified as 6kb products. No PCR products were observed in reactions performed in the absence of template DNA for all reactions. All PCR products were digested with *Dpn1* endonuclease, to digest any parental DNA template and select for the synthesised DNA containing the required mutation. *E.Coli* (XL-1 Blue strain) cells were transformed with the digested PCR products and the plasmid DNA bulked-up and purified. PCR products were verified by sequence analysis (see Appendix I) prior to further investigation.

```
        1            15 16           30 31           45 46           60 61           75 76           90
1 H-Ras ---------------  -----------MTEY KLVVVGAGGVGKSAL TIQLIQNHFVDEYDP TIEDSYRKQVVIDGE TCLLDILDTAGQEEY 64
2 R-Ras MSSGAASGTGRGRPR GGGPGPGPDPPPSETH KLVVVGGGGVGKSAL TIQFIQSYFVSDYDP TIEDSYTKICSVDGI PARLDILDTAGQEEF 90

        91          105 106          120 121          135 136          150 151          165 166          180
1 H-Ras SAMRDQYMRTGEGFL CVFAINNTKSFEDIH QYREQIKRVKDSDDV PMVLVGNKCDLAAR- TVESRQAQDLARSYG IPYIETSAKTRQGVE 153
2 R-Ras GAMREQYMRAGHGFL LVFAINDRQSFNEVG KLFTQILRVKDRDDF PVVLVGNKADLESQR QVPRSEASAFGASHH VAYFEASAKLRLNVD 180

        181         195 196          210 211         225
1 H-Ras DAFYTLVREIRQHKL RKLNPPDESGPG--C MSCKCVLS    189
2 R-Ras EAFEQLVRAVRKYQE QELPPSPPSAPRKKG GGCPCVLL    218
```

Figure 5.1 H-Ras and R-Ras Amino Acid Alignment

H-Ras and R-Ras amino acid sequence alignment with areas targeted by site-directed mutagenesis highlighted in red. Hypervariable regions of H-Ras and R-Ras are underlined.

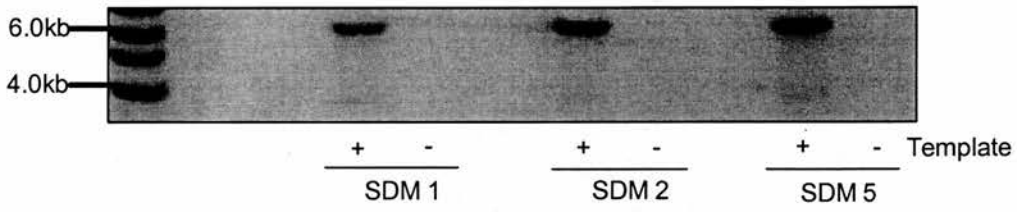

Figure 5.2 Site-directed mutagenesis PCR products.

Using high fidelity PCR, site directed mutagenesis was performed on 50ng of template DNA, R-Ras G38V. The negative controls contained no template DNA. PCR products (10µl) were resolved on 1% agarose gels.

5.2.2 Effect of R-Ras SDM 1, 2 and 5 on H-Ras G12V-mediated integrin suppression

Integrin affinity was determined in $\alpha\beta$-py cells transfected with control vector, R-Ras G38V, R-RasSDM1, R-RasSDM2 and R-RasSDM5 ± H-Ras G12V, see Figure 5.3. As a positive control, full length R-Ras G38V was used to reverse H-Ras-mediated integrin suppression from 40.62 ± 17.18% to -21.52 ± 9.12% ($P<0.01$). SDM1, SDM2 and SDM5 all reversed H-Ras-mediated integrin suppression from 40.62 ± 17.18% to -19.17 ± 6.71%, -24.19 ± 1.21% and -13.23 ± 2.04% respectively ($P<0.05$).

Figures 5.4A and 5.4B show that levels of R-RasSDM1, 2 and 5 expression are all similar and that co-expression with H-Ras G12V did not affect construct expression levels. Figure 5.4C shows that levels of ERK1/2 activation are increased by H-Ras G12V expression but that expression of R-Ras SDM1, SDM2 and SDM5 alone fail to increase ERK1/2 activation levels beyond that observed with control. Total ERK2 remained similar in all transfected cells (Figure 5.4D).

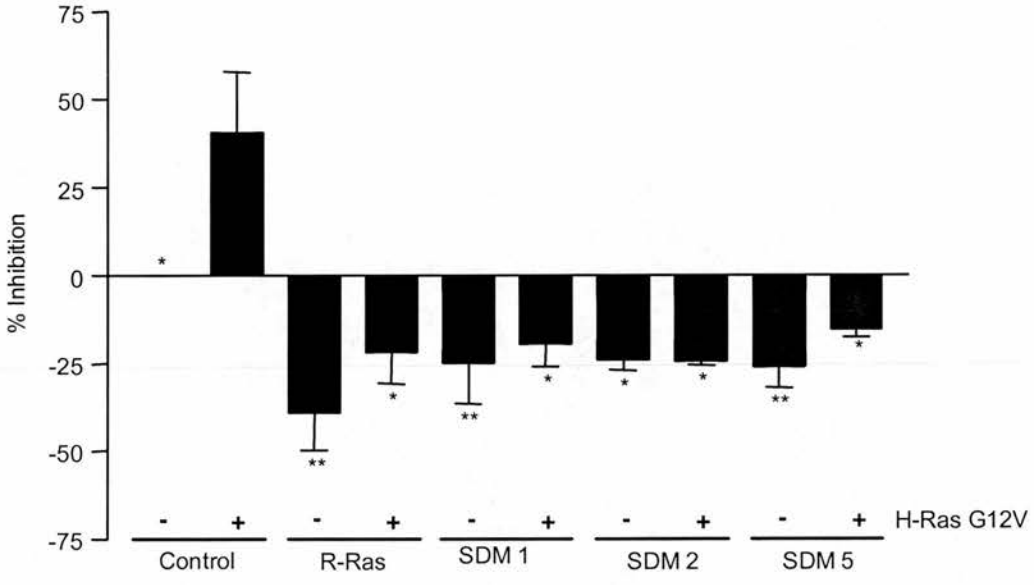

Figure 5.3 Site-directed mutagenesis products show reversal of H-Ras G12V-mediated integrin suppression.

Integrin affinity was determined in $\alpha\beta$-py cells transfected with 1μg of SDM1, SDM2 or SDM5 ± H-Ras G12V (1μg). In each transfection, total DNA content was standardised to 2μg using control vector. Percentage inhibition was calculated in reference to control vector alone. The values represent mean ± SEM of 3 experiments. Statistical analysis was performed by one-way ANOVA test compared to 'Control + H-Ras G12V', * and ** denoting $P<0.05$ and $P<0.01$ respectively.

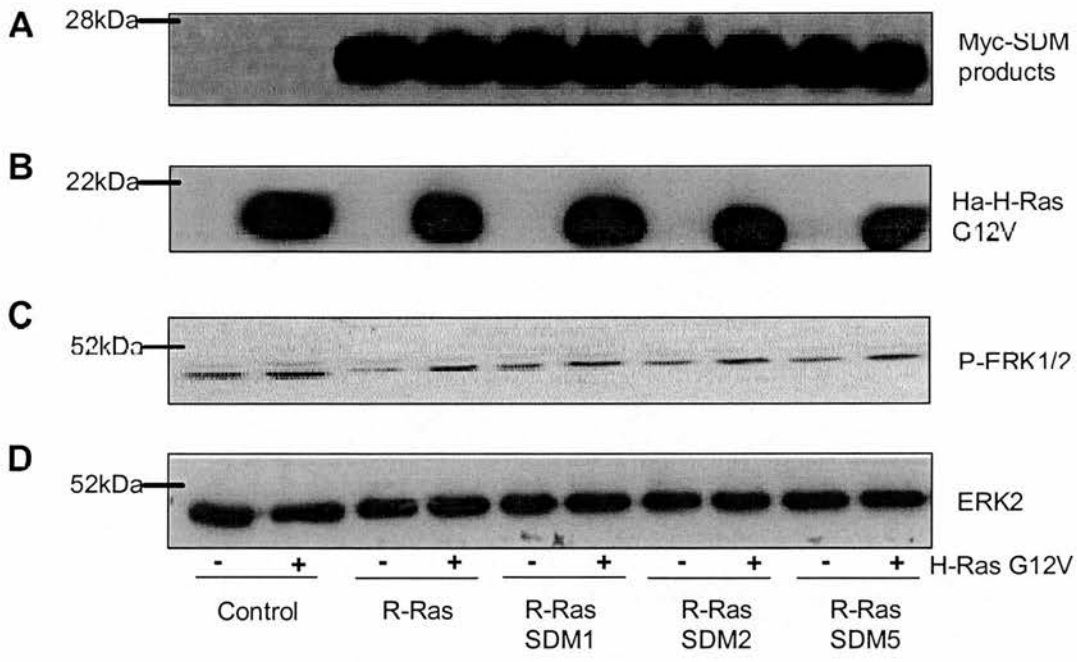

Figure 5.4 SDM product expression levels and effects on ERK1/2 activation.

Cell lysates were prepared from cells transfected with 1μg of R-Ras SDM1, SDM2 or SDM5 ± H-Ras G12V (1μg). In each transfection, total DNA content was standardised to 2μg using control vector. Cell lysates were probed for SDM product expression using anti-Myc antibody (A) and for H-Ras G12V expression levels using anti-Ha antibody (B). ERK1/2 phosphorylation levels were detected with phospho-specific ERK1/2 antibody. Total ERK2 (D) was measured as a control for equal loading of sample.

5.3 Site-directed mutagenesis of R-Ras G38V amino acids Tyr^{193} to Glu^{197}.

5.3.1 High fidelity PCR generation of 5 amino acid site-directed mutagenesis product

Using the QuikChange® Multi Site-Directed Mutagenesis Kit, primers were designed to introduce a 5 amino acid mutation into the R-Ras G38V sequence converting the selected R-Ras G38V amino acids into the equivalent H-Ras G12V amino acid. Figure 5.1 shows the amino acid alignment of H-Ras and R-Ras, the area highlighted in red identifies the specific R-Ras sequences targeted by the site-directed mutagenesis and the equivalent H-Ras sequences. See Table 2.4 for primer sequences. Primers JLsdm5aaF and JLsdm5aaR were used to mutate R-Ras G38V amino acids Tyr^{193}, Gln^{194}, Glu^{195}, Gln^{196} and Glu^{197} into the equivalent H-Ras amino acids His, Lys, Leu, Arg, and Lys respectively. The resulting product R-Ras (G38V/ Y193H/ Q194K/ E195L/ Q196R /E197K) was termed R-Ras5aaSDM.

Figure 5.5 shows that the R-Ras5aaSDM PCR product was amplified as a 6kb product. No PCR products were observed in reactions performed in the absence of template DNA. PCR products were verified by sequence analysis (see Appendix II) prior to further investigation.

5.2.1 Reversal of H-Ras-mediated integrin suppression by R-Ras5aaSDM

Integrin affinity was determined in $\alpha\beta$-py cells transfected with control vector, R-Ras G38Vand R-Ras5aaSDM ± H-Ras G12V, see Figure 5.6. As a positive control, full length R-Ras G38V was used to reverse H-Ras-mediated integrin suppression from 43.13 ± 8.93% to -27.50 ± 5.3% ($P<0.001$). Cells transfected with R-Ras5aaSDM alone did not suppress the integrin (-0.64 ± 14.95%). Cells co-transfected with R-ras5aaSDM + H-Ras G12V, demonstrated a slight reversal of H-Ras-mediated integrin suppression (43.13 ± 8.93% to 15 ± 6.10%), however results were not significant.

Figures 5.7A and 5.7B show that co-expression of R-Ras 5aaSDM with H-Ras G12V does not affect construct expression levels

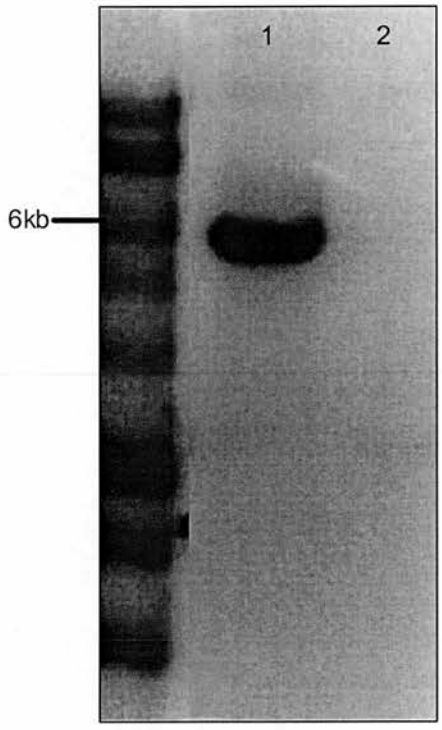

Figure 5.5 Five amino-acid site directed mutagenesis PCR product.

Using high fidelity PCR, site directed mutagenesis was performed on 50ng of template DNA, R-Ras G38V. The negative control (Lane 2) contained no template DNA. PCR products (10µl) were resolved on 1% agarose gel.

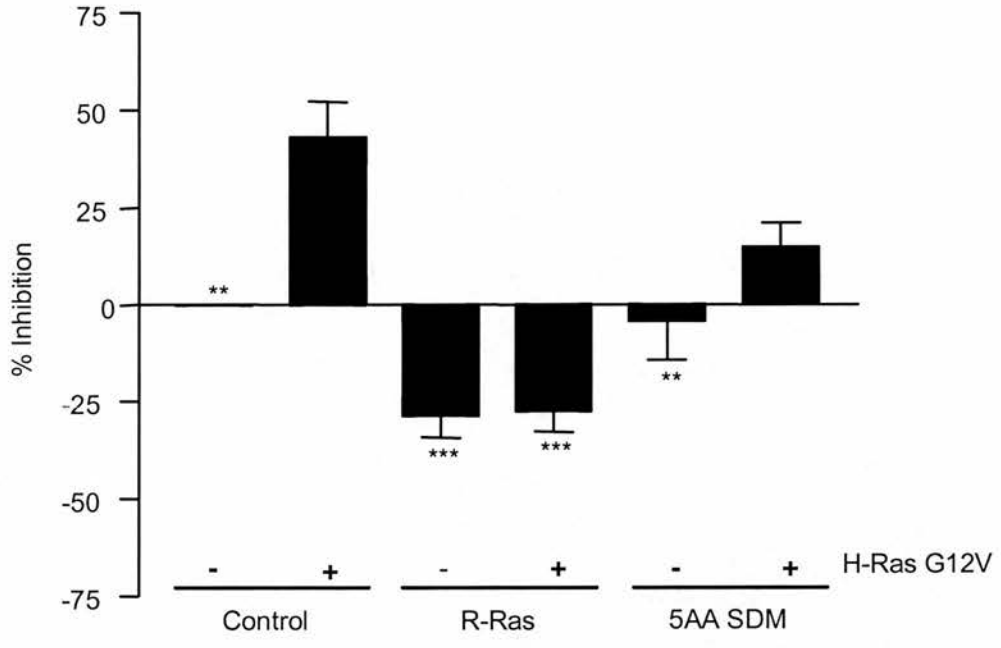

Figure 5.6 R-Ras 5aaSDM does not significantly reverse H-Ras-mediated integrin suppression.

Integrin affinity was determined in $\alpha\beta$-py cells transfected with 1μg of 5aa SDM ± H-Ras G12V (1μg). In each transfection, total DNA content was standardised to 2μg using control vector. Percentage inhibition was calculated in reference to control vector alone. The values represent mean ± SEM of 3 experiments. Statistical analysis was performed by one-way ANOVA test compared to H-Ras G12V, ** and *** denoting $P<0.01$ and $P<0.001$ respectively.

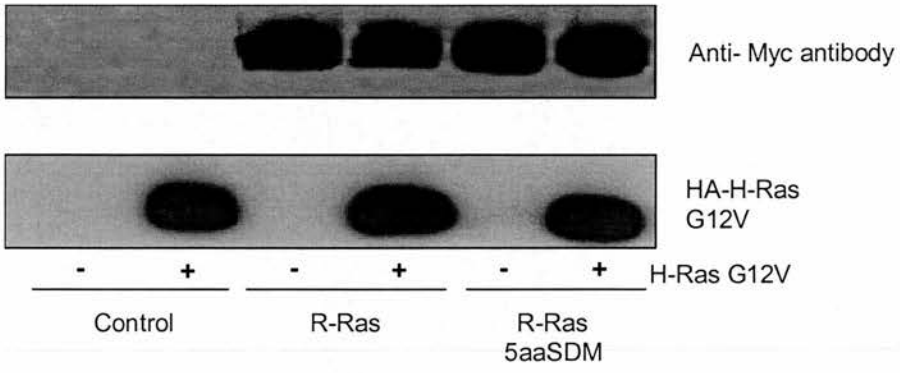

Figure 5.7 R-Ras 5aaSDM expression levels unaffected by co-transfection with H-Ras G12V.

Cell lysates were prepared from cells transfected with 1μg of R-Ras G38V or R-Ras 5aaSDM ± H-Ras G12V (1μg). In each transfection, total DNA content was standardised to 2μg using control vector. Cell lysates were probed for SDM product expression using anti-Myc antibody (A) and for H-Ras G12V expression levels using anti-Ha antibody (B).

5.4 Generation of a new H-and R-Ras chimera using PCR and blunt-ended ligation

To further investigate the importance of the H-Ras and R-Ras C-terminal sequences, a new H-and R-Ras chimera was generated. Thus allowing the investigation of a larger stretch of sequence. Using R-Ras G38V (in pCDNA3.1 (+)) as the template DNA, a series of primers and PCR cycles were utilised in order to exchange R-Ras G38V amino acids Ser^{172} to Tyr^{194} for the equivalent H-Ras G12V amino acid sequences Ser^{145} to His^{166}. Figure 5.8 shows the amino acid alignment of H-Ras and R-Ras, the areas highlighted in red identify the specific R-Ras sequences which will be exchanged for the equivalent H-Ras sequences.

5.4.1 Production of H-and R-Ras chimera blunt-ended PCR products 1 and 2.

Using high fidelity PCR, two separate reactions were used to generate products which would be used to construct a new H-and R-Ras chimera. See Materials and methods (Table 2.5) for primer sequences.

The flanking primers for each reaction, PCR1fwdFLAG and splicePCR2Rev, were designed to include appropriate restriction sites for ligation into the pCDNA3.1(+) vector. The N-terminal flanking primer PCR1fwdFLAG also included a FLAG-tag sequence to allow expression analysis of the resulting protein. The hybrid primers SplicePCR1rev and SPLPCR2fwd each contained sequences homologous to the R-Ras G38V template as well as the relevant H-Ras G12V sequences. SplicePCR1rev contained R-Ras Glu^{171} to Ala^{174}/ H-Ras Lys^{147} to Tyr^{157} and SPLPCR2fwd contained H-Ras Thr^{158} to His^{166}/ R-Ras Glu^{194} to Leu^{198}. The PCR cycle programmes used to generate the two products were repeated on several occasions until the optimal conditions were established.

PCR1fwdFLAG (which includes an EcoRI restriction site) and SplicePCR1rev, with the original PCR cycle conditions (as described in Materials and Methods section 2.12, the first stage reaction cycle) were used to produce product 1, containing the N-terminal sequences of the new H- and R-Ras chimera. Figure 5.9A shows that the amplified product was 500bp. No PCR products were observed in reactions

performed in the absence of template DNA. The PCR product was excised from gel and purified.

Primers SPLPCR2fwd and splicePCR2Rev (which includes a Hind III restriction site), with the original PCR cycle conditions were used to produce product 2, containing the C-terminal sequences of the new H-and R-Ras chimera. Figure 5.9B shows that the amplified product was 125bp. No PCR products were observed in reactions performed in the absence of template DNA. The PCR product was excised from gel and purified.

5.4.2 Ligation of new H-and R-Ras chimera into pCDNA3.1

In preparation for ligation of the new H-and R-Ras chimera into pCDNA3.1, appropriate restriction digests were carried out on the PCR products and pCDNA3.1 vector. The gel purified PCR product 1, containing the N-terminal sequences of the new H-and R-Ras chimera, was digested using the EcoRI restriction enzyme. The gel purified PCR product 2, containing the C-terminal sequences of the new H-and R-Ras chimera, was digested using the HindIII restriction enzyme. The pCDNA3.1 vector was digested using both the EcoRI and HindIII restriction enzymes. Following digestion, all DNA products were ethanol precipitated (Section 2.4). The pCDNA3.1(+) product was treated with shrimp alkaline phosphatase (SAP) for 30 minutes at 37°C then 62°C for 10 minutes, to inhibit self-ligation.

An 18°C ligation reaction was setup overnight using equal (and excess) amounts of products 1 and 2 (at 1:3 total ligation volume, to encourage blunt-ended ligation of the two products) and pCDNA3.1 (at 1:25 total ligation volume). Competent library efficient DH5α cells were transformed using 10µl ligation mix and resulting colonies were selectively grown and mini-prepped. Figure 5.10 shows that ligations were not successful as mini-prep cultures did not contain any plasmid DNA. The ligation reaction was repeated on several occasions with alternative conditions however, subsequent analyses of mini-prep cultures showed a lack of plasmid DNA.

```
        1            15 16           30 31           45 46           60 61           75 76           90
1 H-Ras --------------- -----------MTEY KLVVVGAGGVGKSAL TIQLIQNHFVDEYDP TIEDSYRKQVVIDGE TCLLDILDTAGQEEY 64
2 R-Ras MSSGAASGTGRGRPR GGGPGPGDPPPSETH KLVVVGGGGVGKSAL TIQFIQSYFVSDYDP TIEDSYTKICSVDGI PARLDILDTAGQEEF 90

        91          105 106         120 121         135 136         150 151         165 166         180
1 H-Ras SAMRDQYMRTGEGFL CVFAINNTKSFEDIH QYREQIKRVKDSDDV PMVLVGNKCDLAAR- TVESRQAQDLARSYG IPYIETSAKTRQGVE 153
2 R-Ras GAMREQYMRAGHGFL LVFAINDRQSFNEVG KLFTQILRVKDRDDF PVVLVGNKADLESQR QVPRSEASAFGASHH VAYFEASAKLRLNVD 180

        181         195 196         210 211         225
1 H-Ras DAFYTLVREIRQHKL RKLNPPDESGPG--C MSCKCVLS    189
2 R-Ras EAFEQLVRAVRKYQE QELPPSPPSAPRKKG GGCPCVLL    218
```

Figure 5.8 H-Ras and R-Ras Amino Acid Alignment

H-Ras and R-Ras amino acid sequence alignment with the area of R-Ras to be exchanged for H-Ras, in the generation of a new chimera, highlighted in red.

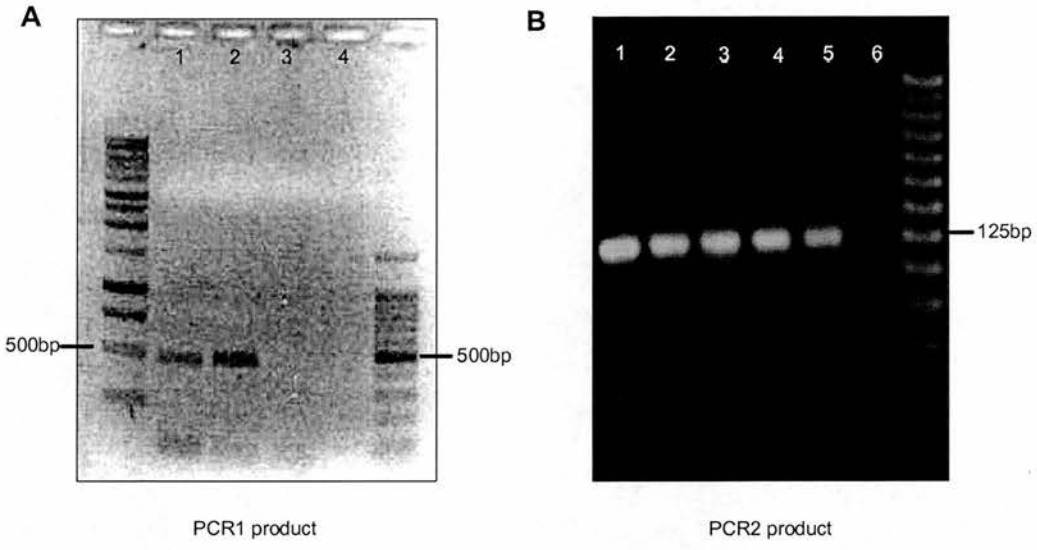

Figure 5.9 High fidelity PCR products for new H-and R-Ras chimera.

Using high fidelity PCR, on R-Ras G38V in pCDNA3.1(+) (50ng), the two products for a new H-and R-Ras chimera were amplified. Gel A (lanes 1 and 2) shows product 1, resolved on a 1% agarose gel, using a 1kb and 100bp ladder. The negative control PCR (lane 3) contained no template. Gel B (lanes 1-5) shows product 2, resolved on a 2% agarose gel, using a 25bp ladder. The negative control PCR (lane 6) contained no template. The image contrast for Gel A has been reversed to allow clear visualisation of bands.

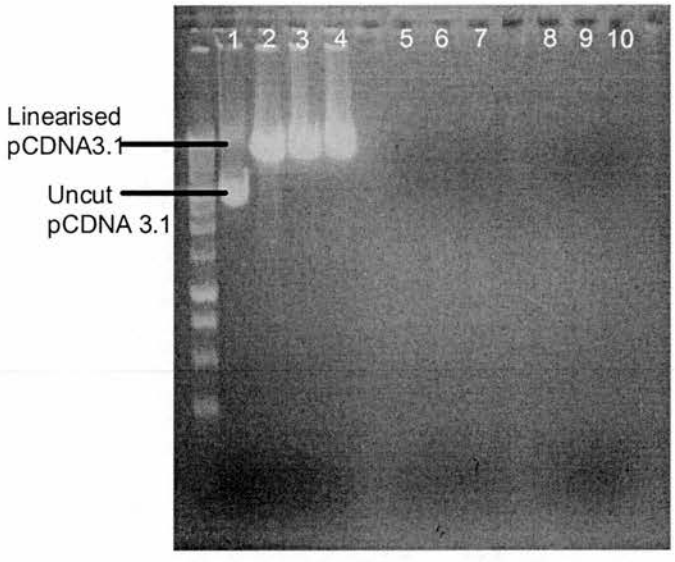

Figure 5.10 Results of blunt-ended ligation of new H-and R-Ras chimera products into pCDNA3.1 (+).

Mini-prepped DNA from blunt-ended ligation of new H-and R-Ras chimera products into pCDNA3.1 (+) were resolved on a 1% agarose gel (Lanes 5-10). Lane 1 contains uncut pCDNA3.1 (+) and Lanes 2-4, contain pCDNA3.1 (+), digested with EcoRI. Samples were resolved against a 1kb ladder.

5.5 Generation of H-and R-Ras chimera using splice-overlap extension by PCR (SOE by PCR).

Subsequent to the unsuccessful blunt-ended ligation of the H-and R-Ras chimera into pCDNA3.1(+), it was decided to redesign the original primers so that the internal hybrid primers contained a site of overlap, thus SOE by PCR could be utilised. Following the first stage generation of PCR products 1 and 2, a second stage PCR would generate the full-length H-and R-Ras chimera with appropriate restriction sites for ligation into pCDNA3.1(+). Figure 5.11 is a schematic representation of the steps involved in the generation of the H-and R-Ras chimera using splice-overlap extension by PCR.

5.5.1 Generation of products 1 and 2 using high fidelity PCR.

Using high fidelity PCR, first stage reactions were used to generate products 1 and 2 which would be used to construct a new H-and R-Ras chimera. New internal hybrid primers were designed to include a sequence overlap between products 1 and 2 (see Table 2.5). The hybrid primer PCR1RevOvlp contained R-Ras Glu171 to Ala174/ H-Ras Lys147 to Val160 and PCR2FwdOvlp contained H-Ras Glu153 to His166/ R-Ras Glu194 to Pro203. The seven amino acid sequence (21 base pair) overlap between PCR1RevOvlp and PCR2FwdOvlp, H-Ras Glu153 to Val160, provided a sequence of homology between the two first stage PCR products. The area of overlap between PCR1RevOvlp and PCR2FwdOvlp is shown in bold type below.

PCR1RevOvlp	5'-**CACCAACGTGTAGAAGGCCTC**CACTCCCTGCCGGGTCTTGGCC GAGGCCTC-3'
PCR2FwdOvlp	5'-**GAGGCCTTCTACACGTTGGTG**CGTGAGATCCGGCAGCACCAG GAACAAGAGCTCCCACCGAGCCCTCCC-3'

It was discovered that the restriction sites originally used for ligation into pCDNA3.1 (5.4.2) were selected for orientation into pCDNA3.1(-) and not pCDNA3.1(+). Therefore, new flanking primers were designed to include the appropriate restriction sites for correct orientation into pCDNA3.1(+).

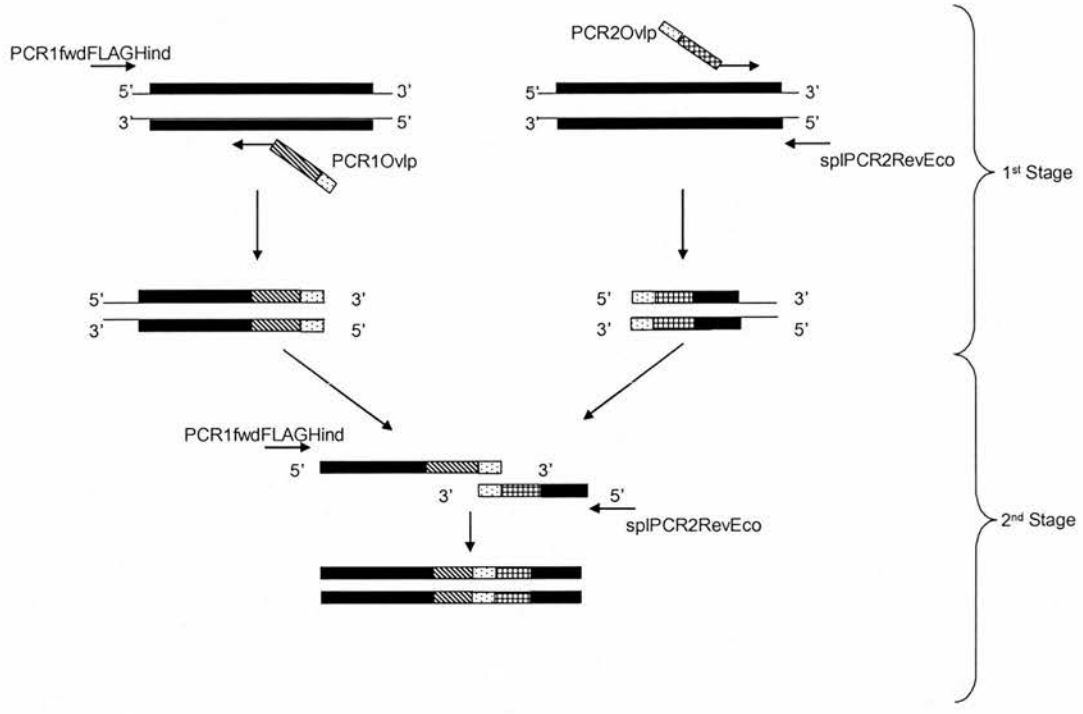

Figure 5.11 Schematic Representation of SOE by PCR

R-Ras G38V cDNA is represented with solid black shading. Flanking oligonucleotide primers (PCR1fwdFLAGHind and splPCR2RevEco) are represented by arrows. Hybrid primers (PCR1Ovlp and PCR2Ovl) are represented by an arrow, with the extended H-Ras sequences represented by a diagonal and hatched fill-effect. Areas of H-Ras sequence overlap on the two hybrid primers are shown with a spotted effect.

Primers PCR1fwdFLAGhind (which includes a HindIII restriction site) and PCR1Ovlp were used to produce product 1, containing the N-terminal sequences of the H-and R-Ras chimera. The final product contains a HindIII restriction site and FLAG-tag at the N-terminus as well as a C-terminal overlap sequence. Figure 5.12A shows that the amplified product was 500bp. No PCR products were observed in reactions performed in the absence of primers or template DNA. The PCR product was excised from the gel and purified.

Primers PCR2Ovlp and splPCR2RevEco (which includes an EcoRI restriction site) were used to produce product 2, containing the C-terminal sequences of the H-and R-Ras chimera. The final product contains an EcoRI restriction site at the C-terminus as well as an N-terminal overlap sequence. Figure 5.12B shows that the amplified product was 125bp. No PCR products were observed in reactions performed in the absence of primers or template DNA. The PCR product was excised from the gel and purified.

5.5.2 High fidelity PCR of H-and R-Ras chimera (CHX).

From Figure 5.11, it can be seen that following the first stage PCRs (5.5.1), it is possible to perform a third high fidelity PCR to generate the full-length H-and R-Ras chimera, termed CHX.

The second stage PCR used the flanking primers PCR1fwdFLAGhind and splPCR2RevEco. The gel purified products 1 and 2 were used as the template DNA. It was necessary to use equal molecular amounts of the two template DNAs. Since product 1 was 500bp and product 2 was 125bp, the concentration of each template used was calculated based on a 4:1 ratio on weight (product 1: product 2, respectively). The PCR cycle programme was adjusted for the second stage PCR (see Materials and Methods, 2.12). The melting temperatures of the flanking primers as well as that of the area of sequence overlap between the two template DNAs were an important consideration in their designs. For the second stage PCR, it was important that the melting temperature of the overlap sequence, H-Ras Glu153 to Val160 (68°C), was lower than the melting temperatures of the two flanking primers PCR1fwdFLAGhind (>75°C) and splPCR2RevEco (>75°C). This encourages the annealing of the two template DNAs during the first PCR cycle (which uses lower

temperatures) prior to increasing the PCR cycle temperatures to allow the flanking primers to anneal and amplify the final product.

Figure 5.13A shows that the amplified CHX was about 600bp. No PCR products were observed in reactions performed in the absence of template DNA. The PCR product was excised from the gel and purified.

Following gel purification, CHX was digested with HindIII and EcoRI, ethanol precipitated and ligated into pCDNA3.1 (+) (pre-digested with both HindIII and EcoRI). The ligation product was subsequently transformed into DH5α competent cells and resulting colonies mini-prepped and digested with HindIII and EcoRI to confirm plasmid DNA content and insert size. Figure 5.13B shows positive plasmid content for all samples, each with an insert measuring between 500 and 750bp. CHX clones 1-6 were all sent for sequence verification. Sequencing not shown.

5.5.3 New H-and R-Ras chimera, CHX, was not expressed in CHO cells.

Following sequencing, one of the CHX clones was selected to test for expression in CHO cells. The N-terminal FLAG-tag on primer PCR1fwdFLAGhind was used so that expression levels of the new chimera (CHX) could be compared with the original H- and R-Ras chimeras, which all contain an N-terminal FLAG-tag. However, using expression of CH1 as a positive FLAG control, CHX showed no expression in αβ-py cells (Figure 5.14A). Furthermore, CHX was not detected even when using an anti-R-Ras antibody with a positive R-Ras G38V control (Figure 5.14B).

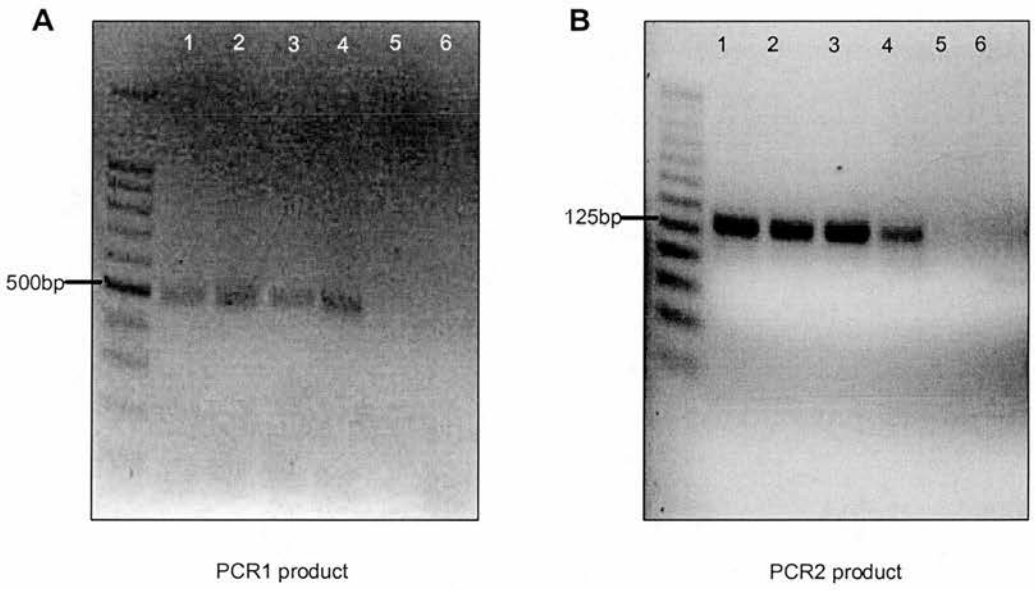

Figure 5.12 First stage PCR products for generation of new H-and R-Ras chimera using splice-overlap extension by PCR.

Using high fidelity PCR, on R-Ras G38V (50ng), the two products for a new H-and R-Ras chimera were amplified using 50µl reaction volumes. Gel A shows product 1 (lanes 1-4), resolved on a 1% agarose gel, using a 1kb ladder. Gel B shows product 2 (lanes 1-4), resolved on a 2% agarose gel, using a 25bp ladder. The negative control PCRs, run in Lanes 5 and 6, of both gels, contain no primers and no template respectively. The image contrast has been reversed to allow clear visualisation of bands.

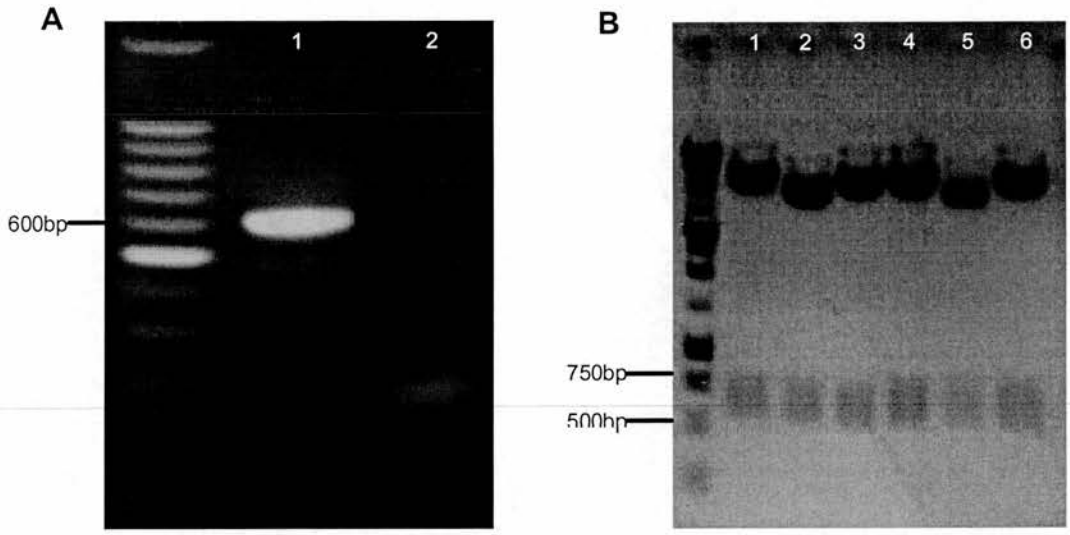

Figure 5.13 Second stage product of slice-overlap extension by PCR

(A) Splice-overlap extension was performed using high fidelity PCR with the products of the first stage PCRs as template DNA. The negative control (Lane 2) contained no template DNA. PCR products were resolved on 1% agarose gel against a 100bp ladder. (B) Restriction digest (HindIII and EcoRI) of plasmid clones from CHX ligations. Products were run on a 1% agarose gel against a 1kb ladder. The image contrast of gel B has been reversed to allow clear visualisation of bands.

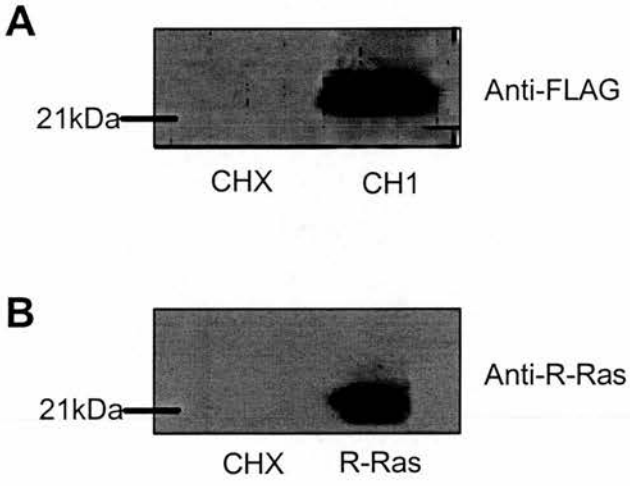

Figure 5.14 Expression of new H-and R-Ras chimera, CHX.

Cell lysates were prepared from $\alpha\beta$-py cells transfected with 1µg of CHX, R-Ras G38V or CH1. Expression of CH1 (A) and R-Ras (B) served as positive controls. Cell lysates were probed for CHX expression using the anti-FLAG monoclonal antibody (A) and the anti-R-Ras antibody (B).

5.6 Correcting CHX N-terminus using unique restriction enzyme sites.

Despite poor N-terminal sequencing of CHX, sequence analysis confirmed that the exchange of R-Ras G38V C-terminal sequences acids Ser^{172} to Tyr^{194} for the equivalent H-Ras G12V amino acid sequences Ser^{145} to His^{166} had been successful. However, it was noticed that there was a one amino acid deletion within the overlap sequence, H-Ras Asp^{154} (base pairs 150-152, GAT) that had accidentally been omitted from PCR1Ovlp and PCR2Ovlp primer sequences.

5.6.1 Ligation of N-terminal sequences of R-Ras G38V into CHX.

Rather than repeat the complicated splice-overlap extension by PCR, it was decided that the N-terminal sequence of CHX could be exchanged for the N-terminal sequence of R-Ras G38V, using a restriction site unique to R-Ras G38V. Figure 5.15 shows a schematic representation for the restriction digests and ligations involved in the exchange of the N-terminus of CHX with that of R-Ras G38V. SacII was selected as the internal R-Ras G38V restriction enzyme for two reasons, it does not cleave the pCDNA3.1 (+) vector and it cleaves R-Ras at position 293 thus removing the poor N-terminal sequences of CHX (base pairs 1-120). Both R-Ras G38V and CHX (cloned into pCDNA3.1 (+)) were digested with HindIII and SacII, to remove the respective N-terminal sequences. Figure 5.16 (lanes 2 and 4) shows that the resulting products are about 6kb and <250bp.

The <250bp product from the R-Ras G38V restriction digest (Lane 2) and the 6kb product from the CHX restriction digest (Lane 4) were gel excised and purified. The 6kb product from CHX (which should contain the base pair sequences 294 to 669 of CHX in pCDNA3.1 (+)) was treated with shrimp alkaline phosphatase (SAP) for 30 minutes at 37°C then 62°C for 10 minutes, to inhibit self-ligation. The <250bp product from the R-Ras G38V digest should contain the N-terminal base pair sequences 1 to 293 of R-Ras G38V. An overnight, 18°C ligation was set up between the <250bp product from the R-Ras G38V restriction digest and the 6kb product from the CHX restriction digest. The ligation product was subsequently transformed into DH5α competent cells and resulting plasmid DNA prepared and tested by restriction digest.

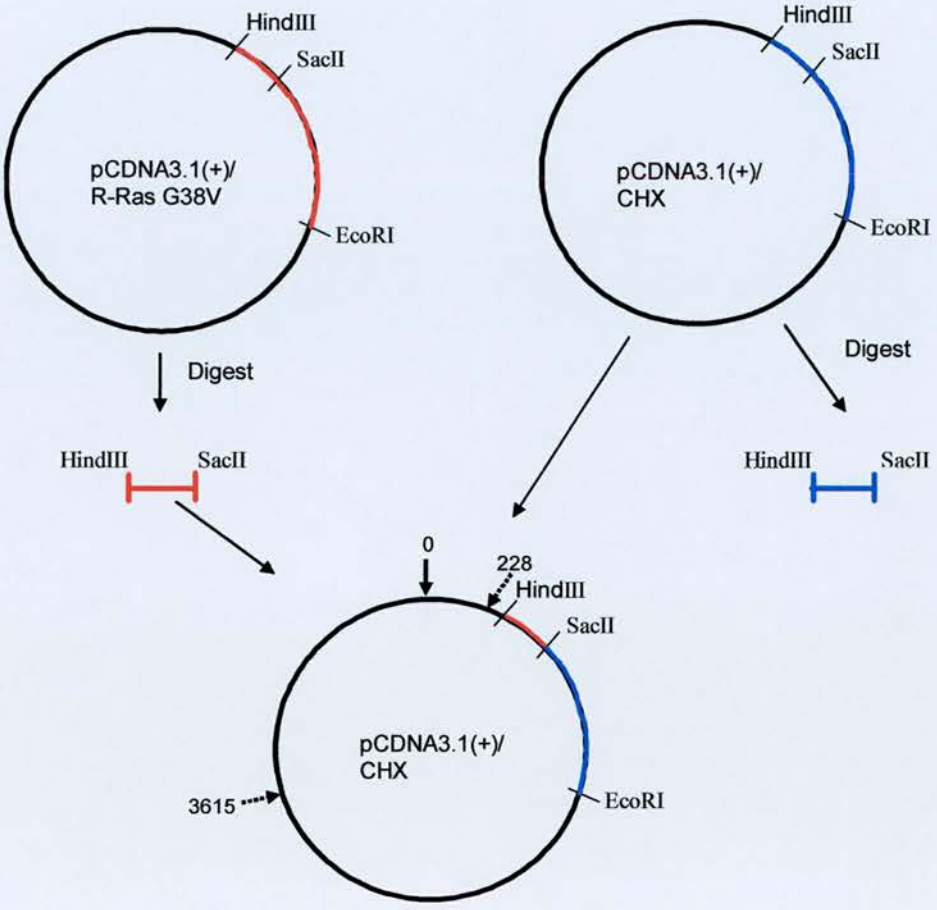

Figure 5.15 Schematic representation of plan to generate full-length CHX

Schematic represents the restriction digests to be carried out on R-Ras G38V (red) and CHX (blue), both cloned into pCDNA3.1(+). N-terminus of R-Ras G38V (red) will be used to replace the N-terminus of CHX (blue), thus generating full-length CHX. Points on pCDNA3.1(+) highlighted by dashed arrows indicate the positions (228 and 3615) where the restriction enzyme AflIII cleaves the vector.

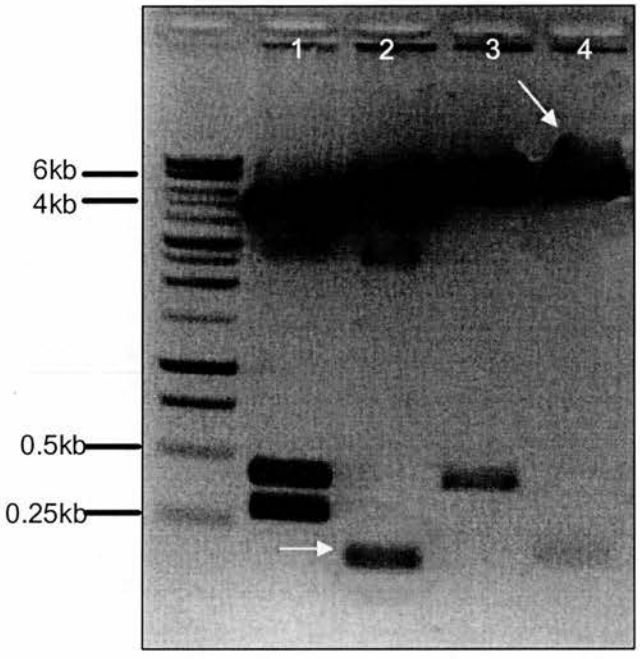

Figure 5.16 Restriction digests of R-Ras G38V and CHX to exchange N-termini.

R-Ras G38V, cloned into pCDNA3.1(+), was digested with EcoRI and SacII (lane1) or HindIII and SacII (lane 2).
CHX, cloned into pCDNA3.1(+), was digested with EcoRI and SacII (lane3) or HindIII and SacII (lane 4).
Products were resolved on a 1% agarose gel against a 1kb ladder. Resulting products from lanes 2 and 4, identified by white arrows, were gel excised.

The restriction enzyme AflIII was selected to test the success of the R-Ras G38V N-terminal ligation since it cleaves pCDNA3.1 (+) at positions 228 and 3615 (see Figure 5.15) but does not cleave R-Ras G38V. An additional advantage of AflIII is that it cleaves H-Ras at position 470, which is found in the area of amino acid exchange between R-Ras and H-Ras for chimera CHX. This meant that restriction analysis would also confirm the success of the SOE by PCR. Sequence analysis of pCDNA3.1(+) and R-Ras G38V suggested that if the ligation of R-Ras G38V N-terminal had been successful, bands were expected at sizes 1183bp, 2958bp and 2041bp.

Figure 5.17 shows the results of an AflIII restriction digest on ten CHX clones. Lanes 4-13 correspond to clones CHX(1) to CHX(10) respectively. Every clone shows evidence of digest products at about 2 and 3 kb, which correspond to the expected 2041bp and 2958bp products. The band corresponding to the third digestion product of clones 1, 3 and 4 (lanes 4, 6 and 7 respectively) ran at just over 1kb. The third digestion product for the other 7 clones ran closer to 1kb.

5.6.2 Expression of CHX clones in CHO cells

A few of the CHX clones were selected for further analysis. The expression of the clones was analysed in $\alpha\beta$-py cells using the N-terminal Myc-tag inherited from ligation of the R-Ras G38V N-terminal.

Figure 5.18A shows that clones CHX(1) and CHX(3) showed positive for Myc-tagged protein expression. The expressed proteins were of a similar size to R-Ras G38V (about 23kDa). The presence of the Myc-tag at the N-terminus of the clones also meant that immunofluorescence analysis could be carried out on transiently transfected cells as a further indication of protein expression. Cells were stained using anti-Myc (9E10) antibody, followed by Alexa 488-conjugated goat anti-mouse IgG (green). Figure 5.18B shows positive staining for expression of a Myc-tagged protein in CHX(1) and CHX(3). The clones CHX(5) and CHX(10), did not show any positive staining (results not shown). Expression of Myc-tagged R-Ras G38V was used as a positive control for both western blot and immunofluorescence analyses.

CHX(1) and CHX(3) were sent for sequence verification. See Appendix (III).

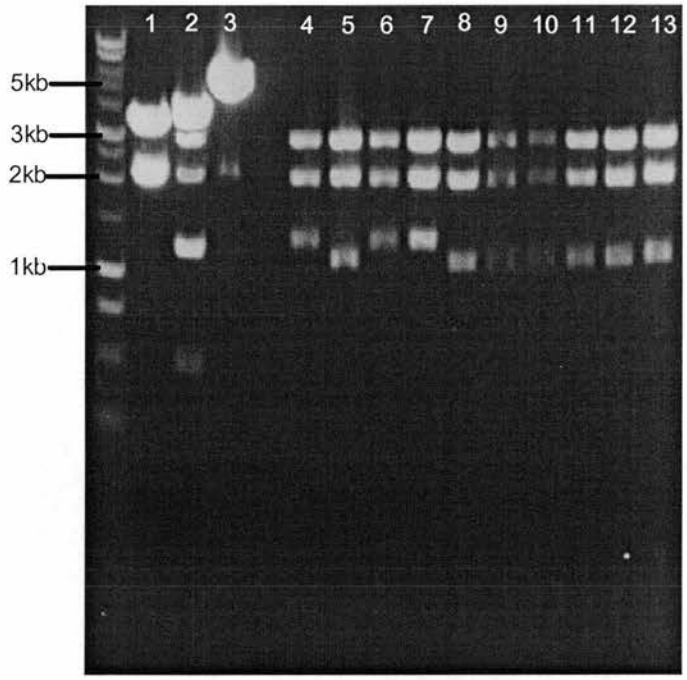

Figure 5.17 Restriction digest of N-terminal R-Ras G38V and C-terminal CHX ligation into pCDNA3.1(+).

Mini-prepped DNA from N-terminal R-Ras G38V and C-terminal CHX ligations (4-13) were digested with Afl III. Control digests carried out on pCDNA3.1(+) alone (lane 1), H-Ras G12V cloned into pCDNA3.1 (+) (lane2) and R-Ras G38V cloned into pCDNA3.1 (+) (lane 3).

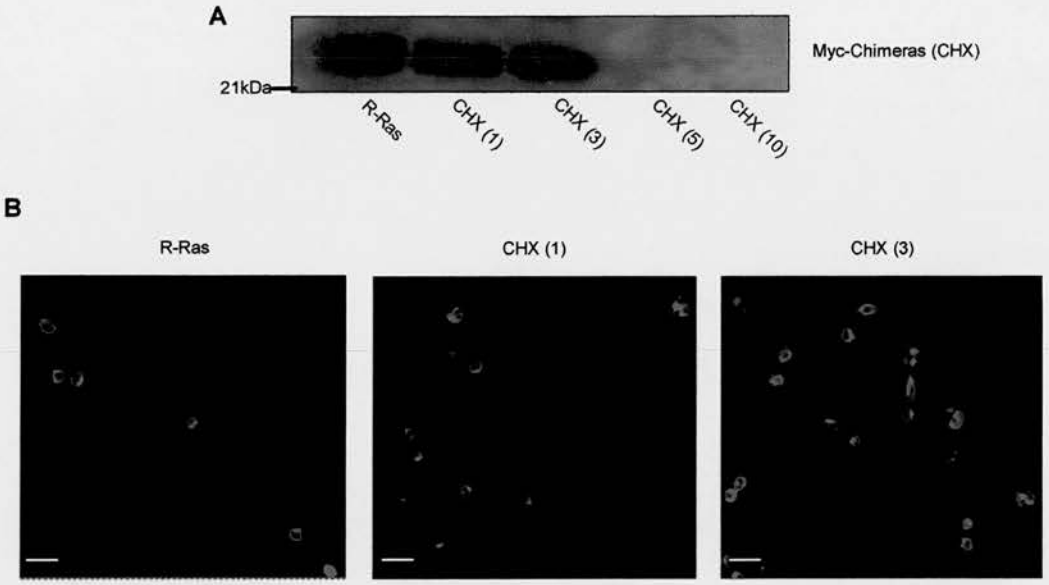

Figure 5.18 Expression of CHX clones

(A) Cell lysates were prepared from αβ-py cells transfected with 1μg of R-Ras G38V or 1μg of each CHX clone. Lysates were probed with anti-Myc antibody to check expression levels.
(B) Expression was confirmed using immunofluorescence. Cells were stained using anti-Myc antibody (green). Bars, 50μm.

5.6.3 Effect of CHX(1) and CHX(3) expression on integrin affinity modulation.

Integrin affinity was determined in $\alpha\beta$-py cells transfected with control vector, R-Ras G38V, CHX(1) and CHX(3) ± H-Ras G12V, see Figure 5.19. As a positive control, full length R-Ras G38V was used to reverse H-Ras-mediated integrin suppression from 50.3% to 10.85%. Preliminary data indicates that cells transfected with CHX(1) alone mediate an activated integrin state similar to that observed with R-Ras G38V however, CHX(1) was not as efficient as R-Ras G38V at reversing H-Ras-mediated integrin suppression (from 50.3% to 29.8%). Cells transfected with CHX(3) show about a 10% suppression of integrin activation which increases to 19.65% in the presence of H-Ras G12V.

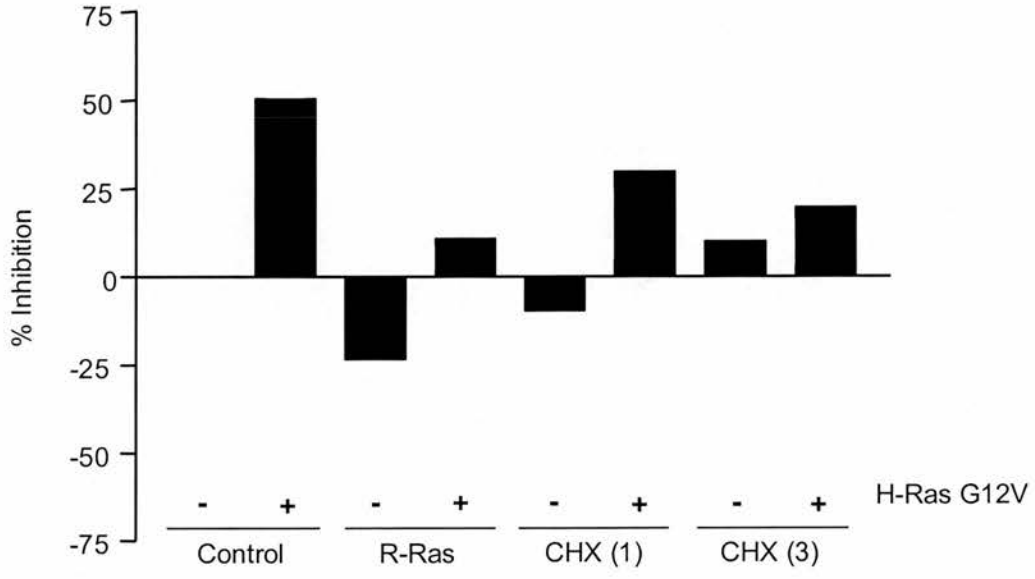

Figure 5.19 Reversal of H-Ras G12V–mediated integrin suppression by CHX clones (n=1).

Integrin affinity was determined in $\alpha\beta$-py cells transfected with 1μg of R-Ras G38V, CHX(1) or CHX (3) ± H-Ras G12V (1μg). In each transfection, total DNA content was standardised to 2μg using control vector. Percentage inhibition was calculated in reference to control vector alone.

5.7 Discussion

In Chapter 4, the C-terminal regions of H-Ras (149-174) and R-Ras (175-203) were found to be required for integrin affinity modulation. In this chapter, these C-terminal regions were further investigated using site-directed mutagenesis and by the generation of a new H-and R-Ras chimera. The major findings in this chapter are: that H-Ras amino acids sequences His^{166} to Glu^{170} are not sufficient to confer H-Ras G12V-mediated integrin suppression properties to R-Ras G38V, however the exchange of R-Ras G38V amino acids Tyr^{193} to Glu^{197} for these equivalent H-Ras amino acids reduces the ability of R-Ras G38V to reverse H-Ras G12V-mediated integrin suppression. Using splice-overlap extension by PCR to generate a new H-and R-Ras chimera, CHX, succeeded in the exchange of R-Ras amino acids Ser^{172} to Tyr^{193} for the equivalent H-Ras amino acids Ser^{145} to His^{166}. CHX clones 1 and 3 were successfully expressed in $\alpha\beta$-py cells.

The differing effects of H-and R-Ras chimeras on integrin-affinity modulation focus attention on the possible influential effects of the hypervariable domains of H-Ras and R-Ras, as well as sequences N-terminal to the HVR. The aims of this chapter were to use a series of site-directed mutations within the C-terminal regions of R-Ras G38V (175-203) and to generate a new H-and R-Ras chimera, where R-Ras G38V domains were replaced with the appropriate H-Ras sequences, to elucidate whether these specific regions are sufficient to confer integrin suppression by H-Ras or if they are required for R-Ras reversal of H-Ras-mediated integrin suppression. The decision to use R-Ras G38V as the template for further investigating the C-terminal domains of H-Ras and R-Ras was based upon it being easier to observe a suppressive effect (i.e. changing an R-Ras G38V effect into an H-Ras G12V effect) than to observe a reversal of integrin suppression.

To further investigate the importance of the hypervariable domains with regard to integrin affinity, site-directed mutagenesis was used to mutate R-Ras amino acids, found within the hypervariable linker domain (Tyr^{193} to Glu^{198}), into the equivalent H-Ras amino acids. These particular amino acids were investigated first as they overlapped with a 6 amino acid area within the HVR of H-Ras shown to be important for efficient interaction with effectors (Jaumot *et al.*, 2002). Single amino-acid

mutations, which required only a single base pair mutation, were attempted first. Results showed that individually, H-Ras amino acids His^{166}, Lys^{167} and Lys^{170} within the linker domain do not confer an ability to suppress integrin affinity. Expanding the region under test, it was decided that the entire five amino acid region of R-Ras G38V should be mutated to the equivalent H-Ras sequence. The reasoning for this action was that if no suppressive effect was conferred by the full five amino acid exchange, then further single amino acid mutations within this region would be unnecessary. While mutation of the entire 5 amino acid sequence did not confer the ability to suppress integrin affinity, the capacity of R-Ras G38V to reverse H-Ras G12V-mediated integrin suppression was diminished.

Although results from Chapter 4 suggested that the C-terminal regions of H-Ras (149-174) and R-Ras (175-203) were found to be required for integrin affinity modulation, the N-terminal sequences of the hypervariable linker domain were investigated first. Several studies have recently identified the importance of the HVR linker domain. Jaumot *et al.*, (2002) showed using amino acid deletion and alanine replacement that the N-terminal sequences of the HVR linker domain (H-Ras amino acids His^{166}- Asn^{172}), in association with C-terminal spacer sequences (H-Ras amino acids Pro^{173}-Pro^{179}) were necessary for the release of activated H-Ras from lipid rafts. Confinement of H-Ras G12V to the lipid rafts abrogated Raf-1, PI 3-kinase and Akt activation (Jaumot *et al.*, 2002). It has been hypothesised that the HVR sequences of H-Ras might transmit conformational changes in the N-terminal domains, coincident with GTP-loading, through to the membrane anchor (Prior *et al.*, 2001).

Results here show that mutation of the HVR N-terminal linker domain had no significant effect on R-Ras-mediated integrin affinity, which suggests that these sequences alone are not sufficient to influence integrin affinity. However, the significant difference in the abilities of R-Ras G38V and the 5aaSDM product to reverse H-Ras-mediated integrin suppression suggests that R-Ras amino acids (Tyr^{193}-Glu^{198}) are required for reversal of H-Ras-mediated integrin affinity. As the equivalent H-Ras amino acids have previously been shown to be required for GTP-loaded release from lipid rafts and subsequent activation of effectors (Jaumot *et al.*, 2002) then perhaps H-Ras substitution of the R-Ras N-terminal linker domain

sequences affects R-Ras interaction with effectors by altering the targeting of the activated protein.

Since site-directed mutagenesis of the five amino acids of R-Ras G38V (Tyr^{193} to Glu^{198}), to the equivalent H-Ras G12V amino acids did not confer integrin suppression properties, it was decided that sequences N-terminal of these five amino acids should be investigated. It is worth mentioning at this point that sequences C-terminal to these five amino acids were not investigated further as current data at the time indicated that the region acted as a spacer element (Jaumot *et* al., 2002) and while the presence of the spacer element was required for proper H-Ras function, amino acid substitution had no effect. Subsequently, this proline-rich region of R-Ras G38V has been found to be a binding site for the Nck adaptor protein, which has been implicated in the recruitment of R-Ras effectors that are employed by R-Ras to augment integrin affinity (Kinbara *et al.*, 2003). If this is the case, then maintaining this proline-rich region in the site-directed mutants may help R-Ras G38V promote an activated integrin state. Whether H-Ras has similar binding sites in this region remains to be investigated.

In order to investigate the importance of the N-terminal regions of H-Ras and R-Ras upstream of the HVR, R-Ras sequences (Ser^{172} to Tyr^{193}) were to be replaced by the equivalent H-Ras sequences (Ser^{145} to His^{166}), using the remaining R-Ras sequences as the backbone of the new H-and R-Ras chimera. Figure 5.8 highlights the area of R-Ras G38V to be exchanged for the equivalent H-Ras sequences. Instead of relying on the presence of restriction sites at appropriate positions of both H-Ras and R-Ras, which would allow the generation of the new chimera, PCR generation of hybrid fragments and subsequent ligation was explored.

The original design of the four primers required for this technique was to rely on a blunt-ended ligation between the two resulting PCR products to form the full-length chimera. While the generation of the DNA fragments was successful (see Figures 5.9A and 5.9B), subsequent blunt-ended ligation of the DNA fragments and overall ligation into the pCDNA3.1(+) vector was unsuccessful (Figure 5.10).

An alternative to the blunt-end ligation procedure, was to employ a technique of splicing by overlap extension by PCR (SOE by PCR) as described by Horton *et al.*,

(1989), where the PCR products contain a region of overlap. In this case, the sequence of overlap was provided by the middle seven amino acids of the H-Ras inserted sequence (Glu^{153} to Val^{160}). The schematic representation of SOE by PCR (Figure 5.11) shows that the first stage PCR generates two DNA fragments containing the H-Ras overlap sequences. As the hybrid oligonucleotides are tipped with a short sequence of homology, when the two first stage products are mixed they can partially anneal and using the original flanking primers, be used as the template for a second stage PCR to produce the final product. Although restriction enzyme analysis of clones of the final product ligated into pCDNA3.1(+) indicated the presence of a 500-750bp insert, sequence analysis could not verify the presence of the N-terminal 120bp of R-Ras G38V. Sequence alignment of the selected clones with R-Ras G38V indicated the poor N-terminal sequencing of each of the six clones (sequences not shown). Although N-terminal sequencing was poor, the insertion of H-Ras sequences Ser^{145} to His^{166} in place of the equivalent R-Ras G38V sequences Ser^{172} to Tyr^{193} was successful. Detailed sequence analysis, however, revealed that a single H-Ras amino acid (Asp^{154}) was absent in all the clones. The omission was tracked down to an error in the hybrid primers PCR1RevOvlp and PCR2FwdOvlp, in which the H-Ras amino acid (Asp^{154}) was absent. Rather than having to start at the beginning again and redesign the hybrid primers for SOE by PCR, it was considered easier to complete the generation of the H-and R-Ras chimera and then using site-directed mutagenesis, re-insert the aspartic acid.

Transfection of $\alpha\beta$-py cells with the chimera DNA and subsequent western blot analysis revealed that the chimeric protein was not expressed, this was most probably due to the poor quality of the N-terminal sequences of R-Ras G38V. Despite extensive repeated manipulation of the buffer conditions and PCR protocol, it was impossible to generate the full-length H-and R-Ras chimera (CHX) with the correct N-terminal sequence. R-Ras G38V is comprised of a very GC-rich section at its N-terminal, with the first 75 base pairs almost 87% GC. As a direct result of this, the PCR1fwdFLAGhind flanking primer at the N-terminus of the R-Ras G38V (which is also GC-rich) may be mis-priming to an alternative section of the N-terminus. Alternatively, the high GC-content may increase the melting temperature of this section of R-Ras, and so it may not be sufficiently denatured in the PCR cycle thus

preventing the annealing of the forward primer. To circumvent this problem, the poor N-terminal sequence could be replaced by restriction digest with the appropriate sequence from R-Ras G38V.

From sequence analyses of the CHX(1-6) clones, it was clear that the sequencing C-terminal to Ras G38V Gly^{39} was satisfactory. As it was only the N-terminal sequences of CHX that seemed to be causing the problem, it was hoped that by replacing these sequences with the appropriate R-Ras G38V sequences that the expression problem may be resolved. The restriction enzyme, SacII (ccgc/gg), cleaves R-Ras G38V at position 254. As this restriction enzyme is unique to R-Ras G38V (when cloned into pCDNA3.1(+)) and cuts sufficiently downstream of the problem N-terminal sequence (base pairs 1-120), it was used to remove the N-terminal sequence of R-Ras G38V from pCDNA3.1(+). This N-terminal R-Ras G38V fragment was used to replace the equivalent section in the new H-and R-Ras chimera (CHX), thus maintaining the hybrid C-terminal section of CHX (see Figure 5.15 for schematic representation of restriction digests and subsequent ligation).

Following ligation, clones were mini-prepped and restriction digest analysis was used to confirm the presence of the N-terminal R-Ras G38V sequences. A diagnostic enzyme, AflIII was selected as it cleaves pCDNA3.1 (+) at positions 228 and 3615 but does not cleave R-Ras G38V. Additionally, AflIII also cleaves H-Ras G12V, at position 470 which is included in the H-Ras sequences of CHX. This meant that further confirmation of the H-Ras insert into R-Ras G38V could be confirmed by restriction digest of the clones with AflIII.

Despite all clones being positive for the H-Ras insert (confirmed by the presence of three bands as opposed to just two) it was more difficult to try and distinguish between clones which contained the N-terminal R-Ras G38V and those that may be missing the N-terminal 254 base pairs, removed by SacII cleavage. Analysis of restriction enzyme maps for AflIII cleavage of pCDNA3.1(+) and H-Ras, suggested that if the chimera contained the N-terminal R-Ras G38V sequences, bands would be expected at 2041bp, 2958bp and 1183bp (the latter being influenced by the presence of the R-Ras N-terminal sequences). However, should the chimera not contain the N-terminal sequences, the third product band would be about 950bp rather than 1183bp.

Consequently, it was expected that clones CHX(1), CHX(3) and CHX(4) (see Figure 5.17) would contain the R-Ras G38V N-terminal sequences as the third digestion product band of these clones ran slightly higher than that of the remaining seven clones. To avoid missing the correct clone, in addition to CHX(1) and CHX(3), the CHX(5) and CHX(10) clones, which contained a smaller sized third product, were also tested. As a consequence of exchanging the N-terminal sequences of CHX with that of R-Ras G38V, the resulting clones inherited the Myc-tag. Western blot analysis showed that CHX(1) and CHX(3) were expressed in $\alpha\beta$-py cells but that CHX(5) and CHX(10) were not. This was further confirmed using immunofluorescence. These results verify the presence of the N-terminal R-Ras G38V sequence on CHX(1) and CHX(3) as the Myc-tagged protein would not otherwise be expressed. As CHX(5) and CHX(10) were not expressed in $\alpha\beta$-py cells would suggest that, in accordance with the AflIII restriction digest results, ligation of the R-Ras G38V N-terminal sequence into CHX was not successful in these clones.

Despite clear evidence that CHX(1) and CHX(3) were both successfully expressed in $\alpha\beta$-py cells and that restriction digest analysis revealed product sizes backing up the presence of the full-length H-and R-Ras chimera, there were problems with the sequencing of full-length CHX(1) and CHX(3). As with earlier sequence analysis of the CHX products, sequencing of the N-terminal region of the chimera was unsuccessful. Appendix III shows that the C-terminal H-Ras sequences equivalent to R-Ras Ser^{172} to Tyr^{193} have been maintained during restriction enzyme manipulation but that sequences N-terminal of R-Ras Val^{40} have not been sufficiently sequenced. The high GC content of the N-terminal is probably responsible for the poor DNA sequencing. R-Ras was first identified by Lowe *et al.*, (1987); this group also had problems with the sequencing of the N-terminal region of R-Ras. They describe that the N-terminal region of R-*ras* mRNA proved refractory to reverse transcription by oligo (dT) priming and from priming from primers complementary to the codon 30 region (Lowe *et al.*, 1987). As yet, PCR conditions to sequence this region have not been identified either by in-house sequencing facilities or commercial facilities. Taking that the proteins could be expressed; it can be assumed that the N-terminal region, carrying the Myc-tag, is present. However, time limitations prevented further attempts to re-sequence the CHX chimeras.

A preliminary experiment was carried out to see how the CHX clones CHX(1) and CHX(3) affected integrin affinity modulation. Results indicated that the exchange of R-Ras amino acids Ser^{172} to Tyr^{193}, for the equivalent H-Ras sequences affects the ability of R-Ras G38V to modulate integrin affinity. CHX(1) and CHX(3) both demonstrated a diminished ability to reverse H-Ras G12V-mediated integrin suppression, compared with R-Ras G38V. The chimeras were not convincing in their suppressive abilities. However as time only permitted a preliminary experiment to be carried out on these new constructs, further investigations are required to fully understand whether this region is sufficient to modulate integrin affinity. These investigations should probably take into account the amino acids C-terminal to the HVR linker domain, as this proline-rich region of R-Ras G38V has recently been implicated in the recruitment of R-Ras effectors that are employed by R-Ras to augment integrin affinity (Kinbara *et al.*, 2003). If this is the case, then perhaps exchange of these amino acids as well as R-Ras amino acids Ser^{172} to Tyr^{193} might confer the full suppressive effect of full-length H-Ras G12V to R-Ras.

5.7.1 Summary

Site-directed mutagenesis of R-Ras G38V to exchange amino acids Tyr^{193} to Glu^{198} for the equivalent H-Ras amino acids His^{166} to Glu^{170} did not confer an ability to R-Ras G38V to suppress integrin affinity. From this it can be deduced that the H-Ras G12V amino acids His^{166} to Glu^{170} alone are not sufficient to suppress integrin affinity modulation. The generation of a new H-and R-Ras chimera to further elucidate the importance of the C-terminal regions, using SOE by PCR, was successful in exchanging the appropriate regions of R-Ras G38V for the equivalent H-Ras sequences.

A preliminary study revealed that H-Ras G12V amino acids Ser^{145} to His^{166} are sufficient to impede the ability of R-Ras G38V to reverse H-Ras–mediated suppression, but not to confer the full suppressive effect of full-length H-Ras G12V. However, time limitations preventing further analysis of integrin-affinity and the reoccurring problems arising from the sequencing of the R-Ras G38V N-terminal sequence mean that the results obtained using the new H-and R-Ras chimera (CHX) are not fully substantiated.

Appendix I

R-Ras SDM1

```
        1              15 16              30 31              45 46              60 61              75 76              90
sdm1    NNGAANATTTAAAGC GTGAGGGGTGGNTTT GGNACAGNTCGGGNT GGTCCANGTGGGGGG AGGTTCAGGGTCCCG GGGAACCNTCCGCCC      90
r-ras   ATGAGCA------GC G---GGGCGGCGTCC GGGACAGGGCGGGGG CGGCCCCG-GGGCGG GGGACCTGGG-CCCG GGGA-CCCCCCGCCC      78

        91            105 106            120 121            135 136            150 151            165 166            180
sdm1    TAGGCGAAACACAAC NAGCCTTGTGGTTTG TGGGNTGGTGTCGGG CGNGGGNCAAGAGCG GGCTGACCATCCCAG TTCATCCAGTCCTAT     180
r-ras   A--GCGAGACACA-C AAGC-TGGTGGTC-G TGGGC-GGCGGCGG- CGTGGGC-AAGAGCG CGCTGACCATCC-AG TTCATCCAGTCCTAC     159

        181           195 196            210 211            225 226            240 241            255 256            270
sdm1    TTGG-GTCTGANTAC GACCCCACTATTGAG GACTCCTACACGAAG ATNTGCAGGTGTGGA TGGCATCCCAGCCCG GGCTGGACATCCTGG     269
r-ras   TTCGTGTCTGACTAC GACCCCACTATTGAG GACTCCTACACGAAG ATCTGCAG-TGTGGA TGGCATCCCAGCCCG G-CTGGACATCCTGG     247

        271           285 286            300 301            315 316            330 331            345 346            360
sdm1    ACACCGCGGGCCAGG AAGAGTTCGGGGCCA TGAGAGAGCAGTACA TGCGTGCTGGCCACG GCTTCCTGCTGGTGT TCGCCATTAATGACC     359
r-ras   ACACCGCGGGCCAGG AAGAGTTCGGGGCCA TGAGAGAGCAGTACA TGCGTGCTGGCCACG GCTTCCTGCTGGTGT TCGCCATTAATGACC     337

        361           375 376            390 391            405 406            420 421            435 436            450
sdm1    GGCAGAGTTTCAACG AGGTGGGCAAGCTCT TCACGCAGATTCTGC GGGTCAAGGACCGCG ACGACTTCCCCGTTG TGTTGGTCGGGAACA     449
r-ras   GGCAGAGTTTCAACG AGGTGGGCAAGCTCT TCACGCAGATTCTGC GGGTCAAGGACCGCG ACGACTTCCCCGTTG TGTTGGTCGGGAACA     427

        451           465 466            480 481            495 496            510 511            525 526            540
sdm1    AGGCAGATCTGGAGT CACAGCGCCAGGTCC CCCGATCAGAAGCCT CTGCCTTCGGCGCCT CCCACCACGTGGCCT ACTTTGAGGCCTCGG     539
r-ras   AGGCAGATCTGGAGT CACAGCGCCAGGTCC CCCGATCAGAAGCCT CTGCCTTCGGCGCCT CCCACCACGTGGCCT ACTTTGAGGCCTCGG     517

        541           555 556            570 571            585 586            600 601            615 616            630
sdm1    CCAAACTGCGTCTCA ACGTGGACGAGGCTT TTGAGCAGCTGGTGC GGGCTGTCCGGAAAC ACCAGGAACAAGAGC TCCCACCGAGCCCTC     629
r-ras   CCAAACTGCGTCTCA ACGTGGACGAGGCTT TTGAGCAGCTGGTGC GGGCTGTCCGGAAAT ACCAGGAACAAGAGC TCCCACCGAGCCCTC     607

Page 8.1
        631           645 646            660 661            675
sdm1    CCAGTGCCCCCAGGA AGAAGGGCGGGGGCT GCCCCTGCGTCCTCC TGTAG
r-ras   CCAGTGCCCCCAGGA AGAAGGGCGGGGGCT GCCCCTGCGTCCTCC TGTAG
```

R-RasSDM2

```
        1              15 16              30 31              45 46              60 61              75 76              90
sdm2    ATGAGCTNNGGTGCT GCNTCTGGTACAGTT CGTGT-CGTCCACGT GGTGGAGGTCCAGGT CCCGGG-ACCCTCCG CCTAGCGAGACACAC      88
r-ras   ATGAGCAGCGGGGCG GCGTCCGGGACAGGG CGGGGGCGGCCCCGG GGCGGGGGACCTGGG CCCGGGGACCCCCCG CCCAGCGAGACACAC      90

        91            105 106            120 121            135 136            150 151            165 166            180
sdm2    AAGCTTGTGGTCGTG GGTGGTGTCGGCGTG GGCAAGAGCGCGCTG ACCATCCAGTTCATC CAGTCCTACTTCGTG TCTGACTACGACCCC     178
r-ras   AAGCTGGTGGTCGTG GGCGGCGGCGGCGTG GGCAAGAGCGCGCTG ACCATCCAGTTCATC CAGTCCTACTTCGTG TCTGACTACGACCCC     180

        181           195 196            210 211            225 226            240 241            255 256            270
sdm2    ACTATTGAGGACTCC TACACGAAGATCTGC AGTGTGGATGGCATC CCAGCCCGGCTGGAC ATCCTGGACACCGCG GGCCAGGAAGAGTTC     268
r-ras   ACTATTGAGGACTCC TACACGAAGATCTGC AGTGTGGATGGCATC CCAGCCCGGCTGGAC ATCCTGGACACCGCG GGCCAGGAAGAGTTC     270

        271           285 286            300 301            315 316            330 331            345 346            360
sdm2    GGGGCCATGAGAGAG CAGTACATGCGTGCT GGCCACGGCTTCCTG CTGGTGTTCGCCATT AATGACCGGCAGAGT TTCAACGAGGTGGGC     358
r-ras   GGGGCCATGAGAGAG CAGTACATGCGTGCT GGCCACGGCTTCCTG CTGGTGTTCGCCATT AATGACCGGCAGAGT TTCAACGAGGTGGGC     360

        361           375 376            390 391            405 406            420 421            435 436            450
sdm2    AAGCTCTTCACGCAG ATTCTGCGGGTCAAG GACCGCGACGACTTC CCCGTTGTGTTGGTC GGGAACAAGGCAGAT CTGGAGTCACAGCGC     448
r-ras   AAGCTCTTCACGCAG ATTCTGCGGGTCAAG GACCGCGACGACTTC CCCGTTGTGTTGGTC GGGAACAAGGCAGAT CTGGAGTCACAGCGC     450

        451           465 466            480 481            495 496            510 511            525 526            540
sdm2    CAGGTCCCCCGATCA GAAGCCTCTGCCTTC GGCGCCTCCCACCAC GTGGCCTACTTTGAG GCCTCGGCCAAACTG CGTCTCAACGTGGAC     538
r-ras   CAGGTCCCCCGATCA GAAGCCTCTGCCTTC GGCGCCTCCCACCAC GTGGCCTACTTTGAG GCCTCGGCCAAACTG CGTCTCAACGTGGAC     540

        541           555 556            570 571            585 586            600 601            615 616            630
sdm2    GAGGCTTTTGAGCAG CTGGTGCGGGCTGTC CGGAAATACAAGGAA CAAGAGCTCCCACCG AGCCCTCCCAGTGCC CCCAGGAAGAAGGGC     628
r-ras   GAGGCTTTTGAGCAG CTGGTGCGGGCTGTC CGGAAATACCAGGAA CAAGAGCTCCCACCG AGCCCTCCCAGTGCC CCCAGGAAGAAGGGC     630

        631           645 646            660 661
sdm2    GGGGGCTGCCCCTGC GTCCTCCTGTAG     655
r-ras   GGGGGCTGCCCCTGC GTCCTCCTGTAG     657
```

R-RasSDM5

```
        1              15 16              30 31              45 46              60 61              75 76              90
sdm5    ATGAGCTNNGGTGCT GCTTCTGGTACAGNT CGTGGTCGTCCAACG TGGTGGAGNTCCAGN TCCCCGGGACCCTCC CGCCTAGCGAGACAC      90
r-ras   ATGAGCAGCGGGGCG GCGTCCGGGACAGGG CGGGGGCGGCCC-CG GGGCGGGGGACCTGG GCCCGGGGACCC-CC CGCCCAGCGAGACAC      88

        91            105 106            120 121            135 136            150 151            165 166            180
sdm5    ACNAGCTTGTGNTCG TGGGTGGTGTCGGCG TGGGCAAGAGCGCGC TGACCATCCAGTTCA TCCAGTCCTACTTCG TGTCTGACTACGACC     180
r-ras   ACAAGCTGGTGGTCG TGGGCGGCGGCGGCG TGGGCAAGAGCGCGC TGACCATCCAGTTCA TCCAGTCCTACTTCG TGTCTGACTACGACC     178

        181           195 196            210 211            225 226            240 241            255 256            270
sdm5    CCACTATTGAGGACT CCTACACGAAGATCT GCAGTGTGGATGGCA TCCCAGCCCGGCTGG ACATCCTGGACACCG CGGGCCAGGAAGAGT     270
r-ras   CCACTATTGAGGACT CCTACACGAAGATCT GCAGTGTGGATGGCA TCCCAGCCCGGCTGG ACATCCTGGACACCG CGGGCCAGGAAGAGT     268

        271           285 286            300 301            315 316            330 331            345 346            360
sdm5    TCGGGGCCATGAGAG AGCAGTACATGCGTG CTGGCCACGGCTTCC TGCTGGTGTTCGCCA TTAATGACCGGCAGA GTTTCAACGAGGTGG     360
r-ras   TCGGGGCCATGAGAG AGCAGTACATGCGTG CTGGCCACGGCTTCC TGCTGGTGTTCGCCA TTAATGACCGGCAGA GTTTCAACGAGGTGG     358

        361           375 376            390 391            405 406            420 421            435 436            450
sdm5    GCAAGCTCTTCACGC AGATTCTGCGGGTCA AGGACCGCGACGACT TCCCCGTTGTGTTGG TCGGGAACAAGGCAG ATCTGGAGTCACAGC     450
r-ras   GCAAGCTCTTCACGC AGATTCTGCGGGTCA AGGACCGCGACGACT TCCCCGTTGTGTTGG TCGGGAACAAGGCAG ATCTGGAGTCACAGC     448

        451           465 466            480 481            495 496            510 511            525 526            540
sdm5    GCCAGGTCCCCCGAT CAGAAGCCTCTGCCT TCGGCGCCTCCCACC ACGTGGCCTACTTTG AGGCCTCGGCCAAAC TGCGTCTCAACGTGG     540
r-ras   GCCAGGTCCCCCGAT CAGAAGCCTCTGCCT TCGGCGCCTCCCACC ACGTGGCCTACTTTG AGGCCTCGGCCAAAC TGCGTCTCAACGTGG     538

        541           555 556            570 571            585 586            600 601            615 616            630
sdm5    ACGAGGCTTTTGAGC AGCTGGTGCGGGCTG TCCGGAAATACCAGG AACAAAAGCTCCCAC CGAGCCCTCCCAGTG CCCCCAGGAAGAAGG     630
r-ras   ACGAGGCTTTTGAGC AGCTGGTGCGGGCTG TCCGGAAATACCAGG AACAAGAGCTCCCAC CGAGCCCTCCCAGTG CCCCCAGGAAGAAGG     628

        631           645 646            660
sdm5    GCGGGGGCTGCCCCT GCGTCCTCCTGTAG
r-ras   GCGGGGGCTGCCCCT GCGTCCTCCTGTAG
```

Appendix II

R-Ras 5aaSDM sequence alignment

```
      1           15 16          30 31          45 46          60 61          75 76          90
R-Ras ATGAGCAGCGGGGCG GCGTCCGGGACAGGG CGGGGGCGGCCCCGG GGCGGGGGACCTGGG CCCGGGGACCCCCCG CCCAGCGAGACACAC     90
5aa   ATGAGTCT-GGTGCT GCTTCTGG-ACAGGT CGTGGTCGTCCACGT GGTGNAGG-CCAGGT CCCGGGGACCCTCCG CCTAGCGAGACACAC     87

      91         105 106         120 121         135 136         150 151         165 166         180
R-Ras AAGCTGGTGGTCGTG GGCGGCGGCGGCGTG GGCAAGAGCGCGCTG ACCATCCAGTTCATC CAGTCCTACTTCGTG TCTGACTACGACCCC    180
5aa   AAGCTTGTGGTCGTG GGTGGTGTCGGCGTG GGCAAGAGCGCGCTG ACCATCCAGTTCATC CAGTCCTACTTCGTG TCTGACTACGACCCC    177

      181         195 196         210 211         225 226         240 241         255 256         270
R-Ras ACTATTGAGGACTCC TACACGAAGATCTGC AGTGTGGATGGCATC CCAGCCCGGCTGGAC ATCCTGGACACCGCG GGCCAGGAAGAGTTC    270
5aa   ACTATTGAGGACTCC TACACGAAGATCTGC AGTGTGGATGGCATC CCAGCCCGGCTGGAC ATCCTGGACACCGCG GGCCAGGAAGAGTTC    267

      271         285 286         300 301         315 316         330 331         345 346         360
R-Ras GGGGCCATGAGAGAG CAGTACATGCGTGCT GGCCACGGCTTCCTG CTGGTGTTCGCCATT AATGACCGGCAGAGT TTCAACGAGGTGGGC    360
5aa   GGGGCCATGAGAGAG CAGTACATGCGTGCT GGCCACGGCTTCCTG CTGGTGTTCGCCATT AATGACCGGCAGAGT TTCAACGAGGTGGGC    357

      361         375 376         390 391         405 406         420 421         435 436         450
R-Ras AAGCTCTTCACGCAG ATTCTGCGGGTCAAG GACCGCGACGACTTC CCCGTTGTGTTGGTC GGGAACAAGGCAGAT CTGGAGTCACAGCGC    450
5aa   AAGCTCTTCACGCAG ATTCTGCGGGTCAAG GACCGCGACGACTTC CCCGTTGTGTTGGTC GGGAACAAGGCAGAT CTGGAGTCACAGCGC    447

       451         465 466         480 481         495 496         510 511         525 526         540
R-Ras CAGGTCCCCCGATCA GAAGCCTCTGCCTTC GGCGCCTCCCACCAC GTGGCCTACTTTGAG GCCTCGGCCAAACTG CGTCTCAACGTGGAC    540
5aa   CAGGTCCCCCGATCA GAAGCCTCTGCCTTC GGCGCCTCCCACCAC GTGGCCTACTTTGAG GCCTCGGCCAAACTG CGTCTCAACGTGGAC    537

      541         555 556         570 571         585 586         600 601         615 616         630
R-Ras GAGGCTTTTGAGCAG CTGGTGCGGGCTGTC CGGAAATACCAGGAA CAAGAGCTCCCACCG AGCCCTCCCAGTGCC CCCAGGAAGAAGGGC    630
5aa   GAGGCTTTTGAGCAG CTGGTGCGGGCTGGT CGGAAACACAAGCTG CGGAAGCTGCCACCG AGCCCTCCCAGTGCC CCCAGGAAGAAGGGC    627

      631         645 646         660
R-Ras GGGGGCTGCCCCTGC GTCCTCCTGTAG
5aa   GGGGGCTGCCCCTGC GTCCTCCTGTAG
```

Appendix III

CHX1 sequence alignment

```
          1              15 16              30 31              45 46              60 61              75 76              90
R-Ras     ATGAGCAGCGGGGCG GCGTCCGGGACAGGG CGGGGGCGGCCCCGG GGCGGGGGACCTGGG CCCGGGGACCCCCCG CCCAGCGAGACACAC      90
chx1      --------------- --------------- --------------- --------------- ----------NTCCG CCTAGCGAGACACAC      20

          91            105 106            120 121            135 136            150 151            165 166            180
R-Ras     AAGCTGGTGGTCGTG GGCGGCGGCGGCGTG GGCAAGAGCGCGCTG ACCATCCAGTTCATC CAGTCCTACTTCGTG TCTGACTACGACCCC      180
chx1      AAGCTTGTG-TCGTG GGTGGTGTCGGCGTG GGCAAGAGCGCGCTG ACCATCCAGTTCATC CAGTCCTACTTCGTG TCTGACTACGACCCC      109

          181            195 196            210 211            225 226            240 241            255 256            270
R-Ras     ACTATTGAGGACTCC TACACGAAGATCTGC AGTGTGGATGGCATC CCAGCCCGGCTGGAC ATCCTGGACACCGCG GGCCAGGAAGAGTTC      270
chx1      ACTATTGAGGACTCC TACACGAAGATCTGC AGTGTGGATGGCATC CCAGCCCGGCTGGAC ATCCTGGACACCGCG GGCCAGGAAGAGTTC      199

          271            285 286            300 301            315 316            330 331            345 346            360
R-Ras     GGGGCCATGAGAGAG CAGTACATGCGTGCT GGCCACGGCTTCCTG CTGGTGTTCGCCATT AATGACCGGCAGAGT TTCAACGAGGTGGGC      360
chx1      GGGGCCATGAGAGAG CAGTACATGCGTGCT GGTCACGGCTTCCTG CTGGTGTTCGCCATT AATGACCGGCAGAGT TTCAACGAGGTGGGC      289

          361            375 376            390 391            405 406            420 421            435 436            450
R-Ras     AAGCTCTTCACGCAG ATTCTGCGGGTCAAG GACCGCGACGACTTC CCCGTTGTGTTGGTC GGGAACAAGGCAGAT CTGGAGTCACAGCGC      450
chx1      AAGCTCTTCACGCAG ATTCTGCGGGTCAAG GACCGCGACAACTTC CCCGTTGTGTTGGTC GGGAACAAGGCAGAT CTGGAGTCACAGCGC      379

          451            465 466            480 481            495 496            510 511            525 526            540
R-Ras     CAGGTCCCCCGATCA GAAGCCTCTGCCTTC GGCGCCTCCCACCAC GTGGCCTACTTTGAG GCCTCGGCCAAACTG CGTCTCAACGTGGAC      540
chx1      CAGGTCCCCCGATCA GAAGCCTCTGCCTTC GGCGCCTCCCACCAC GTGGCCTACTTTGAG GCCTCGGCCAAGACC CGGC---AGGGAGTG      466

          541            555 556            570 571            585 586            600 601            615 616            630
R-Ras     GAGGCTTTTGAGCAG CTGGTGCGGGCTGTC CGGAAATACCAGGAA CAAGAGCTCCCACCG AGCCCTCCCAGTGCC CCCAGGAAGAAGGGC      630
chx1      GAGGCCTTCTACACG TTGGTGCGTGAGATC CGGCAGCACCAGGAA CAAGAGCTCCCACCG AGCCCTCCCAGTGCC CCCAGGAAGAAGGGC      556

          631            645 646            660
R-Ras     GGGGGCTGCCCCTGC GTCC-TCCTGTAG
chx1      GGGGGCTGCCCCTGC GTCCCTCCTGTAG
```

CHX(3) sequence alignment

```
      1            15 16           30 31           45 46           60 61           75 76           90
r-ras ATGAGCAGCGGGGCG GCGTCCGGGACAGGG CGGGGGCGGCCCCGG GGCGGGGGACCTGGG CCCGGGGACCCCCCG CCCAGCGAGACACAC     90
chx3  --------------- --------------- --------------- --------------- --------CCTTCCG CNTAGCGAGACACAC     22

      91          105 106          120 121          135 136          150 151          165 166          180
r-ras AAGCTGGTGGTCGTG GGCGGCGGCGGCGTG GGCAAGAGCGCGCTG ACCATCCAGTTCATC CAGTCCTACTTCGTG TCTGACTACGACCCC     180
chx3  AAGCTTGTGGTCGTG GGTGGTGTCGGCGTG G-CAAGAGCGCGCTG ACCATCCAGTTCATC CAGTCCTACTTCGTG TCTGACTACGACCCC     111

      181         195 196          210 211          225 226          240 241          255 256          270
r-ras ACTATTGAGGACTCC TACACGAAGATCTGC AGTGTGGATGGCATC CCAGCCCGGCTGGAC ATCCTGGACACCGCG GGCCAGGAAGAGTTC     270
chx3  ACTATTGAGGACTCC TACACGAAGATCTGC AGTGTGGATGGCATC CCAGCCCGGCTGGAC ATCCTGGACACCGCG GGCCAGGAAGAGTTC     201

      271         285 286          300 301          315 316          330 331          345 346          360
r-ras GGGGCCATGAGAGAG CAGTACATGCGTGCT GGCCACGGCTTCCTG CTGGTGTTCGCCATT AATGACCGGCAGAGT TTCAACGAGGTGGGC     360
chx3  GGGGCCATGAGAGAG CAGTACATGCGTGCT GGTCACGGCTTCCTG CTGGTGTTCGCCATT AATGACCGGCAGAGT TTCAACGAGGTGGGC     291

      361         375 376          390 391          405 406          420 421          435 436          450
r-ras AAGCTCTTCACGCAG ATTCTGCGGGTCAAG GACCGCGACGACTTC CCCGTTGTGTTGGTC GGGAACAAGGCAGAT CTGGAGTCACAGCGC     450
chx3  AAGCTCTTCACGCAG ATTCTGCGGGTCAAG GACCGCGACAACTTC CCCGTTGTGTTGGTC GGGAACAAGGCAGAT CTGGAGTCACAGCGC     381

      451         465 466          480 481          495 496          510 511          525 526          540
r-ras CAGGTCCCCCGATCA GAAGCCTCTGCCTTC GGCGCCTCCCACCAC GTGGCCTACTTTGAG GCCTCGGCCAAACTG CGTCTCAACGTGGAC     540
chx3  CAGGTCCCCCGATCA GAAGCCTCTGCCTTC GGCGCCTCCCACCAC GTGGCCTACTTTGAG GCCTCGGCCAAGACC CGGC---AGGGAGTG     468

      541         555 556          570 571          585 586          600 601          615 616          630
r-ras GAGGCTTTTGAGCAG CTGGTGCGGGCTGTC CGGAAATACCAGGAA CAAGAGCTCCCACCG AGCCCTCCCAGTGCC CCCAGGAAGAAGGGC     630
chx3  GAGGCCTTCTACACG TTGGTGCGTGAGATC CGGCAGCACCAGGAA CAAGAGCTCCCACCG AGCCCTCCCAGTGCC CCCAGGAAGAAGGGC     558

      631         645 646          660
r-ras GGGGGCTGCCCCTGC GTCC-TCCTGTAG
chx3  GGGGGCTGCCCCTGC GTCCCTCCTGTAG
```

Chapter 6

Analysis of the effects of H-Ras and R-Ras on CHO cell morphology

6.1 Introduction

The main sequence of divergence between the Ras isoforms is the final 24 residues, the hypervariable region (Prior *et al.*, 2001). The hypervariable region contains the signalling sequences that cooperate in targeting Ras to the plasma membrane. An important consequence of the hypervariable divergence is that the plasma membrane anchors of H-Ras, N-Ras and K-Ras are all different. The membrane anchors consist of a methylesterified prenylcysteine group, common to all three Ras proteins, plus one or two palmitoylated cysteine residues in N- and H-Ras, or a polybasic domain of six contiguous lysines in K-Ras (Hancock *et al.*, 1989; Hancock *et al.*, 1990). Prior *et al.*, (2001) showed using GFP-labelled proteins, that the membrane anchor of H-Ras targets to the lipid rafts while the membrane anchor of K-Ras targets predominantly to non-raft plasma membrane. The distinct microlocalisation of the H- and K-Ras proteins has important potential consequences for downstream effector interactions and activation of downstream pathways. Chemically depleting plasma membrane cholesterol selectively abrogates H-Ras- but not K-Ras-mediated activation of Raf-1 (Roy *et al.*, 1999). Expression of a dominant-negative caveolin mutant, caveolin-DGV, which reduces cell surface cholesterol by interfering with intracellular cholesterol transport (Pol *et al.*, 2001), also block H-Ras but not K-Ras signalling pathways (Roy *et al.*, 1999). Therefore, the functional integrity of the H-Ras domain depends on cholesterol.

Like H-Ras, R-Ras contains a palmitoylation site on its membrane anchor, which suggests a similar microlocalisation target to H-Ras which may also be dependent on cholesterol. The targeted microlocalisation of R-Ras has not yet been identified, however, when activated R-Ras is found localised with focal adhesions (Furuhjelm and Peranen, 2003).

Early studies suggested that integrins were not localised to lipid rafts (Fra *et al.*, 1994), but recently integrins such as $\alpha v\beta 3$, LFA-1 and $\alpha 4\beta 1$ have been found to be raft associated (Green *et al.*, 1999; Leitinger and Hogg, 2001). Thorne *et al., (*2000) have also identified $\alpha 6\beta 1$ as being associated with lipid rafts, but a preferential association with the active form of the integrin has not been noted.

The aims of this chapter are to use confocal microscopy to try and elucidate the membrane microlocalisation of R-Ras and to determine the consequences of overexpressing H-Ras G12V and R-Ras G38V on CHO cell cytoskeletal structure. Since H-Ras and integrins have been found to be associated with lipid rafts, it was hoped that by manipulating the cholesterol content of the plasma membrane, it could be determined if the targeting of H-Ras and R-Ras to specific plasma membrane microdomains (such as lipid rafts) is necessary for their effects on integrin affinity modulation.

A further aim of this chapter is to produce CHO-K1 cell lines stably expressing H-Ras G12V, R-Ras G38V and the H-and R-Ras chimeras. It is hoped that by using the stable cell lines, further characterisation of H-Ras and R-Ras sequences may help to determine what role, if any, sequence variations may play in conferring their differing properties with respect to cellular structure and morphology.

6.2 Confocal microscopy to define cellular localisation of activated H-Ras and R-Ras

Immuno-fluorescence has provided an invaluable tool for investigating the specific targeted domains of labelled endogenous proteins and proteins introduced to the cell by means such as transfection. Confocal microscopy improves the quality of immuno-fluorescent images by removing any background staining that may interfere with the required image. It also allows the user to check for 'bleeding' from other fluorescent channels, which may result in a false image being produced. One of the main concerns with immuno-fluorescence is determining whether the staining observed is specific or non-specific. To counteract this problem users provide a negative control for staining, using only the secondary antibody. However, using a transient system in immuno-fluorescence means that you have an in-built negative control for staining. In the transient system, specific staining is very clear, as it is only those cells that have been successfully transfected that express the protein of interest. The in-house confocal facility was used, to study the cellular localisation of transiently over expressed H-Ras G12V and R-Ras G38V in $\alpha\beta$-py cells.

6.2.1 H-Ras G12V and R-Ras G38V both localise to the plasma membrane

The presence of the Ha-tag on H-Ras G12V and the Myc-tag on R-Ras G38V meant that immuno-fluorescence could be performed on transfected cells. Cells were seeded onto coverslips and allowed to adhere overnight prior to transfection. Following transfection, cells were incubated overnight in complete DMEM and then gently washed with PBS prior to staining.

Cells were stained using; anti-HA (Y-11) antibody, followed by Alexa 488-conjugated goat anti-rabbit IgG (green) to determine H-Ras G12V localisation; and anti-Myc (9E10) antibody, followed by Alexa 568-conjugated goat anti-mouse IgG (red) to determine R-Ras G38V localisation. H-Ras G12V, shown in green in Figure 6.1A, localises to the plasma membrane of the cell. R-Ras G38V, shown in red in Figure 6.1B, also localises to the plasma membrane. Cells expressing both proteins allowed a merged image to be produced to compare the localisation of H-Ras G12V and R-Ras G38V. Figure 6.1C shows the merged image of Figures 6.1A and 6.1B. ToPro3 was used to clearly define the nucleus of the cell, allowing us to better judge

the localisation of the proteins compared with the position of the nucleus. The yellow colour observed in Figure 6.1C suggests that H-Ras G12V and R-Ras G38V are both localised to similar areas of the plasma membrane of the transfected cell.

6.2.2 Actin cytoskeleton disrupted in H-Ras G12V transfected cells.

In order to determine the effects that H-Ras G12V and R-Ras G38V may have on the cytoskeleton of cells we made use of phalloidin, a fungal toxin that binds specifically to F-actin. Rhodamine-conjugated phalloidin provides a very convenient tool, in immuno-fluorescence, to study the distribution of F-actin in permeabilised cells. Figure 6.2A reveals the well-defined actin stress fibres (shown in red) of a representative cell transiently transfected with control vector. Cells are well spread (about 100μm diameter) and the stress fibres are distinctly organised across the whole body of the cell.

The staining of H-Ras G12V and R-Ras G38V in the merged images of this experiment is not very apparent. However, in order to clearly visualise stress fibres, cell images need to be taken from the lowest point of the cell i.e. where it has adhered to the coverslip. This can make visualising other proteins difficult as they can be more disperse on this lower plane. Therefore, as well as a final merged image, figures 6.2B and 6.2C provide a separate green and red channel to facilitate visualisation of the tagged proteins and actin cytoskeleton respectively.

In contrast to control cells, H-Ras G12V transfected cells show a much more rounded morphology (Figure 6.2B shows a representative cell). H-Ras G12V cells have a diameter less than half that of the control cell (approximately 40μm in diameter). Figure 6.2B shows positive staining for H-Ras G12V using the anti-HA (Y-11) antibody (shown in green). H-Ras G12V localises to the plasma membrane. Cells have punctate F-actin staining (shown in red) but no stress fibres are visible. Figure 6.2C shows a representative R-Ras G38V transfected cell. R-Ras G38V transfected cells maintain a well spread morphology (approximately 80μm in diameter) and have a much less disrupted cytoskeletal structure (shown in red) compared with H-Ras G12V transfected cells. Figure 6.2C shows positive staining for R-Ras G38V using the anti-Myc (9E10) antibody (shown in green). R-Ras G38V appears to localise to the plasma membrane.

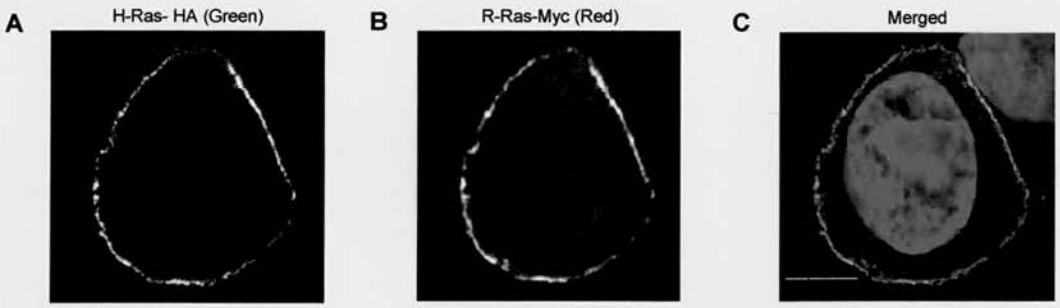

Figure 6.1 Cellular localisation of H-Ras G12V and R-Ras G38V.

Cells co-transfected with 1μg each of H-Ras G12V and R-Ras G38V. Cells were stained with antibodies against; (A) H-Ras G12V expression shown in green; (B) R-Ras G38V expression shown in red; (C) merged image of red and green channels, areas of yellow represent co-incident staining of H-Ras G12V and R-Ras G38V expression. ToPro3 used for nuclear definition (shown in blue). Greyscale images used for the individual green and red channel images to allow optimal visualisation of staining. Bars, 10μm.

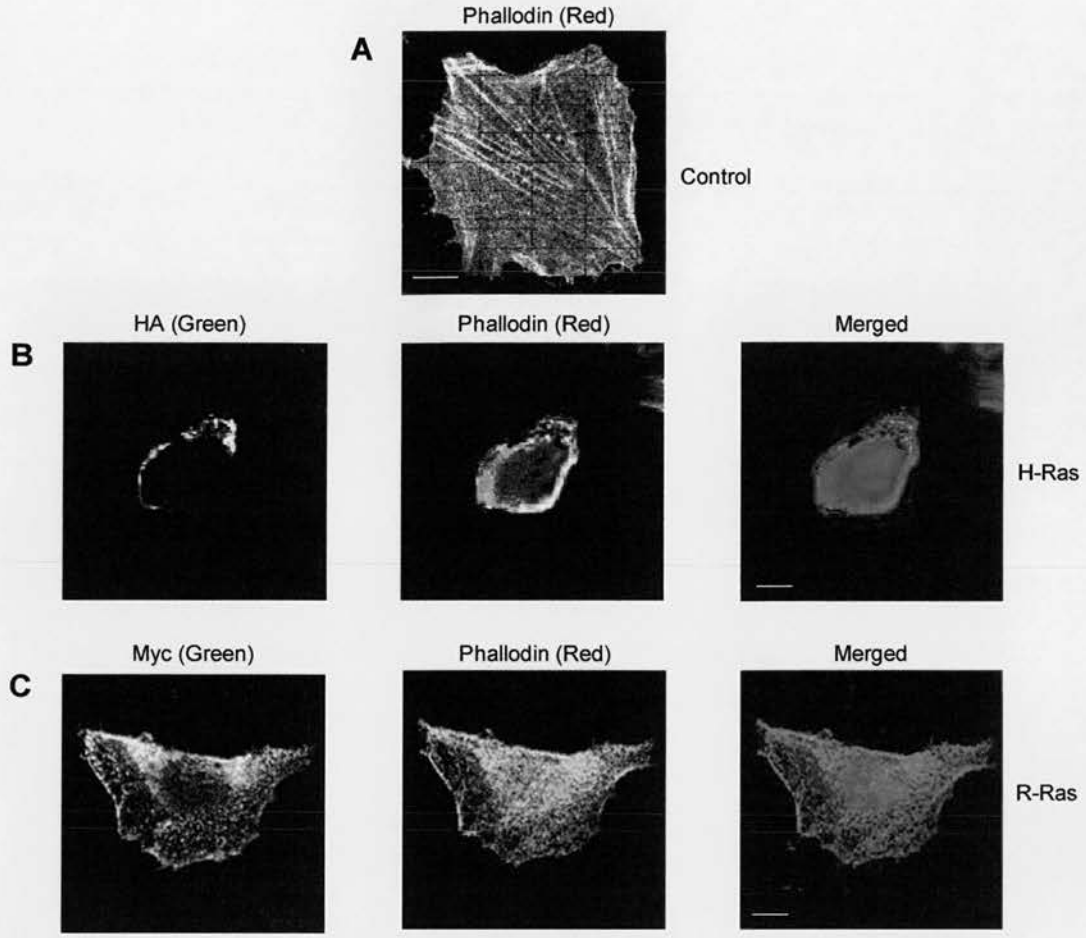

Figure 6.2 Actin cytoskeleton staining in H-Ras G12V and R-Ras G38V transfected cells.

Cells transfected with (A) control vector (1μg), (B) HA-tagged H-Ras G12V (1μg) and (C) Myc-tagged R-Ras G38V (1μg). Expression of H-Ras G12V and R-Ras G38V visualised using Alexa 488-conjugated antibodies, shown in green. Rhodamine-conjugated phallodin used to reveal the actin cytoskeleton, shown in red. In the merged images of red and green channels, areas of yellow represent co-incident staining of H-Ras G12V and R-Ras G38V expression with actin cytoskeleton. ToPro3 (shown in blue) used for nuclear definition. Greyscale images used for the individual green and red channel images to allow optimal visualisation of staining. Bars, 20μm.

6.2.3 H-Ras G12V transfection results in disorganisation of focal adhesions.

To determine whether the disruption of the actin cytoskeleton observed in H-Ras transfected cells reflected a reorganisation of the cellular adhesion sites, we analysed cells transiently transfected with H-Ras G12V and R-Ras G38V using a monoclonal anti-vinculin antibody. Vinculin is a 117kDa protein localised to focal adhesions. Figure 6.3A shows the typical pattern of vinculin staining of a control cell. The control cell has a diameter of about 50μm and vinculin staining can be observed around the periphery of the cell. In order to clearly visualise the transfected tagged proteins and vinculin staining, figures 6.3B and 6.3C provide a separate green and red channel image as well as a final merged image

The rounded morphology of the H-Ras G12V transfected cell (Figure 6.3B) was consistent with a disruption of focal adhesions, with reduced peripheral staining and a cell diameter of about 30μm. H-Ras G12V is shown to be localised to the plasma membrane of the cell, shown by the red staining. Figure 6.3C shows a cell that has been transfected with R-Ras G38V. In this experiment it was necessary to use the anti-Myc (A-14) rabbit polyclonal antibody for staining R-Ras G38V to prevent cross-reaction between the previously used anti-Myc (9E10) antibody and the anti-human vinculin antibody, which are both mouse monoclonals. The vinculin staining in this cell is very pronounced. There are an increased number of focal adhesions around the periphery, compared with the control cell, resulting in a well spread morphology (about 60μm diameter).

Interestingly, Figure 6.3C shows that areas of vinculin expression overlap with areas of R-Ras G38V expression, in particular around the plasma membrane. Although R-Ras G38V is shown to be predominately localised to the plasma membrane of the cell, shown by red staining, some internal staining can be seen in Figure 6.3C.

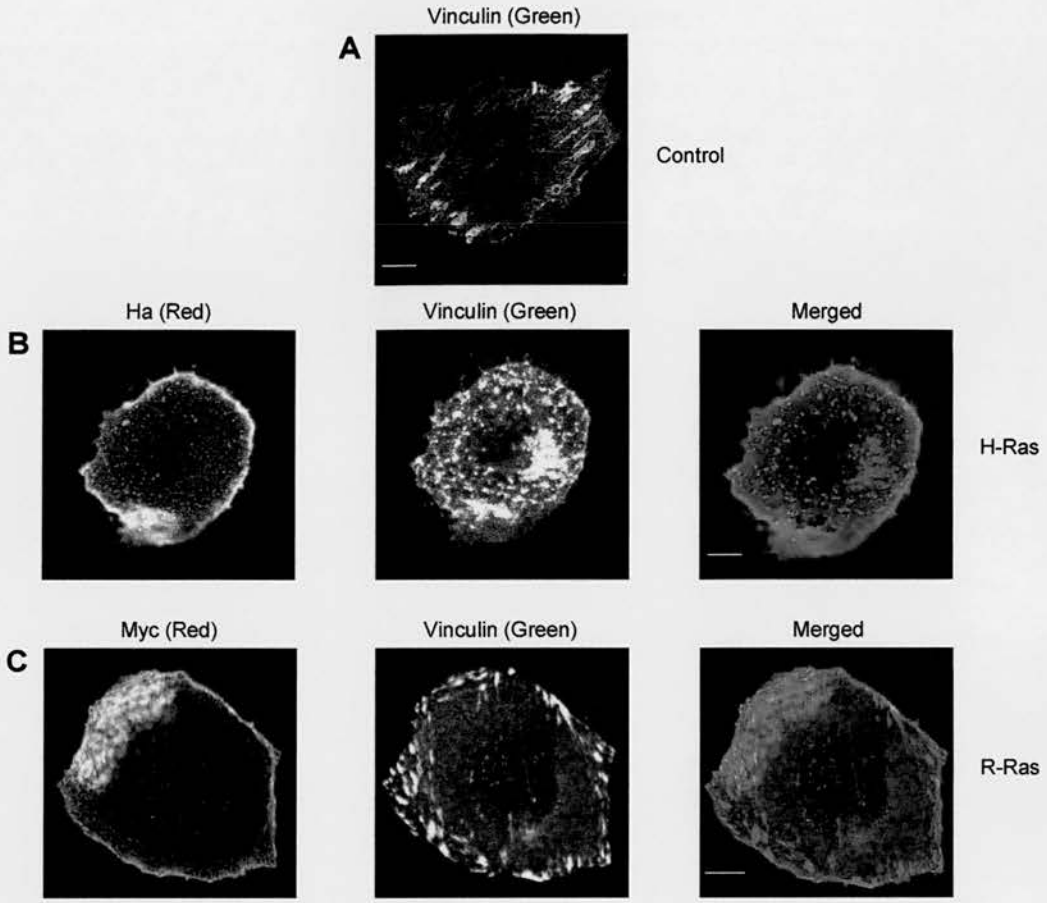

Figure 6.3 Vinculin staining of H-Ras G12V and R-Ras G38V transfected cells.

Cells transfected with (A) control vector (1μg), (B) HA-tagged H-Ras G12V (1μg) and (C) Myc-tagged R-Ras G38V (1μg). Expression of H-Ras G12V and R-Ras G38V visualised using Alexa 568-conjugated antibodies, shown in red. Cells were stained with an anti-vinculin antibody (green). In the merged images of red and green channels, areas of yellow represent co-incident staining of H-Ras G12V and R-Ras G38V expression with vinculin. Greyscale images used for the individual green and red channel images to allow optimal visualisation of staining. Bars, 10μm.

6.3 The effect of cellular localisation of H-Ras G12V and R-Ras G38V on integrin affinity modulation.

Earlier results revealed that both H-Ras G12V and R-Ras G38V localise to the plasma membrane. H-Ras G12V has previously been shown to target to lipid rafts within the plasma membrane (Prior *et al.*, 2001). Methyl-β-cyclodextrin (MβCD) can be used to deplete the cholesterol content and therefore disrupt lipid rafts within the plasma membrane (Hooper, 1999; Ostermeyer *et al.*, 1999). MβCD treatment of cells was used to check for its effects on integrin affinity modulation and to decide whether localisation to specific membrane domains is required for H-Ras G12V suppression of integrin affinity and R-Ras G38V reversal of H-Ras G12V integrin suppression.

6.3.1 Treatment of CHO-K1 cells with MβCD affects lipid raft distribution.

It is possible to detect lipid rafts within the plasma membrane by cross-linking the raft enriched glycosphinolipid GM1 through binding to a rhodamine-conjugated cholera toxin (Ctx) B subunit and patching with rabbit anti-Ctx antibody (Janes *et al.*, 1999). The rhodamine-conjugated Ctx-B allows visualisation of the rafts in immuno-fluorescence studies (Janes *et al.*, 1999).

Preliminary experiments carried out on CHO-K1 cells revealed a problem in detecting the lipid rafts using Ctx-B. Upon investigation it was discovered that unlike wild-type CHO cells, CHO-K1 cells do not synthesise the complex ganglioside, GM1 (Rusnati *et al.*, 1999). It was possible to overcome this by incorporation of exogenous GM1 into the cell membranes (Rusnati *et al.*, 1999). A considerable incorporation of GM1 (approximately 3-fold the amount of endogenous GM3) has been observed when CHO cells were incubated with the exogenous GM1 lipid (Crespo *et al.*, 2002). The exogenous addition of GM1 has been shown to displace GPI-anchored proteins from lipid rafts in living cells (Simons *et al.*, 1999). Exogenously added gangliosides can affect biological systems, leading to increased cell adhesiveness, inhibited cell growth and they can promote cell differentiation (Hakomori and Igarashi, 1995). However, since we are only using GM1 to help identify lipid rafts, the exogenous application of GM1 to CHO-K1 cells was considered a reasonable alternative to obtaining wild-type CHO cells.

Cells were incubated for 96 hours in fresh DMEM containing 0.4% FCS with 100μM GM1 before being used for further investigation (Rusnati *et al.*, 2002). The cell fixation method for immuno-fluorescence utilised elsewhere in this thesis uses 3% paraformaldyhyde. As this may result in the permeabilisation of the cell membrane, which may in turn affect the positioning of GM1, it was decided to observe the lipid raft distribution in live cells.

Employing the method used by Janes *et al.,* (1999), lipid rafts were visualised using fluorescence microscopy. Figure 6.4A shows the homologous distribution of GM1 gangliosides in untreated cells, revealed with rhodamine-conjugated Ctx-B. Cells have a diameter of approximately 50μm. Following treatment with a rabbit anti-Ctx antibody to induce Ctx-B cross-linking, staining became concentrated to distinct patches within the membrane (Figure 6.4B). These distinct patches are caused by the clustering of the GM1 raft marker, caused by the cross-linking of the anti-Ctx antibody. Treatment of cells with the anti-Ctx antibody had no effect on the cell morphology, diameter between 50 and 60μm, compared with the untreated cell.

To assess the effect of MβCD on lipid rafts, cells were incubated with 1% (10mM) MβCD (found to be the optimal concentration) for 1 hour at 37°C prior to staining with rhodamine-conjugated Ctx-B. Figure 6.4C shows cells which are much less spread than either the untreated (6.4A) or cross-linked (6.4B) cells. The cells in 6.4C have diameters of at least half of those cells shown in 6.4A and 6.4B. The Ctx-B staining is less evenly distributed than seen with untreated cells, forming patches within the membrane similar to that observed following antibody cross-linking of the anti-Ctx antibody.

Therefore, these preliminary experiments demonstrated that MβCD disrupts the normal lipid raft distribution of CHO-K1 cells.

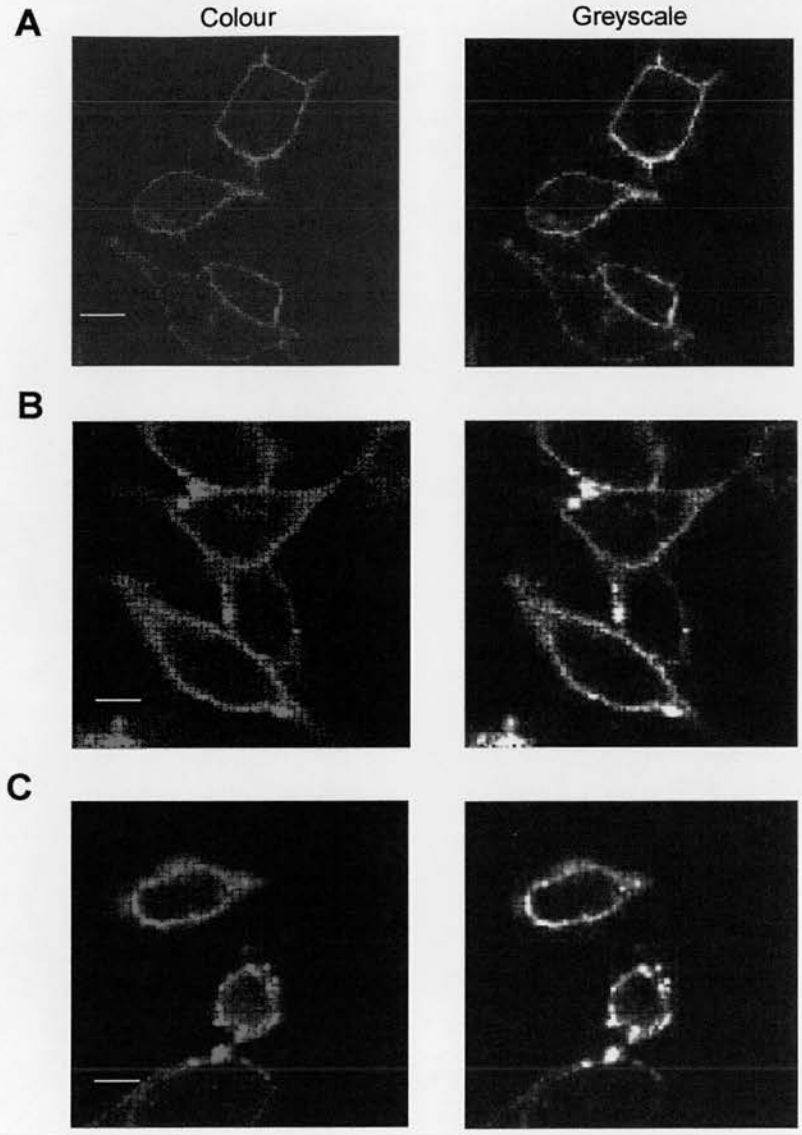

Figure 6.4 Treatment of cells with MβCD affects lipid raft distribution.

CHO-K1 cells were incubated with exogenous GM-1 for 96 hours at 37°C. Immuno-fluorescence performed on live cells. (A) Untreated cells stained with Rhodamine-conjugated Ctx-B. (B) Untreated cells stained with Rhodamine -conjugated Ctx-B, then cross-linked with rabbit anti-Ctx antibody. (C) Cells treated with 1% MβCD for 1 hour at 37°C followed by staining with Rhodamine-conjugated Ctx-B. Greyscale images provided to allow optimal visualisation of staining. Bars, 20μm.

6.3.2 MβCD treatment has no significant effect on integrin affinity modulation by either H-Ras G12V or R-Ras G38V.

It has been demonstrated earlier that treatment of cells with MβCD results in the disruption of lipid rafts distribution in CHO-K1 cells. To test whether integrin affinity modulation by H-Ras G12V or R-Ras G38V requires intact lipid rafts, αβ-py cells were treated with MβCD. To control for non-specific effects of MβCD treatment on cells, cells were treated with 5mM MβCD-cholesterol conjugates (inclusion complexes) for 1 hour at 37°C, following treatment with 1% MβCD. The addition of inclusion complexes provides the cell with cholesterol in the form of MβCD-cholesterol conjugates, which facilitate the incorporation of exogenous cholesterol into membranes (Klein *et al.*, 1995), which reverse the effects of MβCD on lipid rafts. For these experiments, cells were transfected with control vector, H-Ras G12V and R-Ras G38V ± H-Ras G12V and PAC1 binding was assessed.

MβCD treatment of cells had no effect on H-Ras G12V- or R-Ras G38V- mediated changes in integrin affinity. Figure 6.5 shows that levels of integrin affinity of control vector or H-Ras G12V transfected cells did not undergo any significant change during any of the treatments.

However, addition of inclusion complexes significantly attenuated R-Ras G38V activation, and blocked R-Ras G38V reversal of H-Ras G12V-mediated integrin suppression. The levels of integrin affinity in cells transfected with R-Ras G38V alone were significantly reduced to the baseline activity observed with control vector transfection, when compared with untreated and MβCD treated cells. Also, addition of inclusion complexes significantly diminished the ability of R-Ras G38V to reverse H-Ras G12V suppression ($P<0.001$) when compared with untreated and MβCD treated cells. The inclusion complexes did not mediate a toxic effect on R-Ras G38V transfected cells since they did not affect H-Ras G12V or control transfected cells.

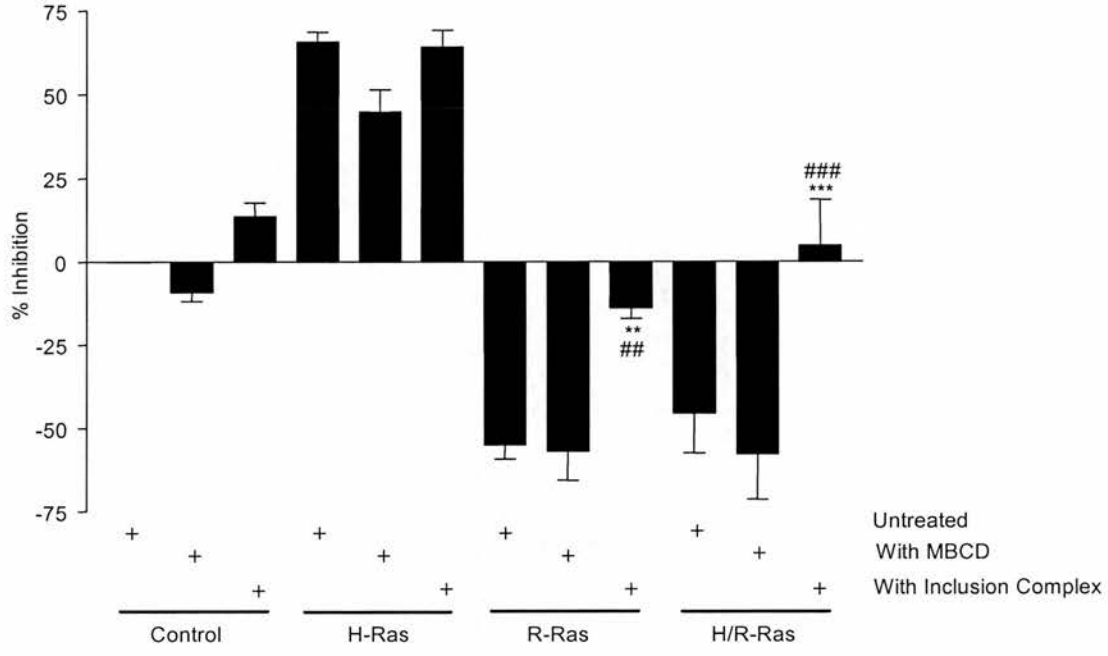

Figure 6.5 Effects of MβCD treatment on integrin affinity modulation by H-Ras G12V and R-Ras G38V.

Flow cytometry was performed on αβ-py cells transfected with control vector (1μg), H-Ras G12V (1μg) or R-Ras G38V ± H-Ras G12V (1μg). In each transfection, total DNA content was standardised to 2μg using control vector. Integrin affinity modulation was determined under three conditions: untreated cells; cells treated with 1% MβCD for 1 hour at 37°C; and cells incubated with inclusion complexes for 1 hour at 37°C, following treatment with 1% MβCD for 1 hour at 37°C. The results shown are the mean ± SEM of 4 independent experiments. Statistical analysis was performed by one-way ANOVA test, within each test DNA sample asterisks represent $P<0.01$ (**) and $P<0.001$ (***) compared with untreated cells, while hashes represent $P<0.01$ (##) and $P<0.001$ (###) compared with MβCD treated cells.

6.3.3 MβCD treatment affects the localisation of wild-type H-Ras but not H-Ras G12V

Using fluorescence confocal microscopy, the effect on cellular localisation of H-Ras by MβCD treatment was examined in CHO-K1 cells transiently expressing pEGFP control vector, GFP-H-Ras (G12V) and GFP-H-Ras (WT). Since the permeabilisation of the cell membrane may affect the positioning of lipid rafts, the localisations of the GFP-tagged proteins were observed in live cells. For each of the above constructs, Figure 6.6 shows images with and without a phase contrast overlay of an untreated control cells and MβCD treated cells. Protein localisation was easily determined by GFP expression (green).

Transfection with pEFGP control vector results in an even distribution of protein throughout the cell and these cells maintain a well spread morphology (about 40μm diameter). MβCD treatment of pEGFP transfected cells has little effect on the distribution of the protein or on the morphology of the cell compared with the untreated control.

GFP-H-Ras (WT) was found to be localised to the plasma membrane, with some perinuclear localisation possibly within the golgi apparatus. GFP-H-Ras (WT) expressing cells maintain morphology similar to that observed with the pEGFP positive cells, with a diameter of about 40μm. MβCD treatment of GFP-H-Ras (WT) transfected cells resulted in a striking change in the compartmentalisation of GFP-H-Ras (WT), which localised mainly to intracellular compartments rather than the intact plasma membrane. MβCD treated cells maintain a spread morphology similar to the pEGFP transfected cells.

GFP-H-Ras (G12V) was found to be localised to the plasma membrane, with some perinuclear localisation possibly within the golgi apparatus. GFP-H-Ras (G12V) expressing cells adopt a rounded morphology, with diameters of around 20μm. MβCD treatment of GFP-H-Ras (G12V) transfected cells has little effect on the distribution of the protein or on the morphology of the cell compared with the untreated control.

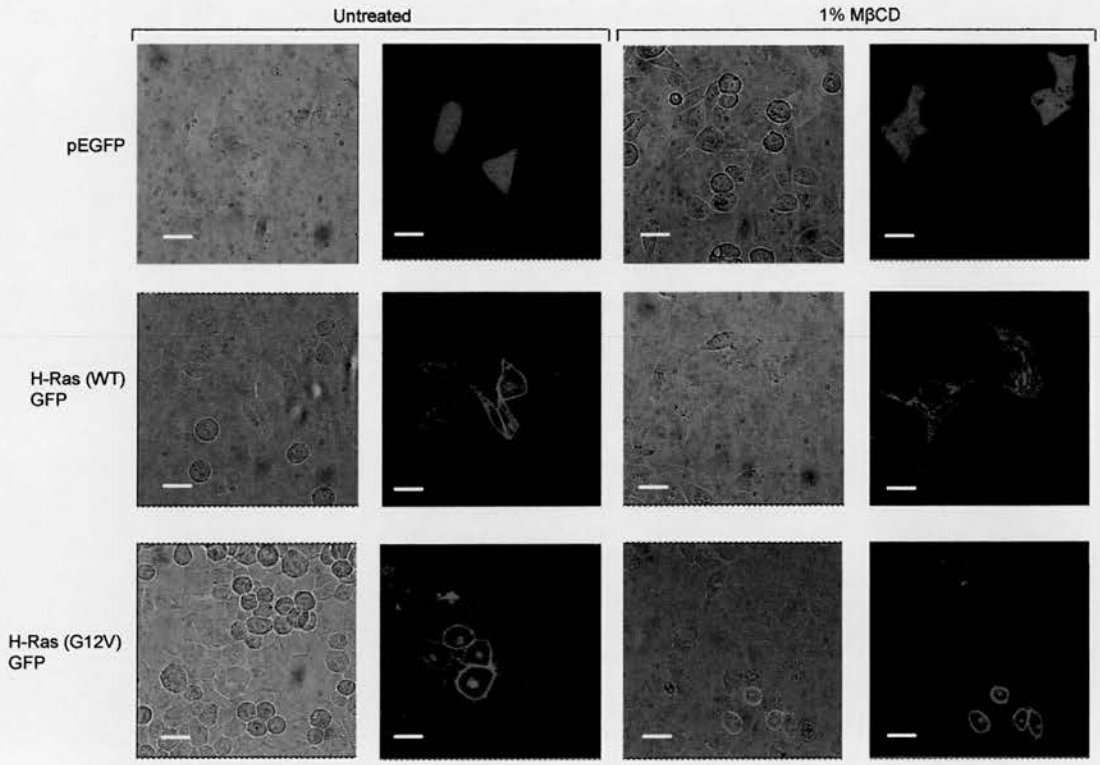

Figure 6.6 Using GFP-labelled proteins to determine if MβCD treatment affects the localisation of H-Ras WT and H-Ras G12V

Confocal microscopy was performed on live cells transfected with pEGFP control vector (1μg), pEGFP-H-Ras WT (1μg) or pEGFP-H-Ras G12V (1μg). Protein localisation, demonstrated by GFP expression, was examined in untreated cells and in cells treated with 1% MβCD for 1 hour at 37°C. Images shown with a phase-contrast overlay for cellular definition and without a phase-contrast overlay to provide a better contrast for observing GFP expression and localisation. Bars, 20μm.

6.4 Production of stable lines expressing chimeric DNA.

Stable lines expressing the H-and R-Ras chimeras, full-length H-Ras G12V and R-Ras G38V were generated to facilitate further structural and functional characterisation. All constructs were cloned into pCDNA3.1(+) encoding the neomycin resistance gene, allowing for G418 selection in CHO-K1 cells. Stable lines were screened by either intracellular FACS analysis or western blotting.

6.4.1 H-Ras G12V fails to express in stable lines.

The N-terminal HA-tag on H-Ras G12V enabled protein expression to be measured by FACS analysis. Intracellular staining was carried out on cells using the anti-Ha (Y-11) antibody followed by a secondary FITC-conjugated anti-rabbit IgG. The histogram shown in Figure 6.7A shows a negative control of Ha-binding, using only the secondary antibody, in the FL-1 channel. Figure 6.7B shows a representative histogram of the negligible levels of positive Ha-antibody staining observed with all the H-Ras G12V clones. FACS analysis on all the remaining H-Ras G12V clones resulted in less than 3% of the population being gated positive for HA-antibody staining. To test the possibility that the poor levels of HA antibody staining was due to a problem with the intracellular FACS analysis, expression was tested by western analysis. Figure 6.7C shows a representative blot indicating that no clone showed positive for H-Ras G12V expression.

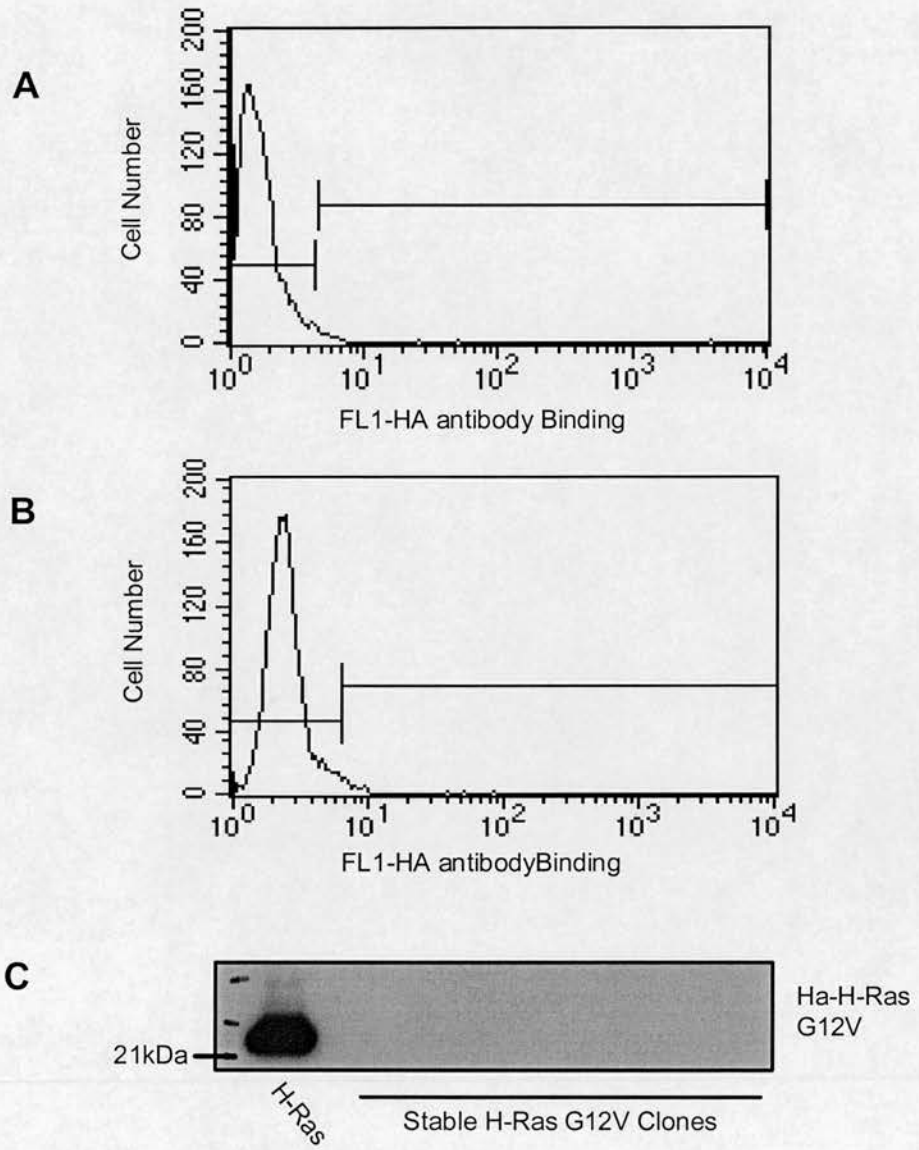

Figure 6.7 Analysis of H-Ras G12V stable lines.

Intracellular FACS staining of H-Ras G12V stable clones was performed using anti-HA (Y-11) antibody. Flow cytometry was performed to determine H-Ras expression levels. (A) Negative control for H-Ras expression using secondary anti-rabbit IgG-FITC staining only. (B) Representative histogram showing HA-staining of an H-Ras G12V stable clone. (C) Cell lysates from stable lines were tested by western analysis with the anti-HA antibody.

6.4.2 Analysis of stable lines expressing R-Ras G38V or H-and R-Ras chimeras.

The N-terminal Myc-tag on R-Ras G38V enabled protein expression in the stable lines to be tested by FACS analysis. Intracellular staining was carried out on cells using the anti-Myc (9E10) antibody followed by a secondary FITC-conjugated anti-mouse IgG. FACS analysis was carried out on a negative control for Myc-binding using only the secondary antibody (see Figure 6.8A). Figure 6.8B shows a representative histogram of the levels of positive Myc antibody staining observed with an R-Ras G38V clone. FACS analysis on all the potential R-Ras G38V clones enabled positive clones to be identified, with the percentage of the populations showing positive for Myc-antibody binding ranging from 10%-98% (data not shown).

Using the N-terminal FLAG-tag on the H-and R-Ras chimeras, stable protein expression was measured by FACS analysis. Intracellular staining was carried out on cells using the anti-FLAG monoclonal antibody followed by a secondary FITC-conjugated anti-mouse IgG. Figures 6.9A and B show histograms representing negative and positive staining for FLAG-binding respectively. As with R-Ras G38V clones, levels of stable protein expression of the H-and R-Ras chimeras varied greatly (data not shown).

For subsequent analyses of the stable lines, clones with comparable levels of chimera expression were selected. Figure 6.10 shows the levels of stable protein expression of the clones selected, ranging between 35-55%.

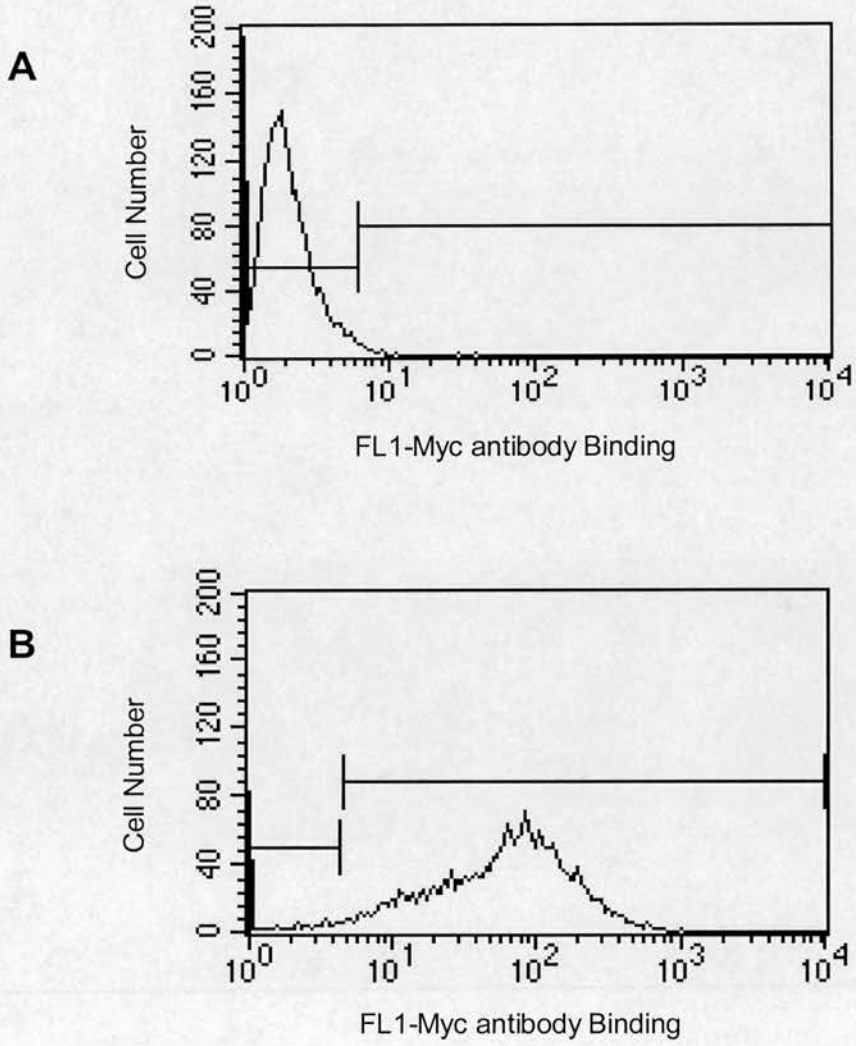

Figure 6.8 Analysis of R-Ras G38V expressing stable lines.

Intracellular staining of R-Ras G38V stable clones was performed using the anti-Myc antibody and the secondary anti-mouse IgG-FITC. Flow cytometry was performed to determine R-Ras expression levels. (A) Negative control for R-Ras expression, determined using secondary anti-rabbit IgG-FITC staining only. (B) Histogram showing R-Ras G38V expression in a stable clone.

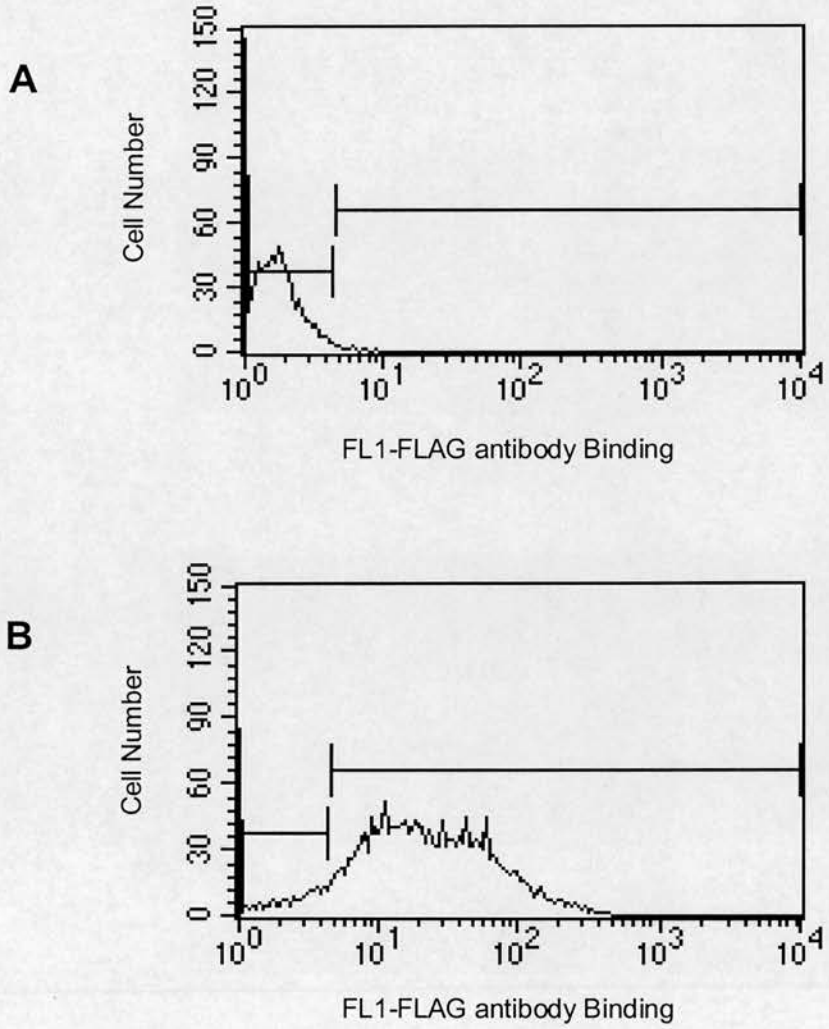

Figure 6.9 Intracellular staining of FLAG-tagged proteins.

Intracellular staining of FLAG-tagged proteins was performed using anti-FLAG monoclonal antibody and the secondary anti-mouse IgG-FITC. Flow cytometry was performed on potential clones. (A) Negative control for FLAG expression, determined by secondary anti-mouse IgG-FITC staining only. (B) Histogram showing FLAG-tagged chimera expression in stable lines.

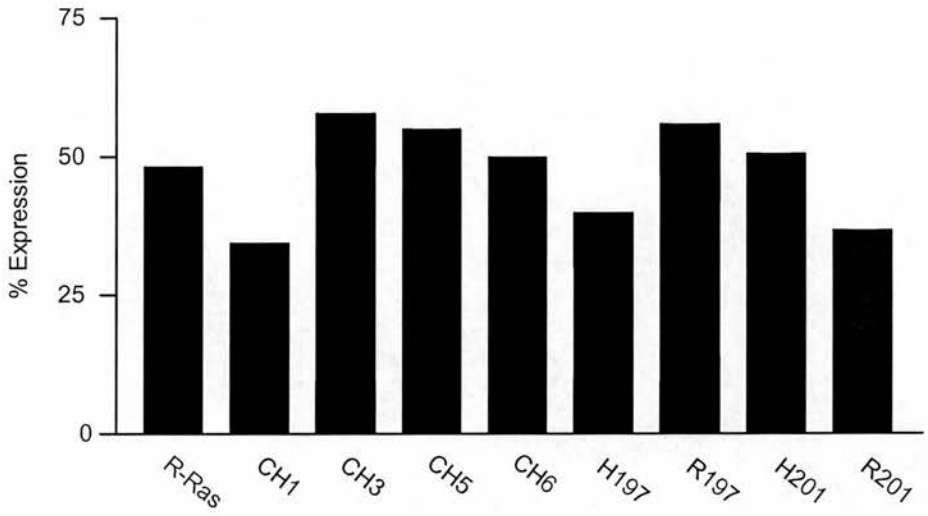

Figure 6.10 Level of protein expression in stable clones.

Intracellular FACS analysis was used to determine protein expression levels of H- and R-Ras chimeras. Data represent the range of protein expression levels for the chimeras.

6.5 Comparing structure and morphology of stable lines

Previous results have shown that transient expression of H-Ras G12V or R-Ras G38V bestow very different structural properties on to cells. The stable H-and R-Ras chimera lines were used to determine the role, if any, the sequence variations of H-Ras G12V and R-Ras G38V may play on their differing properties with respect to cellular structure. Structural and morphological variability will be assessed using immuno-fluorescence and electron microscopy techniques. For each of the stable lines, chimeric protein expression was checked for using immuno-fluorescent staining of the FLAG-tagged proteins. However, in order to clearly visualise stress fibres, cell images need to be taken from the lowest point of the cell i.e. where it has adhered to the coverslip. This can make visualising other proteins difficult as they can be more dispersed on this lower plane.

6.5.1 Cytoskeletal structural variations between H-Ras G12V N-terminal chimeric stable lines

The chimeras CH3, CH6, H197 and H201 all possess, to varying degrees, the N-terminal sequences of H-Ras G12V. Using immuno-fluorescence the structural variance between the stable lines was investigated. Figure 6.11 shows the distribution of F-actin, using rhodamine-conjugated phalloidin (shown in red), of these stable lines. Stable protein expression was confirmed using an anti-FLAG monoclonal antibody followed by a secondary FITC-conjugated anti-mouse IgG antibody (shown in green).

The cell lines stably expressing CH3 and CH6 are well spread (more than 50% of the cells were about 100μm diameter) and have stress fibres organised across the whole body of the cell see Figures 6.11A and B respectively. Protein expression is mainly localised to points around the membrane area of the cells. The H197 and H201 stable lines have markedly different cell morphologies compared with the CH3 and CH6 stable lines. Cells stably expressing H197 and H201, shown by Figures 6.11C and D respectively, are much rounder and have less than half the diameter of CH3 and CH6 stable lines. H197 and H201 cells contain stress fibres and stable protein expression is localised to the membrane.

6.5.2 Cytoskeletal structural variations between R-Ras G38V N-terminal chimeric stable lines

The chimeras CH1, CH5, R197 and R201 all possess, to varying degrees, the N-terminal sequences of R-Ras G38V. As with H-Ras G12V N-terminal chimeric stable lines, the structural variance between these stable lines was investigated. Figure 6.12 shows the distribution of F-actin, using rhodamine-conjugated phalloidin (shown in red). Protein expression was confirmed using an anti-FLAG monoclonal antibody followed by a secondary FITC-conjugated anti-mouse IgG antibody (shown in green).

The CH1 stable cells were well spread (more than 50% of the cells were about 80μm diameter) and had stress fibres organised across the whole body of the cell. Protein expression is localised to the membrane (Figure 6.12A). Figure 6.12B reveals that CH5 stable cells adopt a well spread morphology, like the CH1 stable cells. The cell edges are not clearly defined by F-actin staining in the CH5 stable cells, with the only visible stress fibres arranged internally. Protein expression is localised to the outermost regions of the cells. R197 stable cells are not as well spread as CH1 and CH5 stable lines (less than 60μm in diameter), with stress fibres seen across the length of the cells (Figure 6.12C). Protein expression is localised to the membrane areas of the cells. R201 stable cells (Figure 6.12D), have very well defined stress fibre structures within the cells, stable protein expression can be seen in some internal structures as well as at the membrane.

In brief, the CH3, CH6 and R201 stable lines have a well spread morphology with clearly defined stress fibres organised across the body of the cell. These morphologies are similar to those observed with R-Ras G38V transiently transfected cells (Figure 6.2). The CH1, H197 and H201 stable lines have a less spread, more rounded morphology with a more peripheral pattern of actin staining. These morphologies are similar to those observed with H-Ras G12V transiently transfected cells (Figure 6.2). Results suggest that R-Ras G38V sequences 175 to 203 (residues between CH6 and R201) are required for a well defined actin skeleton, while H-Ras G12V sequences 60 to 199 (residues between CH1 and H197) are required for an H-Ras-like effect on the actin skeleton. See section 6.2.2 for H-Ras and R-Ras effects on the actin cytoskeleton.

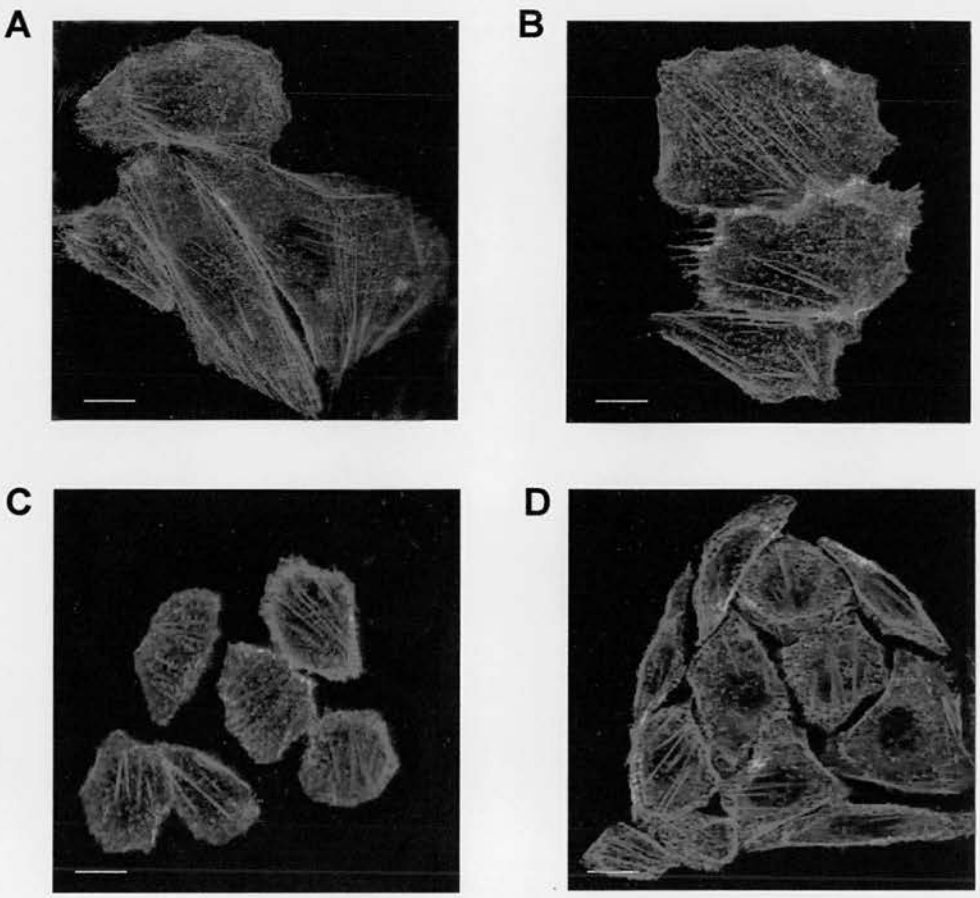

Figure 6.11 Actin cytoskeleton staining of H-Ras G12V N-terminal stable lines.

H-Ras G12V N-Terminal stable lines were stained using anti-FLAG monoclonal antibody followed by the secondary anti-mouse IgG-FITC. F-actin cytoskeleton was stained with rhodamine-conjugated phalloidin for 20mins at room temperature. The panels show the following stable lines: (A) chimera CH3; (B) chimera CH6; (C) chimera H197 and (D) chimera H201. Bars, 20μm.

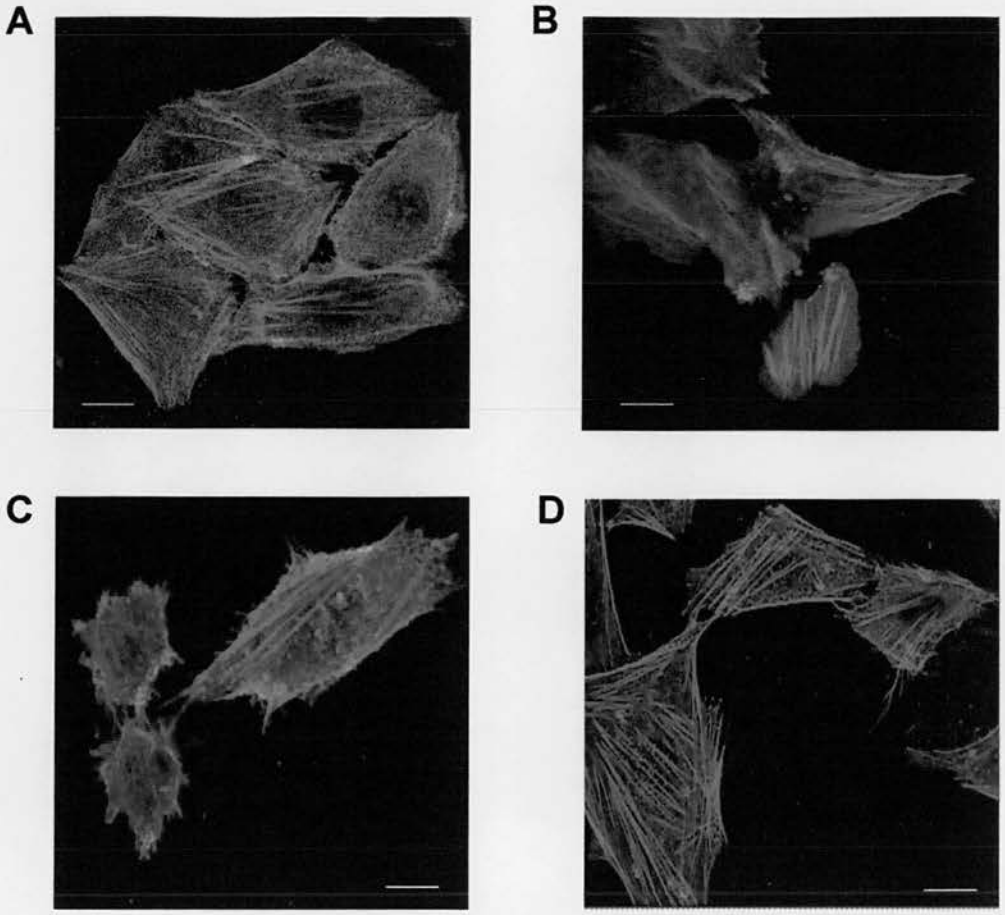

Figure 6.12 Actin cytoskeleton staining of R-Ras G38V N-terminal stable lines.

R-Ras G38V N-Terminal stable lines cells were stained using anti-FLAG monoclonal antibody followed by the secondary anti-mouse IgG-FITC. F-actin cytoskeleton was stained with rhodamine-conjugated phalloidin for 20mins at room temperature. The panels show the following stable lines: (A) chimera CH1; (B) chimera CH5; (C) chimera R197 and (D) chimera R201. Bars, 20μm.

6.5.3 Morphological analysis of R-Ras G38V stable lines.

Scanned electron microscope images of control (pCDNA3.1(+)) and R-Ras G38V stable lines (Figure 6.13) were taken for high resolution cell morphology. Control stable cells (Figures 6.13A and B) are well spread (diameters between 20 and 30μm), with well defined, smooth cell edges and there are the occasional blebs visible on the cell surface (circled areas). R-Ras G38V stable cells (Figures 6.13C and D) are much flatter compared with control cells. They have diameters reaching 40μm, with well defined, smooth cell edges and fewer, smaller surface blebs (circled area) than observed with control stable cells.

6.5.4 Morphological variations between H-Ras G12V N-terminal stable lines.

The chimeric stable lines expressing CH3, CH6, H197 and H201 all possess N-terminal sequences of H-Ras G12V. Images in Figure 6.14 show representative micrographs from each of the individual stable cell lines. CH3 stable cells (Figures 6.14A and B) and CH6 stable cells (Figures 6.14C and D) have very similar morphologies to control cells. In each case the cells are well spread (diameters are about 30μm); they have well-defined, smooth edges and exhibit some membrane blebs over the cell surfaces (circled areas). The H197 (Figures 6.14E and F) and H201 (Figures 6.14G and H) stable cells have strikingly different morphologies compared to control cells. Cells are very rounded up, with diameters barely exceeding 10μm. The cell edges are very ruffled, with a number of protrusions (highlighted with arrows). Cells have larger blebs over their surfaces (circled areas). The ruffled cell edges and the increased number and size of surface blebs are indicative of a transformed phenotype.

6.5.5 Morphological variations between R-Ras G38V N-terminal stable lines.

The chimeric stable lines expressing CH1, CH5, R197 and R201 all possess N-terminal sequences of R-Ras G38V. Images in Figure 6.15 show representative micrographs from each of the individual stable cell lines. CH1 stable cells (Figures 6.15A and B) have diameters of about 20μm. Compared with control cells, CH1 expressing cells have fairly ruffled edges (arrows) and a few large membrane blebs (circled areas). The CH5 stable cells (Figures 6.15C and D) have diameters of about

30μm. They have a very well spread morphology with fairly smooth cell edges and membrane blebs are concentrated around the nuclear area (circled areas). R197 stable cells (Figures 6.15E and F) diameters of about 15μm. These cells are much more rounded than the control cells as well as CH1 and CH5 expressing cells. The surfaces of the R197 stable cells are covered in fairly large membrane blebs (circled areas). Cells have ruffled edges (arrows). The R201 stable cells (Figures 6.15G and H) are very well spread, with diameters reaching 40μm (similar to R-Ras G38V stable lines). Cells have very smooth edges and minimal membrane blebbing.

In brief, the CH3, CH6 and R201 stable lines have flattened cell morphologies similar to control cells and cells stably expressing R-Ras G38V. Cells expressing R201 have the most R-Ras G38V-like cell shape. All these cell lines have smooth, well defined cell edges and minor cell surface blebbing. Results suggest that R-Ras G38V sequences 175 to 203 (residues between CH6 and R201) influence the R-Ras G38V cell morphology.

The CH1, H197 and H201 stable lines have a less spread, more rounded morphology. These stable cell lines have ruffled cell edges and quite large cell surface blebs, indicative of a transformed phenotype. H-Ras G12V sequences 60 to 199 (residues between CH1 and H197) are required for a transformed cell morphology.

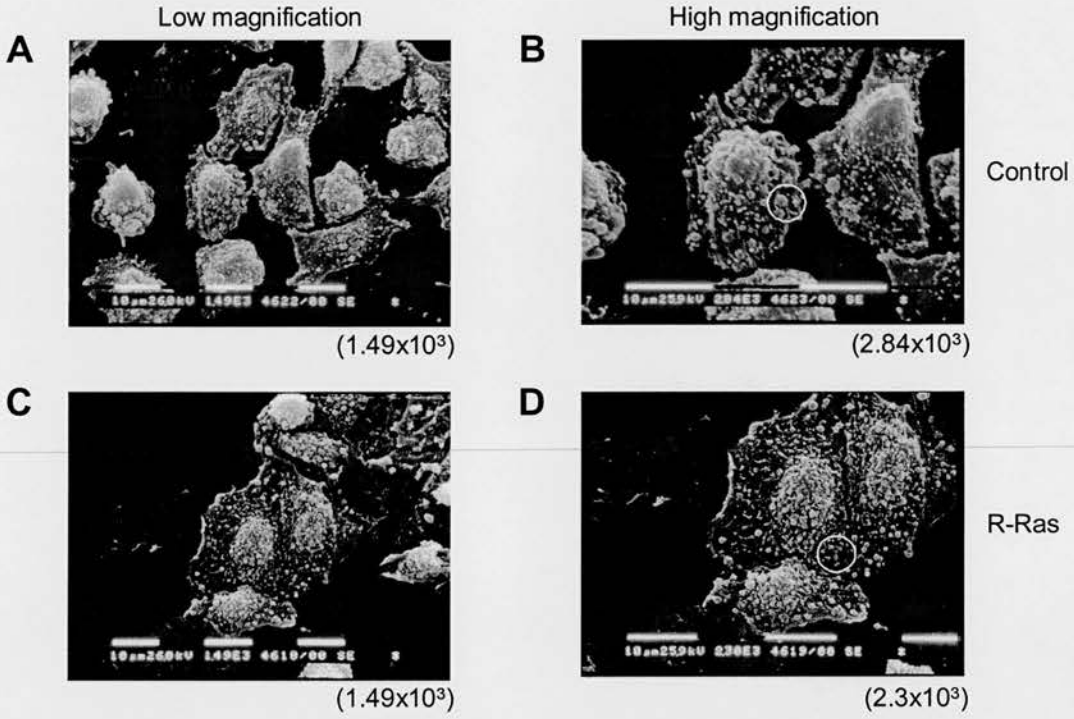

Figure 6.13 Scanning electron micrographs of control and R-Ras G38V stable lines.

Scanning electron micrographs were taken of control vector (panels A and B) and R-Ras G38V (panels C and D) expressing stable lines. Magnifications of each micrograph shown in the lower right hand corner of each panel. Circled areas in higher magnification panels highlight areas of membrane blebbing.
Bars represent 10μm.

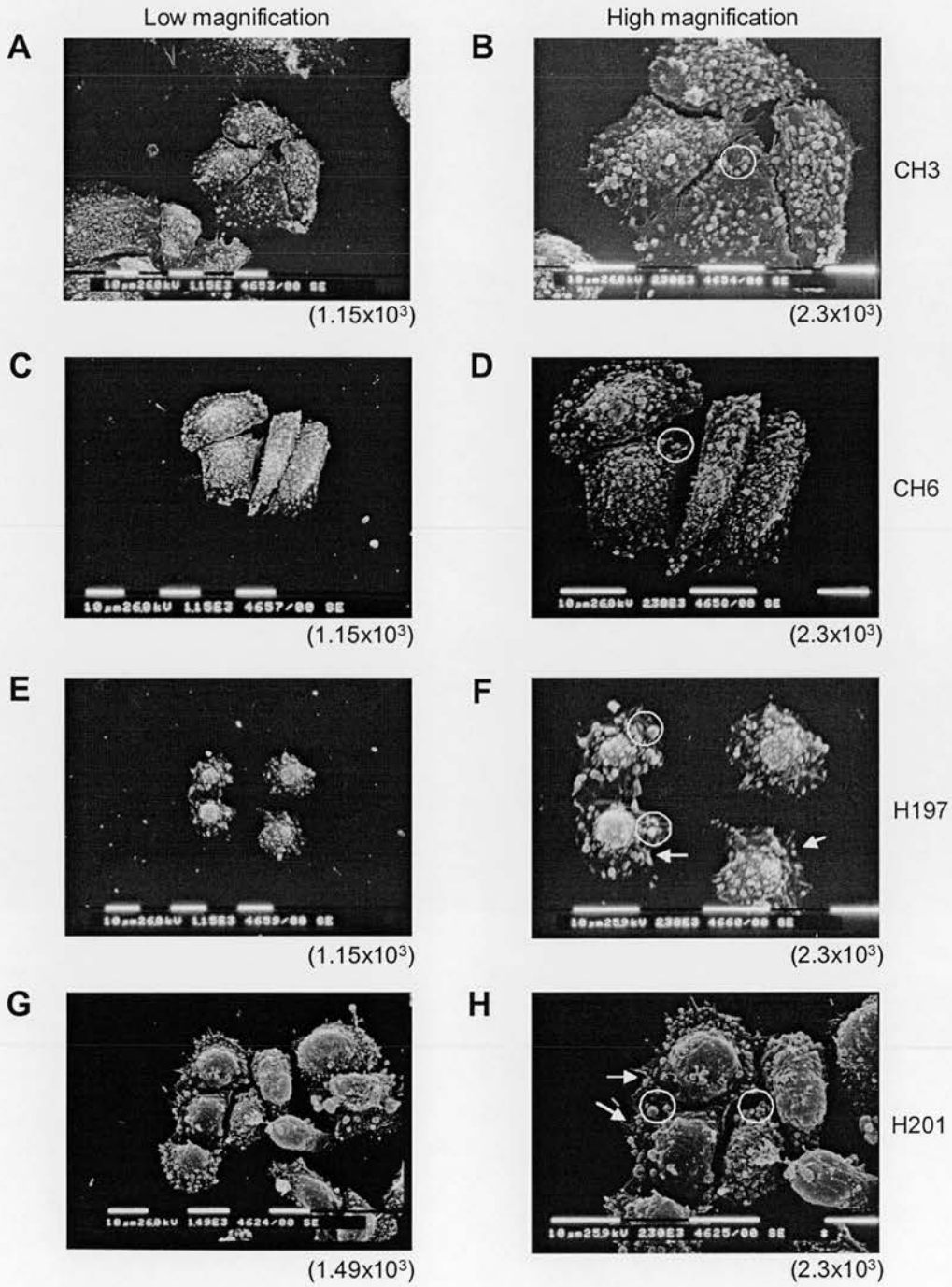

Figure 6.14 Scanning electron micrographs of H-Ras G12V N-Terminal stable lines.

Scanning electron micrographs were taken of CH3 (panels A and B), CH6 (panels C and D), H197 (panels E and F) and H201 (panels G and H) expressing stable lines. Magnifications of each micrograph shown in the lower right hand corner of each panel. Circled areas in higher magnification panels highlight areas of membrane blebbing. Arrows in higher magnification panels indicated areas of membrane ruffling. Bars represent 10μm.

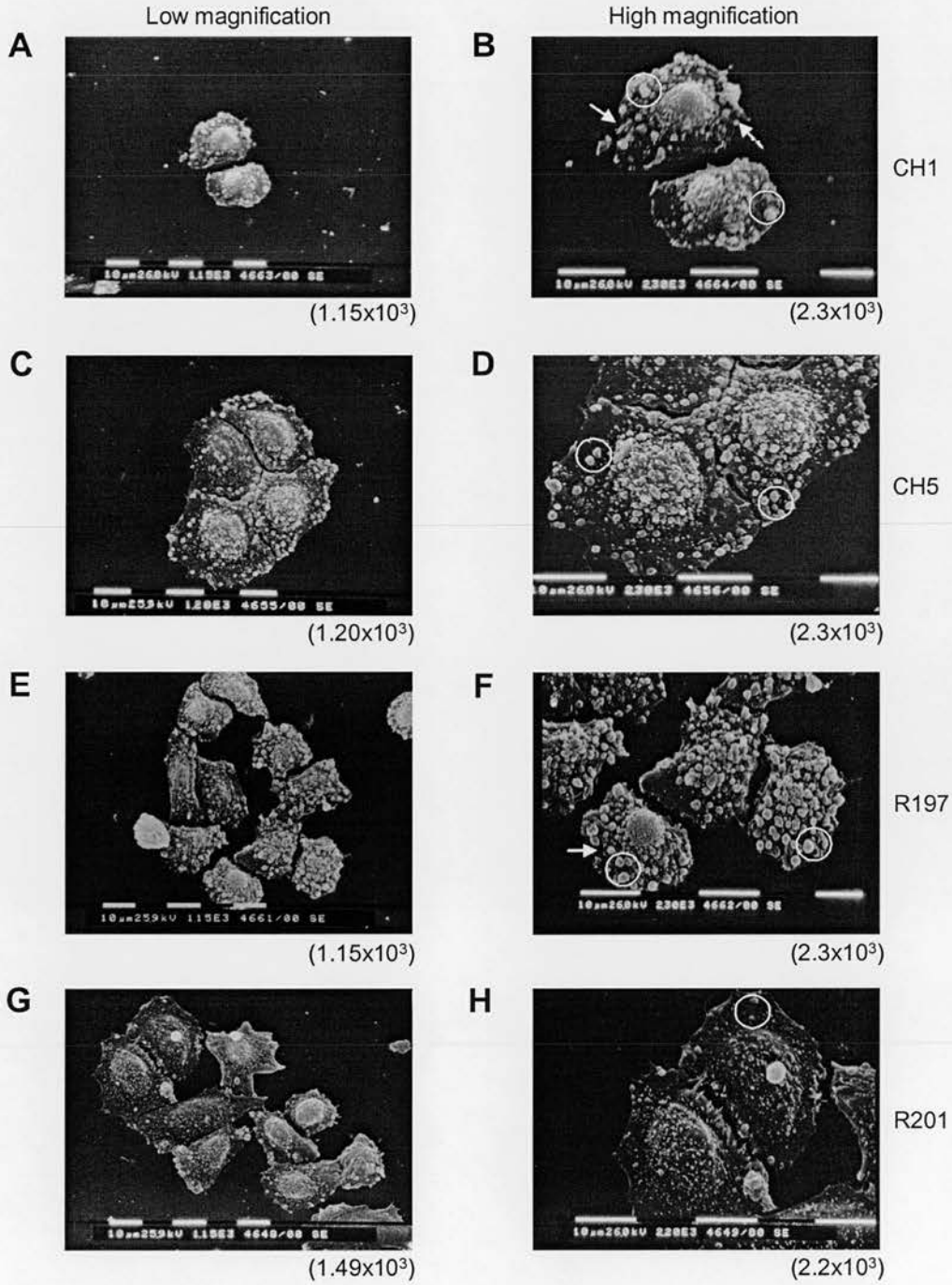

Figure 6.15 Scanning electron micrographs of R-Ras G38V N-Terminal stable lines.

Scanning electron micrographs were taken of CH1 (panels A and B), CH5 (panels C and D), R197 (panels E and F) and R201 (panels G and H) expressing stable lines. Magnifications of each micrograph shown in the lower right hand corner of each panel. Circled areas in higher magnification panels highlight areas of membrane blebbing. Arrows in higher magnification panels indicated areas of membrane ruffling. Bars represent 10μm.

6.6 Discussion

In this chapter, the microlocalisations of H-Ras and R-Ras have been investigated with relation to integrin affinity modulation and using H-and R-Ras chimera stable lines, the regions of H-Ras and R-Ras responsible for conferring their differential effects on cellular structure and morphology have been explored. The major findings of this chapter are as follows: H-Ras G12V and R-Ras G38V localise to similar microdomains within the plasma membrane. Membrane disruption using MβCD has no affect on integrin affinity modulation by H-Ras G12V or R-Ras G38V. Stable expression of H-Ras G12V in CHO-K1 cells is non-viable. The H-Ras sequences Gly^{60} to Leu^{171} are important in conferring H-Ras G12V cytoskeletal structure and cellular morphology, since the CH1, H197 and H201 stable lines are all H-Ras-like. The R-Ras sequences Leu^{175} to Pro^{203} are important in conferring R-Ras G38V cytoskeletal structure and cellular morphology, since the CH6 and R201 stable lines are both R-Ras-like.

The cellular localisation of R-Ras has not been formally identified by any previous studies. Using confocal microscopy, the cellular localisations of transiently expressed H-Ras G12V and R-RasG38V were examined. Results reveal both H-Ras G12V and R-Ras G38V are targeted to similar microdomains within the plasma membrane (Figure 6.1). The earliest insight into Ras microlocalisation came with the observations that disrupting lipid raft structure, by chemically depleting plasma membrane cholesterol, selectively abrogates H-Ras- but not K-Ras-mediated activation of Raf-1 (Roy *et al.*, 1999). More recently, Prior *et al.*, (2001) have shown using the C-terminal 9 amino-acids of H-Ras cloned onto the C-terminus of GFP, that the C-terminal anchor of H-Ras targets to caveolae and lipid rafts. The efficient targeting of H-Ras to lipid rafts and caveolae is dependent on palmitoylation, because non-palmitoylated H-Ras mutants accumulate in the ER (Choy *et al.*, 1999; Apolloni *et al.*, 2000). As a general rule, palmitoylated peripheral membrane proteins can associate with lipid rafts because the saturated palmitate packs well into the liquid-ordered raft structures, whereas unsaturated, branched chain prenyl groups do not (Melkonian *et al.*, 1999). As R-Ras also contains a palmitoylation sequence, it is not unreasonable to assume that it may be targeted to similar lipid raft microdomains

as H-Ras. Also, RhoB and TC10 proteins, which have a geranylgeranylated motif and are palmitoylated, like R-Ras, have been shown to localise at the plasma membrane and golgi (Michaelson *et al.*, 2001), which suggests a similar trafficking pathway to H-Ras. A recent study by Furuhjelm and Peranen, (2003) showed, using EGFP-tagged R-Ras (WT, G38V and 43N) proteins, that each of the proteins localised to the perinuclear region, to the golgi and to the plasma membrane, suggesting that R-Ras does use an analogous endomembrane trafficking route to H-Ras and N-Ras (Choy *et al.*, 1999).

Although inactive H-Ras has been located to lipid rafts and caveolae, it has been demonstrated that GTP loading of H-Ras is sufficient to drive H-Ras out of lipid rafts (Prior *et al.*, 2001). Insolubility in 1% Triton X-100 is widely used as an assay for lipid raft association. The increased detergent solubility of GTP-bound H-Ras G12V, as compared with GDP-bound H-Ras, is consistent with activated H-Ras being driven into disordered plasma membrane (Prior *et al.*, 2001). The results presented in Figure 6.1 show that activated H-Ras G12V and activated R-Ras G38V localise to similar domains within the plasma membrane and so it is probable that upon GTP-loading, R-Ras also migrates to the disordered plasma domain.

The actin cytoskeleton mediates a variety of essential biological functions in all eukaryotic cells. It provides a structural framework around which cell shape and polarity are defined (Hall, 1998). Ras is involved in regulating the organisation of the actin cytoskeleton, with Rho and Rac being downstream effectors (Hall, 1994). Confocal microscopy, following immunostaining with rhodamine-conjugated phalloidin and vinculin, demonstrates the cellular morphological changes correlating with the distribution of cell-substratum contacts, following transient expression of H-Ras G12V and R-Ras G38V in CHO cells. Wild-type CHO cells have the typical well spread, polyglonal shape (Figure 6.2A). Expression of H-Ras G12V results in the loss of stress fibres and a reduction in cell size (Figure 6.2B). The rounded morphology and thickened cortical actin around the periphery of the H-Ras G12V transfected cells are consistent with Ras-transformed epithelial cells (Zhong *et al.*, 1997). The significant effects on cell morphology, inducing loss of adhesions and changes in cell shape, are also typical of the transformed morphology of Swiss 3T3 fibroblasts (Nobes and Hall, 1999). Activated H-Ras has a suppressive function on

integrins, inducing a reduction and enhanced turnover of adhesions (Nobes and Hall, 1999; Hughes *et al.*, 1997), which might help to explain the reduced size of the H-Ras G12V transfected cell. Although the R-Ras G38V transfected cells had fewer stress fibres than the control cell, they maintained a well spread morphology and there was no obvious thickening of cortical actin. This would suggest that unlike H-Ras G12V, R-Ras G38V does not have the ability to transform CHO cells.

Upon adhesion, CHO cell adhesion receptors cluster into highly organised cellular structures named focal contacts that link the extracellular matrix to actin microfilaments and a number of cytoskeleton proteins such as talin, vinculin and α-actinin (reviewed by Turner and Burridge, 1991). Complete spreading is achieved by dynamic peripheral adhesion plaques (focal adhesions) in equilibrium with a pool of free adhesion receptors (such as the $\alpha 5\beta 1$ integrin) subjected to the endocytic cycle (Tranquil *et al.*, 1993). Since H-Ras G12V transfected cells remain adhered to the coverslips, but have a loss of the polygonal shape of the control cells, suggests that focal contacts are formed, however, disorganisation and subsequent disruption of the focal adhesions leading to enhanced turnover of adhesions at the cell periphery, results in a rounded morphology.

Focal adhesions are specialised signalling platforms on the cell surface that mediate cell-matrix interactions via integrins, which are in turn associated with different cytoskeletal proteins (Sastry and Burridge, 2000). Using vinculin as a marker, confocal microscopy showed that R-Ras G38V localised with vinculin and increased the number and size of peripheral focal adhesions (Figure 6.3C). A very recent publication by Furuhjelm and Peranen, (2003) demonstrated, using EGFP-labelled R-Raswt and EGFP-labelled R-RasG38V, that R-Ras is targeted to focal adhesions and that this is dependent on R-Ras being in a GTP-bound state.

Transfection with H-Ras G12V results in an overall reduction in the number and size of focal adhesions, resulting in the rounding up of the cell (Figure 6.3B). When H-Ras G12V is expressed at relatively low levels and at early time points (2 hours), Nobes and Hall, (1999) have clearly observed H-Ras concentrated at focal adhesion sites using the anti-Ras antibody, Y13-238.

The cytoskeletal protein, Talin-1, binds directly to integrins (Liu *et al.*, 2000) and to the actin cytoskeleton (Hemmings *et al.*, 1996). Furuhjelm and Peranen, (2003) showed that the β1-integrin, talin and paxillin localise at focal adhesions. Given that activated R-Ras and H-Ras have been shown to localise to focal adhesions; and that focal adhesions are regions where integrins (such as β1-integrin) can associate with the cytoskeleton of cells (through such proteins as talin-1), it is possible that at, least in adherent cells, focal adhesions provide the opportunity for H-Ras and R-Ras to be in the vicinity of integrins where they may be involved with inside-out signalling.

As previously mentioned, disrupting lipid raft structures, by chemically depleting plasma membrane cholesterol, selectively abrogates H-Ras- but not K-Ras-mediated activation of Raf-1 in baby hamster kidney (BHK) cells (Roy *et al.*, 1999). Furuhjelm and Peranen (2003) have also demonstrated that depleting cholesterol from serum-starved Hela cells expressing EGFP-R-Ras-38V resulted in the loss of EGFP-R-Ras-38V from focal adhesions and a smooth redistribution to the plasma membrane. Lipid rafts consist of dynamic assemblies of cholesterol and sphinolipids (Simons and Toomre, 2000). Cholesterol associates with sphingolipids in the golgi complex and serves to stabilise the lipid raft microdomains, therefore proteins with raft affinity can become associated by way of lipid-lipid interactions (Ilangumaran and Hoessli, 1998). Proteins with lipid raft affinity include glycosylphosphatidylinositol (GPI)-anchored proteins, Src-family kinases, α-subunits of heterotrimeric G proteins, cholesterol and palmitoylated proteins (Simons and Toomre, 2000).

β-cyclodextrins have been found to selectively extract cholesterol from the plasma membrane, in preference to other membrane lipids (Ohtani *et* al., 1989), by complexing with the cholesterol (Klein *et al.*, 1995). Results shown in Figure 6.5 revealed that MβCD treatment of αβ-py cells transfected with H-Ras G12V and R-Ras G38V had no significant effect on their abilities to modulate integrin affinity modulation.

Since MβCD treatment of αβ-py cells transfected with R-Ras G38V did not affect the ability of R-Ras to mediate integrin affinity modulation, but that similar MβCD treatment of Hela cells by Furuhjelm and Peranen, (2003) resulted in a loss of EGFP-

R-Ras G38V from focal adhesions, suggests that R-Ras G38V does not mediate its effect on integrin affinity from focal adhesions. It was interesting to note the significant difference in the effects of R-Ras G38V-mediated, but not H-Ras G12V-mediated, integrin affinity modulation following the addition of the inclusion complexes. Since the incorporation of inclusion complexes had no effect on H-Ras G12V, a toxic effect by the inclusion complexes can be ruled out. It may be possible that the inclusion complexes are simply preventing integrin activation by R-Ras G38V by some non-specific mechanism, such as steric hindrance.

Several hypothesises can be put forward to explain the lack of effect of MβCD treatment, of αβ-py cells transfected with H-Ras G12V and R-Ras G38V, on integrin affinity modulation: First, Figure 6.4 clearly shows the disruption of membrane rafts, following cholesterol depletion by MβCD, in CHO-K1 cells plated onto coverslips resulting in a loss of adhesion and a rounding up of the cells compared with control. Ilangumaran and Hoessli (1998), also describe a rounding up of human umbilical vein-derived endothelial cells (ECV304) following MβCD treatment. A publication by Ilangumaran and Hoessli, (1998) described the successful treatment of suspended murine T-lymphocyte cells with MβCD to remove plasma membrane cholesterol. It was therefore assumed that MβCD treatment of suspended αβ-py cells would have the same cholesterol-depleting effect as that observed with the attached CHO-K1 cells. However, if this is not the case, then this would explain the negligible effect that MβCD treatment has on integrin affinity modulation by H-Ras G12V and R-Ras G38V.

Second, Leitinger and Hogg, (2002) have demonstrated using immunostaining and adhesion studies that disruption of raft integrity through depletion of membrane cholesterol with MβCD completely disrupted α4β1 cluster formation. As membrane disruption, using a similar MβCD treatment as described by Leitinger and Hogg (2002), had little effect on the ability of H-Ras G12V and R-Ras G38V to modulate integrin affinity; this may indicate that lipid rafts play an important role in controlling integrin avidity and not integrin affinity.

Third, it has been demonstrated that GTP loading of H-Ras is sufficient to drive H-Ras out of caveolae (Prior *et al.*, 2001). Consistent with this, the cytoplasmic

localisation of pEGFP-H-Ras WT and not pEGFP-H-Ras G12V, following MβCD treatment (see Figure 6.6) confirms that cholesterol depletion only affects the localisation of the inactivated form of H-Ras and not the H-Ras G12V activated mutant. Prior *et al.,* (2003) further confirmed this using immunogold electron microscopy, showing that activated H-Ras clusters in microdomains and that the cluster patterns are not disrupted by cholesterol depletion. If R-Ras is located to similar cholesterol-sensitive domains as H-Ras, but that a similar displacement is observed with GTP-loaded R-Ras G38V, then treatment to disrupt the cholesterol rich domains of the membrane should not have an effect on GTP-bound H-Ras G12V- and R-Ras G38V-mediated integrin affinity modulation.

Several other methods could also be employed to investigate the compartmentalisation of Ras proteins. Electron microscopy following immunogold labelling of GFP-tagged proteins or fractionating the membranes over sucrose gradients and analysing by immunoblotting (Prior and Hancock, 2001; Prior *et al.,* (2001). Also, filipin could be used in place of MβCD for disrupting the lipid rafts.

It was hoped that by using PCR techniques R-Ras WT and G38V could be cloned into a dsRed-expressing construct allowing us to visualise their distributions in live cells and compare them to the GFP-tagged H-Ras constructs (Figure 6.6). However, due to the high GC content of the N-terminus of R-Ras, it was very difficult to sequence the resulting PCR products. After several failed attempts to sequence PCR products, time constraints prevented further investigations using this method.

Stable lines expressing R-Ras G38V and the H-and R-Ras chimeras (schematic representation shown in Chapter 4, Figure 4.1) were produced in CHO-K1 cells in order to elucidate which areas of H-Ras and R-Ras were important in conferring their different effects on cellular morphology.

Although H-Ras G12V was successfully expressed in a transient system, repeated attempts to produce an H-Ras G12V stable line in CHO-K1 cells proved futile. Despite G418 selection, none of the prospective clones expressed H-Ras G12V. We suspect that perhaps the CHO-K1 cells became spontaneously G418 resistant, explaining why they were capable of growing in the selection media without plasmid expression.

Previous studies have shown H-Ras stables lines to be successfully produced in NIH 3T3 cells (Hansen *et al.*, 2002; Kawano *et al.*, 2000). However, Kawano *et al.*, (2000) used an H-Ras G12V gene that was under the control of an IPTG-inducible promoter and therefore the transient expression of the H-Ras G12V gene could be regulated. Hansen *et al.*, (2002) used an H-Ras with mutations G12R and A59T, which may have contributed to its ability to be expressed in a stable system. H-Ras has been shown to have a lethal effect on cells. Expression of H-Ras (wt) or H-Ras G12V in a neuroblastoma cell line caused the cells to round up and fragment (Kitanaka *et al.*, 2002). This H-Ras-mediated cell death is a process distinct from apoptosis, since it was not prevented by the overexpression of the anti-apoptotic protein Bcl2 or by the addition of caspase inhibitors (Kitanaka *et al.*, 2002). Other results from this group showed that the H-Ras G12V/D38N mutant failed to induce cell death (Kitanaka *et al.*, 2002). The H-Ras D38N mutation abolishes Raf-1 binding, which suggests that the H-Ras-mediated cell death requires Raf-1 activation. This may help to explain why it was possible to produce a stable line expressing H201 (which comprises 88% H-Ras, residues 1-174). This chimera was not as effective as H-Ras G12V at activating Raf and so, unlike the overexpression of H-Ras G12V, H201 overexpression may not induce cell death.

Although it would have been ideal to have both H-Ras G12V and R-Ras G38V stable lines to use as controls for comparing differences in phenotypes, it was decided that the cells transiently transfected with H-Ras G12V and R-Ras G38V (see Figures 6.2B and 6.2C) would serve as comparisons for actin cytoskeleton structure. The H201 stable line was used in place of an H-Ras G12V stable in comparing the electron microscopy images as it had a similar transforming effect on CHO-K1 cellular morphology to transiently transfected H-Ras G12V (see Figures 6.11D and 6.2B respectively).

Comparing the actin cytoskeleton structures and electron-microscopy images of the chimeric stables has indicated the importance of the hypervariable N-terminal linker region of H-Ras for conferring activated H-Ras transforming effect on cells. This conclusion was drawn from two observations; first, that the CH1 stables, comprising H-Ras sequences C-terminal of Gly^{60}, (R-Ras 85; H-Ras 60-198), was sufficient to convey a transformed phenotype (Figures 6.12A, 6.14A and 6.14B). Second, that the

H197 stable, that contains H-Ras residues N-terminal of Leu^{171} (H-Ras 171; R-Ras 199-219) was able to confer a transformed phenotype (Figures 6.11C, 6.13E and 6.13F). Results also suggest that H-Ras sequences N-terminal of the H-Ras HVR linker domain are necessary to confer a transformed phenotype. This conclusion was drawn from the observation that while expression of CH1 (comprising H-Ras sequences C-terminal of Gly60), was sufficient to confer a transformed phenotype, expression of CH5 (comprising H-Ras sequences C-terminal of Lys^{149}) was not sufficient to confer a transformed phenotype (Figures 6.12B, 6.14C and 6.14D). The sequence divergence between CH1 and CH5 overlaps with the Switch II region (H-Ras residues 60 to 149). Upon activation, the exchange of GDP for GTP drives an allosteric change in the Switch I and Switch II regions (Boriack-Sjodin *et al.*, 1998). This conformational change allows the Switch I region to bind effectors (Ehrhardt *et al.*, 2002). It may be that the presence of the R-Ras Switch II region in chimera CH5, in place of the H-Ras Switch II region, may alter the GTP-bound conformation and impair the ability of this protein to interact efficiently with the H-Ras effectors required for a fully-transformed phenotype.

The 28-amino-acid stretch of R-Ras, which includes the R-Ras hypervariable region, comprising residues 175-203, is sufficient to confer an R-Ras G38V-like phenotype to CHO-K1 cells. This conclusion was drawn from the following observations; first, the CH6 stables, comprising R-Ras sequences C-terminal of Leu^{175}, (H-Ras 146; R-Ras 175-219), was sufficient to confer an R-Ras G38V-like phenotype to CHO-K1 cells (Figures 6.11B, 6.13C and 6.13D). Second, that R201 stables, that contain R-Ras residues N-terminal of Pro^{203} (R-Ras 203; H-Ras 175-189) convey an R-Ras-like phenotype (Figures 6.12D, 6.14E and 6.14H).

Of particular interest are the differences in morphology seen with chimera stables R197 and R201. While expression of R201 confers an R-Ras like phenotype, cells expressing R197 exhibit some properties indicative of a transformed phenotype (Figures 6.12 and 6.14) i.e. a slight rounded morphology. These chimeras comprise N-terminal R-Ras sequences, differing in only five R-Ras amino acids at the C-terminal end of the R-Ras hypervariable region. These five amino acids comprise the proline-rich domain of R-Ras, which has previously been shown to have influence over the ability of R-Ras G38V to modulate integrin affinity (see Chapter 4). Here,

the presence of the proline-rich domain of R-Ras seems necessary to fully bestow the well spread, 'fried egg', phenotype of R-Ras G38V. However, the transformed phenotype of H197 (H-Ras 171; R-Ras 199-219) (Figures 6.11C, 6.13E and 6.13F) implies that the presence of R-Ras C-terminal sequences alone, including the proline–rich domain, are not wholly sufficient to confer an R-Ras G38V phenotype and that R-Ras C-terminal sequences 175-199, the residues of divergence between CH6 stable (which have an R-Ras like phenotype) and H197 stables (which have a transformed phenotype), are also important in determining phenotype.

In Chapter 4, the hypervariable regions of H-Ras and R-Ras have already been shown to be of importance in modulating integrin affinity. In this chapter, it has been shown that the hypervariable domains are also important in the transforming abilities of H-Ras and R-Ras. The importance of the hypervariable domains has also been confirmed by Prior *et al.* (2001), who showed that the removal of the hypervariable domain of H-Ras (HΔhvrG12V) abrogates the GTP-dependent redistribution of H-Ras from rafts to the bulk plasma membrane thus preventing Raf activation. Also, the recent publication by Furuhjelm and Peranen, (2003) demonstrated that when the hypervariable region of R-Ras (amino acids 175-218) was replaced with the corresponding region (amino acids 147-189) of H-Ras, the targeting of R-Ras to focal adhesions was inhibited. Furthermore, when the hypervariable region of H-Ras (amino acids 147-189) was replaced by the corresponding region (amino acids 175-218) of R-Ras, the H-Ras molecule was targeted to focal adhesions (Furuhjelm and Peranen, 2003). Hancock (2003) postulates that the hypervariable region might interact with other plasma-membrane proteins to regulate the later segregation of H-Ras and that galectin-1 was a possible candidate. Galectin-1 interacts with H-Ras GTP (Paz *et al.*, 2001). Down-regulation of galectin-1 expression abolishes H-Ras G12V clustering at the plasma membrane, resulting in partial mislocalisation of H-Ras G12V to the cytosol (Paz *et al.*, 2001; Prior *et al.*, 2003).

6.6.1 Summary

Both H-Ras G12V and R-Ras G38V are targeted to similar domains within the plasma membrane. Integrin affinity modulation by these proteins is not affected by the depletion of plasma membrane cholesterol, which suggests that they do not

influence integrin affinity from cholesterol-sensitive microdomains such as the lipid rafts and focal adhesions.

Confocal microscopy has shown that transient transfection of CHO-K1 cells with H-Ras G12V results in a transformed phenotype. In contrast, R-Ras G38V expression does not transform CHO-K1 cells.

Results in Chapter 4 revealed that a 25-amino acid stretch of H-Ras (Arg^{149} to Pro^{174}) is required for integrin suppression. Results from this chapter suggest that a 111-amino stretch of H-Ras (Gly^{60} to Leu^{171}) is required for conferring a transformed phenotype. This area overlaps with the 25-amino acid stretch required for integrin affinity modulation, but includes the Switch II region of H-Ras (Gly^{60} to Gly^{75}), which may be important for efficient effector binding.

Results from Chapter 4 revealed that a 28-amino acid stretch of R-Ras (Leu^{175} to Pro^{203}) is sufficient to reverse H-Ras mediated integrin suppression. Results from this chapter show that the same 28-amino acid stretch is sufficient to confer an R-Ras-like phenotype. Interestingly, the presence of the proline-rich domain of R-Ras (residues 198 to 203) seems to be required for conferring the full R-Ras phenotype, since expression of R201 confers a full R-Ras-like phenotype while expression of R197 does not. This region has also been shown to be important for modulating integrin affinity (chapter 4).

Since the presence of H-Ras amino acids Leu^{171} to Pro^{174} are not required for a transformed phenotype but that the equivalent proline-rich amino acids of R-Ras (Pro^{198} to Pro^{203}) are required for a full R-Ras phenotype, suggests an important role for these amino acids in R-Ras signalling.

Stable or prolonged transient expression of H-Ras G12V in CHO-K1 cells may result in H-Ras-mediated cell death. This process may be dependent on full activation of Raf-1, since stable lines expressing the H201 chimera (which activated Raf-1 to a lesser extent than H-Ras G12V) are viable.

Chapter 7

Functional characterisation of H-Ras and R-Ras

7.1 Introduction

In Chapter 6, results showed that transfection of CHO cells with R-Ras G38V increased cell spreading and focal adhesion formation. In contrast, H-Ras G12V expression resulted in a rounding up of CHO cells, which correlated with a decrease in focal adhesion formation and disruption of the actin cytoskeleton. The regulation of cell migration and adhesion are central to many normal and pathological processes including wound healing, inflammation and tumor metastasis. Regulation is dependent upon rapid, controlled alterations in integrin affinity for their extracellular ligands (Huttenlocher *et al.*, 1996).

In vitro and *in vivo* growth properties that distinguish transformed cells from normal counterparts include alterations in cellular morphology, decreased dependence on serum growth factors, loss of cell-cell contact growth inhibition, the ability to proliferate in suspension or semi-solid growth medium and the ability to form tumours when introduced into the appropriate host (Freedman and Shin, 1974; Stanbridge and Wilkinson, 1978).

The ease of transfection and sensitivity to transformation of rodent fibroblastic cell lines make them the system of choice for analysing the alterations in cell phenotype induced by oncogenic expression (Clark *et al.*, 1995). *In vitro*, fibroblastic-like CHO cells grow as an adherent monolayer. Following transformation by cytoplasmic oncogenes such as *Ras* or *Src*, cell detachment induced apoptosis does not occur and is accompanied by the ability to grown in suspension (Frisch and Francis, 1994).

The aims of this chapter are as follows: First, to compare the effects of integrin affinity modulation by H-Ras G12V and R-Ras G38V expression on the adhesion and migration properties of CHO cells using the $\alpha\beta$-py cells to relate integrin-affinity state to cell adhesion and migration. Second, using CHO cells stably expressing H- and R-Ras chimeras, determine if specific regions of H-Ras and R-Ras are required for their effects on cell adhesion and migration. Thirdly, using the H-and R-Ras

chimera stable lines, determine which specific sequences of H-Ras G12V are required to convey transformation of CHO cells, as characterised by enhanced proliferation and anchorage-independent growth and to determine if integrin-affinity modulation by H-Ras and R-Ras bears any relation to their transforming abilities.

7.2 Effects of integrin affinity modulation on cell adhesion and migration.

It has previously been reported that H-Ras G12V suppresses integrin affinity while R-Ras G38V promotes an activated state of integrin. As integrins mediate cell adhesion (Hynes, 1987; Hynes, 1992), it was decided to investigate if expression of H-Ras G12V or R-Ras G38V affects cellular adhesion and migration in CHO cells. Furthermore, examination of adhesion and migration of CHO cells stably expressing H-and R-Ras chimeras may help to determine if the specific domains of H-Ras and R-Ras required for integrin affinity modulation (see Chapter 4) also affect cellular adhesion and migration. In each of the following experiments, cells transfected with pCDNA3.1(+) serve as control cells.

7.2.1 Transient expression of H-Ras G12V reduces cell adhesion.

The presence of the stably expressed $\alpha_{IIb}\alpha_{6A}\beta_3\beta_1$ chimeric integrin on $\alpha\beta$-py cells allows for these cells to be used in an adhesion assay to assess the abilities of H-Ras G12V and R-RasG38V, to regulate cell adhesion to the natural $\alpha_{IIb}\beta_3$ ligand, fibrinogen. As this was an assay based on transient expression of DNA and not stable expression, it was deemed necessary to co-transfect test DNA with a GFP-expressing vector to serve as a co-reporter for transfection, allowing only those cells expressing GFP to be assessed. Also, expression of GFP permitted the use of a fluorescent plate reader to evaluate cell adhesion, which proved to be a much more efficient method than traditional staining methods.

Adhesion was compared between cells plated onto untreated wells and cells plated onto wells that had been pre-coated with 10µg/ml fibrinogen, following incubation at 37°C for 15 minutes. Figure 7.1 shows that there is only minor adhesion observed in cells plated on untreated (plastic) wells compared with samples plated onto the fibrinogen-coated wells. There were no significant changes in adhesion observed

between cells plated onto plastic. When plated onto fibrinogen, H-Ras G12V transfected cells showed a significant decrease ($P<0.01$) in the levels of adhesion when compared with control cells. R-Ras G38V transfection had no significant effect on levels of adhesion when compared with control however, levels of adhesion were significantly increased ($P<0.001$) when compared with H-Ras G12V transfected cells.

7.2.2 Stable expression of H- and R-Ras chimeras does not affect cell adhesion

Cell adhesion was assessed in CHO-K1 cells stably expressing control vector, R-Ras G38V and the H-and R-Ras chimeras. Stable protein expression eliminated the need to transfect cells with GFP-expressing construct to act as a reporter of transfection. Fibronectin was used to coat the wells, as CHO-K1 cells do not naturally express the $\alpha_{IIb}\beta_3$ integrin. Cells were plated onto untreated wells (plastic) and onto wells pre-coated with 20μg/ml fibronectin and adhesion compared following incubation at 37°C for 15 minutes. Figure 7.2 shows no significant difference between levels of adhesion between stable lines plated onto fibronectin, compared with control.

The average percentage adhesion of control cells for each experiment, i.e. percentage of total cell count, was about 60% (data not shown). Therefore, the lack of significant difference between the stable cell lines and the control cells was not as a result of maximum adhesion of control cells (i.e. 100% of total cell count) following incubation at 37°C for 15 minutes on 20μg/ml fibronectin.

There were no significant changes in adhesion observed between stables plated onto plastic (data not shown).

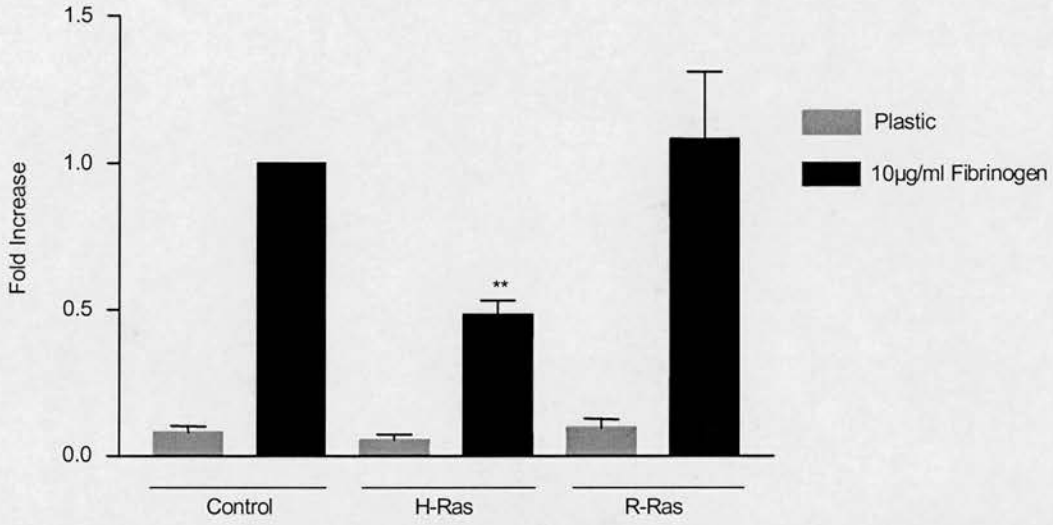

Figure 7.1 H-Ras G12V reduces cell adhesion.

Cell adhesion was determined in $\alpha\beta$-py cells co-transfected with control vector (3µg), H-Ras G12V (3µg) or R-Ras G38V (3µg) and a GFP reporter construct (1.5µg). Cell adhesion was carried out for 15 minutes at 37°C on wells left uncoated (plastic) or coated with 10µg/ml fibrinogen. Fold increase was calculated where control cells on fibrinogen = 1. Values represent mean ± SEM of 3 experiments. Statistical analysis was performed by one-way ANOVA test within each individual condition. ** = significant difference, $P<0.01$, compared with pCDNA3.1(+).

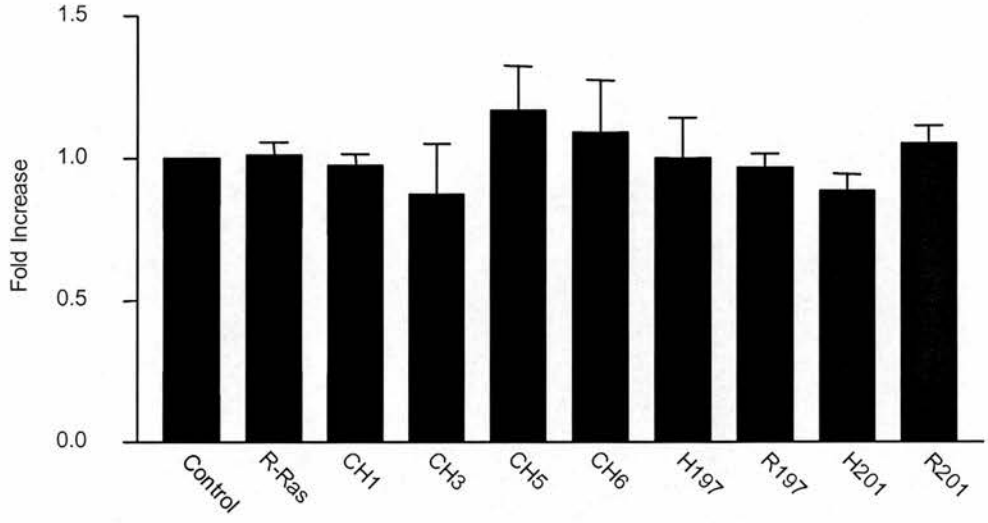

Figure 7.2 H- and R-Ras chimera stable lines have no significant effect on cell adhesion.

Cell adhesion was determined in CHO-K1 cells stably expressing H-and R-Ras chimeras. Cell adhesion was carried out for 15 minutes at 37°C on wells coated with 20μg/ml fibronectin. Cell adhesion was assessed by colorimetric detection. Fold increase was calculated where control cells on fibronectin = 1. Values represent mean ± SEM of 3-5 experiments

7.2.3 Transient expression of R-Ras G38V reduces cell migration

The abilities of transiently expressed H-Ras G12V and R-Ras G38V to regulate cell migration in $\alpha\beta$-py cells, to the natural platelet ligand fibrinogen, was determined using a Boyden chamber haptotactic assay (Keely *et al.*, 1995; Keely *et al.*, 1999) in which transwells were coated on the underside with 10μg/ml fibrinogen and migration compared in the absence of serum. Cell migration was also determined chemo-tactically, where transwells were left uncoated and migration compared in the presence of 10% serum. Cells were transiently transfected with control vector, H-Ras G12V and R-Ras G38V, together with GFP to serve as a reporter of transfected cells. A fluorescent plate reader was used to evaluate cell migration of GFP-expressing cells. Figure 7.3 shows that R-Ras G38V significantly inhibited cell migration in the haptotactic assay ($P<0.05$) compared with control. The migration of cells expressing R-Ras G38V was significantly reduced ($P<0.01$) in response to serum, compared with H-Ras G12V expressing cells.

7.2.4 Stable expression of H- and R-Ras chimeras does not affect cell migration

The ability of stably expressed chimeras to regulate the migration of CHO-K1 cells on fibronectin was determined using a Boyden chamber haptotatic assay, in which transwells were coated on the underside with 20μg/ml fibronectin. As with the stable adhesion assays, stable protein expression eliminated the need to transfect cells with a GFP-expressing reporter construct. Cells were plated onto chambers pre-coated with 20μg/ml fibronectin and migration compared following incubation at 37°C for 4 hours. Figure 7.4 shows no significant difference between levels of adhesion between stable lines plated onto fibronectin, in the absence of serum, compared with control. Moreover, there were no significant changes in migration observed between stable cell lines plated onto uncoated transwells migrating towards 10% serum conditions (data not shown). The average percentage migration of control cells for each experiment, i.e. percentage of total cell count, was about 55% (data not shown). Therefore, the lack of significant difference between the stable cell lines and the control cells was not as a result of maximum migration of control cells (i.e. 100% of total cell count) following incubation at 37°C for 4 hours on 20μg/ml fibronectin.

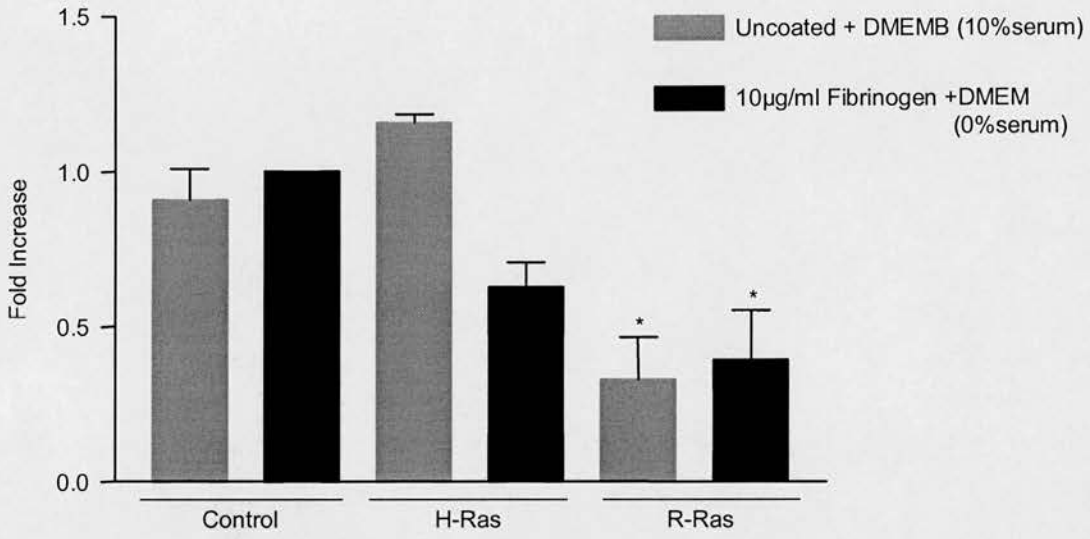

Figure 7.3 Transient expression of R-Ras G38V reduces cell migration.

Cell migration was determined in $\alpha\beta$-py cells transfected with control vector (3µg), H-Ras G12V (3µg) or R-Ras G38V (3µg) a GFP reporter construct (1.5µg). Cell migration was carried out for 4 hours at 37°C on chambers left uncoated or coated from the underside with 10µg/ml fibrinogen. Readings were taken using a fluorescent plate reader. Fold increase was calculated where control cells on fibrinogen = 1. Values represent mean ± SEM of 3 experiments. Statistical analysis was performed by one-way ANOVA test, within each individual condition. * = significant difference, $P<0.05$, compared with control.

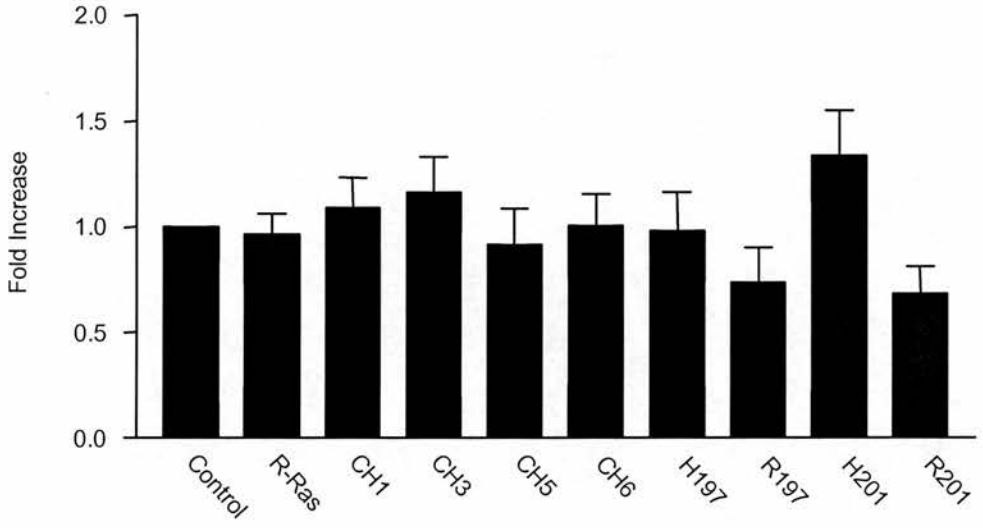

Figure 7.4 H- and R-Ras chimera stable lines have no significant effect on cell migration.

Cell migration was determined in CHO-K1 cells stably expressing H-and R-Ras chimeras. Cell migration was carried out on chambers coated from the underside with 20μg/ml fibronectin and left to migrate towards DMEM (without serum) for 4 hours at 37°C. Cell migration was assessed by colorimetric detection Fold increase was calculated where control cells on fibronectin = 1. Values represent mean ± SEM of 3-5 experiments.

7.2.5 Wound assay analysis of cell migration.

To investigate the role of H-Ras and R-Ras in CHO-K1 cell motility, cell motility was assessed by the wound assay method. Following wounding, cells were maintained in a serum-free growth media to reduce levels of cell proliferation. Thus, any movement into the wound space should be a consequence of cellular migration and not cell growth. Identical wound areas were assessed at 0, 24 and 48 hour time points (see Figures 7.5, 7.6 and 7.7), to help determine the extent of cell movement into the wound. The original wound width, at 0 hours, has been marked onto the each of the subsequent time point images to allow for easier interpretation. Figure 7.5 shows the migration of control vector and R-Ras G38V stable lines. By 24 hours, control cells at the wound edge have become less rounded and have started to respread and extend into the open space. By 48 hours, cells have developed an elongated morphology and there are areas where the wound has almost closed. In contrast, R-Ras G38V stables show negligible movement into the wound. The wound edges are well defined throughout the assay and cells remain tightly packed and maintain a polygonal morphology.

Figure 7.6 shows the cell migration of H-Ras G12V N-terminal stable line chimeras. Compared with the control cells (Figure 7.5), CH3 and H201 stables show negligible movement into the wound space throughout the 48 hour assay, maintaining well defined wound edges similar to that observed with the R-Ras G38V stables (Figure 7.5). In contrast, the CH6 and H197 stables show cells extending into the open space of the wound at 48 hours. The CH6 stable cells have taken on a more noticeably elongated, spindle-shaped morphology than observed with control cells. While the H197 cells have migrated into the wound space, have a less spindle shape and more polarised morphology than the control cells. Interestingly, both the CH6 and H197 stables have developed areas of cell aggregation surrounding the wound area. The areas immediately surrounding the cell aggregates are clear of cells, suggesting migration/aggregation of cells from the original monolayer rather than cell proliferation. CH6 stables have formed very large cell aggregates, which seemed to merge into each other. In contrast, the H197 stable line had much smaller, clearly defined aggregates.

Figure 7.7 shows the migration of R-Ras G38V N-terminal stable lines. Compared with control cells (Figure 7.5), R197 and R201 stables show negligible movement into the wound space throughout the 48-hour assay. As with the R-Ras G38V stables, (Figure 7.5) the wound edges remain clearly defined and the cells maintain a normal morphology. As with the control cells, CH1 and CH5 stables show movement into the wound space at both 24 and 48-hour time points. CH1 stable cells have a spindle-shaped morphology similar to that observed with the control cells and by 24 hours they have developed areas of cell aggregation within the cellular monolayer, similar to CH6 and H197. In contrast, CH5 stable cells maintained a very flat, polarised morphology with extensions localised only at the leading edges of the cells.

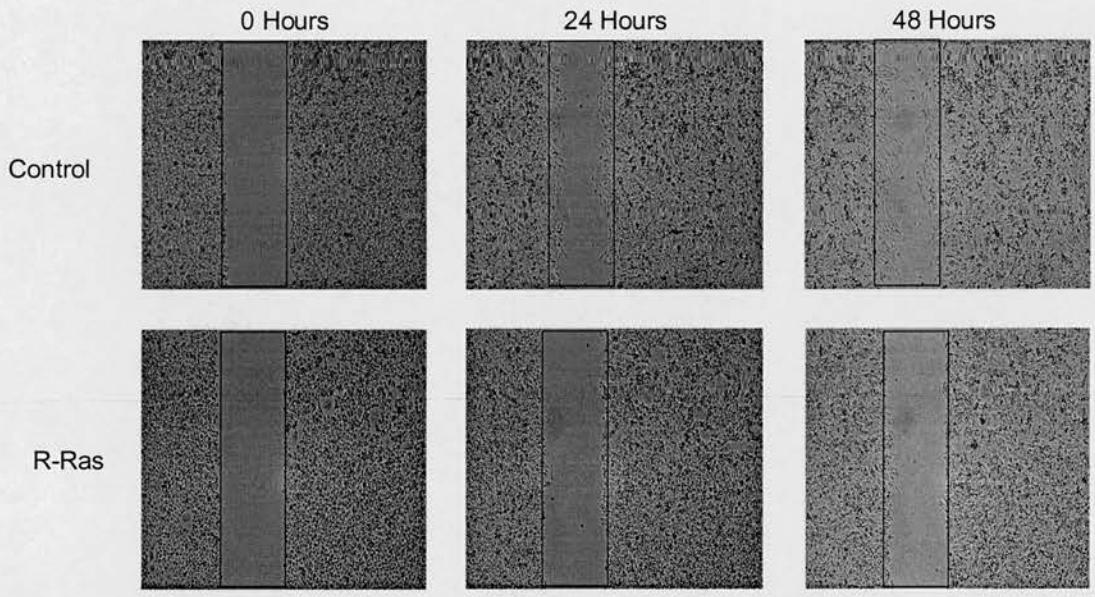

Figure 7.5 Wound assays of control and R-Ras G38V stable lines

Plates were seeded with stable cell lines expressing control vector and R-Ras G38V. Cell monolayers were wounded and images were taken at 0, 24 and 48 hour time points. Original wound width, at 0 hours, has been marked on all subsequent images. Images are representative of 4 individual experiments.

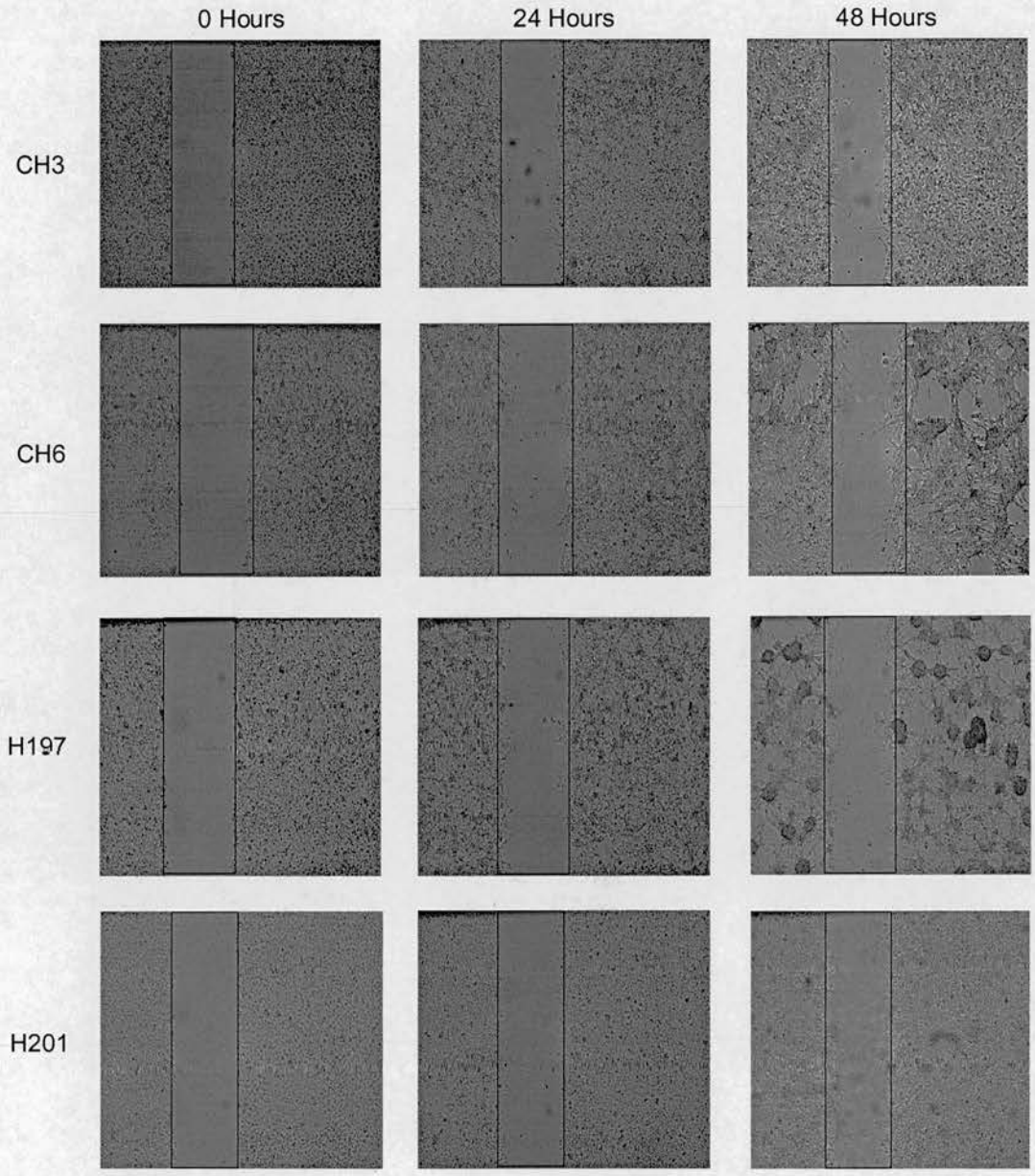

Figure 7.6 Wound assays of H-Ras G12V N-terminal chimeric stable lines

Plates were seeded with stable cell lines expressing H-and R-Ras chimeras CH3, CH6, H197 and H201. Cell monolayers were wounded and cell images were taken at 0, 24 and 48 hour time points. Original wound width, at 0 hours, has been marked on all subsequent images. Images are representative of 4 individual experiments.

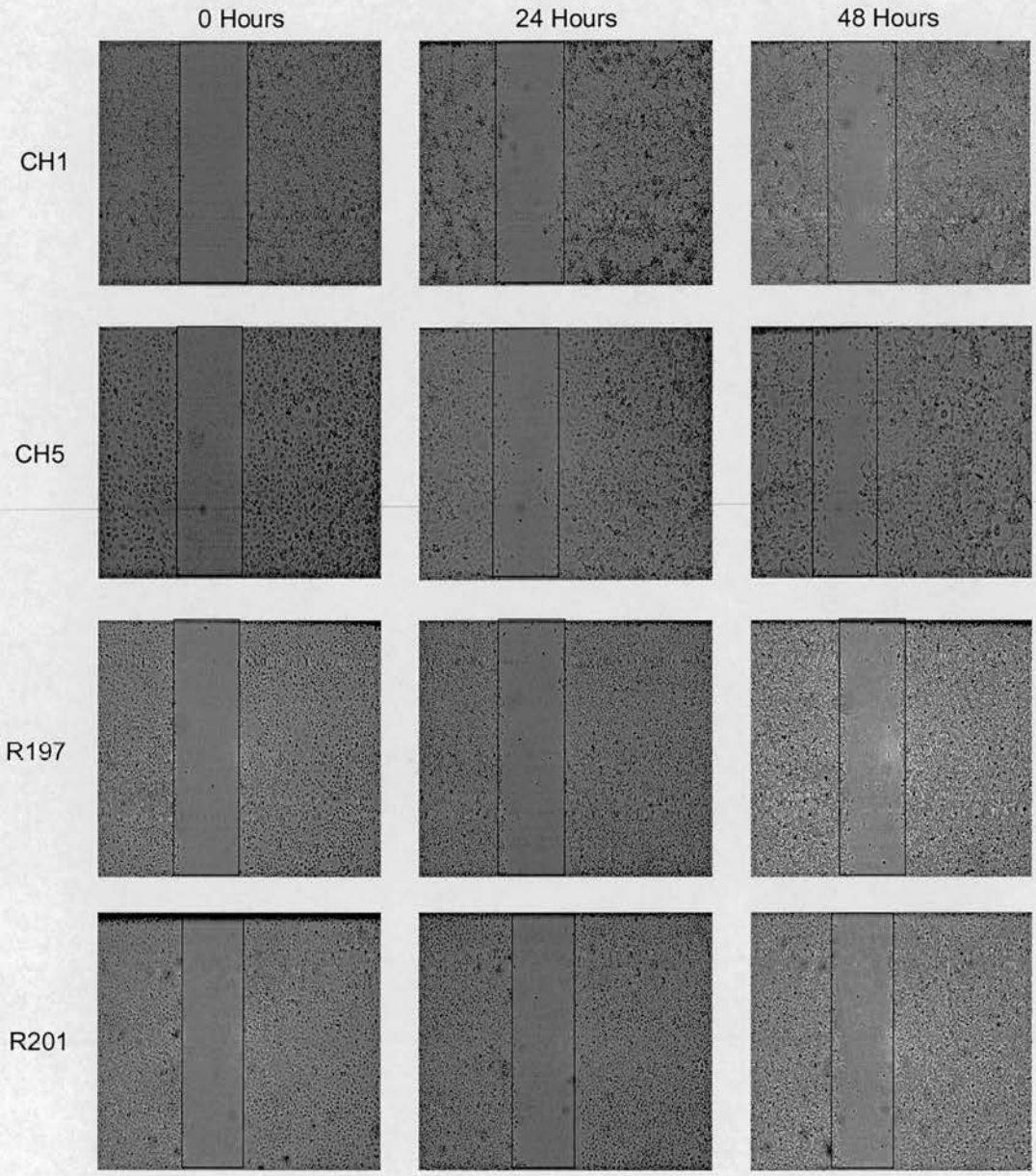

Figure 7.7 Wound assays of R-Ras G38V N-terminal chimeric stable lines

Plates were seeded with stable cell lines expressing H-and R-Ras chimeras CH1, CH5, R197 and R201.Cell monolayers were wounded and cell images were taken at 0, 24 and 48 hour time points. Original wound width, at 0 hours, has been marked on all subsequent images. Images are representative of 4 individual experiments.

7.3 Analysis of anchorage-independent growth potential

An excellent *in vitro* indicator of the ability of a gene to provoke malignant turmorigenicity is an ability to promote growth in an anchorage-independent environment (Der *et al.*, 1988; Clark *et al.*, 1995). Untransformed CHO-K1 cells need to adhere to a solid substratum in order to grow whereas Ras-transformed cells lose this requirement and readily proliferate in suspension in liquid culture or when suspended in semisolid medium (Stanbridge and Wilkinson, 1978). Growth in soft agar is the most commonly used assay for Ras-transformed cells, this assay currently represents the best *in vitro* correlate to *in vivo* growth potential (Clark *et al.*, 1995).

7.3.1 Transient expression of H-Ras G12V confers anchorage independent growth in CHO-K1 cells.

The abilities of H-Ras G12V and R-Ras G38V to induce colony formation were compared. As attempts to produce an H-Ras G12V stable line were unsuccessful (see Chapter 6), it was necessary to use transient colony assays. As expression of H-Ras G12V and R-Ras G38V was only transient, colony counts were taken on Days 1 and 2 post-seeding. Assays were set up using untransfected CHO-K1 cells and cells transiently transfected with control vector, H-Ras G12V and R-Ras G38V. Colonies of three or more cells were counted and represented as cloning efficiency.

Figure 7.8A compares Day 2 colony formation in 1% serum. The data shows that there was no significant difference in the cloning efficiency of untransfected cells (2.52 ± 0.73%), cells transfected with control vector (3.38 ± 0.18%) and R-Ras G38V (1.96 ± 0.47%). The cloning efficiency of H-Ras G12V transfected cells (6.18 ± 0.35%) was significantly increased ($P<0.01$), compared with control vector cells. There was a highly significant difference in the cloning efficiencies of cells transfected with H-Ras G12V and R-Ras G38V ($P<0.001$). A similar trend in cloning efficiencies was observed when colony assays were performed in the presence of 5% serum. Figure 7.8B shows that H-Ras G12V transfected cells (6.76 ± 0.47%) significantly increased cloning efficiency compared with control cells ($P<0.001$). The data also showed that there was a significant difference in the cloning efficiencies of cells transfected with H-Ras G12V and R-Ras G38V ($P<0.01$).

7.3.2 Stable expression of H201 confers anchorage-independent growth in CHO-K1 cells.

Percentage cloning efficiencies were compared between CHO-K1 cells stably expressing control vector and H-and R-Ras chimeras. Colonies were counted where they consisted of three or more cells and represented as cloning efficiency. In order to extend the colony assays to Day 6, cells were maintained in 5% serum conditions. Figure 7.9 shows the cloning efficiencies of stable lines on Day 4, which was shown to be the optimal day for comparing cloning efficiencies.

R-Ras G38V stables have a reduced cloning efficiency (2.86 ± 0.8%) compared with control stables (8.21 ± 2.8%). CH3 (2.76 ± 0.74%), CH6 (2.56 ± .78%), H197 (3.73 ± 0.88%) and R201 (2.31 ± 0.8%) stable lines also demonstrate a reduced cloning efficiency compared with control cells.

CH1 (7.81 ± 3.4%) and CH5 (6.67 ± 1.25%) stable lines show levels of cloning efficiency similar to control stables while stable expression of H201 (20.54 ± 6.31%) significantly increased the cloning efficiency of cells ($P<0.01$). The data also shows that there was a significant difference in the cloning efficiencies of cells stably expressing H201 and R201 ($P<0.01$).

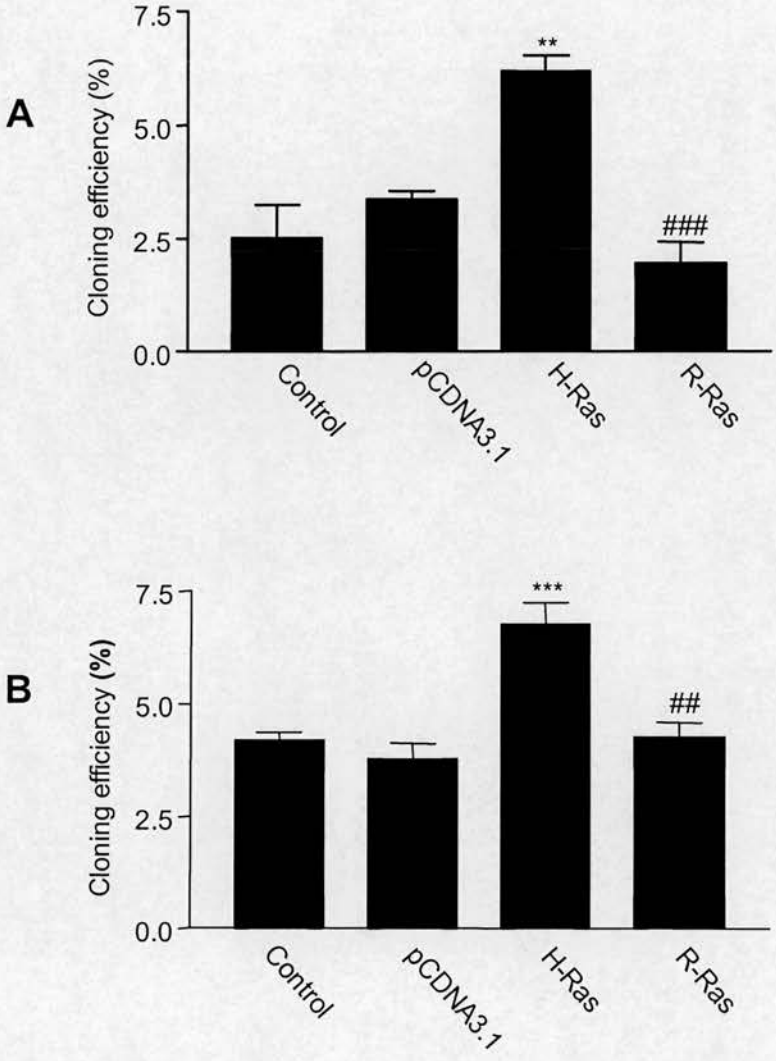

Figure 7.8 Transient expression of H-Ras G12V confers anchorage-independent growth.

Colony formation was determined in CHO-K1 cells transfected with pCDNA3.1(+) (3μg), H-Ras G12V (3μg), R-Ras G38V(3μg) or left untransfected (control). Cells were plated out in triplicate in either 1% serum conditions (A) or 5% serum conditions (B), and incubated at 37°C. Colonies were counted on day 2 and percentage cloning efficiency was calculated for each of the samples.
Values represent mean ± SEM of 3 experiments. Statistical analysis was performed, ** and *** denoting $P<0.01$ and $P<0.001$ respectively, compared with pCDNA3.1. The significant difference between H-Ras and R-Ras are shown by ## and ### denoting $P<0.01$ and $P<0.001$ respectively.

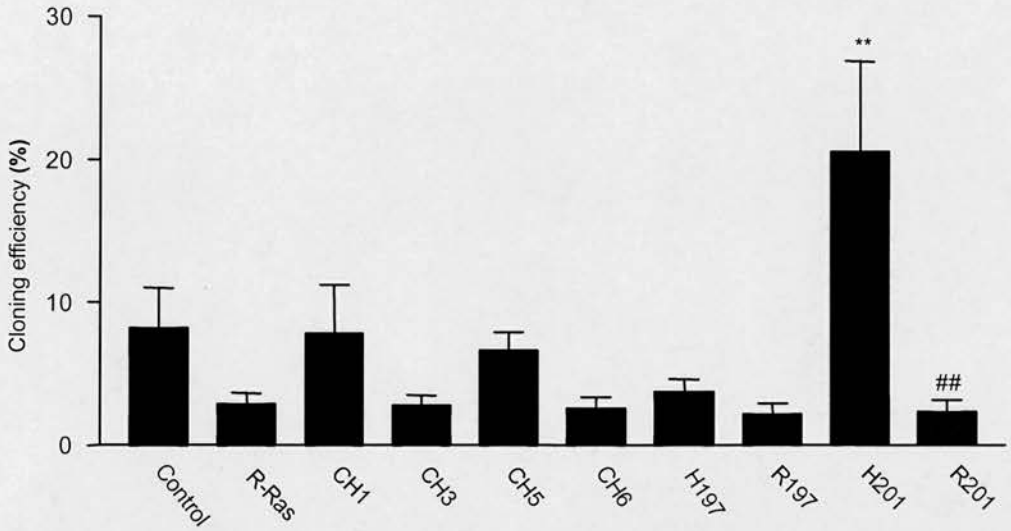

Figure 7.9 Stable expression of H201 confers anchorage-independent growth.

Colony formation was determined in CHO-K1 cells stably expressing H-and R-Ras chimeras. Cells were plated out in triplicate in 5% serum conditions, and incubated at 37°C. Colonies were counted on day 4 and percentage cloning efficiency was calculated for each of the samples.

Values represent mean ± SEM of 5 experiments. Statistical analysis was performed, ** = $P<0.01$ compared with pCDNA3.1. The significant difference between H201 and R201 is shown by ## denoting $P<0.01$.

7.3.3 Activation and inhibition of β-1 integrin has a significant effect on anchorage-independent growth

The H201 and R201 stable lines show H-Ras and R-Ras-like effects on cloning efficiency respectively (Figure 7.9). Previous results have shown that H201 and R201 transient expression in αβ-py cells modulated integrin affinity similarly to H-Ras G12V and R-Ras G38V respectively. In an effort to determine whether anchorage-independent growth was influenced by integrin activation state, it was decided to investigate the abilities of H201 and R201 stables to form colonies following treatment with β-1 integrin activating (TS2-16) and blocking (4B4) antibodies. As controls, stables were left untreated or treated with IgG_1 isotype antibody.

Figure 7.10 shows the percentage cloning efficiencies for H201 (black bars) and R201 (grey bars) from day 6, which was shown to be the optimal day for comparing cloning efficiencies following antibody treatment. H201 stables treated with the β-1 integrin activating integrin, TS2-16, significantly decreased cloning efficiency compared with untreated control (from 22.71 ± 5.21% to 4.9 ± 2.18%) ($P<0.05$). In contrast, H201 stables showed no significant difference in percentage cloning efficiency between untreated (22.71 ± 5.21%), isotype control (25.83 ± 8.4%) and 4B4 treated (30.61 ± 7.59%) cells.

With the R201 stables, treatment with the β-1 integrin blocking antibody, 4B4, significantly increased cloning efficiency compared with untreated control (from 5.26 ± 1.46% to 26.03 ± 6.13%) ($P<0.05$). There was no significant difference in percentage cloning efficiency between untreated (5.26 ± 1.46%), isotype control (4.8 ± 2.03%) and TS2-16 treated (5.74 ± 1.78%) cells.

We were concerned by the possibility of the sodium azide (NaN_3) concent in the IgG1 isotype and 4B4-inhibiting antibody solutions affecting the results. To test this hypothesis, a control colony assay was performed in the presence of NaN_3. Figure 7.11 shows that addition of 15μM NaN_3 to H201 and R201 stables did not affect the colony forming abilities of H201 and R201 stable lines.

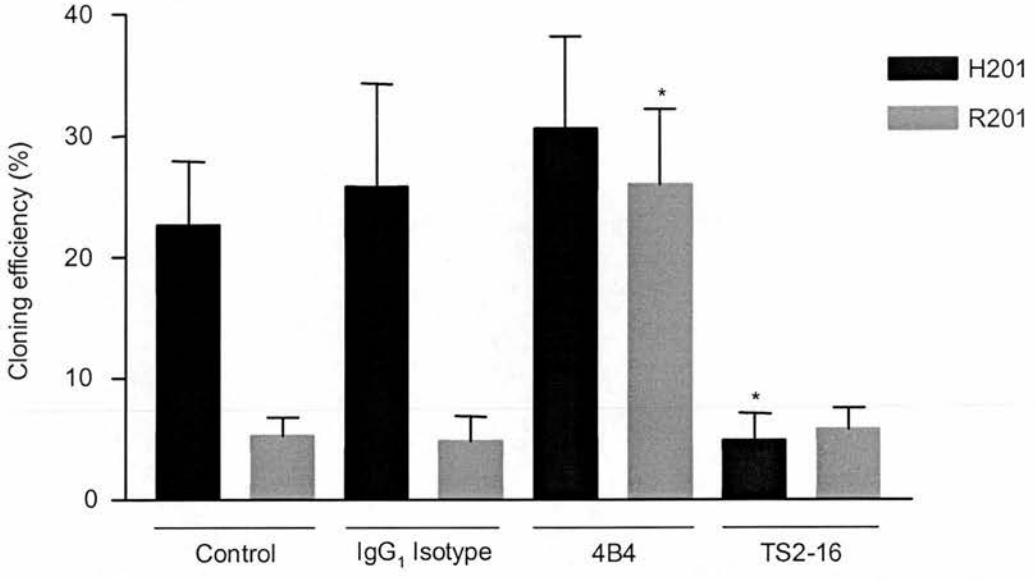

Figure 7.10 Anti β1-integrin antibodies affect colony formation by H201 and R201 stable lines.

Colony formation was determined in CHO-K1 cells stably expressing H201and R201 chimeras. Cells were plated out in triplicate in DMEM containing 5% serum and were left untreated (control) or treated with the addition of IgG_1 isotype, 4B4 or TS2-16 antibodies at 10μg/ml, and incubated at 37°C. Antibodies were added to the 0.3% agarose layer. Colonies were counted on day 6 and percentage cloning efficiency was calculated for each of the samples. Values represent mean ± SEM of 4 experiments. Statistical analysis was performed, * = $P<0.05$, compared with control sample within each individual stable line.

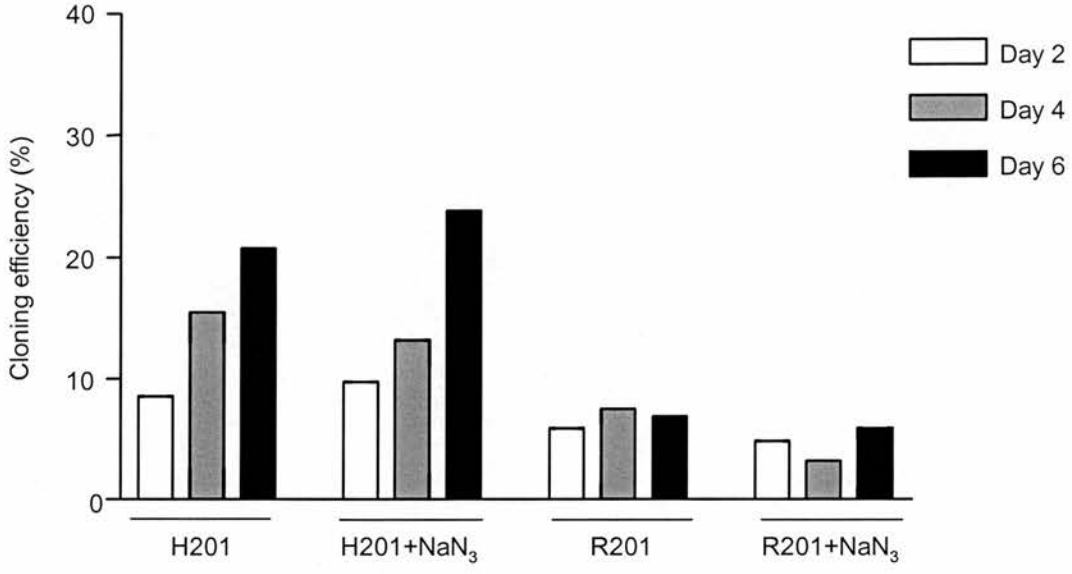

Figure 7.11 The NaN_3 content of antibody solutions does not affect colony formation by H201 and R201 stable lines.

Colony formation was determined in CHO-K1 cells stably expressing H201and R201 chimeras in DMEMB containing 5% serum ± 15μM NaN_3, and incubated at 37°C. Colonies were counted on days 2, 4 and 6. Percentage cloning efficiency was calculated for each of the samples.

7.4 Comparison of stable proliferation rates

Previous studies have demonstrated that transformed adherent cell types have the ability to proliferate in suspension. It was decided to compare the proliferation rates of control, R-Ras G38V and H-and R-Ras chimeric stable lines. Proliferation rates were assessed in conditions where cells were allowed to adhere.

7.4.1 Growth curves for stable lines

To assess the normal growth curves of the control, R-Ras G38V and H-and R-Ras stable lines, cells were seeded at $2x10^4$ cells per 10cm plate and ten plates were seeded for each stable line for each experiment.

Figure 7.12 shows the growth curves for control, R-Ras G38V and H-Ras N-terminal stables. Like the R-Ras G38V stable, CH3 and CH6 stables grow at a consistent, but slightly slower rate to control stables. The H197 stables reach a peak at Day 8 ($4.16x10^6 \pm 2.26x10^5$ cells) and then cell number begins to decrease. From Day 6, the H201 stables proliferate at a higher rate than the control cells, reaching a density of $5.3x10^6 \pm 5.21x10^5$ cells by day 10 compared with $4.78x10^6 \pm 1.06x10^5$ for control cells.

Figure 7.13 shows the growth curves for control, R-Ras G38V and R-Ras N-terminal stables. Like the R-Ras G38V stables, CH5 and R201 stables grow at a consistent, but slightly slower rate to control cells. The R197 stables reach a peak at day 8 ($3.19x10^6 \pm 2.84x10^5$) and then cell number begins to decrease. From day 8, the CH1 stables begin to proliferate at a higher rate than control cells, reaching a density of $5.5x10^6 \pm 1.4x10^5$ cells by day 10 compared with $4.78x10^6 \pm 1.06x10^5$ for control cells.

Statistical analysis showed that only the saturation densities (day 10 data) of the H197 and R197 stable lines were significantly lower than control, $P<0.01$ and $P<0.05$ respectively.

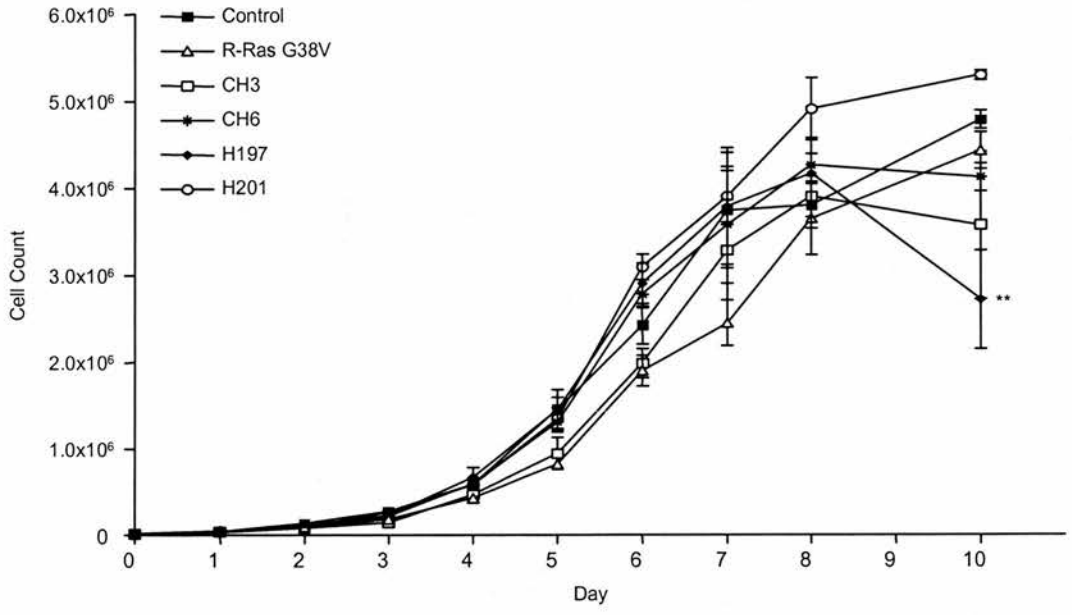

Figure 7.12 Growth curves of H-Ras G12V N-terminal stable lines

Proliferation was determined in CHO-K1 cells stably expressing H-and R-Ras chimeras. Cell number for each stable line was determined using a coulter counter on ten consecutive days. Values represent mean ± SEM of 3-6 experiments. Statistical analysis was performed on day 10 saturation densities , ** = $P<0.01$, compared with control sample.

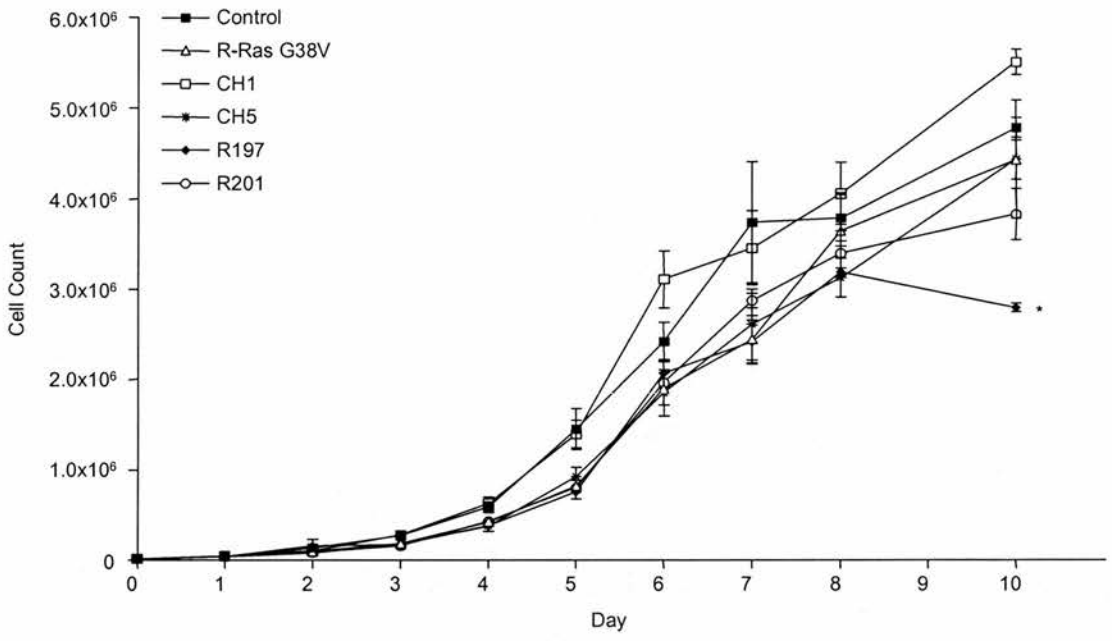

Figure 7.13 Growth curves of R-Ras G38V N-terminal stable lines

Proliferation was determined in CHO-K1 cells stably expressing H-and R-Ras chimeras. Cell number for each stable line was determined using a coulter counter on ten consecutive days. Values represent mean ± SEM of 3-6 experiments. Statistical analysis was performed on day 10 saturation densities, * = $P<0.05$, compared with control sample.

7.5 Discussion

In this chapter, the effects of H-Ras and R-Ras on cell motility and transformation have been investigated. Studies have been carried out using CHO-K1 cells stably expressing H- and R-Ras chimeras, with the aim of mapping the regions of H-Ras and R-Ras responsible for their effects on cell function. The major findings of this chapter are as follows: Expression of full-length H-Ras G12V reduces cell adhesion. Expression of full-length R-Ras G38V reduces chemotactic and haptotactic cell migration, while expression of H-Ras G12V only reduces haptotactic migration. H-Ras G12V sequences 60-174 are sufficient to increase proliferation rates of CHO cells however H-Ras sequences 1-174 are required to promote a fully-transformed phenotype, confirmed by anchorage-independent growth.

7.5.1 Cell motility

The initial attachment of many cell types to extracellular matrix proteins is a prerequisite for many adhesion-dependent processes including cell migration, survival and proliferation. A mathematical relationship between the extent of cell adhesion and migration has been described by Palecek *et al.*, (1997). These authors determined that the rate of cell migration could be plotted as an approximate bell-shaped curve against adhesion, whereby the extent of cell adhesion increases with increasing substrate concentration, cell surface integrin expression or increased integrin affinity. The adhesive state of the cell can potentially cause either an increase or decrease in cell migration, depending on where one starts on the bell-shaped curve (Holly *et al.*, 2000).

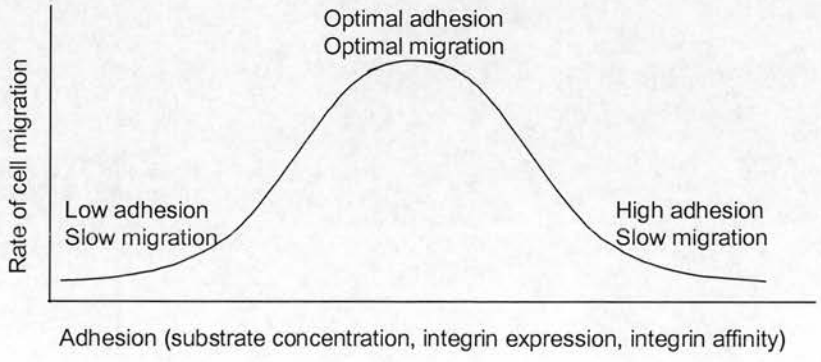

Integrins form a structural link between the extracellular matrix and the cell's cytoskeletal and signal transduction apparatus (Berrier *et al.*, 2000). Integrin affinity modulation is thought to be the major mechanism for activating the adhesion ability of the major platelet integrin $\alpha_{IIb}\beta_3$ (Ginsberg., *et al* 1992). Integrin affinity modulation and integrin avidity also stimulate adhesion mediated by leukocyte $\beta 2$ subunit-containing integrins (Schwartz *et al.*, 1995). Studies carried out using $\alpha\beta$-py cells represent a useful system for the interactions between integrins and substrate, as CHO-K1 cells do not express an endogenous receptor for fibrinogen. This was highlighted by Huttenlocher *et al.*, (1996) who showed that the migration of $\alpha_{IIb}\beta_3$–expressing CHO-K1 cells on a fibrinogen substrate was inhibited by a specific fibrinogen receptor peptide, RO43-5054, and a function-blocking antibody specific to the $\alpha_{IIb}\beta_3$ receptor, 2G12. Using $\alpha\beta$-py cells, transiently transfected with H-Ras G12V and R-Ras G38V, revealed that H-Ras G12V resulted in a significant ($P<0.01$) reduction in $\alpha\beta$-py cell adhesion to the $\alpha_{IIb}\beta_3$ ligand fibrinogen (Figure 7.1). The levels of adhesion with control and R-Ras G38V transfected cells were about two fold greater than observed with H-Ras G12V expressing cells (Figure 7.1). Zhang *et al.*, (1996) demonstrated that constitutively active R-Ras G38V could enhance the adhesion of CHO2b3a cells which express the full length $\alpha_{IIb}\beta_3$ integrin, in a low affinity state, (O'Toole *et al.*, 1991; O'Toole *et al.*, 1994) by enhancing the ligand binding affinity of the $\alpha_{IIb}\beta_3$. That R-Ras G38V enhances adhesion in the CHO2b3a cells but confers levels of adhesion similar to control in the $\alpha\beta$-py cells can be explained by the basal $\alpha_{IIb}\beta_3$ affinity state of the model cell systems, which is constitutively low in the CHO2b3a cells and constitutively high in the $\alpha\beta$-py cells. A number of recent studies carried out to investigate the effects of integrin signalling on the initial attachment and subsequent spreading of cells on substratum may help to elucidate the reasons for the differences between H-Ras G12V and R-Ras G38V mediated cell adhesion.

The reduced cell adhesion observed with the H-Ras G12V transfected $\alpha\beta$-py cells to fibrinogen may simply be explained by the suppression of the $\alpha_{IIb}\beta_3$ integrin (shown in Chapters 3 and 4). In its inactive conformation, this integrin has a reduced capacity to bind to its ligand, fibrinogen. Conversely, R-Ras has no overall effect on cell adhesion, compared to control cells. R-Ras promotes an activated integrin state

and therefore expression of R-Ras in αβ-py cells, expressing the constitutively active $\alpha_{IIb}\alpha_{6A}\beta_3\beta_1$ chimera should not affect cell adhesion. For the cell adhesion assays, an incubation time of 15 minutes was used as this was found to be the optimal time point for observing differences between the transiently transfected cells. H-Ras G12V transfected cells, left to adhere for longer time points showed levels of adhesion comparable to control vector or R-Ras G38V transfected cells.

R-Ras has previously been implicated in the control of integrin-mediated adhesion, converting the suspension-cell lines, mouse 32D and human myeloid cells, into highly adherent cells (Zhang *et al.*, 1996). Expression of R-Ras G38V also induces the adhesion of bone-marrow-derived mast cells through activation of $\alpha_5\beta_1$ (Kinashi *et al.*, 2000). The Ras-like small GTPase, Rap1, has also been shown to be involved in integrin-mediated cell adhesion (Bos *et al.*, 2003; Caron, 2003). Katagiri *et al.*, (2000) showed that, in Jurkat cells, the introduction of Rap1 induces integrin αLβ2 (LFA1)-mediated adhesion to ICAMS. Furthermore, in Jurkat cells, ligation of the adhesion molecule CD31 induces activation of αLβ2, which was inhibited by blocking Rap1 signalling (Reedquist *et al.*, 2000). The studies mentioned show, by using the binding of a soluble ligand (Katagiri *et al.*, 2000) or a conformation-specific antibody (Reedquist *et al.*, 2000; Katagiri *et al.*, 2000) rather than mere adhesion to substratum (which results from both inside-out and outside-in signalling), that Rap1 controls inside-out rather than outside-in signalling to integrins in Jurkat cells. Although it remains to be established whether active R-Ras induces cell adhesion through activation of Rap1, it has been shown that RapGAP expression blocks R-Ras-induced effects in several cell types, which suggests that Rap1 acts downstream of R-Ras (Self *et al.*, 2001).

The fibronectin receptor (FnR) of CHO cells is the counterpart of the human VLA_5 or α5β1 (Hemler, 1990). The α5β1 expressed by adherent cells (such as CHO cells) is intrinsically activated, and the maintenance of this activated state is dependent on intracellular signalling (Faull *et al.*, 1994). As previously mentioned, R-Ras can induce the adhesion of bone-marrow-derived mast cells to fibronectin through activation of $\alpha_5\beta_1$ (Kinashi *et al.*, 2000). In contrast, H-Ras G12V expression has been shown to markedly reduce the levels of a β_1-dependent osteoblast adhesion to fibronectin (FN) via signals mediated by the Raf-1/ERK pathway, as demonstrated

by the H-Ras G12V Y40C mutant (Tanaka *et al.*, 2002). Despite the contrasting effects of activated H-Ras and R-Ras on cellular adhesion mediated though $\alpha_5\beta_1$, no significant changes in cell adhesion were observed with the H-and R-Ras CHO-K1 stable lines plated onto fibronectin (Figure 7.2). If H-Ras G12V expression reduces the levels of adhesion in CHO cells via signals mediated by the Raf-1/ERK pathway, like that observed with osteoblasts, then the insignificant levels of Raf-1/ERK activation seen with expression of the chimeras in Chapter 4 (Figures 4.4, 4.5 and 4.6) may explain the negligible effects on CHO cell adhesion.

Integrins play an important role during cell migration by linking the extracellular matrix and the actin cytoskeleton and by transmitting the forces required for migration (Laufenburger and Horwitz, 1996). Cell migration plays a central role in diverse processes including embryonic development, wound healing, inflammation and tumour metastasis (Huttenlocher *et al.*, 1998). Migration can be divided up into four distinct phases: initial attachment, spreading, contraction and tail retraction (Holly *et al.*, 2000). Each phase of cell migration requires the regulation of integrin-mediated ligand binding.

Since integrins play an important role in cell migration, the effects of H-Ras G12V- and R-Ras G38V-mediated integrin affinity on cell motility were investigated. Using $\alpha\beta$-py cells, transiently transfected with H-Ras G12V and R-Ras G38V, migration assays revealed that expression of R-Ras G38V significantly inhibited both chemotactic and haptotactic migration ($P<0.05$) (Figure 7.4). Huttenlocher *et al.*, (1996) found that an inverse relationship between focal adhesion organisation and cell migration rates existed, using CHO cells expressing an $\alpha_{IIb}\Delta 9966\beta_3$ mutant (which produced increased organisation of focal adhesions and actin microfilament bundles). Dunlevy and Couchman, (1993) also showed that fibroblast migration rate decreases as focal adhesion increases. In Chapter 6, (Figure 6.3) expression of R-Ras G38V in CHO cells was shown to increase the size and number of focal adhesions. Therefore, the reduced migration of R-Ras G38V transfected cells could be as a result of increased focal adhesion assembly. The increase in focal adhesion assembly may impede cell detachment from matrix, resulting in reduced migration rate. As H-Ras G12V transfected cells showed reduced adhesion (Figure7.1) and a reduced number of focal adhesions (Figure 6.3), it was hypothesised that they might show an

increase in cell migration. Results revealed that levels of chemotactic migration (towards serum) in H-Ras G12V transfected cells are slightly higher than those observed with control cells, while levels of haptotactic migration are lower than with control cells (Figure 7.3). That H-Ras G12V expression reduced haptotactic and not chemotactic migration may be interpreted as follows: chemotactic migration may be limited by the ability of the cell to release adhesions at the cell rear (tail retraction), thus in H-Ras G12V expressing cells the increased rate of adhesive release at the rear of the cell, caused by suppression of integrins, may promote the increase in migration. However, haptotactic migration may be inhibited by an inability to form adhesions at the cell front that are strong enough to mediate the migration through the transwell membrane.

Haptotactic migration assays with R-Ras G38V and H-and R-Ras stable lines demonstrated no significant difference between the stable lines compared with control cells on a fibronectin matrix (Figure 7.4). In CHO cells, $\alpha_5\beta_1$-mediated activation of Rac1 and Cdc42 is maximal at intermediate fibronectin levels whereas Rho activity continues to increase with increasing fibronectin levels (Cox *et al.*, 2001). Since Rac1 and Cdc42 promote, but RhoA inhibits membrane protrusions, increased integrin-mediated activation of Rho halts migration in these cells (Cox *et al.*, 2001). Expression of chimeras CH3, CH6 and R201, which promote an activated state of integrin, therefore increasing integrin-ligand binding, may inhibit migration through increased activation of Rho. Studies with H-Ras G12V transiently transfected $\alpha\beta$-py cells show an inhibition of haptotactic migration, which may be due to an inability to efficiently form adhesions at the cell front to mediate migration. By reducing ligand-integrin binding (suppressed integrins) in chimeras CH1, CH5 and H201, the decreased RhoA activity may result in the reduced degree of haptotactic migration. Studies to investigate the levels of RhoA activity in the cells expressing H-Ras G12V or R-Ras G38V would determine if RhoA activity is affected by the expression of these proteins. Rho activity in these cells could be investigated using the method described by Nobes and Hall, (1999) who determined Rho activity in Swiss 3T3 fibroblasts by visualising the formation of stress fibres, since Rho activity is required for both the formation and maintenance of actin stress fibres and focal adhesions (Ridley and Hall, 1992; Hotchin and Hall, 1995).

Other cell signalling pathways have also been implicated in control of cell migration. Cellular transformation by H-Ras is associated with increased MAP kinase activity and enhanced cell proliferation and migration in human breast epithelial cells (Ochieng *et al.*, 1991). A study by Klemke *et al.*, (1997) provided evidence that MAP kinase (ERK1 and ERK2) signalling can regulate cell migration by directly impacting the migratory machinery. MAP kinase enhances the activity of myosin light chain kinase (MLCK) leading to the phosphorylation and increased function of myosin light chain (MLC) (Klemke *et al.*, 1997). MLC promotes myosin ATPase activity and polymerisation of actin, resulting in a fully functional actin-myosin motor unit used to generate the contractile force required for cell motility (Klemke *et al.*, 1997).

Wound assays examine the cell's ability to migrate once contact-inhibition has been removed. Where cells are in contact with each other, cadherins as well as integrin receptors co-ordinately regulate cell migration (Huttenlocher *et al.*, 1998). Cadherins promote strong intercellular adhesions, and their expression is associated with decreased tumor cell invasiveness and metastasis *in vivo* (Takeichi, 1993). Two probable mechanisms for this inhibition are increased cell-cell adhesion and effects on cell motility (Chen and Obrink, 1997; Chen *et al.*, 1997). Wound assay studies by Huttenlocher *et al.*, (1998) which examined the effects of integrin-mediated signalling on myoblast migration, revealed that enhanced integrin-mediated signalling promotes contact-mediated inhibition of migration by N-cadherin and as a result wound closure was inhibited. Huttenlocher *et al.*, (1998) demonstrated that enhanced adhesive signalling through ectopic α_5 or β_1 expression on myoblasts, led to an upregulation of N-cadherin expression and inhibition of cell migration through enhanced cell-cell aggregation and cessation of motile activity. Integrin-mediated signalling is required for the cessation of motile activity, as ectopic N-cadherin expression alone does not result in contact-mediated suppression of motile activity that is seen in ectopic α_5-expressing myoblasts (Huttenlocher *et al.*, 1998).

The characteristics of contact-mediated suppression of motile activity can be seen with the CH3, CH6 and H197 stables (Figure 7.6) where cells demonstrate aggregation and delayed wound closure (compared with control cells, Figure 7.5). Stable expression of R-Ras G38V and R201 (Figures 7.5 and 7.7 respectively) both

show signs of inhibited wound closure however this was not accompanied by any cell aggregation. An increase in the number of focal adhesions (promoting cell spreading) and RhoA activation (which inhibits cell migration) by increased integrin-mediated signalling may explain the complete cessation of migration by these cell lines.

Transient expression of CH1, CH5 and H201 has previously been shown to mediate integrin suppression (Chapter 4, Figure 4.2). The resulting decrease in integrin-mediated signalling may therefore release the contact-mediated inhibition. In support of this, CH5 and to a lesser extent CH1 stable lines both initiate wound closure (Figure 7.7). The CH1 and CH5 cells do not display aggregated growth to the same extent as CH6 and H197; this could be explained by a reduction of N-cadherin regulation. Although H201 expression also suppresses integrins, there was a complete cessation of cell motility observed in the forty-eight hour wound assay (Figure 7.6). This could be explained by a reduced ability of integrins to form adhesive contacts at the leading edge of the cells that are strong enough to mediate the migration, thus disrupting the balance between cell adhesion and detachment required for cell migration. The formation of focal adhesions and actin stress fibres could be compared for each stable line during the wound assays by fixing the wounds at specified time points, and then staining the cells with anti-vinculin antibody (vinculin is a protein which is localised to focal adhesions) or rhodamine-conjugated phallodin (which binds to F-actin).

It is important to note that the effects of H-Ras G12V and R-Ras G38V expression on cell motility are cell-type and integrin specific. We have found that expression of activated R-Ras significantly inhibits cell migration of $\alpha\beta$-py cells on fibrinogen and has no significant effect on CHO cell migration on fibronectin. However, R-Ras has been shown to enhance migration in breast epithelial cells on collagen through the α_2 integrin cytoplasmic domain (Keely *et al.*, 1999). Here, expression of H-Ras G12V has been shown to reduce adhesion of $\alpha\beta$-py cells on fibrinogen, conversely H-Ras has been shown to activate $\alpha_5\beta_1$ in mast cells to stimulate adhesion on fibronectin (Kinashi *et al.*, 2000).

7.5.2 Cellular transformation

Many mammalian cell types are dependent on adhesion to the extracellular matrix for their continued survival. Primary cells of epithelial (MDCK) and endothelial (HUVEC) origin undergo rapid apoptosis when denied proper substrate adhesion in a process called anoikis (Frisch and France, 1994). Transformed cells are frequently characterised by their ability to grow in the absence of contacts with a solid extracellular matrix (Stoker *et al.*, 1968). As well as the ability to proliferate in suspension, other properties commonly associated with the transformed phenotype induced by most oncogenes include a loss of density-dependent growth, enhanced growth rates and a reduction in the requirement for serum growth factors (Cox and Der , 1994). Here, the effects of H-Ras G12V, R-Ras G38V and H-and R-Ras chimera expression on CHO cell transformation have been investigated using anchorage-independent growth assays (colony assays) and proliferation assays.

Results from colony assays carried out with CHO cells show a significant increase in percentage cloning efficiency with H-Ras G12V transfected cells in 1% serum and 5% serum conditions ($P<0.01$ and $P<0.001$ respectively) (Figure 7.8A and B). Results suggested that transient transfection of H-Ras G12V in CHO-K1 cells confers a transformed phenotype that is capable of anchorage-independent growth in serum-deprived conditions. Transient transfection of CHO-K1 cells with R-Ras G38V did not confer a transformed phenotype, percentage cloning efficiency was significantly lower that that observed with H-Ras G12V transfected cells in both 1% and 5% serum conditions ($P<0.001$ and $P<0.01$ respectively).

Anchorage-independent growth assays were carried out with the H-and R-Ras chimera stable lines to try and elucidate if any specific regions of H-Ras G12V have the ability to confer a transformed phenotype. The only stable line to display a significant increase in percentage cloning efficiency was the H201 stable line (Figure 7.9). This suggests that H-Ras sequences 1-174, which include the effector binding domains and C-terminal integrin-affinity modulating sequences, are required to confer significant anchorage-independent growth. It was of interest to note that stable lines that have an R-Ras like effect on the integrin affinity state i.e. CH3, CH6, H197, R197 and R201 (Chapter 4, Figure 4.2) demonstrated cloning efficiencies

consistently less than control cells. The results suggest a relative trend between integrin affinity state and cloning efficiency.

Alterations in integrins have been shown to play a role in the phenotype of transformed cells. Studies on rodent cell lines have shown that the level of expression of the $\alpha_5\beta_1$ integrin (fibronectin receptor), is reduced in Ras-transformed cells compared to normal cells (Plantefaber and Hynes, 1989), resulting in anchorage-independent growth in agar and tumor formation in nude mice (Giancotti and Ruoslahti, 1990) and that elevated levels of $\alpha_5\beta_1$ can suppress the transformed phenotype of CHO cells. Results here confirm the transforming abilities of H-Ras G12V in CHO-K1 cells (Figure 7.8). Confirming that H-Ras G12V is not only capable of suppressing the chimeric integrin expressed on $\alpha\beta$-py cells, but that it is also capable of suppressing the endogenous integrins such as $\alpha_5\beta_1$.

Further investigations of the role of the $\alpha_5\beta_1$ integrin in anchorage-independent growth, were carried out using the most H-Ras-like and R-Ras-like stable lines (H201 and R201 respectively) along with β_1-integrin mAbs. The β_1 integrin activating (TS2-16) and blocking (4B4) monoclonal antibodies bind to residues 207 to 218 of the β_1 subunit (Takada and Puzon, 1993). Studies have suggested that activating mAbs may change the conformation of the β_1 subunit upon binding, and that this is a direct antibody-induced change that does not require intracellular signalling (Faull *et al.*, 1993). It has been suggested that activating mAbs might fix the conformation in an activated state, while inhibiting mAbs may fix the integrin conformation in an inactive conformation (Takada and Puzon, 1993). The finding that anchorage-independent growth could be abrogated by a function-activating β_1 antibody (TS2-16) and enhanced by a function-blocking β_1 antibody (4B4), confirms a β_1 integrin-mediated role in CHO cell transformation (Figure 7.11).

The loss of fibronectin matrix assembly has been associated with acquisition of a transformed phenotype. Hughes *et al.*, (1997) showed that expression of H-Ras G12V in fibroblasts resulted in decreased fibronectin matrix assembly. Transformed cells frequently show decreased synthesis and increased degradation of fibronectin (Olden and Yamada, 1977). A study by Brenner *et al.*, (2000) showed that matrix formation by HT1080, human fibrosarcoma, cells was triggered by decreasing the

amount of Ras signalling with a MEK1 inhibitor or by increasing integrin activity with an anti-β_1 integrin stimulatory antibody. If fibronectin matrix assembly is linked to cellular transformation then observations made in this study, see Figure 7.10, suggest that the integrin-suppressing ability of the H201 chimera or the function blocking anti-β_1 antibody, 4B4, promote anchorage-independent growth by reducing the ability of the cells to form a fibronectin matrix and that these effects can be negated by addition of the function activating anti-β_1 antibody, TS2-16. The integrin-activating ability of R201 may enhance levels of $\alpha_5\beta_1$ activation, which has been shown to suppress the transformed phenotype of CHO cells (Giancotti and Ruoslahti, 1990). Expression of R201 may increase fibronectin matrix assembly by activating the $\alpha_5\beta_1$ integrin and this activity can be blocked using the anti-β_1 antibody 4B4. It would be of interest to determine if the magnitude of matrix assembly by chimera stable-lines is inversely related to the ability to promote anchorage-independent growth.

Enhanced growth rates and saturation densities were observed with the CH1 and H201 stable lines (Figures 7.12 and 7.13), suggesting that H-Ras sequences 60-174 are sufficient to promote the characteristic increase in proliferation rates observed with transformed cells. However, as only the H201 stable line (H-Ras sequences 1-174) showed any significant ability to promote anchorage-independent growth would suggest that for a fully transformed phenotype, the N-terminal effector binding sequences of H-Ras are also required. The downstream effectors of H-Ras have been associated with cellular transformation. PI 3-Kinase activation has been implicated in anchorage-independent growth, metastasis and cell invasion (Shaw *et al.*, 1997; Keely *et al.*, 1997) and with integrin-dependent proliferation through the downregulation of p27kip resulting in cyclin D1 induction (Feng *et al.*, 2000). Integrin-mediated proliferation also depends on the activation of the ERK1/2 pathway, which controls expression of cyclin D1 and p21cip (Brakebuch *et al.*, 2002). Integrins and growth factor receptors regulate some of the same signalling pathways; in many instances both are required for activation of downstream signalling events. It has been hypothesised that constitutive activation of the downstream signalling events by oncogenes overrides the requirement for integrin activation, resulting in increased proliferation and anchorage-independence. Studies

have shown that the loss of integrin-mediated adhesion inhibits the activation of MAP kinase by serum or active forms of Ras and Raf (Lin *et al.*, 1997; Renshaw *et al.*, 1996). However, cytoplasmic oncogenes may provide a constitutively activated signal, usually initiated by ligand-bound integrins, and in doing so overcome anchorage dependence (Sethi *et al.*, 1999). Expression of oncogenic Ras and Raf can induce ERK1/2 activation in suspension cells to levels which revoke the need for adhesion, resulting in anchorage-independent survival (Schwartz, 1997). However, as the H-and R-Ras chimeras were incapable of activating Raf and ERK1/2 to levels observed with full-length H-Ras G12V (Chapter 4, Figures 4.4, 4.5 and 4.6), then it is unlikely that the increased proliferation rates observed with CH1 and H201 and the anchorage-independent growth of H201 stables are simply due to activation of the ERK1/2 pathway.

Upon engagement of integrins to ECM proteins, PI 3-kinase becomes constitutively activated to a significant level in MDCK cells (Khwaja *et al.*, 1997). The PI 3-kinase lipid products provide a protective signal acting through PKB/Akt, which has previously been reported to be required for cell survival (Yao and Cooper, 1996). Upon cell detachment from matrix, PI 3-kinase and PKB/Akt become inactive, even in the presence of serum factors and an apoptosis pathway is engaged. The ability of oncogenic Ras to activate PI 3-kinase, by binding directly to p110 (Rodriguez-Viciana *et al.*, 1994, Rodriguez-Viciana *et al.*, 1996), and hence PKB/Akt, in the absence of adhesion to the ECM, promotes anchorage-independent survival. As PI 3-kinase has also been implicated in cell proliferation, it would be interesting to assess the abilities of the chimeras to activate PI 3-kinase using either PI 3-kinase assays or by western blot analysis with phospho-AKT antibodies. It would also be interesting to determine whether PI-3-kinase inhibitors affect cell growth and to find out if proliferation rates are a consequence of cell survival or cell death eg. by measuring levels of apoptosis.

The results here show that H-Ras G12V can transform CHO cells. However, while R-Ras is incapable of transforming CHO cells, it has demonstrated transforming abilities in NIH3T3 cells, inducing anchorage-independent growth (Cox *et al.*, 1994) and foci-formation (Hansen *et al.*, 2002). Investigations show that the effects of H-Ras and R-Ras are cell type specific. Studies of the transforming effects of Ras or

Ras effectors make use of rodent cell lines due to their ease of transfection and because they are easily transformed by oncoproteins (Gupta *et al.*, 2000). However, it is possible that rodent models may not accurately reflect the functional consequences of the expression of oncogenic Ras proteins in human cells. Further investigations to compare transforming abilities of H-Ras and R-Ras in a human cell line to their transforming abilities in CHO cells would be appealing.

7.5.3 Summary

The extent of cell adhesion and cell migration rate can both be affected by integrin affinity state. Cell adhesion assays revealed that expression of full-length H-Ras G12V (which suppresses integrin affinity) reduced CHO cell adhesion to fibrinogen. Cell migration assays revealed that H-Ras increased chemotactic migration of CHO cells however, haptotactic migration was reduced. The reduced degree of haptotactic migration of H-Ras G12V transfected cells is probably due to the suppressive effects upon the integrins, which prevent the formation of adhesive contacts at the front of the cell required for directional migration. Integrin activation in R-Ras G38V transfected cells results in increased cell spreading and focal adhesion formation, which in turn inhibits CHO cell migration in chemotactic and haptotactic migration assays. Stable lines expressing the H-and R-Ras chimeras had little overall effect on CHO cell adhesion and rate of migration.

Transient expression of full-length H-Ras G12V and stable expression of H201 both resulted in anchorage-independent growth of CHO cells, indicative of a transformed phenotype. As H201 stable cells were the only chimeric stables to induce a transformed phenotype, suggests that the entire 174 N-terminal stretch of H-Ras (1-174) is required to confer a transformed phenotype in CHO cells. Anchorage-independent growth appears to be influenced by the activation state of the CHO cell β_1 integrin since suppression of the integrin by expression of H-Ras G12V or H201, or by the use of a the β_1–blocking antibody, 4B4, leads to anchorage-independent growth. In contrast, activation of the integrin by expression of R-Ras G38V or R201, or the use of the β_1–activating antibody prevents anchorage independent growth. These results may be a consequence of the changes in fibronectin-matrix assembly, which has been shown to be mediated via the $\alpha_5\beta_1$ integrin and reduced in transformed cells.

Chapter 8

Concluding remarks and future directions

In order to achieve correct cellular function, the interactions between integrins and their ligands must be strictly regulated. The rapid activation of integrins is essential for the ability of a cell to respond to environmental changes. Integrins in the β_1, β_2, β_3 and β_7 subfamilies have been shown to modulate their integrin-binding affinity through conformational changes, in response to inside-out signalling (Hughes and Pfaff, 1998). A number of intracellular signalling pathways have been implicated in modulating integrin affinity; however they have yet to be fully defined. Recent studies have indicated that the Ras family of small GTP-binding proteins, and their effectors, play a crucial role in integrin affinity modulation (Keely *et al.*, 1998; Hughes *et al.*, 1997).

Despite their sequence homology and overlapping use of effectors and GEFs, H-Ras and R-Ras have different functional effects on integrins. In CHO cells, expression of R-Ras promotes the active integrin state while expression of H-Ras suppresses integrin activation. Furthermore, co-expression of active R-Ras G38V with active H-Ras G12V, in CHO cells, reversed H-Ras-mediated integrin suppression (Sethi *et al.*, 1999). The central aim of this thesis was to use a series of H-and R-Ras chimeras to elucidate the role, if any, the sequence variations in H-Ras and R-Ras may play in their differing properties with respect to integrin affinity modulation. Table 8.1 shows the effects of the chimeras on integrin affinity, compared to H-Ras and R-Ras, and their effects on ERK1/2 phosphorylation.

The H/R-Ras chimeras imply that the C-terminal sequences of H-Ras and R-Ras are critical to determining their different effects on integrin affinity. More specifically, a 25-amino acid stretch of H-Ras (Arg^{149} to Pro^{174}) is required for integrin suppression, and a 28-amino acid stretch of R-Ras (Leu^{175} to Pro^{203}) is sufficient to reverse H-Ras mediated integrin suppression. Like H-Ras G12V, chimeras CH1, CH5 and H201, all suppressed integrin affinity. However, only H201 induced integrin suppression correlated with ERK1/2 activation, which suggests that Ras-induced integrin

suppression may be independent of the bulk activation of ERK1/2. Recently, PLCϵ has been identified as a new H-Ras effector (Wing *et al.*, 2003). Work carried out by our group has implicated PLCϵ in a Raf-independent integrin suppression pathway. PLCϵ has been shown to be activated by the H-Ras E37G mutant (which does not bind Raf) and that kinase-dead PLCϵ blocks H-Ras-mediated integrin suppression (personal communication, Dr. Yatish Lad). Results presented in this thesis also imply the presence of a Raf-independent integrin suppression pathway; the CH1, CH5 and H201 chimeras all demonstrate the ability to confer integrin suppression despite being less competent at activating Raf-1 than H-Ras G12V.

Characterisation of the H-and R-Ras chimeras suggested an important role for the R-Ras G38V proline-rich domain Ras (residues Pro^{199} to Pro^{206}), particularly for the reversal of H-Ras-mediated integrin suppression. This domain has been shown to bind the adaptor protein Nck (Wang *et al.*, 2000) and so it was hypothesised that the relationship between R-Ras and the Nck adaptor protein may be important for conferring R-Ras's properties. However, a publication released during the course of the write-up of this thesis, showed that alanine substitution of the proline-rich domain had no effect on the R-Ras modulation of integrin function (Hansen *et al.*, 2003). Investigations using H-and R-Ras chimeras demonstrated that R-Ras amino acids Tyr^{193} to Pro^{203}, which include the proline-rich domain, are necessary but not sufficient, for increased integrin activation (Hansen *et al.*, 2003). This area overlaps with the HVR linker domain of R-Ras. Results from this thesis would suggest that sequences N-terminal to the residues Tyr^{193} to Pro^{203} of R-Ras are involved (the 28-amino acid stretch from Leu^{175} to Pro^{203}).

It has been hypothesised that one way in which H-Ras and R-Ras could confer their contrasting properties is by targeting to different membrane microdomains. H-Ras has been demonstrated to redistribute from lipid rafts into the bulk plasma membrane upon GTP-loading (Niv *et al.*, 2002; Prior *et al.*, 2001; Prior *et al.*, 2003). Experiments were carried out to disrupt the membrane cholesterol content of CHO cells, in order to help determine the importance of membrane localisation with regards to integrin affinity modulation and to help reveal the subcellular localisation of R-Ras. Results demonstrated that cholesterol depletion, and subsequent disruption of lipid rafts, had no effect on the abilities of H-Ras and R-Ras to modulate integrin

affinity. However, the ability of R-Ras to mediate its effect on integrin affinity was diminished by the repletion of membrane cholesterol in the form of inclusion complexes.

We had hypothesised that the reason that lipid raft disruption had no effect on the ability of R-Ras to modulate integrin affinity might be due to a similar redistribution of the GTP-bound protein as that observed with activated H-Ras i.e. migration out of the cholesterol sensitive lipid rafts and into the bulk plasma membrane. Attempts to produce GFP-tagged R-Ras constructs to confirm this were unsuccessful due to poor sequencing of the N-terminal R-Ras residues. Investigations by Hansen *et al.*, (2003) showed that the activated mutant GFP-R-Ras 87L seemed to be more enriched in lipid rafts/caveolae fractions than wildtype GFP-R-Ras. This suggests that unlike H-Ras, which upon activation migrates out of the lipid rafts/caveolae, R-Ras does not and is in fact more enriched in these fractions when activated. Further investigations by these authors, using GFP-tagged H-and R-Ras chimeras demonstrated that the microlocalisation of these proteins specifies their capacity to activate downstream effectors, such as Raf-1, but does not correlate with their effects on integrins (Hansen *et al.*, 2003). This would explain why MβCD treatment of CHO cells had no effect on H-Ras-and R-Ras-mediated integrin affinity.

The diminished R-Ras effects on integrin affinity following the addition of inclusion complexes may be explained by the targeting of activated R-Ras to cholesterol sensitive lipid rafts (Hansen *et al.*, 2003). It had been hypothesised that perhaps the addition of cholesterol inclusion complexes resulted in some form of steric hindrance. This seems to be a very likely situation since we now know that activated R-Ras is targeted to microdomains sensitive to cholesterol content. The addition of inclusion complexes may increase the basal levels of cholesterol found in lipid rafts and as a result may prevent normal R-Ras signalling. Using GFP-tagged R-Ras (wt) and (G38V) constructs, confocal microscopy could be used to visualise the effects of MβCD treatment on R-Ras membrane microlocalisation.

The cellular consequences of H-Ras-and R-Ras-mediated integrin affinity have also been investigated in this thesis. The adhesion of H-Ras G12V transfected $\alpha\beta$-py cells on fibrinogen is significantly reduced, suggesting that H-Ras G12V–mediated

integrin suppression (of the chimeric integrin) does affect cell adhesion. Confocal microscopy has revealed that these cells have a rounded shape with reduced numbers of focal adhesions. In contrast, R-Ras G38V transfected cells have an increased number of focal adhesions and a well-spread polygonal shape and cells adhere as well as to fibrinogen as the control $\alpha\beta$-py cells.

Cell migration requires the transient adhesion and detachment of the cell at the leading and trailing edge respectively (Lauffenburger and Horwitz, 1996). These effects can be mediated by the cycling of focal adhesions during cell ligation (Petit and Thiery, 2000). The integrin-activating effect of R-Ras G38V reduces both chemotactic and haptotactic migration of $\alpha\beta$-py cells, this is probably due to the increased number of focal adhesions. H-Ras G12V reduced haptotactic migration, this may be due to the suppressed state of the integrin and may inhibit the formation of adhesions at the cell front that are strong enough to mediate the migration through across the matrix

The H-and R-Ras chimeras had no overall effect on CHO cell adhesion to fibronectin or cell migration. This suggests that cell adhesion and migration, although partially correlating with integrin affinity state, also rely on downstream effectors involved with cytoskeletal machinery. A study by Klemke *et al.*, (1997) provided evidence that MAP kinase (ERK1 and ERK2) signalling can regulate cell migration by directly impacting the migratory machinery. ERK1/2 enhances the activity of myosin light chain kinase (MLCK) leading to the phosphorylation and increased function of myosin light chain (MLC) (Klemke *et al.*, 1997). The low levels of ERK1/2 activation seen by the H-and R-Ras chimeras may explain their insignificant effect on CHO cell migration, despite mediating effects on integrin affinity.

CHO cells are readily transformed by H-Ras, resulting in anchorage-independent growth. Of all the chimeras only H201 showed any transforming abilities, which suggests that H-Ras amino acids 1-174 are required to confer a transformed phenotype. Investigations into how integrin affinity state influences cellular transformation has suggested that suppression of the β_1-integrin, by H201 expression or by use of a β_1-integrin blocking antibody (4B4), can increase anchorage-independent growth. In contrast, activation of this integrin either by expression of the

R201 chimera or by use of a β_1-integrin activating antibody (TS2-16) inhibits anchorage-independent growth. It would be of interest to investigate the effects that the β_1-integrin antibodies alone have on control cells.

It is important to note that the investigations described in this thesis have relied on the over-expression of proteins, which may affect normal cellular events. It would be interesting to use methods such as siRNA and dominant negative protein expression, and compare results to control cells, to further substantiate the findings made here. Also, further analysis of the 3D-protein structures of the chimeric proteins may help to elucidate whether the folding of the proteins impairs the normal interactions with effectors, compared with full length H-Ras and R-Ras.

Overall, this thesis has highlighted the importance of the HVR domain and N-terminal sequences to the HVR, in conferring the contrasting abilities of H-Ras G12V and R-Ras G38V to mediate integrin affinity. All chimeras containing H-Ras residues Arg^{149} to Pro^{174} suppressed integrin affinity (CH1, CH5 and H201)., conversely all chimeras containing R-Ras residues Leu^{175} to Pro^{203}) reversed H-Ras G12V-and Raf-BxB CAAX- mediated integrin suppression (CH3, CH6 and R201). The microlocalisation of H-Ras and R-Ras does not correlate with their effects on integrins. The extreme C-terminal residues of H-Ras and R-Ras, while important for targeting the plasma membrane, are not necessary for mediating integrin affinity modulation. The N-terminal and HVR sequences of H-Ras are required for CHO cell transformation, which suggests that integrin state alone is not sufficient to confer a transformed phenotype but the signalling to downstream effectors is also required.

Table 8.1 provides a summary of all the findings made in this thesis with regards to the H-and R-Ras chimeras; please refer to schematic representation of chimeras for sequence comparisons

Chimera	Integrin affinity	Reversal of H-Ras suppression	Reversal of Raf-BxB CAAX suppression	ERK1/2 Activation	Cell Morphology (EM micrographs)	Anchorage-independence
Full-length R-Ras	Activated	***	***	+	Well spread, smooth edges	N/A
Full-length H-Ras	Suppressed	N/A	N/A	+++	Rounded, ruffled edges and surface blebbing	***
CH3	Activated	***	***	+	R-Ras-like	N/A
CH6	Activated	***	***	+	R-Ras-like	N/A
H197	Little effect	*	*	+	H-Ras-like	N/A
H201	Suppressed	N/A	N/A	++	H-Ras-like	***
CH1	Suppressed	N/A	N/A	+	H-Ras-like	N/A
CH5	Suppressed	N/A	N/A	+	R-Ras-like	N/A
R197	Little effect	*	*	+	H-Ras-like	N/A
R201	Activated	***	***	+	R-Ras-like	N/A

Table 8.1 Summary of H-and R-Ras Chimera effects

Key: Influence on the reversal of suppression of H-Ras G12V and Raf-BxB CAAX shown with asterisks, where * = small reversal and *** = highly significant reversal. Effect on ERK1/2 activation shown using crosses, where + = control level activation, ++ = slight increase in activation and +++ = significant increase in activation. Cell morphologies are compared to full-length H-Ras and R-Ras Anchorage-independent growth shown with asterisks, where ***=significant growth.

Reference List

Abrams,C., Deng,Y.J., Steiner,B., Otoole,T., Shattil,S.J. (1994). Determinants of Specificity of A Baculovirus-Expressed Antibody Fab Fragment That Binds Selectively to the Activated Form of Integrin Alpha(Iib)Beta(3). Journal of Biological Chemistry 269, 18781-18788.

Albanese,C., Johnson,J., Watanabe,G., Eklund,N., Vu,D., Arnold,A., Pestell,R.G. (1995). Transforming P21(Ras) Mutants and C-Ets-2 Activate the Cyclin D1 Promoter Through Distinguishable Regions. Journal of Biological Chemistry 270, 23589-23597.

Alessi,D.R., Saito,Y., Campbell,D.G., Cohen,P., Sithanandam,G., Rapp,U., Ashworth,A., Marshall,C.J., Cowley,S. (1994). Identification of the Sites in Map Kinase Kinase-1 Phosphorylated by P74(Raf-1). Embo Journal 13, 1610-1619.

Alessi,D.R., Smythe,C., Keyse,S.M. (1993). The Human Cl100 Gene Encodes A Tyr/Thr-Protein Phosphatase Which Potently and Specifically Inactivates Map Kinase and Suppresses Its Activation by Oncogenic Ras in Xenopus-Oocyte Extracts. Oncogene 8, 2015-2020.

Anderson,D.C., Springer,T.A. (1987). Leukocyte Adhesion Deficiency - An Inherited Defect in the Mac- 1, Lfa-1, and P150,95 Glycoproteins. Annual Review of Medicine 38, 175-194.

Anderson,N.G., Maller,J.L., Tonks,N.K., Sturgill,T.W. (1990). Requirement for Integration of Signals from 2 Distinct Phosphorylation Pathways for Activation of Map Kinase. Nature 343, 651-653.

Apolloni,A., Prior,I.A., Lindsay,M., Parton,R.G., Hancock,J.F. (2000). H-ras but not K-ras traffics to the plasma membrane through the exocytic pathway. Molecular and Cellular Biology 20, 2475-2487.

Arai,A., Nosaka,Y., Kanda,E., Yamamoto,K., Miyasaka,N., Miura,O. (2001). Rap1 is activated by erythropoietin or interleukin-3 and is involved in regulation of beta(1) integrin-mediated hematopoietic cell adhesion. Journal of Biological Chemistry 276, 10453-10462.

Arroyo,A.G., Garciapardo,A., Sanchezmadrid,F. (1993). A High-Affinity Conformational State on Vla Integrin Heterodimers Induced by An Anti-Beta-1 Chain Monoclonal-Antibody. Journal of Biological Chemistry 268, 9863-9868.

Bajt,M.L., Loftus,J.C. (1994). Mutation of A Ligand-Binding Domain of Beta(3) Integrin - Integral Role of Oxygenated Residues in Alpha(Iib)Beta(3) (Gpiib-Iiia) Receptor Function. Journal of Biological Chemistry 269, 20913-20919.

Ballester,R., Marchuk,D., Boguski,M., Saulino,A., Letcher,R., Wigler,M., Collins,F. (1990). The Nf1 Locus Encodes A Protein Functionally Related to Mammalian Gap and Yeast Ira Proteins. Cell 63, 851-859.

Barbacid,M. (1987). Ras Genes. Annual Review of Biochemistry 56, 779-827.

Bazzoni,G., Hemler,M.E. (1998). Are changes in integrin affinity and conformation overemphasized? Trends in Biochemical Sciences 23, 30-34.

Bennett,J.S., Vilaire,G. (1979). Exposure of platelet fibrinogen receptors by ADP and epinephrine. Journal of Clinical Investigation 64, 1393-1401.

Berrier,A.L., Mastrangelo,A.M., Downward,J., Ginsberg,M., LaFlamme,S.E. (2000). Activated R-Ras, Rac1, PI 3-kinase and PKC is an element of can each restore cell spreading inhibited by isolated integrin beta 1 cytoplasmic domains. Journal of Cell Biology 151, 1549-1560.

Bertoni,A., Tadokoro,S., Eto,K., Pampori,N., Parise,L.V., White,G.C., Shattil,S.J. (2002). Relationships between Rap1b, affinity modulation of integrin alpha(IIb)beta(3), and the actin cytoskeleton. Journal of Biological Chemistry 277, 25715-25721.

Birge,R.B., Knudsen,B.S., Besser,D., Hanafusa,H. (1996). SH2 and SH3-containing adaptor proteins: Redundant or Independent mediators of intracellular signal transduction. Genes to Cells 1, 595-613.

Bodeau,A.L., Berrier,A.L., Mastrangelo,A.M., Martinez,R., LaFlamme,S.E. (2001). A functional comparison of mutations in integrin beta cytoplasmic domains: effects on the regulation of tyrosine phosphorylation, cell spreading, cell attachment and beta 1 integrin conformation. Journal of Cell Science 114, 2795-2807.

Boriack-Sjodin,P.A., Margarit,S.M., Bar-Sagi,D., Kuriyan,J. (1998). The structural basis of the activation of Ras by Sos. Nature 394, 337-343.

Bos,J.L. (1989). Ras Oncogenes in Human Cancer - A Review. Cancer Research 49, 4682-4689.

Bos,J.L., de Bruyn,K., Enserink,J., Kuiperij,B., Rangarajan,S., Rehmann,H., Riedl,J., de Rooij,J., van Mansfeld,F., Zwartkruis,F. (2003). The role of Rap1 in integrin-mediated cell adhesion. Biochemical Society Transactions 31, 83-86.

Bowtell,D., Fu,P., Simon,M., Senior,P. (1992). Identification of Murine Homologs of the Drosophila Son of Sevenless Gene - Potential Activators of Ras. Proceedings of the National Academy of Sciences of the United States of America 89, 6511-6515.

Brakebusch,C., Bouvard,D., Stanchi,F., Saki,T., Fassler,R. (2002). Integrins in invasive growth. Journal of Clinical Investigation 109, 999-1006.

Brenner,K.A., Corbett,S.A., Schwarzbauer,J.E. (2000). Regulation of fibronectin matrix assembly by activated Ras in transformed cells. Oncogene 19, 3156-3163.

Brown,E., Hogg,N. (1996). Where the outside meets the inside: Integrins as activators and targets of signal transduction cascades. Immunology Letters 54, 189-193.

Brown,H.A., Gutowski,S., Moomaw,C.R., Slaughter,C., Sternweis,P.C. (1993). Adp-Ribosylation Factor, A Small Gtp-Dependent Regulatory Protein, Stimulates Phospholipase-D Activity. Cell 75, 1137-1144.

Burridge,K., Fath,K., Kelly,T., Nuckolls,G., Turner,C. (1988). Focal Adhesions - Transmembrane Junctions Between the Extracellular-Matrix and the Cytoskeleton. Annual Review of Cell Biology 4, 487-525.

Calderwood,D.A., Zent,R., Grant,R., Rees,D.J.G., Hynes,R.O., Ginsberg,M.H. (1999). The talin head domain binds to integrin beta subunit cytoplasmic tails and regulates integrin activation. Journal of Biological Chemistry 274, 28071-28074.

Campbell,S.L., Khosravi-Far,R., Rossman,K.L., Clark,G.J., Der,C.J. (1998). Increasing complexity of Ras signaling. Oncogene 17, 1395-1413.

Capon,D.J., Chen,E.Y., Levinson,A.D., Seeburg,P.H., Goeddel,D.V. (1983). Complete Nucleotide-Sequences of the T24 Human Bladder- Carcinoma Oncogene and Its Normal Homolog. Nature 302, 33-37.

Caron,E. (2003). Cellular functions of the Rap1 GTP-binding protein: a pattern emerges. Journal of Cell Science 116, 435-440.

Caron,E., Self,A.J., Hall,A. (2000). The GTPase Rap1 controls functional activation of macrophage integrin alpha M beta 2 by LPS and other inflammatory mediators. Current Biology 10, 974-978.

Carpenter,C.L., Cantley,L.C. (1996). Phosphoinositide kinases. Current Opinion in Cell Biology 8, 153-158.

Chan,B.M.C., Matsuura,N., Takada,Y., Zetter,B.R., Hemler,M.E. (1991). Invitro and Invivo Consequences of Vla-2 Expression on Rhabdomyosarcoma Cells. Science 251, 1600-1602.

Chang,D.D., Wong,C., Smith,H., Liu,J. (1997). ICAP-1, a novel beta(1) integrin cytoplasmic domain-associated protein, binds to a conserved and functionally important NPXY sequence motif of beta(1) integrin. Journal of Cell Biology 138, 1149-1157.

Chen,H.C., Appeddu,P.A., Isoda,H., Guan,J.L. (1996). Phosphorylation of tyrosine 397 in focal adhesion kinase is required for binding phosphatidylinositol 3-kinase. Journal of Biological Chemistry 271, 26329-26334.

Chen,H.Y., Paradies,N.E., FedorChaiken,M., Brackenbury,R. (1997). E-cadherin mediates adhesion and suppresses cell motility via distinct mechanisms. Journal of Cell Science 110, 345-356.

Chen,W.C., Obrink,B. (1991). Cell Cell Contacts Mediated by E-Cadherin (Uvomorulin) Restrict Invasive Behavior of L-Cells. Journal of Cell Biology 114, 319-327.

Choy,E., Chiu,V.K., Silletti,J., Feoktistov,M., Morimoto,T., Michaelson,D., Ivanov,I.E., Philips,M.R. (1999). Endomembrane trafficking of Ras: The CAAX motif targets proteins to the ER and Golgi. Cell 98, 69-80.

Clark,G.J., Cox,A.D., Graham,S.M., Der,C.J. (1995). Biological Assays for Ras Transformation. Small Gtpases and Their Regulators, Pt A 255, 395-412.

Clemetson,K.J., Clemetson,J.M. (1998). Integrins and cardiovascular disease. Cellular and Molecular Life Sciences 54, 502-513.

Cowley,S., Paterson,H., Kemp,P., Marshall,C.J. (1994). Activation of Map Kinase Kinase Is Necessary and Sufficient for Pc12 Differentiation and for Transformation of Nih 3T3 Cells. Cell 77, 841-852.

Cox,A.D., Brtva,T.R., Lowe,D.G., Der,C.J. (1994). R-Ras Induces Malignant, But Not Morphologic, Transformation of Nih3T3 Cells. Oncogene 9, 3281-3288.

Cox,A.D., Der,C.J. (1994). Biological Assays for Cellular-Transformation. Heterotrimeric G-Protein Effectors 238, 277-294.

Cox,E.A., Sastry,S.K., Huttenlocher,A. (2001). Integrin-mediated adhesion regulates cell polarity and membrane protrusion through the Rho family of GTPases. Molecular Biology of the Cell 12, 265-277.

Crespo,P.M., Zurita,A.R., Daniotti,J.L. (2002). Effect of gangliosides on the distribution of a glycosylphosphatidylinositol-anchored protein in plasma membrane from Chinese hamster ovary-K1 cells. Journal of Biological Chemistry 277, 44731-44739.

Crews,C.M., Alessandrini,A., Erikson,R.L. (1992). The Primary Structure of Mek, A Protein-Kinase That Phosphorylates the Erk Gene-Product. Science 258, 478-480.

Crews,C.M., Erikson,R.L. (1993). Extracellular Signals and Reversible Protein-Phosphorylation - What to Mek of It All. Cell 74, 215-217.

Datta,S.R., Brunet,A., Greenberg,M.E. (1999). Cellular survival: a play in three Akts. Genes & Development 13, 2905-2927.

Dedhar,S., Hannigan,G.E. (1996). Integrin cytoplasmic interactions and bidirectional transmembrane signalling. Current Opinion in Cell Biology 8, 657-669.

Defeojones,D., Scolnick,E.M., Koller,R., Dhar,R. (1983). Ras-Related Gene-Sequences Identified and Isolated from Saccharomyces-Cerevisiae. Nature 306, 707-709.

Denhardt,D.T. (1996). Signal-transducing protein phosphorylation cascades mediated by Ras/Rho proteins in the mammalian cell: The potential for multiplex signalling. Biochemical Journal 318, 729-747.

Der,C.J., Krontiris,T.G., Cooper,G.M. (1982). Transforming Genes of Human Bladder and Lung-Carcinoma Cell- Lines Are Homologous to the Ras Genes of Harvey and Kirsten Sarcoma-Viruses. Proceedings of the National Academy of Sciences of the United States of America-Biological Sciences 79, 3637-3640.

Der,C.J., Weissman,B., Macdonald,M.J. (1988). Altered Guanine-Nucleotide Binding and H-Ras Transforming and Differentiating Activities. Oncogene 3, 105-112.

Dhanasekaran,N., Reddy,E.P. (1998). Signaling by dual specificity kinases. Oncogene 17, 1447-1455.

Downward,J. (1998). Ras signalling and apoptosis. Current Opinion in Genetics & Development 8, 49-54.

Downward,J. (2003). Targeting RAS signalling pathways in cancer therapy. National Review Cancer 3, 11-22.

Dsouza,S.E., Haas,T.A., Piotrowicz,R.S., Byersward,V., Mcgrath,D.E., Soule,H.R., Cierniewski,C., Plow,E.F., Smith,J.W. (1994). Ligand and Cation-Binding Are Dual Functions of A Discrete Segment of the Integrin Beta(3) Subunit - Cation Displacement Is Involved in Ligand-Binding. Cell 79, 659-667.

Dunlevy,J.R., Couchman,J.R. (1993). Controlled Induction of Focal Adhesion Disassembly and Migration in Primary Fibroblasts. Journal of Cell Science 105, 489-500.

Ebinu,J.O., Bottorff,D.A., Chan,E.Y.W., Stang,S.L., Dunn,R.J., Stone,J.C. (1998). RasGRP, a Ras guanyl nucleotide-releasing protein with calcium- and diacylglycerol-binding motifs. Science 280, 1082-1086.

Ehrhardt,A., Ehrhardt,G.R.A., Guo,X., Schrader,J.W. (2002). Ras and relatives - job sharing and networking keep an old family together. Experimental Hematology 30, 1089-1106.

Ellis,R.W., Defoe,D., Shih,T.Y., Gonda,M.A., Young,H.A., Tsuchida,N., Lowy,D.R., Scolnick,E.M. (1981). The p21 src genes of Harvey and Kirsten sarcoma viruses originate from divergent members of a family of normal vertebrate genes. Nature 292, 506-511.

Emkey,R., Freedman,S., Feig,L.A. (1991). Characterization of A Gtpase-Activating Protein for the Ras- Related Ral Protein. Journal of Biological Chemistry 266, 9703-9706.

Esteban,L.M., Vicario-Abejon,C., Fernandez-Salguero,P., Fernandez-Medarde,A., Swaminathan,N., Yienger,K., Lopez,E., Malumbres,M., Mckay,R., Ward,J.M., Pellicer,A., Santos,E. (2001). Targeted genomic disruption of H-ras and N-ras, individually or in combination, reveals the dispensability of both loci for mouse growth and development. Molecular and Cellular Biology 21, 1444-1452.

Etzioni,A. (1999). Integrins - the glue of life. Lancet 353, 341-343.

Fam,N.P., Fan,W.T., Wang,Z.X., Zhang,L.J., Chen,H., Moran,M.F. (1997). Cloning and characterization of Ras-GRF2, a novel guanine nucleotide exchange factor for Ras. Molecular and Cellular Biology 17, 1396-1406.

Fang,F., Orend,G., Watanabe,N., Hunter,T., Ruoslahti,E. (1996). Dependence of cyclin E-CDK2 kinase activity on cell anchorage. Science 271, 499-502.

Farnsworth,C.L., Freshney,N.W., Rosen,L.B., Ghosh,A., Greenberg,M.E., Feig,L.A. (1995). Calcium Activation of Ras Mediated by Neuronal Exchange Factor Ras-Grf. Nature 376, 524-527.

Fassler,R., Meyer,M. (1995). Consequences of Lack of Beta-1 Integrin Gene-Expression in Mice. Genes & Development 9, 1896-1908.

Faull,R.J., Ginsberg,M.H. (1996). Inside-out signaling through integrins. Journal of the American Society of Nephrology 7, 1091-1097.

Faull,R.J., Kovach,N.L., Harlan,J.M., Ginsberg,M.H. (1993). Affinity Modulation of Integrin Alpha-5-Beta-1 - Regulation of the Functional-Response by Soluble Fibronectin. Journal of Cell Biology 121, 155-162.

Faull,R.J., Kovach,N.L., Harlan,J.M., Ginsberg,M.H. (1994). Stimulation of Integrin-Mediated Adhesion of T-Lymphocytes and Monocytes - 2 Mechanisms with Divergent Biological Consequences. Journal of Experimental Medicine 179, 1307-1316.

Favata,M.F., Horiuchi,K.Y., Manos,E.J., Daulerio,A.J., Stradley,D.A., Feeser,W.S., Van Dyk,D.E., Pitts,W.J., Earl,R.A., Hobbs,F., Copeland,R.A., Magolda,R.L., Scherle,P.A., Trzaskos,J.M. (1998). Identification of a novel inhibitor of mitogen-activated protein kinase kinase. Journal of Biological Chemistry 273, 18623-18632.

Feng,L.X., Ravindranath,N., Dym,M. (2000). Stem cell factor/c-kit up-regulates cyclin D3 and promotes cell cycle progression via the phosphoinositide 3-kinase/p70 S6 kinase pathway in spermatogonia. Journal of Biological Chemistry 275, 25572-25576.

Fernandez C, Clark C, Burrows L, Schofield M.R., Humphries M.J. (1998). Regulation of the extracellular ligand binding activity of integrins. Frontiers in Bioscience 3, 684-700.

Fernandezsarabia,M.J., Bischoff,J.R. (1993). Bcl-2 Associates with the Ras-Related Protein R-Ras P23. Nature 366, 274-275.

Field,J., Broek,D., Kataoka,T., Wigler,M. (1987). Guanine-Nucleotide Activation Of, and Competition Between, Ras Proteins from Saccharomyces-Cerevisiae. Molecular and Cellular Biology 7, 2128-2133.

Finlin,B.S., Crump,S.M., Satin,J., Andres,D.A. (2003). Regulation of voltage-gated calcium channel activity by the Rem and Rad GTPases. Proceedings of the National Academy of Sciences of the United States of America 100, 14469-14474.

Finlin,B.S., Shao,H.P., Kadono-Okuda,K., Guo,N., Andres,D.A. (2000). Rem2, a new member of the Rem/Rad/Gem/Kir family of Ras-related GTPases. Biochemical Journal 347, 223-231.

Formstecher,E., Ramos,J.W., Fauquet,M., Calderwood,D.A., Hsieh,J.C., Canton,B., Nguyen,X.T., Barnier,J.V., Camonis,J., Ginsberg,M.H., Chneiweiss,H. (2001). PEA-15 mediates cytoplasmic sequestration of ERK MAP kinase. Developmental Cell 1, 239-250.

Fra,A.M., Williamson,E., Simons,K., Parton,R.G. (1994). Detergent-Insoluble Glycolipid Microdomains in Lymphocytes in the Absence of Caveolae. Journal of Biological Chemistry 269, 30745-30748.

Freedman V.H., Shin S.I. (1974). Cellular tumorigenicity in nude mice: correlation with cell growth in semi-solid medium. Cell 4, 355-359.

Frisch,S.M., Francis,H. (1994). Disruption of Epithelial Cell-Matrix Interactions Induces Apoptosis. Journal of Cell Biology 124, 619-626.

Fujimoto,H., Tanaka,Y., Liu,Z.J., Yagita,H., Okumura,K., Kosugi,A., Morinobu,A., Umehara,H., Yamamura,H., Minami,Y. (2001). Down-regulation of alpha 6 integrin, an anti-

oncogene product, by functional cooperation of H-Ras and c-Myc. Genes to Cells 6, 337-343.

Furuhjelm,J., Peranen,J. (2003). The C-terminal end of R-Ras contains a focal adhesion targeting signal. Journal of Cell Science 116, 3729-3738.

Gale,N.W., Kaplan,S., Lowenstein,E.J., Schlessinger,J., Barsagi,D. (1993). Grb2 Mediates the Egf-Dependent Activation of Guanine- Nucleotide Exchange on Ras. Nature 363, 88-92.

Garcia-Alvarez,B., de Pereda,J.M., Calderwood,D.A., Ulmer,T.S., Critchley,D., Campbell,I.D., Ginsberg,M.H., Liddington,R.C. (2003). Structural determinants of integrin recognition by Talin. Molecular Cell 11, 49-58.

Giancotti,F.G., Ruoslahti,E. (1990). Elevated Levels of the Alpha-5-Beta-1-Fibronectin Receptor Suppress the Transformed Phenotype of Chinese Hamster Ovary Cells. Cell 60, 849-859.

Giancotti,F.G., Ruoslahti,E. (1999). Transduction - Integrin signaling. Science 285, 1028-1032.

Gibbs,J.B., Sigal,I.S., Poe,M., Scolnick,E.M. (1984). Intrinsic Gtpase Activity Distinguishes Normal and Oncogenic Ras-P21 Molecules. Proceedings of the National Academy of Sciences of the United States of America-Biological Sciences 81, 5704-5708.

Ginsberg,M.H., Du,X.P., Plow E.F. (1992). Inside-out integrin signalling. Current Opinion in Cell Biology 4, 766-771.

Ginsberg,M.H., Yaspan,B., Forsyth,J., Ulmer,T.S., Campbell,I.D., Slepak,M. (2001). A membrane-distal segment of the integrin alpha(IIb) cytoplasmic domain regulates integrin activation. Journal of Biological Chemistry 276, 22514-22521.

Gotoh,T., Tian,X.J., Feig,L.A. (2001). Prenylation of target GTPases contributes to signaling specificity of Ras-guanine nucleotide exchange factors. Journal of Biological Chemistry 276, 38029-38035.

Green,N., Rosebrook,J., Cochran,N., Tan,K., Wang J.H., Springer,T.A., Briskin,M.J. (1999). Mutational analysis of MAdCAM-1/alpha4beta7 interactions reveals significant binding determinants in both the first and second immunuglobulin domains. Cell Adhes Commun 167-181.

Gupta,S., Plattner,R., Der,C.J., Stanbridge,E.J. (2000). Dissection of ras-dependent signaling pathways controlling aggressive tumor growth of human fibrosarcoma cells: Evidence for a potential novel pathway. Molecular and Cellular Biology 20, 9294-9306.

Haimovich,B., Lipfert,L., Brugge,J.S., Shattil,S.J. (1993). Tyrosine Phosphorylation and Cytoskeletal Reorganization in Platelets Are Triggered by Interaction of Integrin Receptors with Their Immobilized Ligands. Journal of Biological Chemistry 268, 15868-15877.

Hall,A. (1994). Small Gtp-Binding Proteins and the Regulation of the Actin Cytoskeleton. Annual Review of Cell Biology 10, 31-54.

Hall,A. (1998). Rho GTPases and the actin cytoskeleton. Science 279, 509-514.

Hall,A., Marshall,C.J., Spurr,N.K., Weiss,R.A. (1983). Identification of Transforming Gene in 2 Human Sarcoma Cell- Lines As A New Member of the Ras Gene Family Located on Chromosome-1. Nature 303, 396-400.

Halliday,K.R. (1984). Regional Homology in Gtp-Binding Proto-Oncogene Products and Elongation-Factors. Journal of Cyclic Nucleotide and Protein Phosphorylation Research 9, 435-448.

Hancock,J.F. (2003). Ras proteins: Different signals from different locations. Nature Reviews Molecular Cell Biology 4, 373-384.

Hancock,J.F., Magee,A.I., Childs,J.E., Marshall,C.J. (1989). All Ras Proteins Are Polyisoprenylated But Only Some Are Palmitoylated. Cell 57, 1167-1177.

Hancock,J.F., Paterson,H., Marshall,C.J. (1990). A Polybasic Domain Or Palmitoylation Is Required in Addition to the Caax Motif to Localize P21Ras to the Plasma-Membrane. Cell 63, 133-139.

Hanks,S.K., Polte,T.R. (1997). Signaling through focal adhesion kinase. Bioessays 19, 137-145.

Hansen,M., Prior,I.A., Hughes,P.E., Oertli,B., Chou,F.L., Willumsen,B.M., Hancock,J.F., Ginsberg,M.H. (2003). C-terminal sequences in R-Ras are involved in integrin regulation and in plasma membrane microdomain distribution. Biochemical and Biophysical Research Communications 311, 829-838.

Hansen,M., Rusyn,E.V., Hughes,P.E., Ginsberg,M.H., Cox,A.D., Willumsen,B.M. (2002). R-Ras C-terminal sequences are sufficient to confer R-Ras specificity to H-Ras. Oncogene 21, 4448-4461.

Harvey J.J. (1964). An unidentified virus which causes the rapid production of tumours in mice. Nature 204, 1104-1105.

Hato,T., Pampori,N., Shattil,S.J. (1998). Complementary roles for receptor clustering and conformational change in the adhesive and signaling functions of integrin alpha(IIb)beta(3). Journal of Cell Biology 141, 1685-1695.

Hemler,M.E. (1990). Vla Proteins in the Integrin Family - Structures, Functions, and Their Role on Leukocytes. Annual Review of Immunology 8, 365-400.

Hemmings,L., Rees,D.J.G., Ohanian,V., Bolton,S.J., Gilmore,A.P., Patel,B., Priddle,H., Trevithick,J.E., Hynes,R.O., Critchley,D.R. (1996). Talin contains three actin-binding sites each of which is adjacent to a vinculin-binding site. Journal of Cell Science 109, 2715-2726.

Henry,D.O., Moskalenko,S.A., Kaur,K.J., Fu,M.F., Pestell,R.G., Camonis,J.H., White,M.A. (2000). Ral GTPases contribute to regulation of cyclin D1 through activation of NF-kappa B. Molecular and Cellular Biology 20, 8084-8092.

Hillis,G.S., MacLeod,A.M. (1996). Integrins and disease. Clinical Science 91, 639-650.

Hodivala-Dilke,K.M., Mchugh,K.P., Tsakiris,D.A., Rayburn,H., Crowley,D., Ullman-Cullere,M., Ross,F.P., Coller,B.S., Teitelbaum,S., Hynes,R.O. (1999). beta 3-integrin-deficient mice are a model for Glanzmann thrombasthenia showing placental defects and reduced survival. Journal of Clinical Investigation 103, 229-238.

Hofer,F., Fields,S., Schneider,C., Martin,G.S. (1994). Activated Ras Interacts with the Ral Guanine-Nucleotide Dissociation Stimulator. Proceedings of the National Academy of Sciences of the United States of America 91, 11089-11093.

Hogg,N., Bates,P.A. (2000). Genetic analysis of integrin function in man: LAD-1 and other syndromes. Matrix Biology 19, 211-222.

Holland,S.J., Peles,E., Pawson,T., Schlessinger,J. (1998). Cell-contact-dependent signalling in axon growth and guidance: Eph receptor tyrosine kinases and receptor protein tyrosine phosphatase beta. Current Opinion in Neurobiology 8, 117-127.

Holly,S.P., Larson,M.K., Parise,L.V. (2000). Multiple roles of integrins in cell motility. Experimental Cell Research 261, 69-74.

Hooper,N.M. (1999). Detergent-insoluble glycosphingolipid/cholesterol-rich membrane domains, lipid rafts and caveolae (review). Molecular Membrane Biology 16, 145-156.

Horton,R.M., Hunt,H.D., Ho,S.N., Pullen,J.K., Pease,L.R. (1989). Engineering Hybrid Genes Without the Use of Restriction Enzymes - Gene-Splicing by Overlap Extension. Gene 77, 61-68.

Hotchin,N.A., Hall,A. (1995). The assembly of integrin adhesion complexes requires both extracellular matrix and intracellular rho/rac GTPases. Journal of Cell Biology 131, 1857-1865.

Howe,L.R., Leevers,S.J., Gomez,N., Nakielny,S., Cohen,P., Marshall,C.J. (1992). Activation of the Map Kinase Pathway by the Protein-Kinase Raf. Cell 71, 335-342.

Hu,C.D., Kariya,K., Okada,T., Qi,X.D., Song,C.H., Kataoka,T. (1999). Effect of phosphorylation on activities of Rap1A to interact with Raf-1 and to suppress Ras-dependent Raf-1 activation. Journal of Biological Chemistry 274, 48-51.

Huff,S.Y., Quilliam,L.A., Cox,A.D., Der,C.J. (1997). R-Ras is regulated by activators and effectors distinct from those that control Ras function. Oncogene 14, 133-143.

Hughes,P.E., DiazGonzalez,F., Leong,L., Wu,C.Y., McDonald,J.A., Shattil,S.J., Ginsberg,M.H. (1996). Breaking the integrin hinge - A defined structural constraint regulates integrin signaling. Journal of Biological Chemistry 271, 6571-6574.

Hughes,P.E., Oertli,B., Hansen,M., Chou,F.L., Willumsen,B.M., Ginsberg,M.H. (2002). Suppression of integrin activation by activated Ras or Raf does not correlate with bulk activation of ERK MAP kinase. Molecular Biology of the Cell 13, 2256-2265.

Hughes,P.E., Pfaff,M. (1998). Integrin affinity modulation. Trends in Cell Biology 8, 359-364.

Hughes,P.E., Renshaw,M.W., Pfaff,M., Forsyth,J., Keivens,V.M., Schwartz,M.A., Ginsberg,M.H. (1997). Suppression of integrin activation: A novel function of a Ras/Raf-initiated MAP kinase pathway. Cell 88, 521-530.

Humphries,M.J. (2000). Integrin structure. Biochemical Society Transactions 28, 311-340.

Huttenlocher,A., Ginsberg,M.H., Horwitz,A.F. (1996). Modulation of cell migration by integrin-mediated cytoskeletal linkages and ligand-binding affinity. Journal of Cell Biology 134, 1551-1562.

Huttenlocher,A., Lakonishok,M., Kinder,M., Wu,S., Truong,T., Knudsen,K.A., Horwitz,A.F. (1998). Integrin and cadherin synergy regulates contact inhibition of migration and motile activity. Journal of Cell Biology 141, 515-526.

Hynes,R.O. (1987). Integrins - A Family of Cell-Surface Receptors. Cell 48, 549-554.

Hynes,R.O. (1992). Integrins - Versatility, Modulation, and Signaling in Cell- Adhesion. Cell 69, 11-25.

Hynes,R.O., Yamada,K.M. (1982). Fibronectins - Multifunctional Modular Glycoproteins. Journal of Cell Biology 95, 369-377.

Ilangumaran,S., Hoessli,D.C. (1998). Effects of cholesterol depletion by cyclodextrin on the sphingolipid microdomains of the plasma membrane. Biochemical Journal 335, 433-440.

Ivins,J.K., Yurchenco,P.D., Lander,A.D. (2000). Regulation of neurite outgrowth by integrin activation. Journal of Neuroscience 20, 6551-6560.

Janes,P.W., Ley,S.C., Magee,A.I. (1999). Aggregation of lipid rafts accompanies signaling via the T cell antigen receptor. Journal of Cell Biology 147, 447-461.

Janknecht,R., Ernst,W.H., Pingoud,V., Nordheim,A. (1993). Activation of Ternary Complex Factor Elk-1 by Map Kinases. Embo Journal 12, 5097-5104.

Jaumot,M., Yan,J., Clyde-Smith,J., Sluimer,J., Hancock,J.F. (2002). The linker domain of the Ha-Ras hypervariable region regulates interactions with exchange factors, Raf-1 and phosphoinositide 3-kinase. Journal of Biological Chemistry 277, 272-278.

Juliano R.L., Varner J.A. (1993). Adhesion molecules in cancer: the role of integrins. Current Opinion in Cell Biology 5, 812-818.

Katagiri,K., Hattori,M., Minato,N., Irie,S., Takatsu,K., Kinashi,T. (2000). Rap1 is a potent activation signal for leukocyte function- associated antigen 1 distinct from protein kinase C and phosphatidylinositol-3-OH kinase. Molecular and Cellular Biology 20, 1956-1969.

Keely,P., Parise,L., Juliano,R. (1998). Integrins and GTPases in tumour cell growth, motility and invasion. Trends in Cell Biology 8, 101-106.

Keely,P.J., Fong,A.M., Zutter,M.M., Santoro,S.A. (1995). Alteration of Collagen-Dependent Adhesion, Motility, and Morphogenesis by the Expression of Antisense Alpha(2) Integrin Messenger-Rna in Mammary Cells. Journal of Cell Science 108, 595-607.

Keely,P.J., Rusyn,E.V., Cox,A.D., Parise,L.V. (1999). R-Ras signals through specific integrin alpha cytoplasmic domains to promote migration and invasion of breast epithelial cells. Journal of Cell Biology 145, 1077-1088.

Keely,P.J., Westwick,J.K., Whitehead,I.P., Der,C.J., Parise,L.V. (1997). Cdc42 and Rac1 induce integrin-mediated cell motility and invasiveness through PI(3)K. Nature 390, 632-636.

Keyse,S.M. (2000). Protein phosphatases and the regulation of mitogen-activated protein kinase signalling. Current Opinion in Cell Biology 12, 186-192.

Khwaja,A., RodriguezViciana,P., Wennstrom,S., Warne,P.H., Downward,J. (1997). Matrix adhesion and Ras transformation both activate a phosphoinositide 3-OH kinase and protein kinase B/Akt cellular survival pathway. Embo Journal 16, 2783-2793.

Kinashi,T., Katagiri,K., Watanabe,S., Vanhaesebroeck,B., Downward,J., Takatsu,K. (2000). Distinct mechanisms of alpha(5)beta(1) integrin activation by Ha-Ras and R-Ras. Journal of Biological Chemistry 275, 22590-22596.

Kinbara,K., Goldfinger,L.E., Hansen,M., Chou,F.L., Ginsberg,M.H. (2003). Ras GTPases: Integrins' friends or foes? Nature Reviews Molecular Cell Biology 4, 767-776.

Kirsten,W.H., Mayer,L.A. (1969). Malignant lymphomas of extrathymic origin induced in rats by murine erythroblastosis virus. Journal of the National Cancer Institute 43, 735-746.

Kitanaka,C., Kato,K., Ijiri,R., Sakurada,K., Tomiyama,A., Noguchi,K., Nagashima,Y., Nakagawara,A., Momoi,T., Toyoda,Y., Kigasawa,H., Nishi,T., Shirouzu,M., Yokoyama,S., Tanaka,Y., Kuchino,Y. (2002). Increased Ras expression and caspase-independent neuroblastoma cell death: Possible mechanism of spontaneous neuroblastoma regression. Journal of the National Cancer Institute 94, 358-368.

Klein,U., Gimpl,G., Fahrenholz,F. (1995). Alteration of the Myometrial Plasma-Membrane Cholesterol Content with Beta-Cyclodextrin Modulates the Binding-Affinity of the Oxytocin Receptor. Biochemistry 34, 13784-13793.

Klemke,R.L., Cai,S., Giannini,A.L., Gallagher,P.J., deLanerolle,P., Cheresh,D.A. (1997). Regulation of cell motility by mitogen-activated protein kinase. Journal of Cell Biology 137, 481-492.

Koera,K., Nakamura,K., Nakao,K., Miyoshi,J., Toyoshima,K., Hatta,T., Otani,H., Aiba,A., Katsuki,M. (1997). K-ras is essential for the development of the mouse embryo. Oncogene 15, 1151-1159.

Kolch,W. (2000). Meaningful relationships: the regulation of the Ras/Raf/MEK/ERK pathway by protein interactions. Biochemical Journal 351, 289-305.

Kozak,C., Gunnell,M.A., Rapp,U.R. (1984). A New Oncogene, C-Raf, Is Located on Mouse Chromosome-6. Journal of Virology 49, 297-299.

Kucik,D.F., Dustin,M.L., Miller,J.M., Brown,E.J. (1996). Adhesion-activating phorbol ester increases the mobility of leukocyte integrin LFA-1 in cultured lymphocytes. Journal of Clinical Investigation 97, 2139-2144.

Kuijpers,T.W., vanLier,R.A.W., Hamann,D., deBoer,M., Thung,L.Y., Weening,R.S., Verhoeven,A.J., Roos,D. (1997). Leukocyte adhesion deficiency type 1 (LAD-1)/variant - A novel immunodeficiency syndrome characterized by dysfunctional beta(2) integrins. Journal of Clinical Investigation 100, 1725-1733.

Kumar,C.C. (1998). Signaling by integrin receptors. Oncogene 17, 1365-1373.

Kunicki,T.J., Annis,D.S., Deng,Y.J., Loftus,J.C., Shattil,S.J. (1996). A molecular basis for affinity modulation of Fab ligand binding to integrin alpha(IIb)beta(3). Journal of Biological Chemistry 271, 20315-20321.

Lai,C.C., Boguski,M., Broek,D., Powers,S. (1993). Influence of Guanine-Nucleotides on Complex-Formation Between Ras and Cdc25 Proteins. Molecular and Cellular Biology 13, 1345-1352.

Langbeheim,H., Shih,T.Y., Scolnick,E.M. (1980). Identification of a normal vertebrate cell protein related to the p21 src of Harvey murine sarcoma virus. Virology 106, 292-300.

Lauffenburger,D.A., Horwitz,A.F. (1996). Cell migration: A physically integrated molecular process. Cell 84, 359-369.

Leberman,R., Egner,U. (1984). Homologies in the Primary Structure of Gtp-Binding Proteins - the Nucleotide-Binding Site of Ef-Tu and P21. Embo Journal 3, 339-341.

Leevers,S.J., Paterson,H.F., Marshall,C.J. (1994). Requirement for Ras in Raf Activation Is Overcome by Targeting Raf to the Plasma-Membrane. Nature 369, 411-414.

Leitinger,B., Hogg,N. (2002). The involvement of lipid rafts in the regulation of integrin function. Journal of Cell Science 115, 963-972.

Lenzen,C., Cool,R.H., Prinz,H., Kuhlmann,J., Wittinghofer,A. (1998). Kinetic analysis by fluorescence of the interaction between Ras and the catalytic domain of the guanine nucleotide exchange factor Cdc25(Mm). Biochemistry 37, 7420-7430.

Levy,L., Broad,S., Diekmann,D., Evans,R.D., Watt,F.M. (2000). beta 1 integrins regulate keratinocyte adhesion and differentiation by distinct mechanisms. Molecular Biology of the Cell 11, 453-466.

Lewis,J.M., Schwartz,M.A. (1995). Mapping In-Vivo Associations of Cytoplasmic Proteins with Integrin Beta-1 Cytoplasmic Domain Mutants. Molecular Biology of the Cell 6, 151-160.

Li,L.M., Okura,M., Imamoto,A. (2002). Focal adhesions require catalytic activity of Src family kinases to mediate integrin-matrix adhesion. Molecular and Cellular Biology 22, 1203-1217.

Li,N., Batzer,A., Daly,R., Yajnik,V., Skolnik,E., Chardin,P., Barsagi,D., Margolis,B., Schlessinger,J. (1993). Guanine-Nucleotide-Releasing Factor Hsos1 Binds to Grb2 and Links Receptor Tyrosine Kinases to Ras Signaling. Nature 363, 85-88.

Li,S.W., Satoh,H., Watanabe,T., Nakamura,S., Hattori,S. (1996). cDNA cloning and chromosomal mapping of a novel human GAP (GAP1M), a GTPase-activating protein of Ras. Genomics 35, 625-627.

Lin,T.H., Chen,Q.M., Howe,A., Juliano,R.L. (1997). Cell anchorage permits efficient signal transduction between Ras and its downstream kinases. Journal of Biological Chemistry 272, 8849-8852.

Liu,S., Thomas,S.M., Woodside,D.G., Rose,D.M., Kiosses,W.B., Pfaff,M., Ginsberg,M.H. (1999). Binding of paxillin to alpha(4) integrins modifies integrin- dependent biological responses. Nature 402, 676-681.

Liu,S.C., Calderwood,D.A., Ginsberg,M.H. (2000). Integrin cytoplasmic domain-binding proteins. Journal of Cell Science 113, 3563-3571.

Lobo,S., Greentree,W.K., Linder,M.E., Deschenes,R.J. (2002). Identification of a Ras palmitoyltransferase in Saccharomyces cerevisiae. Journal of Biological Chemistry 277, 41268-41273.

Lowe,D.G., Capon,D.J., Delwart,E., Sakaguchi,A.Y., Naylor,S.L., Goeddel,D.V. (1987). Structure of the Human and Murine R-Ras Genes, Novel Genes Closely Related to Ras Protooncogenes. Cell 48, 137-146.

Lowe,D.G., Goeddel,D.V. (1987). Heterologous Expression and Characterization of the Human R-Ras Gene-Product. Molecular and Cellular Biology 7, 2845-2856.

Lowe,D.G., Ricketts,M., Levinson,A.D., Goeddel,D.V. (1988). Chimeric Proteins Define Variable and Essential Regions of Ha- Ras-Encoded Protein. Proceedings of the National Academy of Sciences of the United States of America 85, 1015-1019.

Lowenstein,E.J., Daly,R.J., Batzer,A.G., Li,W., Margolis,B., Lammers,R., Ullrich,A., Skolnik,E.Y., Barsagi,D., Schlessinger,J. (1992). The Sh2 and Sh3 Domain Containing Protein Grb2 Links Receptor Tyrosine Kinases to Ras Signaling. Cell 70, 431-442.

Lowes,V.L., Ip,N.Y., Wong,Y.H. (2002). Integration of signals from receptor tyrosine kinases and G protein-coupled receptors. Neurosignals 11, 5-19.

Lowy,D.R., Willumsen,B.M. (1993). Function and Regulation of Ras. Annual Review of Biochemistry 62, 851-891.

Macaluso,M., Russo,G., Cinti,C., Bazan,V., Gebbia,N., Russo,A. (2002). Ras family genes: An interesting link between cell cycle and cancer. Journal of Cellular Physiology 192, 125-130.

Malumbres,M., Barbacid,M. (2003). Timeline - RAS oncogenes: the first 30 years. Nature Reviews Cancer 3, 459-465.

Manes,S., Mira,E., Gomez-Mouton,C., Lacalle,R.A., Keller,P., Labrador,J.P., Martinez,A. (1999). Membrane raft microdomains mediate front-rear polarity in migrating cells. Embo Journal 18, 6211-6220.

Manser,E., Huang,H.Y., Loo,T.H., Chen,X.Q., Dong,J.M., Leung,T., Lim,L. (1997). Expression of constitutively active alpha-PAK reveals effects of the kinase on actin and focal complexes. Molecular and Cellular Biology 17, 1129-1143.

Manser,E., Leung,T., Salihuddin,H., Zhao,Z.S., Lim,L. (1994). A Brain Serine Threonine Protein-Kinase Activated by Cdc42 and Rac1. Nature 367, 40-46.

Mansour,S.J., Matten,W.T., Hermann,A.S., Candia,J.M., Rong,S., Fukasawa,K., Vandewoude,G.F., Ahn,N.G. (1994). Transformation of Mammalian-Cells by Constitutively Active Map Kinase Kinase. Science 265, 966-970.

Marais,R., Wynne,J., Treisman,R. (1993). The Srf Accessory Protein Elk-1 Contains A Growth Factor- Regulated Transcriptional Activation Domain. Cell 73, 381-393.

Marshall,C.J. (1996). Ras effectors. Current Opinion in Cell Biology 8, 197-204.

Marshall,M.S., Davis,L.J., Keys,R.D., Mosser,S.D., Hill,W.S., Scolnick,E.M., Gibbs,J.B. (1991). Identification of Amino-Acid-Residues Required for Ras-P21 Target Activation. Molecular and Cellular Biology 11, 3997-4004.

Marte,B.M., RodriguezViciana,P., Wennstrom,S., Warne,P.H., Downward,J. (1997a). R-Ras can activate the phosphoinositide 3-kinase but not the MAP kinase arm of the Ras effector pathways. Current Biology 7, 63-70.

Marte,B.M., RodriguezViciana,P., Wennstrom,S., Warne,P.H., Downward,J. (1997b). R-Ras can activate the phosphoinositide 3-kinase but not the MAP kinase arm of the Ras effector pathways (vol 7, pg 63, 1997). Current Biology 7, R261.

Mastrangelo,A.M., Homan,S.M., Humphries,M.J., LaFlamme,S.E. (1999). Amino acid motifs required for isolated beta cytoplasmic domains to regulate 'in trans' beta 1 integrin conformation and function in cell attachment. Journal of Cell Science 112, 217-229.

McCarty,J.H. (1998). The Nck SH2/SH3 adaptor protein: a regulator of multiple intracellular signal transduction events. Bioessays 20, 913-921.

McCormick,F. (1998). Going for the GAP. Current Biology 8, R673-R674.

McDowall,A., Inwald,D., Leitinger,B., Jones,A., Liesner,R., Klein,N., Hogg,N. (2003). A novel form of integrin dysfunction involving beta 1, beta 2, and beta 3 integrins. Journal of Clinical Investigation 111, 51-60.

Mcgrath,J.P., Capon,D.J., Goeddel,D.V., Levinson,A.D. (1984). Comparative Biochemical-Properties of Normal and Activated Human Ras P21 Protein. Nature 310, 644-649.

Melkonian,K.A., Ostermeyer,A.G., Chen,J.Z., Roth,M.G., Brown,D.A. (1999). Role of lipid modifications in targeting proteins to detergent- resistant membrane rafts - Many raft proteins are acylated, while few are prenylated. Journal of Biological Chemistry 274, 3910-3917.

Meredith,J.E., Fazeli,B., Schwartz,M.A. (1993). The Extracellular-Matrix As A Cell-Survival Factor. Molecular Biology of the Cell 4, 953-961.

Michaelson,D., Silletti,J., Murphy,G., D'Eustachio,P., Rush,M., Philips,M.R. (2001). Differential localization of Rho GTPases in live cells: Regulation by hypervariable regions and RhoGDI binding. Journal of Cell Biology 152, 111-126.

Miyamoto,S., Teramoto,H., Gutkind,J.S., Yamada,K.M. (1996). Integrins can collaborate with growth factors for phosphorylation of receptor tyrosine kinases and MAP kinase activation: Roles of integrin aggregation and occupancy of receptors. Journal of Cell Biology 135, 1633-1642.

Moodie,S.A., Willumsen,B.M., Weber,M.J., Wolfman,A. (1993). Complexes of Ras.Gtp with Raf-1 and Mitogen-Activated Protein- Kinase Kinase. Science 260, 1658-1661.

Morrison,D.K., Cutler,R.E. (1997). The complexity of Raf-1 regulation. Current Opinion in Cell Biology 9, 174-179.

Morrison,D.L., Sanghera,J.S., Stewart,J., Sutherland,C., Walsh,M.P., Pelech,S.L. (1996). Phosphorylation and activation of smooth muscle myosin light chain kinase by MAP kinase

and cyclin-dependent kinase-1. Biochemistry and Cell Biology-Biochimie et Biologie Cellulaire 74, 549-557.

Muda,M., Theodosiou,A., Rodrigues,N., Boschert,U., Camps,M., Gillieron,C., Davies,K., Ashworth,A., Arkinstall,S. (1996). The dual specificity phosphatases M3/6 and MKP-3 are highly selective for inactivation of distinct mitogen-activated protein kinases. Journal of Biological Chemistry 271, 27205-27208.

Mulrooney,J.P., Hong,T., Grabel,L.B. (2001). Serine 785 phosphorylation of the beta 1 cytoplasmic domain modulates beta 1A-integrin-dependent functions. Journal of Cell Science 114, 2525-2533.

Nermut,M.V., Green,N.M., Eason,P., Yamada,S.S., Yamada,K.M. (1988). Electron-Microscopy and Structural Model of Human Fibronectin Receptor. Embo Journal 7, 4093-4099.

Neuman-Silberberg,F.S., Schejter,E., Hoffmann,F.M., Shilo,B.Z. (1984). The Drosophila ras oncogenes: structure and nucleotide sequence. Cell 37, 1027-1033.

Newham,P., Humphries,M.J. (1996). Integrin adhesion receptors: Structure, function and implications for biomedicine. Molecular Medicine Today 2, 304-313.

Newman,P.J., Seligsohn,U., Lyman,S., Coller,B.S. (1991). The Molecular Genetic-Basis of Glanzmann Thrombasthenia in the Iraqi-Jewish and Arab Populations in Israel. Proceedings of the National Academy of Sciences of the United States of America 88, 3160-3164.

Niv,H., Gutman,O., Kloog,Y., Henis,Y.I. (2002). Activated K-Ras and H-Ras display different interactions with saturable nonraft sites at the surface of live cells. Journal of Cell Biology 157, 865-872.

Nobes,C.D., Hall,A. (1995). Rho, Rac, and Cdc42 Gtpases Regulate the Assembly of Multimolecular Focal Complexes Associated with Actin Stress Fibers, Lamellipodia, and Filopodia. Cell 81, 53-62.

Nobes,C.D., Hall,A. (1999). Rho GTPases control polarity, protrusion, and adhesion during cell movement. Journal of Cell Biology 144, 1235-1244.

Ochieng,J., Basolo,F., Albini,A., Melchiori,A., Watanabe,H., Elliott,J., Raz,A., Parodi,S., Russo,J. (1991). Increased Invasive, Chemotactic and Locomotive Abilities of C- Ha-Ras-Transformed Human Breast Epithelial-Cells. Invasion & Metastasis 11, 38-47.

Oertli,B., Han,J., Marte,B.M., Sethi,T., Downward,J., Ginsberg,M., Hughes,P.E. (2000). The effector loop and prenylation site of R-Ras are involved in the regulation of integrin function. Oncogene 19, 4961-4969.

Ohba,Y., Mochizuki,N., Yamashita,S., Chan,A.M., Schrader,J.W., Hattori,S., Nagashima,K., Matsuda,M. (2000). Regulatory proteins of R-Ras, TC21/R-Ras2, and M-Ras/R-Ras3. Journal of Biological Chemistry 275, 20020-20026.

Ohtani,Y., Irie,T., Uekama,K., Fukunaga,K., Pitha,J. (1989). Differential-Effects of Alpha-Cyclodextrins, Beta-Cyclodextrins and Gamma-Cyclodextrins on Human-Erythrocytes. European Journal of Biochemistry 186, 17-22.

Okada,T., Masuda,T., Shinkai,M., Kariya,K., Kataoka,T. (1996). Post-translational modification of H-Ras is required for activation of, but not for association with, B-Raf. Journal of Biological Chemistry 271, 4671-4678.

Okutani,T., Okabayashi,Y., Kido,Y., Sugimoto,Y., Sakaguchi,K., Matuoka,K., Takenawa,T., Kasuga,M. (1994). Grb2/Ash Binds Directly to Tyrosine-1068 and Tyrosine-1086 and Indirectly to Tyrosine-1148 of Activated Human Epidermal Growth-Factor Receptors in Intact-Cells. Journal of Biological Chemistry 269, 31310-31314.

Olden K., Yamada,K.M. (1977). Mechanism of the decrease in the major cell surface protein of chick embryo fibroblasts after transformation. Cell 4, 957-969.

Osada,M., Tolkacheva,T., Li,W.Q., Chan,T.O., Tsichlis,P.N., Saez,R., Kimmelman,A.C., Chan,A.M.L. (1999). Differential roles of Akt, Rac, and Ral in R-Ras-mediated cellular transformation, adhesion, and survival. Molecular and Cellular Biology 19, 6333-6344.

Ostermeyer,A.G., Beckrich,B.T., Ivarson,K.A., Grove,K.E., Brown,D.A. (1999). Glycosphingolipids are not essential for formation of detergent-resistant membrane rafts in melanoma cells - Methyl- beta-cyclodextrin does not affect cell surface transport of a GPI-anchored protein. Journal of Biological Chemistry 274, 34459-34466.

Otey,C.A., Vasquez,G.B., Burridge,K., Erickson,B.W. (1993). Mapping of the Alpha-Actinin Binding-Site Within the Beta-1 Integrin Cytoplasmic Domain. Journal of Biological Chemistry 268, 21193-21197.

Otoole,T.E., Katagiri,Y., Faull,R.J., Peter,K., Tamura,R., Quaranta,V., Loftus,J.C., Shattil,S.J., Ginsberg,M.H. (1994). Integrin Cytoplasmic Domains Mediate Inside-Out Signal- Transduction. Journal of Cell Biology 124, 1047-1059.

Otoole,T.E., Loftus,J.C., Du,X.P., Glass,A.A., Ruggeri,Z.M., Shattil,S.J., Plow,E.F., Ginsberg,M.H. (1990). Affinity Modulation of the Alpha-Iib-Beta-3 Integrin (Platelet Gpiib-Iiia) Is An Intrinsic Property of the Receptor. Cell Regulation 1, 883-893.

Otoole,T.E., Mandelman,D., Forsyth,J., Shattil,S.J., Plow,E.F., Ginsberg,M.H. (1991). Modulation of the Affinity of Integrin-Alpha-Iib-Beta-3 (Gpiib- Iiia) by the Cytoplasmic Domain of Alpha-Iib. Science 254, 845-847.

Otoole,T.E., Ylanne,J., Culley,B.M. (1995). Regulation of Integrin Affinity States Through An Npxy Motif in the Beta-Subunit Cytoplasmic Domain. Journal of Biological Chemistry 270, 8553-8558.

Palecek,S.P. (1997). Integrin-ligand binding properties govern cell migration speed through cell-substratum adhesiveness (vol 385, pg 537, 1997). Nature 388, 210.

Palecek,S.P., Loftus,J.C., Ginsberg,M.H., Lauffenburger,D.A., Horwitz,A.F. (1997). Integrin-ligand binding properties govern cell migration speed through cell-substratum adhesiveness. Nature 385, 537-540.

Parada,L.F., Tabin,C.J., Shih,C., Weinberg,R.A. (1982). Human Ej Bladder-Carcinoma Oncogene Is Homolog of Harvey Sarcoma-Virus Ras Gene. Nature 297, 474-478.

Payne,D.M., Rossomando,A.J., Martino,P., Erickson,A.K., Her,J.H., Shabanowitz,J., Hunt,D.F., Weber,M.J., Sturgill,T.W. (1991). Identification of the Regulatory Phosphorylation Sites in Pp42/Mitogen-Activated Protein-Kinase (Map Kinase). Embo Journal 10, 885-892.

Payrastre,B., Missy,K., Trumel,C., Bodin,S., Plantavid,M., Chap,H. (2000). The integrin alpha IIb/beta 3 in human platelet signal transduction. Biochemical Pharmacology 60, 1069-1074.

Paz,A., Haklai,R., Elad-Sfadia,G., Ballan,E., Kloog,Y. (2001). Galectin-1 binds oncogenic H-Ras to mediate Ras membrane anchorage and cell transformation. Oncogene 20, 7486-7493.

Pazin,M.J., Williams,L.T. (1992). Triggering Signaling Cascades by Receptor Tyrosine Kinases. Trends in Biochemical Sciences 17, 374-378.

Peterson,S.N., Trabalzini,L., Brtva,T.R., Fischer,T., Altschuler,D.L., Martelli,P., Lapetina,E.G., Der,C.J., White,G.C. (1996). Identification of a novel RalGDS-related protein

as a candidate effector for Ras and Rap1. Journal of Biological Chemistry 271, 29903-29908.

Petit,V., Thiery,J.P. (2000). Focal adhesions: structure and dynamics. Biology of the Cell 92, 477-494.

Phillips,D.R., Charo,I.F., Scarborough,R.M. (1991). Gpiib-Iiia - the Responsive Integrin. Cell 65, 359-362.

Pierschbacher,M.D., Ruoslahti,E. (1984). Cell Attachment Activity of Fibronectin Can be Duplicated by Small Synthetic Fragments of the Molecule. Nature 309, 30-33.

Plantefaber,L.C., Hynes,R.O. (1989). Changes in Integrin Receptors on Oncogenically Transformed- Cells. Cell 56, 281-290.

Plow,E.F., Haas,T.K., Zhang,L., Loftus,J., Smith,J.W. (2000). Ligand binding to integrins. Journal of Biological Chemistry 275, 21785-21788.

Pol,A., Luetterforst,R., Lindsay,M., Heino,S., Ikonen,E., Parton,R.G. (2001). A caveolin dominant negative mutant associates with lipid bodies and induces intracellular cholesterol imbalance. Journal of Cell Biology 152, 1057-1070.

Price,M.A., Hill,C., Treisman,R. (1996). Integration of growth factor signals at the c-fos serum response element. Philosophical Transactions of the Royal Society of London Series B-Biological Sciences 351, 551-559.

Prior,I.A., Hancock,J.F. (2001). Compartmentalization of Ras proteins. Journal of Cell Science 114, 1603-1608.

Prior,I.A., Harding,A., Yan,J., Sluimer,J., Parton,R.G., Hancock,J.F. (2001). GTP-dependent segregation of H-ras from lipid rafts is required for biological activity. Nature Cell Biology 3, 368-375.

Prior,I.A., Muncke,C., Parton,R.G., Hancock,J.F. (2003). Direct visualization of Ras proteins in spatially distinct cell surface microdomains. Journal of Cell Biology 160, 165-170.

Pritchard,C.A., Samuels,M.L., Bosch,E., McMahon,M. (1995). Conditionally Oncogenic Forms of the A-Raf and B-Raf Protein- Kinases Display Different Biological and Biochemical-Properties in Nih 3T3 Cells. Molecular and Cellular Biology 15, 6430-6442.

Ramos,J.W., Kojima,T.K., Hughes,P.E., Fenczik,C.A., Ginsberg,M.H. (1998). The death effector domain of PEA-15 is involved in its regulation of integrin activation. Journal of Biological Chemistry 273, 33897-33900.

Rapp,U.R., Goldsborough,M.D., Mark,G.E., Bonner,T.I., Groffen,J., Reynolds,F.H., Stephenson,J.R. (1983). Structure and Biological-Activity of V-Raf, A Unique Oncogene Transduced by A Retrovirus. Proceedings of the National Academy of Sciences of the United States of America-Biological Sciences 80, 4218-4222.

Reddy,E.P. (1983). Nucleotide-Sequence Analysis of the T24 Human Bladder-Carcinoma Oncogene. Science 220, 1061-1063.

Reedquist,K.A., Ross,E., Koop,E.A., Wolthuis,R.M.F., Zwartkruis,F.J.T., van Kooyk,Y., Salmon,M., Buckley,C.D., Bos,J.L. (2000). The small GTPase, Rap1, mediates CD31-induced integrin adhesion. Journal of Cell Biology 148, 1151-1158.

Renshaw,M.W., Toksoz,D., Schwartz,M.A. (1996). Involvement of the small GTPase Rho in integrin-mediated activation of mitogen-activated protein kinase. Journal of Biological Chemistry 271, 21691-21694.

Reszka,A.A., Hayashi,Y., Horwitz,A.F. (1992). Identification of Amino-Acid-Sequences in the Integrin-Beta-1 Cytoplasmic Domain Implicated in Cytoskeletal Association. Journal of Cell Biology 117, 1321-1330.

Reuther,G.W., Der,C.J. (2000). The Ras branch of small GTPases: Ras family members don't fall far from the tree. Current Opinion in Cell Biology 12, 157-165.

Rey,I., Taylorharris,P., Vanerp,H., Hall,A. (1994). R-Ras Interacts with Rasgap, Neurofibromin and C-Raf But Does Not Regulate Cell-Growth Or Differentiation. Oncogene 9, 685-692.

Richardson,A., Parsons,T. (1996). A mechanism for regulation of the adhesion-associated protein tyrosine kinase pp125(FAK) (vol 380, pg 538, 1996). Nature 381, 810.

Ridley,A.J., Hall,A. (1992). The Small Gtp-Binding Protein Rho Regulates the Assembly of Focal Adhesions and Actin Stress Fibers in Response to Growth- Factors. Cell 70, 389-399.

Robbins,D.J., Zhen,E.Z., Owaki,H., Vanderbilt,C.A., Ebert,D., Geppert,T.D., Cobb,M.H. (1993). Regulation and Properties of Extracellular Signal-Regulated Protein Kinase-1 and Kinase-2 Invitro. Journal of Biological Chemistry 268, 5097-5106.

RodriguezViciana,P., Warne,P.H., Dhand,R., Vanhaesebroeck,B., Gout,I., Fry,M.J., Waterfield,M.D., Downward,J. (1994). Phosphatidylinositol-3-Oh Kinase As A Direct Target of Ras. Nature 370, 527-532.

RodriguezViciana,P., Warne,P.H., Vanhaesebroeck,B., Waterfield,M.D., Downward,J. (1996). Activation of phosphoinositide 3-kinase by interaction with Ras and by point mutation. Embo Journal 15, 2442-2451.

Roy,M.O., Leventis,R., Silvius,J.R. (2000). Mutational and biochemical analysis of plasma membrane targeting mediated by the farnesylated, polybasic carboxy terminus of K-ras4B. Biochemistry 39, 8298-8307.

Roy,S., Luetterforst,R., Harding,A., Apolloni,A., Etheridge,M., Stang,E., Rolls,B., Hancock,J.F., Parton,R.G. (1999). Dominant-negative caveolin inhibits H-Ras function by disrupting cholesterol-rich plasma membrane domains. Nature Cell Biology 1, 98-105.

Rozakisadcock,M., Fernley,R., Wade,J., Pawson,T., Bowtell,D. (1993). The Sh2 and Sh3 Domains of Mammalian Grb2 Couple the Egf Receptor to the Ras Activator Msos1. Nature 363, 83-85.

Ruoslahti,E. (1992). Control of Cell Motility and Tumor Invasion by Extracellular- Matrix Interactions. British Journal of Cancer 66, 239-242.

Ruoslahti,E., Pierschbacher,M.D. (1987). New Perspectives in Cell-Adhesion - Rgd and Integrins. Science 238, 491-497.

Rusnati,M., Tanghetti,E., Urbinati,C., Tulipano,G., Marchesini,S., Ziche,M., Presta,M. (1999). Interaction of fibroblast growth factor-2 (FGF-2) with free gangliosides: Biochemical characterization and biological consequences in endothelial cell cultures. Molecular Biology of the Cell 10, 313-327.

Rusnati,M., Urbinati,C., Tanghetti,E., Dell'Era,P., Lortat-Jacob,H., Presta,M. (2002). Cell membrane GM(1) ganglioside is a functional coreceptor for fibroblast growth factor 2. Proceedings of the National Academy of Sciences of the United States of America 99, 4367-4372.

Santos,E., Tronick,S.R., Aaronson,S.A., Pulciani,S., Barbacid,M. (1982). T24 Human Bladder-Carcinoma Oncogene Is An Activated Form of the Normal Human Homolog of Balb-Msv and Harvey-Msv Transforming Genes. Nature 298, 343-347.

Sastry,S.K., Burridge,K. (2000). Focal adhesions: A nexus for intracellular signaling and cytoskeletal dynamics. Experimental Cell Research 261, 25-36.

Schaeffer,H.J., Weber,M.J. (1999). Mitogen-activated protein kinases: Specific messages from ubiquitous messengers. Molecular and Cellular Biology 19, 2435-2444.

Schaller,M.D., Hildebrand,J.D., Shannon,J.D., Fox,J.W., Vines,R.R., Parsons,J.T. (1994). Autophosphorylation of the Focal Adhesion Kinase, Pp125(Fak), Directs Sh2 Dependent Binding of Pp60(Src). Molecular and Cellular Biology 14, 1680-1688.

Schimmoller,F., Simon,I., Pfeffer,S.R. (1998). Rab GTPases, directors of vesicle docking. Journal of Biological Chemistry 273, 22161-22164.

Schlaepfer,D.D., Hanks,S.K., Hunter,T., Vandergeer,P. (1994). Integrin-Mediated Signal-Transduction Linked to Ras Pathway by Grb2 Binding to Focal Adhesion Kinase. Nature 372, 786-791.

Schmits,R., Kundig,T.M., Baker,D.M., Shumaker,G., Simard,J.J.L., Duncan,G., Wakeham,A., Shahinian,A., vanderHeiden,A., Bachmann,M.F., Ohashi,P.S., Mak,T.W., Hickstein,D.D. (1996). LFA-1-deficient mice show normal CTL responses to virus but fail to reject immunogenic tumor. Journal of Experimental Medicine 183, 1415-1426.

Schwartz,M.A. (1997). Integrins, oncogenes, and anchorage independence. Journal of Cell Biology 139, 575-578.

Schwartz,M.A., Schaller,M.D., Ginsberg,M.H. (1995). Integrins: Emerging paradigms of signal transduction. Annual Review of Cell and Developmental Biology 11, 549-599.

Schwartz,M.A., Toksoz,D., KhosraviFar,R. (1996). Transformation by Rho exchange factor oncogenes is mediated by activation of an integrin-dependent pathway. Embo Journal 15, 6525-6530.

Self,A.J., Caron,E., Paterson,H.F., Hall,A. (2001). Analysis of R-Ras signalling pathways. Journal of Cell Science 114, 1357-1366.

Sethi,T., Ginsberg,M.H., Downward,J., Hughes,P.E. (1999a). The small GTP-binding protein R-Ras can influence integrin activation by antagonizing a Ras/Raf-initiated integrin suppression pathway. Molecular Biology of the Cell 10, 1799-1809.

Sethi,T., Rintoul,R.C., Moore,S.M., MacKinnon,A.C., Salter,D., Choo,C., Chilvers,E.R., Dransfield,I., Donnelly,S.C., Strieter,R., Haslett,C. (1999b). Extracellular matrix proteins protect small cell lung cancer cells against apoptosis: A mechanism for small cell lung cancer growth and drug resistance in vivo. Nature Medicine 5, 662-668.

Sharma,C.P., Ezzell,R.M., Arnaout,M.A. (1995). Direct Interaction of Filamin (Abp-280) with the Beta-2- Integrin Subunit Cd18. Journal of Immunology 154, 3461-3470.

Shattil,S.J., Brass,L.F. (1987). Induction of the Fibrinogen Receptor on Human-Platelets by Intracellular Mediators. Journal of Biological Chemistry 262, 992-1000.

Shattil,S.J., Hoxie,J.A., Cunningham,M., Brass,L.F. (1985). Changes in the Platelet Membrane Glycoprotein-Iib-Iiia Complex During Platelet Activation. Journal of Biological Chemistry 260, 1107-1114.

Shaw,L.M., Rabinovitz,I., Wang,H.H.F., Toker,A., Mercurio,A.M. (1997). Activation of phosphoinositide 3-OH kinase by the alpha 6 beta 4 integrin promotes carcinoma invasion. Cell 91, 949-960.

Sheppard,D. (2000). In vivo functions of integrins: lessons from null mutations in mice. Matrix Biology 19, 203-209.

Shibayama,H., Anzai,N., Braun,S.E., Fukuda,S., Mantel,C., Broxmeyer,H.E. (1999). H-Ras is involved in the inside-out signaling pathway of interleukin-3-induced integrin activation. Blood 93, 1540-1548.

Shields,J.M., Pruitt,K., McFall,A., Shaub,A., Der,C.J. (2000). Understanding Ras: 'it ain't over 'til it's over'. Trends in Cell Biology 10, 147-154.

Shih,T.Y., Weeks,M.O., Young,H.A., Scholnick,E.M. (1979). Identification of a sarcoma virus-coded phosphoprotein in nonproducer cells transformed by Kirsten or Harvey murine sarcoma virus. Virology 96, 64-79.

Shimizu,K., Birnbaum,D., Ruley,M.A., Fasano,O., Suard,Y., Edlund,L., Taparowsky,E., Goldfarb,M., Wigler,M. (1983). Structure of the Ki-Ras Gene of the Human-Lung Carcinoma Cell- Line Calu-1. Nature 304, 497-500.

Shin,E.Y., Lee,J.Y., Park,M.K., Jeong,G.B., Kim,E.G., Kim,S.Y. (1999). H-Ras is a negative regulator of alpha(3)beta(1) integrin expression in ECV304 endothelial cells. Biochemical and Biophysical Research Communications 257, 95-99.

Simons,K., Ikonen,E. (1997). Functional rafts in cell membranes. Nature 387, 569-572.

Simons,K., Toomre,D. (2000). Lipid rafts and signal transduction. Nature Reviews Molecular Cell Biology 1, 31-39.

Simons,M., Friedrichson,T., Schulz,J.B., Pitto,M., Masserini,M., Kurzchalia,T.V. (1999). Exogenous administration of gangliosides displaces GPI-anchored proteins from lipid microdomains in living cells. Molecular Biology of the Cell 10, 3187-3196.

Spaargaren,M., Bischoff,J.R. (1994). Identification of the Guanine-Nucleotide Dissociation Stimulator for Ral As A Putative Effector Molecule of R-Ras, H- Ras, K-Ras, and Rap. Proceedings of the National Academy of Sciences of the United States of America 91, 12609-12613.

Spaargaren,M., Martin,G.A., McCormick,F., Fernandezsarabia,M.J., Bischoff,J.R. (1994). The Ras-Related Protein R-Ras Interacts Directly with Raf-1 in A Gtp-Dependent Manner. Biochemical Journal 300, 303-307.

Springer,T.A. (1990). Adhesion Receptors of the Immune-System. Nature 346, 425-434.

Springer,T.A. (1997). Folding of the N-terminal, ligand-binding region of integrin alpha-subunits into a beta-propeller domain. Proceedings of the National Academy of Sciences of the United States of America 94, 65-72.

Stanbridge E.J., Wilkinson J (1978). Analysis of malignancy in human cells: malignant and transformed phenotypes are under separate genetic control. Proceedings of the National Academy of Sciences of the United States of America 75, 1466-1469.

Stephens,L.E., Sutherland,A.E., Klimanskaya,I.V., Andrieux,A., Meneses,J., Pedersen,R.A., Damsky,C.H. (1995). Deletion of Beta-1 Integrins in Mice Results in Inner Cell Mass Failure and Periimplantation Lethality. Genes & Development 9, 1883-1895.

Stewart,M., Hogg,N. (1996). Regulation of leukocyte integrin function: Affinity vs avidity. Journal of Cellular Biochemistry 61, 554-561.

Stoker M, O'Neill C, Berryman S, Waxman V (1968). Anchorage and growth regulation in normal and virus-transformed cells. International Journal of Cancer 3, 683-693.

Sweet,R.W., Yokoyama,S., Kamata,T., Feramisco,J.R., Rosenberg,M., Gross,M. (1984). The Product of Ras Is A Gtpase and the T24 Oncogenic Mutant Is Deficient in This Activity. Nature 311, 273-275.

Tabin,C.J., Bradley,S.M., Bargmann,C.I., Weinberg,R.A., Papageorge,A.G., Scolnick,E.M., Dhar,R., Lowy,D.R., Chang,E.H. (1982). Mechanism of Activation of A Human Oncogene. Nature 300, 143-149.

Takada,Y., Puzon,W. (1993). Identification of A Regulatory Region of Integrin-Beta-1 Subunit Using Activating and Inhibiting Antibodies. Journal of Biological Chemistry 268, 17597-17601.

Takagi,J., Petre,B.M., Walz,T., Springer,T.A. (2002). Global conformational rearrangements in integrin extracellular domains in outside-in and inside-out signaling. Cell 110, 599-611.

Takagi,J., Strokovich,K., Springer,T.A., Walz,T. (2003). Structure of integrin alpha(5)beta(1) in complex with fibronectin. Embo Journal 22, 4607-4615.

Takeichi M (1993). Cadherins in cancer: implications for invasion and metastasis. Current Opinion in Cell Biology 5, 806-811.

Tamkun,J.W., Desimone,D.W., Fonda,D., Patel,R.S., Buck,C., Horwitz,A.F., Hynes,R.O. (1986). Structure of Integrin, A Glycoprotein Involved in the Transmembrane Linkage Between Fibronectin and Actin. Cell 46, 271-282.

Tanaka,Y., Minami,Y., Mine,S., Hirano,H., Hu,C.D., Fujimoto,H., Fujii,K., Saito,K., Tsukada,J., van Kooyk,Y., Figdor,C.G., Kataoka,T., Eto,S. (1999). H-ras signals to cytoskeletal machinery in induction of integrin-mediated adhesion of T cells. Journal of Immunology 163, 6209-6216.

Tanaka,Y., Nakayamada,S., Fujimoto,H., Okada,Y., Umehara,H., Kataoka,T., Minami,Y. (2002). H-Ras/mitogen-activated protein kinase pathway inhibits integrin-mediated adhesion and induces apoptosis in osteoblasts. Journal of Biological Chemistry 277, 21446-21452.

Thorne,R.F., Marshall,J.F., Shafren,D.R., Gibson,P.G., Hart,I.R., Burns,G.F. (2000). The integrins alpha(3)beta(1) and alpha(6)beta(1) physically and functionally associate with CD36 in human melanoma cells - Requirement for the extracellular domain of CD36. Journal of Biological Chemistry 275, 35264-35275.

Tranqui,L., Usson,Y., Marie,C., Block,M.R. (1993). Adhesion of Cho Cells to Fibronectin Is Mediated by Functionally and Structurally Distinct Adhesion Plaques. Journal of Cell Science 106, 377-387.

Travis,M.A., Humphries,J.D., Humphries,M.J. (2003). An unraveling tale of how integrins are activated from within. Trends in Pharmacological Sciences 24, 192-197.

Turner C.E., Burridge K (1991). Transmembrane molecular assemblies in cell-extracellular matrix interactions. Current Opinion in Cell Biology 5, 849-853.

Urano,T., Emkey,R., Feig,L.A. (1996). Ral-GTPases mediate a distinct downstream signaling pathway from Ras that facilitates cellular transformation. Embo Journal 15, 810-816.

van Kooyk,Y., Figdor,C.G. (2000). Avidity regulation of integrins: the driving force in leukocyte adhesion. Current Opinion in Cell Biology 12, 542-547.

Vinogradova,O., Velyvis,A., Velyviene,A., Hu,B., Haas,T.A., Plow,E.F., Qin,J. (2002). A structural mechanism of integrin alpha(IIb)beta(3) "inside- out" activation as regulated by its cytoplasmic face. Cell 110, 587-597.

Vojtek,A.B., Hollenberg,S.M., Cooper,J.A. (1993). Mammalian Ras Interacts Directly with the Serine Threonine Kinase Raf. Cell 74, 205-214.

Vuori,K., Hirai,H., Aizawa,S., Ruoslahti,E. (1996). Induction of p130(cas) signaling complex formation upon integrin-mediated cell adhesion: A role for Src family kinases. Molecular and Cellular Biology 16, 2606-2613.

Wang,B.C., Zou,J.X., Ek-Rylander,B., Ruoslahti,E. (2000). R-Ras contains a proline-rich site that binds to SH3 domains and is required for integrin activation by R-Ras. Journal of Biological Chemistry 275, 5222-5227.

Warrens,A.N., Jones,M.D., Lechler,R.I. (1997). Splicing by overlap extension by PCR using asymmetric amplification: An improved technique for the generation of hybrid proteins of immunological interest. Gene 186, 29-35.

Wartmann,M., Davis,R.J. (1994). The Native Structure of the Activated Raf Protein-Kinase Is A Membrane-Bound Multisubunit Complex. Journal of Biological Chemistry 269, 6695-6701.

Wary,K.K., Mainiero,F., Isakoff,S.J., Marcantonio,E.E., Giancotti,F.G. (1996). The adaptor protein Shc couples a class of integrins to the control of cell cycle progression. Cell 87, 733-743.

Wary,K.K., Mariotti,A., Zurzolo,C., Giancotti,F.G. (1998). A requirement for caveolin-1 and associated kinase Fyn in integrin signaling and anchorage-dependent cell growth. Cell 94, 625-634.

Willumsen,B.M., Christensen,A., Hubbert,N.L., Papageorge,A.G., Lowy,D.R. (1984). The P21 Ras C-Terminus Is Required for Transformation and Membrane Association. Nature 310, 583-586.

Willumsen,B.M., Cox,A.D., Solski,P.A., Der,C.J., Buss,J.E. (1996). Novel determinants of H-Ras plasma membrane localization and transformation. Oncogene 13, 1901-1909.

Wing M.R., Bourdon D.M., Harden T.K. (2003). PLC-{varepsilon} A shared effector protein in Ras-, Rho-, and G{alpha}{beta}{gamma}-mediated signaling. Mol Intervent 5, 273-280.

Wittinghofer,A., Scheffzek,K., Ahmadian,M.R. (1997). The interaction of Ras with GTPase-activating proteins. Febs Letters 410, 63-67.

Wolthuis,R.M.F., Bos,J.L. (1999). Ras caught in another affair: the exchange factors for Ral. Current Opinion in Genetics & Development 9, 112-117.

Woods,D., Cherwinski,H., Venetsanakos,E., Bhat,A., Gysin,S., Humbert,M., Bray,P.F., Saylor,V.L., McMahon,M. (2001). Induction of beta 3-integrin gene expression by sustained activation of the Ras-regulated Raf-MEK-extracellular signal- regulated kinase signaling pathway. Molecular and Cellular Biology 21, 3192-3205.

Woods,D., Parry,D., Cherwinski,H., Bosch,E., Lees,E., McMahon,M. (1997). Raf-induced proliferation or cell cycle arrest is determined by the level of Raf activity with arrest mediated by p21(Cip1). Molecular and Cellular Biology 17, 5598-5611.

Xia,Z.G., Dickens,M., Raingeaud,J., Davis,R.J., Greenberg,M.E. (1995). Opposing Effects of Erk and Jnk-P38 Map Kinases on Apoptosis. Science 270, 1326-1331.

Xiong,J.P., Stehle,T., Diefenbach,B., Zhang,R.G., Dunker,R., Scott,D.L., Joachimiak,A., Goodman,S.L., Arnaout,M.A. (2001). Crystal structure of the extracellular segment of integrin alpha V beta 3. Science 294, 339-345.

Yamada,K.M., Miyamoto,S. (1995). Integrin Transmembrane Signaling and Cytoskeletal Control. Current Opinion in Cell Biology 7, 681-689.

Yamamoto,T., Matsui,T., Nakafuku,M., Iwamatsu,A., Kaibuchi,K. (1995). A novel GTPase-activating protein for R-Ras. Journal of Biological Chemistry 270, 30557-30561.

Yan,J., Roy,S., Apolloni,A., Lane,A., Hancock,J.F. (1998). Ras isoforms vary in their ability to activate Raf-1 and phosphoinositide 3-kinase. Journal of Biological Chemistry 273, 24052-24056.

Yang,J.T., Rayburn,H., Hynes,R.O. (1993). Embryonic Mesodermal Defects in Alpha(5) Integrin-Deficient Mice. Development 119, 1093-1105.

Yao,R., Cooper,G.M. (1996). Growth factor-dependent survival of rodent fibroblasts requires phosphatidylinositol 3-kinase but is independent of pp70(S6K) activity. Oncogene 13, 343-351.

Zhang,X.F., Settleman,J., Kyriakis,J.M., Takeuchisuzuki,E., Elledge,S.J., Marshall,M.S., Bruder,J.T., Rapp,U.R., Avruch,J. (1993). Normal and Oncogenic P21(Ras) Proteins Bind to the Amino- Terminal Regulatory Domain of C-Raf-1. Nature 364, 308-313.

Zhang,Z.H., Vuori,K., Reed,J.C., Ruoslahti,E. (1995). The Alpha-5-Beta-1 Integrin Supports Survival of Cells on Fibronectin and Up-Regulates Bcl-2 Expression. Proceedings of the National Academy of Sciences of the United States of America 92, 6161-6165.

Zhang,Z.H., Vuori,K., Wang,H.G., Reed,J.C., Ruoslahti,E. (1996). Integrin activation by R-ras. Cell 85, 61-69.

Zhong,C.L., Kinch,M.S., Burridge,K. (1997). Rho-stimulated contractility contributes to the fibroblastic phenotype of ras-transformed epithelial cells. Molecular Biology of the Cell 8, 2329-2344.

Zhu,X.Y., Ohtsubo,M., Bohmer,R.M., Roberts,J.M., Assoian,R.K. (1996). Adhesion-dependent cell cycle progression linked to the expression of cyclin D1, activation of cyclin E-cdk2, and phosphorylation of the retinoblastoma protein. Journal of Cell Biology 133, 391-403.

Zou,J.X., Liu,Y.Q., Pasquale,E.B., Ruoslahti,E. (2002). Activated Src oncogene phosphorylates R-Ras and suppresses integrin activity. Journal of Biological Chemistry 277, 1824-1827.

Zou,J.X., Wang,B.C., Kalo,M.S., Zisch,A.H., Pasquale,E.B., Ruoslahti,E. (1999). An Eph receptor regulates integrin activity through R-Ras. Proceedings of the National Academy of Sciences of the United States of America 96, 13813-13818.